The role of different subtypes of olfactory bulb interneurons in olfactory behavior

Thèse

Sarah Malvaut

Doctorat en neurobiologie
Philosophiæ doctor (Ph. D.)

Québec, Canada

The role of different subtypes of olfactory bulb interneurons in olfactory behavior

Thèse

Sarah MALVAUT

Sous la direction de :

Armen SAGHATELYAN, directeur de recherche

RÉSUMÉ

Le bulbe olfactif (BO) représente dans le cerveau le premier relai dans le traitement des informations olfactives. Au niveau de cette structure, plusieurs types de neurones sont impliqués dans la modulation de l'information odorante, avant même que celle-ci ne soit envoyée vers des structures corticales supérieures. Parmi eux se trouvent les cellules granulaires (CGs), une population d'interneurones régulant de manière importante l'activité des cellules principales du BO. De manière intéressante, le BO est capable à l'âge adulte de produire et régénérer une partie de sa population interneuronale via le processus de neurogénèse adulte. Il est ainsi possible de faire la distinction entre les CGs générées au cours de la période postnatale (CGs postnatales) des CGs générées à l'âge adulte (CGs nouvellement générées). Le rôle que jouent ces CGs dans le traitement olfactif mais aussi dans les différents comportements olfactifs a pendant très longtemps donné lieu à des interprétations contradictoires. Le manque de cohérence au niveau des données peut s'expliquer par le fait que pendant longtemps, les CGs ont été considérées comme étant une population homogène de cellules. Néanmoins, des études ont montré que les CGs peuvent exprimer différents marqueurs neurochimiques. Notamment, nous nous sommes intéressés dans le cadre de notre étude à deux de ces marqueurs : la protéine kinase calcium calmoduline dépendante IIα (CaMKIIα) et la Calrétinine (CR). Une telle hétérogénéité au sein des cellules interneuronales du BO pourrait également refléter une hétérogénéité fonctionnelle, chaque sous-population de CGs pouvant contribuer de façon propre et unique au traitement des informations olfactives et donc au comportement olfactif.

Dans la première partie de ces travaux, nous avons étudié le rôle fonctionnel des cellules exprimant la CaMKIIα et l'avons comparé à la population générale de CGs. De manière intéressante, nous montrons que, bien que ces deux populations de cellules soient en tous points semblables au niveau morphologique, les cellules CaMKIIα reçoivent un niveau d'inhibition moindre par rapport à leurs homologies négatives, les rendant plus susceptibles d'être activées suite à des tâches

comportementales spécifiques. De plus, l'inhibition spécifique des cellules CaMKIIα-positive entraine une perturbation des performances de discrimination fine.

Dans la seconde partie de ces travaux, nous nous sommes intéressés cette fois-ci à la sous-population de CGs exprimant la CR, en tenant compte également de la période développementale de ces cellules (i.e CGs post-natales ou nouvellement générées). Nous montrons que les cellules nouvellement générées exprimant ou non la CR, ainsi que les cellules CR-positives postnatales diffèrent quant à leurs propriétés électrophysiologiques. De plus, tout comme les cellules exprimant la CaMKIIα, les cellules exprimant la CR présentent un niveau d'activation plus important à la suite de certaines tâches comportementales et sont également nécessaires à la bonne réalisation de tâches de discrimination olfactive.

ABSTRACT

The olfactory bulb (OB) is considered as the first relay in the brain during olfactory processing. Several types of neurons are involved at the level of this structure in the refinement of the olfactory information before it is sent to higher cortical structures. Among the cell types involved is the population of granule cells (GC), a population of interneurons largely regulating the activity of OB principal cells. Interestingly, the OB retain during adulthood the ability to produce and renew part of its interneuronal pool through a process called adult neurogenesis. Therefore, it is possible to distinguish in the adult OB between GCs born during the early postnatal period (early-born GCs) to the one that were generated during adulthood (adult-born GCs). Several studies aimed at determining the precise role played by GC in olfactory processing and olfactory behavior, giving rise quite often to conflicting results. This absence of coherence in the data could come from the fact that for long, the population of GCs was considered as a homogeneous cell population. However, GCs were shown to express diverse neurochemical markers. In this study we investigated more particularly into two of those markers, showed to be expressed by GCs: the Ca^{2+}/calmodulin-dependent protein kinase IIα (CaMKIIα) and Calretinin (CR). Hence, such a heterogeneity in the phenotype of OB interneurons could also underlie a functional heterogeneity of the different GC subpopulation, each one contributing in a unique way to olfactory processing and thus olfactory behavior.

In the first part of this work, we investigated the functional role of CaMKIIα-expressing cells and compared it to the general population of GCs. Interestingly we revealed that CaMKIIα-positive GCs are more prone to activation following specific behavioral tasks, likely due to a decreased level of inhibition as compared to their negative counterparts. Moreover, the specific inhibition of this GC subpopulation let to alteration of animals' fine discrimination abilities.

In the second part of our work, when focusing this time on the subpopulation of CR-expressing GCs, taking this time also into account the developmental period at which they were generated (i.e early- versus adult-born cells), we showed that adult-born CR-expressing and non-expressing GCs, but also early-born CR-expressing

GCs display different electrophysiological characteristics. Moreover, as for CaMKIIα-positive GCs, CR-positive GCs present a higher level of activation following specific olfactory tasks and are also important for a proper ability to perform olfactory discrimination tasks.

TABLE OF CONTENTS

LIST OF FIGURES

LIST OF TABLES

LIST OF ABBREVIATIONS

AAV	adeno-associated virus
ACSF	artificial cerebrospinal fluid
AMPA	2-amino-3-(3-hydroxy-5-methyl-isoxazol-4-yl) propanoic acid
AON	anterior olfactory nucleus
AP	action potential
AraC	β-D-arabinofuranoside
BDNF	brain-derived neurotrophic factor
BF	basal forebrain
BMI	bicuculline methochlorine
BrdU	bromo-desoxy-uridine
CAG	cytomegalovirus early enhancer/chicken β actin
CaMKIIα	Ca^{2+}/calmodulin-dependent protein kinase IIα
CaMKIV	Ca^{2+}/calmodulin-dependent protein kinase IV
CB	calbindin
CBA	chicken β-actin
cFos	cellular oncogene response 1
ChR2	channel-rhodopsin
CNO	clozapine-N-oxide
CR	calretinin
DAB	diaminobenzidine
dpi	day post-injection
DREADDs	Designer receptors exclusively activated by designer drugs
DV	dorso-ventral
EF1α	elongation factor 1α
EGFR	epidermal growth factor receptor
EPL	external plexiform layer
EPSC	excitatory post-synaptic current
GABA	γ-aminobutyric acid
GC	granule cell
GCL	granule cell layer
GFAP	glial fibrillary acidic protein
GFP	green fluorescent protein
GL	glomerular layer
HDB	horizontal limb of diagonal band of Broca
IEG	immediate early gene
IPL	internal plexiform layer
IPSC	inhibitory post-synaptic current
Kyn	kynurenic acid
LTP	long-term potentiation
M/T cells	mitral/tufted cells
MC	mitral cell
MCPO	magnocellular preoptic nucleus
mEPSC	miniature excitatory post-synaptic current

mGluR2	metabotropic glutamate receptor 2
mIPSC	miniature inhibitory post-synaptic current
ML	medio-lateral
NCAM	neural cell adhesion molecule
NeuN	neuronal nuclei
NpHR	halorhodospin
NSC	neural stem cell
OB	olfactory bulb
OE	olfactory epithelium
ONL	olfactory nerve layer
OPR	olfactory bulb projecting region
OSN	olfactory sensory neuron
OT	olfactory tubercle
PC	piriform cortex
PCNA	proliferating cell nuclear antigen
PFA	paraformaldehyde
PG	periglomerular cell
PGC	periglomerular cell
PV	parvalbumin
RFP	red fluorescent protein
RMS	rostral migratory stream
ROI	region of interest
SAC	short-axon cell
SD	standard deviation
sEPSC	spontaneous excitatory post-synaptic current
SHF	spine head filopodia
sIPSC	spontaneous inhibitory post-synaptic current
SVZ	subventricular zone
Syn	synapsin
TC	tufted cell
TH	tyrosine-hydroxylase
TTX	tetrodotoxin
TVA	avian tumor virus receptor A
Val66Met	variant brain-derived neurotrophic factor
wpi	week post-injection
Zif268	zinc finger protein 268

A ma famille, mon mari et mes amis

REMERCIEMENTS

Je tiens tout d'abord à remercier mon directeur de thèse, le Dr. Armen Saghatelyan pour m'avoir offert la chance il y a maintenant presque 6 ans de commencer un doctorat dans son laboratoire. Il a toujours su se montrer disponible pour me guider, discuter et répondre à mes parfois nombreuses interrogations tout au long de ces années. Venir étudier au Québec est probablement ce que je considère comme l'un des plus grands défis de ma vie et cette expérience dans son laboratoire m'aura permis d'enrichir à la fois mon panel de connaissances et d'expertises, tout en développant un intérêt et une curiosité pour les approches d'optique et d'imagerie.

Je tiens également à remercier tous les membres de mon jury, le Dr. Paul de Koninck, le Dr. Christophe Proulx ainsi que le Dr. Diane Lagace, pour avoir accepté de réviser ma thèse.

Je remercie tous mes collègues du laboratoire du Dr. Saghatelyan, actuels ou anciens, Marina, Cédric, Archana, Delphine, Arthur, Tiziano, Alessandra, Aymeric, Vlad, Majid, Qian, Marcos, Caroline, et Rodrigo.

Les prochains remerciements vont à mes amis, tant outre-atlantique : Amélie, Rémy et Sophie, qu'à ma famille du Québec : Cédric et Thierry, Archana, Axelle et Yoann, Léa, Louis, Mélina et Mike, Aymeric, Karen et Armina, Alessandra, Romina, Delphine et Flavien. Être loin de sa famille et de son pays peut parfois, même souvent, être difficile, et je n'oublierai jamais tous nos repas, brunchs du dimanche, soirées ou tout simplement nos moments partagés ensemble ainsi que votre présence et soutien lors d'évènements importants de ma vie. Je ne doute pas qu'il y en aura beaucoup d'autres et pour tout cela, un énorme merci !

Je remercie maintenant tout naturellement ma famille, et notamment mon père, ma mère, ainsi que mes deux (petites mais grandes) sœurs Fanny et Raphaëlle. Partir loin de vous pour faire ma thèse a probablement été la décision la plus dure à prendre, et même si celle-ci n'a pas forcément fait l'unanimité au départ, vous avez toujours

été présents pour moi dans tous les moments, les bons comme les moins bons, ces 6 dernières années et pour cela je vous en remercie tellement. Comme l'a dit une fois une poète de la famille « la distance n'enlève en rien tout l'amour que j'ai pour vous ».

Enfin, je remercie mon mari Julien. Tu es celui qui m'accompagne au quotidien, a su me supporter et me soutenir dans les dernières étapes de mon doctorat. Tu sais toujours me redonner le sourire par ton humour (certes un peu spécial…) et me remonter le moral lorsque je doute ou stresse, tout simplement.

AVANT-PROPOS

La première partie des résultats présentés dans ce manuscrit de thèse, et qui représente le projet principal sur lequel j'ai travaillé au cours de mon doctorat, a fait l'objet d'une publication dans le journal *Current Biology* en Octobre 2017. Dans le cadre de cet article, j'ai réalisé l'intégralité des expériences d'imagerie calcique *in vivo*, ainsi qu'une grande majorité des expériences comportementales ayant permis de caractériser par immunohistochimie l'activation des sous-types cellulaires d'intérêt dans l'étude. Plusieurs personnes ont également collaboré à la réalisation de ce travail. Delphine Hardy a participé à l'analyse de la morphologie et de l'activation des cellules à la suite des paradigmes comportementaux. Linda David a réalisé les enregistrements électrophysiologiques. L'équipe du Dr. Alain Trembleau, composée des Drs. Simona Gribaudo, Laura Daroles, Alain Trembleau et Isabelle Caillé, a également contribué à l'analyse morphologique des populations neuronales d'intérêt ainsi qu'à l'analyse de l'activation de ces populations site à différents comportements olfactifs. Les Drs. Martin Holzenberger et Zayna Chaker nous ont permis d'obtenir des cerveaux d'animaux transgéniques CaMKIIa-cre-tdTomato utilisés lors de notre analyse immunohistochimique. Les expériences d'imagerie deux-photons *in vivo* ont été effectuées sur le système du Dr. Daniel Côté et l'analyse de ces imageries calciques a été permise grâce à l'élaboration de codes Matlab par le Dr. Simon Labrecque, le Dr. Paul de Koninck et Marie-Anne Lebel-Cormier. Ce projet a été supervisé par le Dr. Armen Saghatelyan, avec qui j'ai écrit l'article, en tenant compte des commentaires et remarques émis par chacun des co-auteurs.

Dans le cadre de l'étude présentée en seconde partie de cette thèse, la majorité des résultats a été obtenue par ma collègue Delphine Hardy qui a réalisé les analyses électrophysiologiques, morphologiques et immunohistochimiques. Nous avons toutes deux également réalisé des tâches de comportements olfactifs (conditionnement opérant pour sa part et discrimination olfactive pour ma part) ayant permis de caractériser l'activation cellulaire à la suite de ces différentes tâches. Le Dr. Vincent Breton-Provencher a contribué à la conception des expériences d'électrophysiologie

aux premières étapes de développement du projet. Enfin le Dr. Armen Saghatelyan a supervisé le projet.

INTRODUCTION

The olfactory environment by which we are surrounded and live is in constant flux. The sense of smell plays a vital role for some species, allowing them to find food, detect potential threats, and interact with conspecifics. Animals encounter new odors every day. To detect these new odors, they need to discriminate them from previously experienced ones. Among the structures involved, the olfactory bulb (OB) is pivotal since it represents the first relay of olfactory inputs coming from the olfactory epithelium (OE). It has the ability to decode the olfactory information before sending it, without any thalamic relay, to other brain regions such as the olfactory cortex, amygdala, olfactory tubercle, hippocampus, and entorhinal cortex (Davis, 2004; Ghosh et al., 2011; Miyamichi et al., 2011; Sosulski et al., 2011). Interestingly, the OB, even during adulthood, retains the ability to regenerate some of its neuronal population by constantly integrating new cells through a process called adult neurogenesis (Altman, 1969; Alvarez-Buylla and Garcia-Verdugo, 2002; Lagace et al., 2007; Lepousez et al., 2015; Lois and Alvarez-Buylla, 1994). This regenerative process poses a “stability-plasticity” dilemma in that the normal functioning of the OB network must be maintained despite its constant structuro-functional reorganization.

In this chapter, I will first briefly describe the architecture and cellular organization of the OB. I will then present and discuss the current state of knowledge concerning the processes by which the OB can partly regenerate its cellular pool and also adapt to an environment undergoing constant change. In addition, I will present the roles that such phenomena may play in the bulbar network and odor behavior. Lastly, I will discuss how the olfactory bulb functioning is shaped and complexified by the existence of subgroups of cells that play distinct roles in the bulbar network functioning but also sensory processing.

1. Structure and organization of the mammalian olfactory bulb

The structure of the OB has been well characterized, and several cellular layers are easily identifiable, depending on their location in the OB (***Figure 1.1***). The outermost layer, the olfactory nerve layer (ONL), conveys the axons of olfactory

sensory neurons (OSNs) that project to a very well-organized structure in the glomerular layer (GL), the glomerulus. Interestingly, axons from OSNs scattered throughout the OE that express the same olfactory receptor gather together in the same glomeruli, creating an odorant map in the OB (Mombaerts et al., 1996; Mori et al., 2006). Inside the glomeruli, OSN axons form synapses with the primary dendrites of OB principal cells, that is, mitral and tufted cells (MCs and TCs). Short-axon cells (SACs) and periglomerular cells (PGs), the first type of OB resident interneurons, also reside in the GL and play important roles in information processing. The external plexiform layer (EPL) lies below the GL and is home to the dendrites of MCs, the apical dendrites of granule cells (GCs), and the soma and lateral dendrites of TCs and parvalbumin-expressing neurons (Miyamichi et al., 2013).

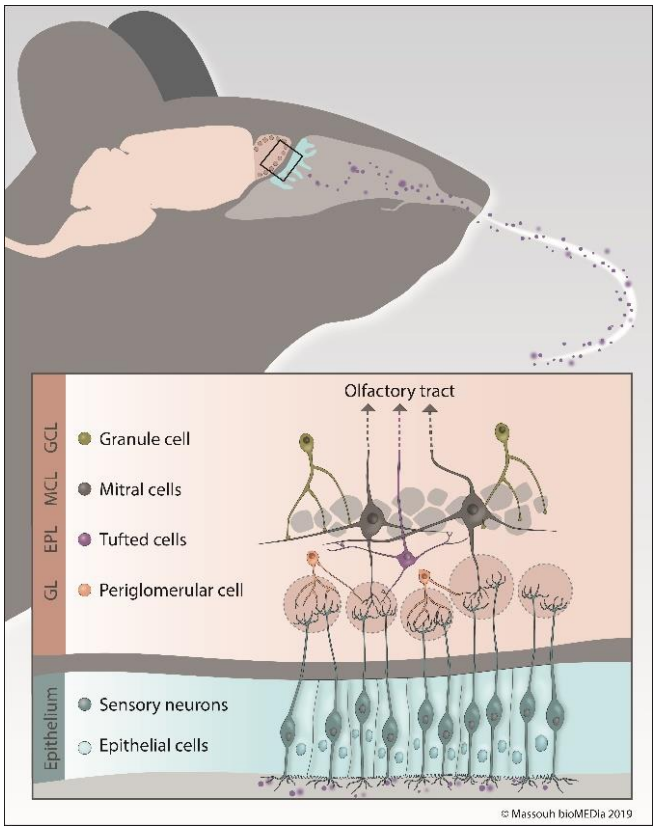

Figure 1.1: Schematic representation of the OB.

Volatile odorant molecules, once they enter the nasal cavity, bind to olfactory receptors on the surface of OSNs in the OE. Odorant information is then transduced into an electrical signal and is transmitted to the glomerular layer of the olfactory bulb via OSN axons. Each OSN expresses one of the thousands of olfactory receptors and all OSNs expressing the same olfactory receptor project to the same pair of glomeruli. Inside the glomeruli, OSN axons form synapses with MCs and TCs, the output neurons of the OB. PGs are the first population of resident interneurons and are also found inside the GL. The cell bodies of TCs reside in the EPL, which is located deeper in the OB. The inner part of the EPL is lined with the MCs layer, which encloses the cell bodies of MCs. The GCL is the largest layer of the OB and is composed of GCs (*source: Massouh bioMEDia*).

The inner part of the EPL is delimited by the mitral cell layer (MCL), which is formed by the cell bodies of MCs. The granule cell layer (GCL), the largest and deepest layer of the OB, is composed of GC cell bodies. GCs are axon-less resident

interneurons in the OB. They send long, ramified secondary dendrites toward the EPL to form synapses with the lateral dendrites of principal cells. Lastly, the OB portion of the rostral migratory stream (RMS-OB) is the innermost layer of the OB and constantly replenishes the OB with immature neurons (***Figure 1.1***).

In the OB network, GC and PG interneurons play a major role in modulating the output of olfactory information sent by principal cells to higher brain regions. Interestingly, GCs constitute the most numerous cell population, and it is estimated that individual MCs can receive inputs from approximately 100 individual GCs and that each GC may contact hundreds of MCs (Shepherd, 1972). This important inhibitory drive on bulbar principal neurons allows the tight spatio-temporal modulation of information processing (Arevian et al., 2008; Gschwend et al., 2015; Urban, 2002; Yokoi et al., 1995). To modulate principal cell activity, PGs and GCs form a unique type of synapse: the reciprocal dendro-dendritic synapse (Isaacson and Strowbridge, 1998; Jahr and Nicoll, 1982) (***Figure 1.2***). Following their activation, MCs and TCs release glutamate onto GC or PG spines, which in turn leads to the release, within the same synapse, of the inhibitory neurotransmitter γ-aminobutyric acid (GABA) back to principal cell dendrites (Rojas-Libano and Kay, 2008; Whitman and Greer, 2007).

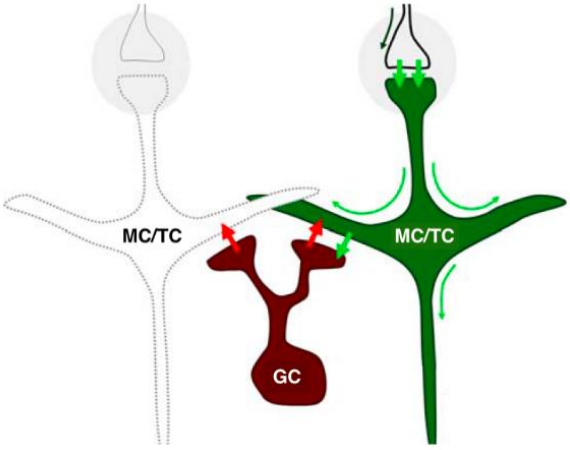

Figure 1.2: Reciprocal dendrodendritic synapse between mitral/tufted cells and granule cells

Action potentials from OSNs arrive at glomeruli (gray circles) and excite (short green arrows) MC\TC. This depolarization propagates from the postsynaptic membrane through the entire cell (long green arrows), resulting in excitation of GCs through glutamate liberation at the dendro-dendritic synapse. The excitation of granule cells causes them to liberate GABA (red arrows), eliciting recurrent and lateral inhibition of M/T cells. Note that due to the geometry of the arrangement, the same dynamical interactions can be elicited by antidromic activation of M/T cells *Adapted from Rojas-Libano and Kay, 2008.*

Individual MCs/TCs respond to only a few odorants by changing their firing rates, supporting the idea of sparse encoding of odor information in the OB (Bathellier et al., 2008; Davison and Katz, 2007; Fantana et al., 2008; Nagayama et al., 2004). Moreover, the inhibition of principal cells by GCs at dendrodendritic reciprocal synapses generates fast oscillations in the gamma range (20-80 Hz) (Fukunaga et al., 2014), resulting in the synchronization of MC activity (Arevian et al., 2008; Lagier et al., 2004; Lagier et al., 2007; Lepousez and Lledo, 2013). The proper functioning of the recurrent inhibition of MCs by GCs and the generation of gamma rhythms is also of particular relevance in the context of odor discrimination (Abraham et al., 2010; Lepousez and Lledo, 2013). In fact, modulating the imbalance between the excitation/inhibition of these synapses using picrotoxin, a GABA(A)-receptor antagonist, is sufficient to decrease the frequency of gamma oscillations and concomitantly alter the performance of animals in odor discrimination tasks (Lepousez and Lledo, 2013). This effect has been corroborated by inhibiting GC activity using a pharmacogenetic approach (use of designer receptors exclusively activated by designer drugs or DREADDs), which decreases pattern separation and slows down the learning of an odor discrimination task involving complex odor mixtures (Gschwend et al., 2015) (***Figure 1.3***). On the other hand, optogenetically activating GCs using channel-rhodopsin (ChR2) resulted in increased pattern separation (Gschwend et al., 2015) (***Figure 1.3***). These results thus highlight the importance of GCs and their inhibitory drive on principal cells regarding the decorrelation of overlapping MC/TC ensembles, an ability that underlies the capacity of animals to properly discriminate related odorants. The inhibition provided by PGs is also important for information processing and coding in the OB. PGs coordinate theta activity in the OB and regulate baseline and odor-evoked inhibition (Fukunaga et al., 2014). These GC- and PG-associated inhibitory networks thus control OB activities at different timescales, with PGs being involved in regulating the theta rhythm and GCs controlling gamma oscillations (Fukunaga et al., 2014).

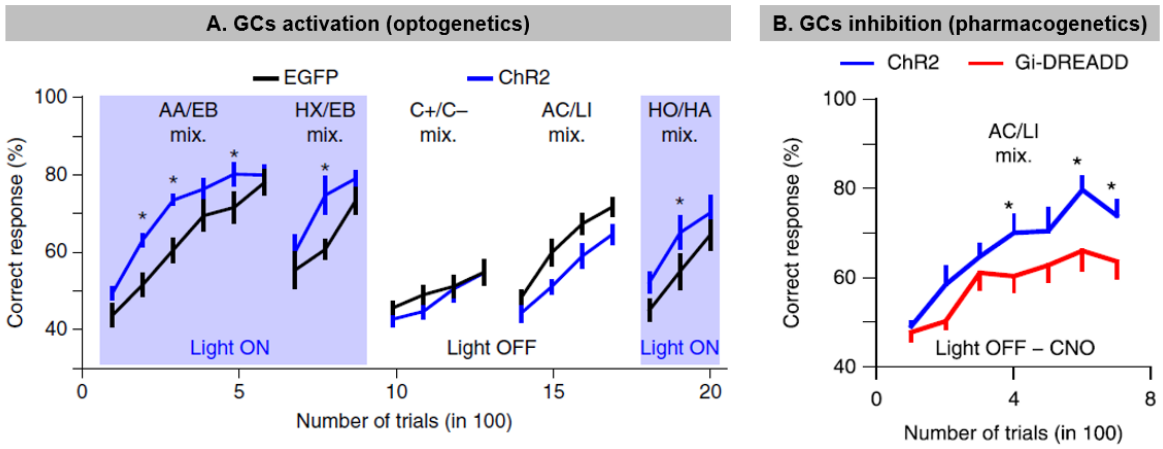

Figure 1.3: Modulation of granule cells activity influences odor discrimination performances

A. Optogenetic stimulation of GCL improves odor discrimination learning. Discrimination performances for different groups of mice, which received injection of an adeno-associated virus (AAV) expressing either ChR2 or EGFP) in the GCL. Performances of ChR2-expressing mice (blue lines, n = 7) were specifically improved by photo-stimulation in comparison with EGFP-expressing mice (black lines, n = 7; Light ON: repeated-measures ANOVA, F = 8.3, P = 0.015, *post hoc* Fisher test at least *P < 0.034; Light OFF: repeated-measures ANOVA, F = 3.7, P = 0.08). Blue boxes indicate light ON episodes. Data are presented as mean ± sem. The odor pairs used were (all gas mixes): amyl acetate/ethyl butyrate (AA/EB) 60/40 versus AA/EB 40/60, ethyl butyrate/3-hexanone (EB/HX) 60/40 versus EB/HX 40/60, (+)-Carvone/(-)Carvone (C+/C–) 60/40 versus C+/C– 40/60, acetophenone/limonene (AC/LI) 60/40 versus AC/LI 40/60, and heptanol/hexanal (HO/HA) 60/40 versus HO/HA 40/60. **B.** Pharmacogenetic inhibition of GCL neurons deteriorates odor discrimination learning. CNO injection (2 mg per kg; all groups injected) decreased learning performances in Gi-DREADD–expressing mice in comparison with ChR2-expressing mice (n = 9 mice in each group; repeated-measures ANOVA F = 6.32 P = 0.023, *post hoc* LSD test at least *P < 0.045). Data are presented as mean ± sem. Odor pair used: AC/LI 60/40 versus AC/LI 40/60 (gas mixes). *Adapted from Gschwend et al., 2015*.

2. Regeneration of the olfactory bulb during adulthood: the process of adult neurogenesis

A. Adult neurogenesis: an overview

The OB is in direct contact with the outside environment through its contacts with OSNs. As already mentioned, the OE is responsible for the transduction of olfactory information to the OB via the axons of OSNs. Interestingly, the OE has a marked ability to regenerate since OSNs are in direct contact with the external environment. They thus have a short lifetime and are constantly being replenished (Calof et al., 1998; Graziadei and Graziadei, 1979; Murray and Calof, 1999). The axons of these newly generated OSNs form new connections with MCs and TCs in

the glomeruli of the OB (Mombaerts, 2001) and induce morpho-functional rearrangements of the GL circuitry.

The constant regeneration of OSNs and axonal remodeling in the glomeruli implies that an adaptive process that adjusts the bulbar network should also occur intrinsically in the OB. One current assumption is that the turnover of OSNs in the OE may underlie another regenerative process in the OB. Adult neurogenesis, which will be more extensively discussed below, provides the OB daily with thousands of newly generated cells by constantly renewing approximately 10-15% of GCs and 30% of PGs each (Ninkovic et al., 2007). Until now, no clear evidence has emerged of a direct link between these two neurogenic processes in the OE and the OB. However, it appears that both phenomena are sensitive to the level of sensory activity. For instance, olfactory enrichment results in increased OE neurogenesis and survival of adult-born OB interneurons (Cavallin et al., 2010; Rochefort et al., 2002; Rochefort and Lledo, 2005; Watt et al., 2004; Woo et al., 2006). On the other hand, sensory deprivation via a mechanical blockade of olfactory input entry or a lesion of the sensory epithelium results in a reduction in the thickness of the OE, a loss of olfactory sensory neurons and basal cells in the occluded side (Cavallin et al., 2010; Farbman et al., 1988), and a reduction in OB volume (Cummings et al., 1997) and the number of adult-born interneurons (Corotto et al., 1994; Petreanu and Alvarez-Buylla, 2002; Saghatelyan et al., 2005; Yamaguchi and Mori, 2005). It remains, however, to be determined whether the constant arrival of new sensory axons drives synaptic remodeling between interneurons and principal cells in the OB network and whether neurogenesis in the OE drives neurogenesis in the OB. OB neurogenesis involves a succession of processes, beginning with stem cell division and ending with the morpho-functional integration of adult-born neurons into the OB neuronal circuitry. Below, I briefly describe the generation and migration of neuronal precursors, with an emphasis on the developmental processes leading to the maturation and integration of adult-born neurons into the OB.

a. From stem cells to neuronal progenitors

The adult neural stem cells (NSCs) that produce neuronal precursors for the OB are located at the border of the lateral ventricle in the subventricular zone (SVZ) (***Figure 1.4, Insight 1***). These stem cells are derived from embryonic radial glial cells (Fuentealba et al., 2015; Furutachi et al., 2015; Redmond et al., 2019) and express astrocytic markers such as glial fibrillary acidic protein (GFAP) and brain-lipid binding proteins (Codega et al., 2014; Fuentealba et al., 2015). NSCs exist in either a quiescent or proliferative state (Codega et al., 2014). Once activated, $GFAP^+$ B1 cells express the epidermal growth factor receptor (EGFR) and give rise to rapidly dividing progenitors (type C cells) (Codega et al., 2014; Fuentealba et al., 2015; Obernier and Alvarez-Buylla, 2019). These cells in turn divide to generate migrating neuroblasts (***Figure 1.4, Insight 1***). Cells that express both GFAP and EGFR (or proliferative markers such as proliferating cell nuclear antigen (PCNA) and Ki67) are activated B1 stem cells (Codega et al., 2014; Pastrana et al., 2009). On the other hand, $GFAP^+$ cells that do not express EGFR and proliferative markers may be either quiescent stem cells or SVZ niche astrocytes. These two populations can be further distinguished by the expression of prominin, which is present on the primary cilia of NSCs and ependymal cells, but not niche astrocytes (Beckervordersandforth et al., 2010; Codega et al., 2014; Mirzadeh et al., 2008). It is currently thought that some of embryonic radial glia enters a long quiescent state until their re-activation in adulthood (Fuentealba et al., 2015; Furutachi et al., 2015). Adult NSCs are located in a specialized microenvironment and encounter multiple inter-cellular interactions and myriads of molecular factors derived from blood vessels, cerebrospinal fluid, niche astrocytes, neuroblasts, and other cells in the SVZ (Gengatharan et al., 2016; Obernier and Alvarez-Buylla, 2019). Adult NSCs have to decode and integrate all these microenvironmental factors to either remain in a quiescent state or become activated to generate neurons and glia. Once activated, adult NSCs undergo self-renewing or differentiating divisions that either lead to the expansion and maintenance of the NSC pool or to the production of rapidly dividing transient amplifying C-type cells (Obernier et al., 2018). C-type cells in turn generate neuroblasts (Alvarez-Buylla and Garcia-Verdugo, 2002; Doetsch et al., 1999; Luskin,

1993) that migrate long distances toward the OB (Gengatharan et al., 2016; Saghatelyan, 2009).

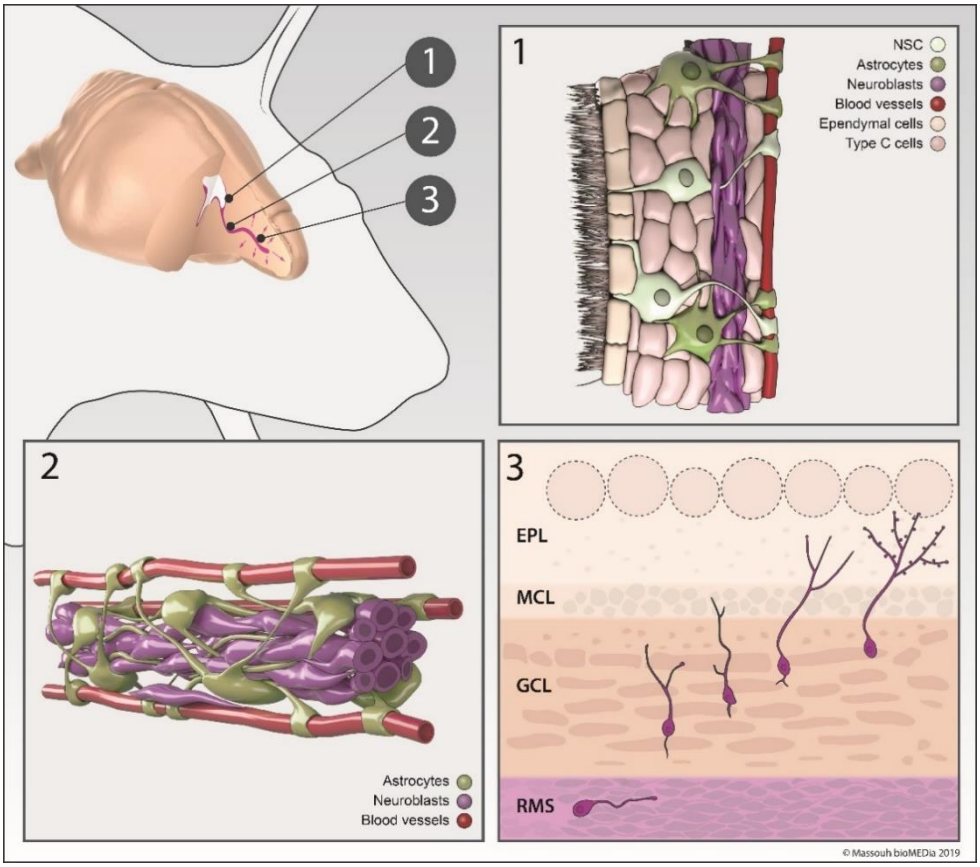

Figure 1.4: Adult neurogenesis in the olfactory bulb

A scheme of the adult mouse forebrain showing the different steps of adult neurogenesis, from the subventricular zone (SVZ) to the olfactory bulb (OB). **Insight 1**: Cellular organization of the SVZ: Type B cells are neural stem cells (NSCs). Once activated, these NSCs either self-renew or give rise to transient amplifying C-type cells, which in turn generate neuroblasts. **Insight 2:** Migration in the rostral migratory stream (RMS). Once neuroblasts enter the RMS, they migrate tangentially in chains along blood vessels and inside astrocytic tunnels. **Insight 3:** Differentiation and maturation of adult-born neurons in the OB. In the case of GCs, immature neurons go through five developmental stages. Neuroblasts first finish migrating tangentially in the RMS-OB (class 1 cells) and then migrate radially in the OB to reach their final location in the GCL where they become class 2 cells. In the GCL, immature GCs (class 3 cells) start extending their primary dendrites toward the EPL. Their dendritic arborization will later complexify and form spineless secondary dendrites in the EPL (class 4 cells). Lastly, type 5 GCs form spines and fully integrate the OB network, forming synapses with principal cells. *Source: Massouh bioMEDia*.

b. Neuroblasts migration in the adult brain

To reach the OB, neuroblasts follow the RMS, a long and intricate migratory pathway (***Figure 1.4, Insight 2***). The neuroblasts first migrate tangentially along the RMS and, once in the OB, turn to migrate radially and individually out of the RMS into the GCL and GL. In the adult RMS, neuroblasts travel in chains unsheathed by astrocytic processes (Kaneko et al., 2010; Lois and Alvarez-Buylla, 1994), and their migration is under the control of various signaling molecules, including those derived from astrocytes (Gengatharan et al., 2016). Cellular interactions between neuroblasts and blood vessels are also required for faithful migration toward the OB. Neuronal precursors use blood vessels that topographically outline the RMS for their migration (Snapyan et al., 2009; Whitman et al., 2009). Furthermore, endothelial cells release trophic factors that foster neuronal migration (Snapyan et al., 2009), indicating that blood vessels provide not only a physical scaffold but also molecular cues required for neuroblast migration. In addition to factors derived from astrocytes and endothelial cells, factors released by neuroblasts themselves affect their own migration. For example, the autocrine action of GABA on neuronal migration through $GABA_A$ receptors on neuroblasts has been documented (Bolteus and Bordey, 2004; Platel et al., 2008; Snapyan et al., 2009). Some 30,000 to 40,000 neuroblasts arrive in the OB every day (Petreanu and Alvarez-Buylla, 2002). This massive and unique migration of neuronal precursors in the adult brain is under the tight control of several molecular signals (Gengatharan et al., 2016; Kaneko et al., 2017).

c. Becoming a functional neuron in a pre-existing network

The vast majority of neuroblasts (approximately 90%) in the OB become GCs that mostly populate the deep layer of the GCL (Imayoshi et al., 2008), whereas the remaining immature neurons differentiate into PGs (Winner et al., 2002). Approximately four weeks are required from the moment immature neuronal precursors are generated in the SVZ to the full morpho-functional maturation of adult-born neurons in the OB (Carleton et al., 2003; Petreanu and Alvarez-Buylla, 2002). As they mature through the development periods, adult-born neurons undergo increasingly complex changes in their morphology, functions, and

channel/receptor repertoires. Five developmental classes (***Figure 1.4, Insight 3***) have been described for GCs (Carleton et al., 2003; Petreanu and Alvarez-Buylla, 2002). Class 1 cells correspond to neuroblasts that migrate tangentially in the RMS-OB. Class 2 cells correspond to neuroblasts that migrate radially in the OB toward their final destination in the GCL. Once installed in the GCL, immature class 3 GCs start to extend their primary dendrite toward the EPL, with no contacts with MCs. At the end of the second week, adult-born GCs undergo the final maturational steps. They first extend and complexify their dendritic arborization to form spineless secondary dendrites in the EPL (class 4 cells) and ultimately, after a process of spinogenesis, fully integrate the bulbar circuitry and form synapses with MCs as class 5 GCs (Carleton et al., 2003; Petreanu and Alvarez-Buylla, 2002).

From a functional point of view, adult-born neuroblasts express both AMPA and GABA receptors and start to receive spontaneous synaptic inputs at early stages of their maturation, that is, shortly after completion of the migration phase (Carleton et al., 2003). They first receive excitatory glutamatergic and inhibitory GABAergic inputs on their soma and proximal part of their apical dendrites (Kelsch et al., 2008; Panzanelli et al., 2009; Whitman and Greer, 2007) (***Figure 1.5***). Driven partly by these synaptic inputs, adult-born neurons mature and extend their dendrites from the GCL to the EPL, which is followed by the formation of axo-dendritic inputs impinging on their basal dendrites and dendro-dendritic inputs on their secondary dendrites. The end of GC synaptic maturation is marked by the establishment of the major output synapses that GCs establish in the OB, that is, the dendro-dendritic inhibitory synapses with MCs/TCs (Kelsch et al., 2008) (***Figure 1.5***). This sequential acquisition of input and output synapses differentiates adult-born cells from early-born ones, with early-born cells acquiring outputs and inputs simultaneously (Kelsch et al., 2008) (***Figure 1.5***). Another particularity of adult-born GC maturation is delayed action potential (AP) firing (Carleton et al., 2003) which may allow adult-born GCs to silently integrate into the bulbar network, without disturbing it by “uncontrolled” neurotransmitter release (Lledo et al., 2004).

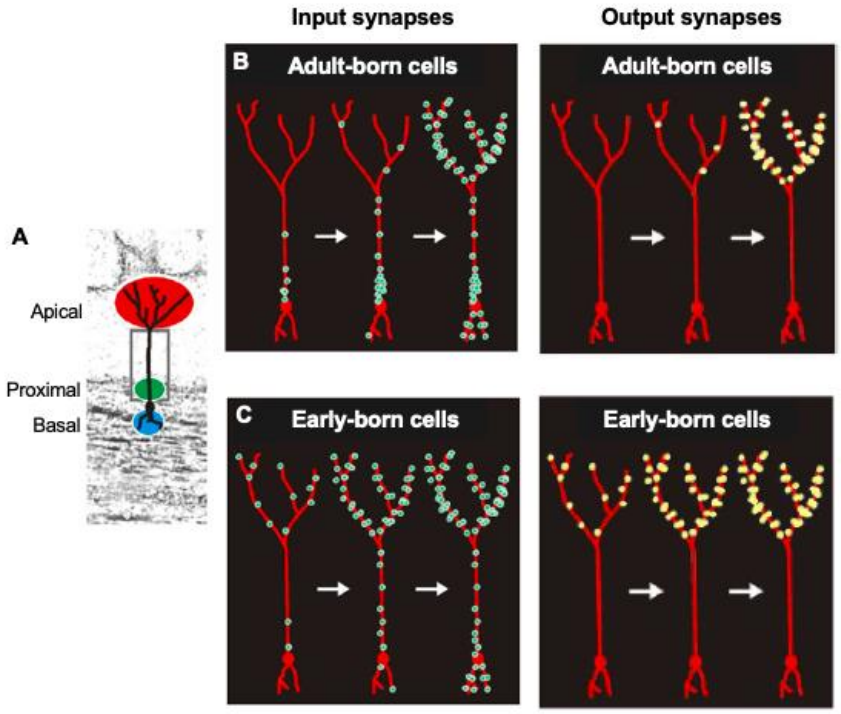

Figure 1.5: Synaptic development on adult- and early-born GCs.

A. Schematic of the dendritic domains of a GC, showing the basal (blue), proximal (green) and apical (red) domains of the dendritic tree. **B.** Diagrams illustrating the developmental pattern of input (left diagram) and output (right diagram) synapses during maturation of adult-born GCs. **C.** Diagrams illustrating the developmental pattern of input (left diagram) and output (right diagram) synapses during maturation of early-born GCs. *Adapted from Kelsch et al., 2008.*

Unlike GCs, adult-born PGs fire APs, have fully developed voltage-gated sodium and potassium conductances at early stages of their maturation (Belluzzi et al., 2003), and reach their final location in the OB faster than the GCs despite the fact that they have to move over longer distances (Hack et al., 2005). Interestingly, *in vivo* two-photon imaging combined with sensory stimulation has shown that while adult-born PGs are still migrating in the GL, approximately half have functional responses to odor stimulation that are undistinguishable from their early-born counterparts (Kovalchuk et al., 2015). The structuro-functional maturation and integration of PGs thus occurs very rapidly and concurrently in the GL.

B. Adult neurogenesis generates a specific subset of olfactory bulb interneurons

The odor environment is in constant flux and the OB has to adapt and reorganize its network to deal with these changes. Adult-born cells are constantly supplied to the bulbar network, which could facilitate the adaptive response of the bulbar network to changing environmental conditions. In the following paragraphs, I discuss the unique properties intrinsic to adult-born interneurons as well as the specific roles played by this particular population of cells in OB functioning and behavior.

a. Properties of adult-born neurons

Early-born and adult-born interneurons undergo different survival and targeting dynamics. It has been reported that early-born interneurons have longer lifetimes than their adult-born counterparts (Lemasson et al., 2005; Petreanu and Alvarez-Buylla, 2002). These two populations of GCs also colonize different parts of the GCL. GCs born during the first post-natal weeks are found mostly in the superficial GCL (Lemasson et al., 2005). On the contrary, a genetic ablation of adult-born GCs results in a loss of cells predominantly in the deep GCL, while the superficial GCL is spared (Imayoshi et al., 2008). Since no morphological differences between deep and superficial GCs have been observed, and since deep GCs may form synapses preferentially with MCs whereas superficial GCs tend to form synapses with TCs (Greer, 1987; Shepherd et al., 2007), it is conceivable that early-born GCs mainly regulate the synaptic activity of TCs whereas adult-born GCs regulate the activities of both MCs and TCs. Indeed, it has been shown that the ablation of neurogenesis using an antimitotic drug results in a 45% decrease in the inhibition received by MCs after 28 days (Breton-Provencher et al., 2009). The same decrease has also been observed following sensory deprivation (Saghatelyan et al., 2005). This marked effect of adult-born cells on the activity of principal cells is corroborated by the fact that adult-born cells display higher excitability than pre-existing neurons in the OB. Indeed, both fully mature adult-born GCs and PGs display larger sodium currents with steeper conductance-voltage relationships and more negative activation

voltages than early-born interneurons. This may result in greater excitability to incoming sensory inputs and thus greater recruitment for odor processing.

Adult-born neurons appear to play a major role in mediating the ability of the OB network to rapidly adapt to changes in the external olfactory environment. Indeed, an analysis of immediate early genes has revealed that adult-born neurons have stronger responses to novel odors than early-born interneurons, at least during the second week after their birth, a period known as their critical period (Belnoue et al., 2011; Magavi et al., 2005) (***Figure 1.6***). This critical period also coincides with the time window during which a process of long-term potentiation of excitatory inputs on the proximal dendrites of adult-born cells can be induced (Nissant et al., 2009). Similarly, *in vivo* two-photon targeted recordings of adult-born PGs at different developmental stages has revealed that their responsiveness increases after the start of their synaptic integration, even when they are still migrating in the GL (Livneh et al., 2014).

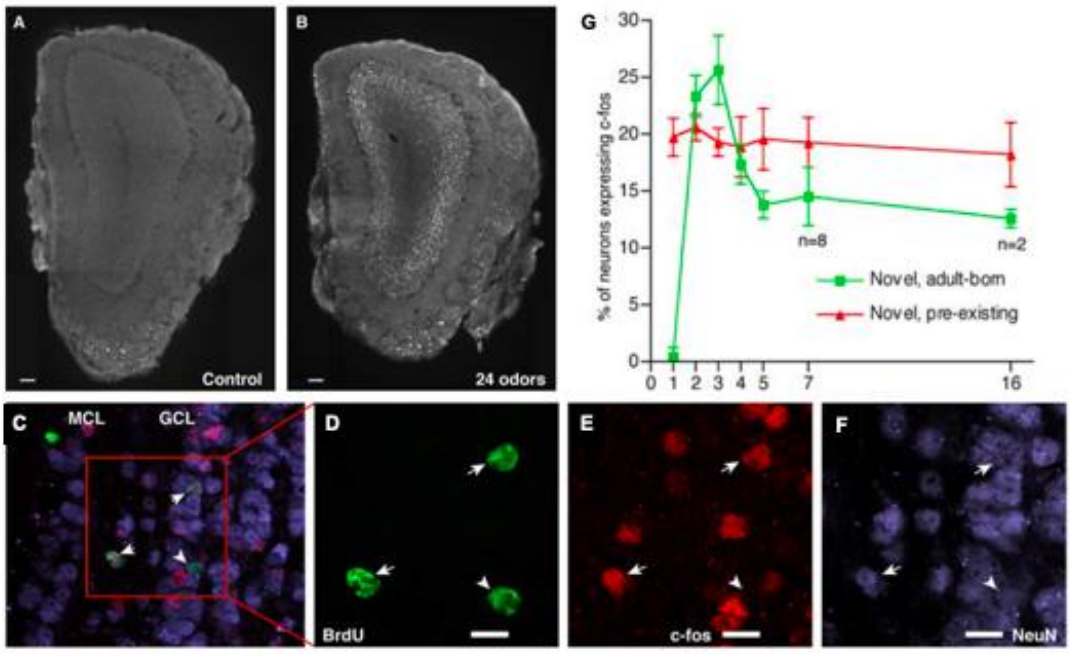

Figure 1.6: Adult-born neurons are more sensitive to novel odors

A. Mice receiving only clean, HEPA-filtered air have very few c-*fos*-positive (white) GCs. The specks in the ventral glomerular layer are autofluorescent fixation artifacts and are easily distinguished from genuine cellular labeling at higher magnification. **B.** Novel odor exposure dramatically increases the

number of c-*fos*-positive GCs, MCs, and PGs. **C-F.** Confocal imaging reveals that Bromo-desoxy-uridine (BrdU, green) adult-born cells in the GCL differentiate into mature NeuN-expressing neurons (blue) and express c-*fos* (red) in response to olfactory stimulation. The arrows indicate activated adult-born neurons. The arrowhead indicates an inactive adult-born neuron. Scale bar, 10µm. **G.** Adult-born neurons are most responsive soon after they synaptically integrate; as they mature, they become less responsive. Pre-existing granule neurons maintain a stable response. *Adapted from Magavi et al., 2005*.

OB interneurons remain plastic well beyond their final maturational stages. In fact, spine turnover, i.e., the addition of new spines and the elimination of pre-existing ones, remains at the level of the secondary dendrites of mature GCs for extended periods of time, even up to one year following the generation of the cells in the SVZ (Sailor et al., 2016). It has been estimated that approximately 20% of the spines on GCs, either pre-existing or adult-generated, are being continuously renewed (Sailor et al., 2016). However, although this constant synaptic turnover could be one of the mechanisms underlying OB adaptability and plasticity in response to environmental changes, synaptogenesis is a slow process and cannot cope with rapid changes in the odor environment. The bulbar network thus requires a fast adaptation process to rapidly respond and adjust to the changing olfactory environment. In line with this, a new phenomenon of structural plasticity in the OB has recently been described and involves the relocation of mature GC spines in an activity-dependent manner (***Figure 1.7***). Two-photon *in vitro* and *in vivo* experiments have revealed that adult-born GCs, in response to a stimulus, are able to extend a protrusion or spine head filopodia (SHF) from their spines and toward an activated principal cell (Breton-Provencher et al., 2016). SHFs are found almost exclusively on the spines of the secondary dendrites of adult-born neurons and are guided by MC odor-evoked activity. The protrusion of SHFs is followed by the relocation of the spine in the direction of the activated MC, an event that depends on the secretion of brain-derived neurotrophic factor (BDNF) by the principal cell (Breton-Provencher et al., 2016). Such rapid structural modifications, which have also been observed in other brain regions during the critical period (Majewska and Sur, 2003; Weinhard et al., 2018), may allow for rapid adaptive responses in the bulbar network to changing environmental conditions. Indeed, a modeling study has corroborated this notion by showing that as few as 3% of the spines relocating to activated MC dendrites may

allow the synchronization of MCs in response to a sensory stimulation (Breton-Provencher et al., 2016).

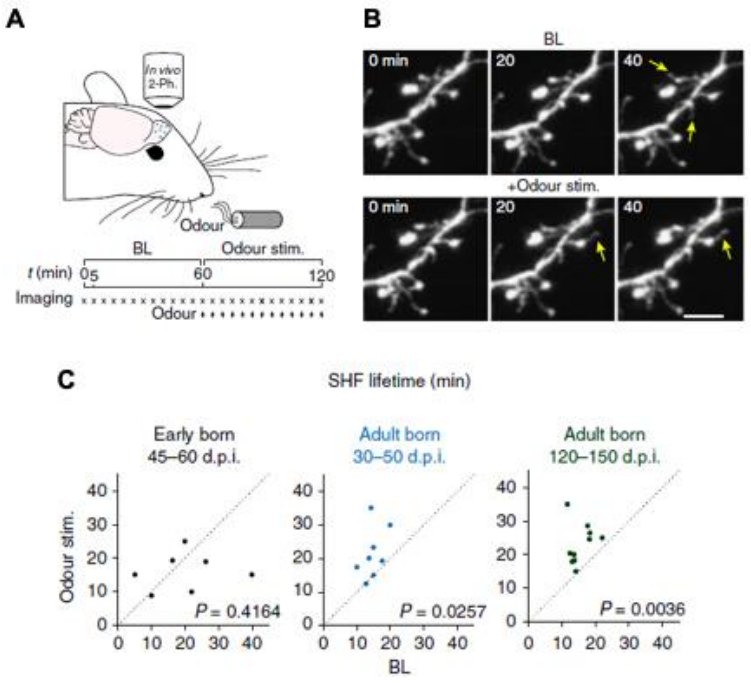

Figure 1.7: Plasticity of adult-born neuron spines is driven by sensory activity

A-B. Experimental procedure and time-lapse imaging during sensory stimulation *in vivo*. Scale bar, 5µm. **C**. Quantification of effects of sensory stimulation on the SHF lifetime *in vivo* for early-born GCs at 45–60 days post-injection (dpi). and adult-born GCs at 30–50 and 120–150 d.p.i. (n=7, 8 and 7 cells from 6, 6 and 4 mice, respectively). *Adapted from Breton-Provencher et al., 2016.*

b. Responses of adult-born cells to sensory stimulations

It is well now established that environmental factors, specifically sensory experiences, have a substantial impact on the fate of adult-born OB neurons (***Figure 1.8***). Exposure for an extended period of time to an enriched olfactory environment results in a noticeable increase in the survival and maturation of adult-born neurons (Moreno et al., 2009; Rochefort et al., 2002; Rochefort and Lledo, 2005). *In vivo* two-photon imaging of mature adult-born PGs and GCs has revealed that their synapses stabilize following odor enrichment (Livneh and Mizrahi, 2012) and that depriving animals of olfactory inputs negatively impacts the survival rate of immature adult-born OB interneurons, resulting in an overall decrease in the size of the deprived OB. This effect occurs more specifically at the moment of their synaptic integration

into the pre-existing bulbar network, i.e., the critical period of adult-born cells (Corotto et al., 1994; Petreanu and Alvarez-Buylla, 2002; Saghatelyan et al., 2005; Yamaguchi and Mori, 2005). These data are also corroborated by a recent *in vivo* imaging study suggesting that while most adult-born GCs survive in the OB following their arrival, sensory deprivation reduces the survival rate and maintenance of adult-born neurons (Platel et al., 2019).

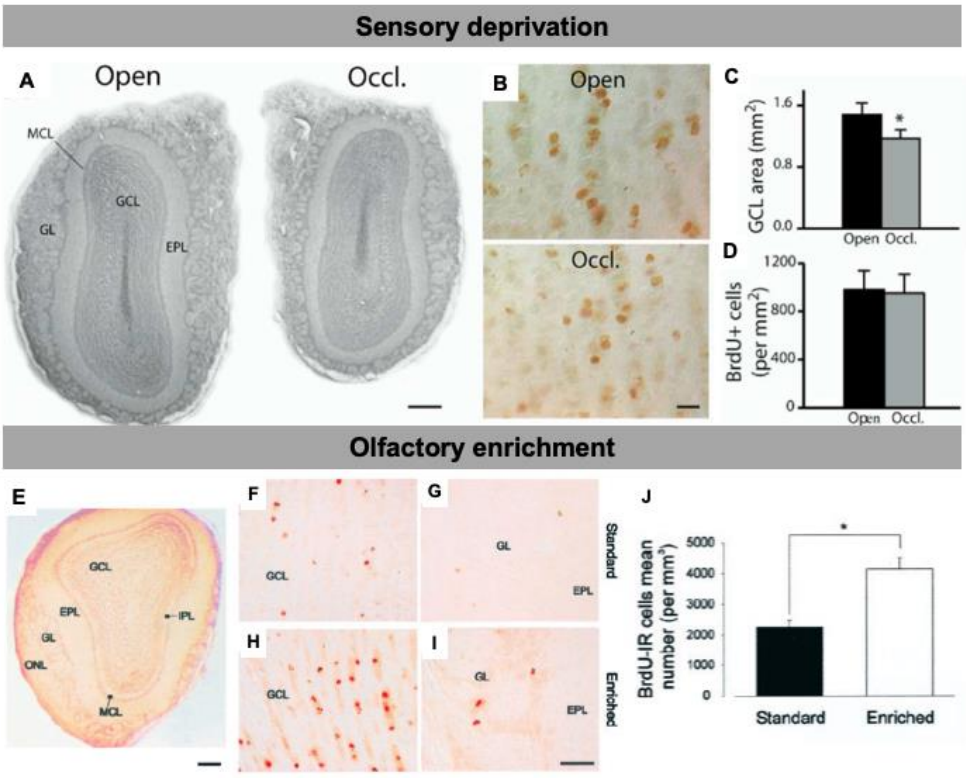

Figure 1.8: Adult-born neurons are sensitive to the level of olfactory activity

A. Photomicrographs of coronal sections displaying the different layers of the MOB. Note the size difference between the control (Open) and the occluded (Occl.) bulb sections of the same animal taken at the same rostrocaudal position. **B.** BrdU-positive cells in the granule cell layer of the control (Open) and odor-deprived (Occl.) bulbs. **C.** Decrease in the GCL area following odor deprivation. **D.** Density of BrdU-labeled cells in the control and odor-deprived bulbs. BrdU counting was performed 21 days following BrdU injections and 33 days following unilateral nostril occlusion. *p < 0.05 with a Student's t test. **E.** Photomicrograph of a coronal section of the main olfactory bulb displaying the different layers. **F-I**. BrdU-IR cells in the GCL (**F,H**) and in the GL (**G,I**) of standard (**F,G**) and enriched (**H,I**) mice. **H**, Mean number of BrdU-IR cells per millimeters cubed. *p<0.05 with a Student's t test. Scale bars: **E**, 300 µm; **F-I**, 20 µm. IPL, internal plexiform layer. *Adapted from Saghatelyan et al., 2005 and Rochefort et al., 2002.*

Sensory deprivation also has an effect on the maturation of adult-born cells, resulting in a decrease in the spine density of their secondary dendrites and a decrease in overall dendritic length (Kelsch et al., 2008; Saghatelyan et al., 2005). Interestingly, despite such drastic morphological changes, adult-born GCs retain their functional role in the OB network by increasing their excitability, indicating that adult-born interneurons possess intrinsic adaptive plasticity mechanisms that respond to changing environmental conditions (Saghatelyan et al., 2005).

All the unique features provided by adult-born neurons to the OB network underscore their importance as well as their specific signature and contribution to olfactory processing. In fact, they are one of the ways the OB can adapt and respond to new incoming odorant inputs. Moreover, if one considers the populations of adult-born and early-born interneurons as physiologically independent cell populations, it is conceivable that adult-born neurons also contribute in unique way to different olfactory behaviors.

3. Functions of olfactory bulb interneurons in olfactory functioning and behavior

The process of adult neurogenesis remains a fascinating topic given that the brain was once considered as being unable to replenish its neuronal pool. Nevertheless, the reasons for and the role played by such a process in the OB remain to be fully elucidated. When it comes to odor behavior, it is possible to distinguish between odor-based behaviors that have a social relevance for the animals and behaviors involving neutral odorants in ambient air and that are divided into spontaneous and reward-associated behaviors. Below, I discuss the role of OB interneurons in these different types of olfactory behaviors.

A. Role of OB interneurons in socially relevant behaviors

Olfaction intervenes at the different steps of an animal's development, shaping the interactions or reactions that an individual has with its conspecifics and with predators. The involvement of bulbar adult neurogenesis in ethologically relevant odor behavior differs depending on the sex of the animal and the type of behavior.

In fact, the ablation of neurogenesis in mice using either an irradiation or a genetic strategy counteracts several innate behaviors, including male-male aggression, sexual behavior toward females, and recognition of predators (Feierstein et al., 2010; Sakamoto et al., 2011). Neurogenesis also increases in males that interact with their offspring during the postnatal period. This increase is required for paternal recognition once the offspring reaches adulthood (Mak and Weiss, 2010).

The link between adult neurogenesis in the SVZ and social behavior has been more extensively studied in females, more specifically in the context of pregnancy and maternal behavior. Pregnancy per se has been reported to have different effects on adult neurogenesis, including a prolactin-mediated increase in SVZ proliferation during gestation in rodents (Larsen and Grattan, 2010; Shingo et al., 2003; Wang et al., 2013) and a downregulation of neurogenesis in parturient ewes compared to non-pregnant ewes (Brus et al., 2014). Another study reported a more specific effect on the dendritic arborization of adult-born cells (Belnoue et al., 2016), indicating that these cells may contribute to the OB network and olfactory processing. In line with this, *in vivo* recordings of neurons generated during the pregnancy of lactating mice revealed enhanced synaptic integration reflected by the stabilization of their spines compared to naïve subjects (Kopel et al., 2012). Moreover, pregnancy appears to increase the specificity of adult-born cells toward certain types of odorants (Vinograd et al., 2017). Motherhood also increases the inhibitory drive of interneurons onto MCs, which respond more strongly to behaviorally relevant odors and more sparsely to neutral odors (Vinograd et al., 2017).

Several studies have also tried to link adult neurogenesis in the OB to the establishment of maternal behavior. In mother ewes, interactions with lambs result in an increased activation of adult-born neurons in the GCL, an effect that is specific to lamb-related odorants (Corona et al., 2017). It has also been shown that the ablation of neurogenesis using a genetic approach (Sakamoto et al., 2011) or the reduction of the pregnancy-induced increase in neurogenesis using bromocriptine, a prolactin secretion suppressor, affects maternal interactions with their offspring (Larsen and Grattan, 2010). In contrast, focal irradiation of the SVZ spares the

establishment of normal maternal behavior in treated females and does not affect maternal discrimination of their own pups from strange pups (Feierstein et al., 2010). Maternal recognition is, however, altered in gestationally stressed mothers in which the beneficial effect of motherhood on the dendritic arborization of adult-born GCs is counteracted (Belnoue et al., 2016). Hence, all the results presented above highlight the importance of OB adult neurogenesis in socially relevant behaviors.

B. Role of OB interneurons in spontaneous odor-behavior

Spontaneous odor behaviors are based on the motivation of the animals to perform the task. The time spent exploring is recorded, which gives an indication as to whether the animal performed the task correctly or not. The involvement of adult-born neurons in spontaneous odor behavior tasks such as the odor detection threshold, habituation/dishabituation odor discrimination, short-term odor memory, and perceptual learning has been investigated. The odor detection threshold corresponds to the minimal concentration at which an animal is able to detect the presence of an odorant and is reflected by an increase in exploration time. Habituation/dishabituation odor discrimination is based on the successive exposure of the animal to the same odorant (habituation phase), which is reflected by a decrease in the exploration time of the odorant in successive sessions. During the second phase of the test, a novel odor (dishabituation odor), which is different from the habituation odor, is introduced, leading to an increase in exploration time and thus discrimination between the two odorants. Different versions of this task exist, depending on the molecular similarity of the habituation and dishabituation odors. The use of chemically similar odorants increases the difficulty of the task. In the short-term olfactory memory task, the animals are exposed twice to the same odorant separated by various time intervals ranging from several minutes to several hours. Once again, a decrease in exploration time during the second presentation of the odor attests to the animal's memory of the odor. For the perceptual learning task, the animals are first submitted to a habituation/dishabituation task using very similar odorants that animals are naturally unable to discriminate. Following a 10-day period

of olfactory enrichment with these two odorants, the animals are resubmitted to the discrimination task and are now able to complete it.

Many studies have addressed the role(s) of adult-born neurons in olfactory behavior but have given conflicting results. The approaches used to modulate the levels of adult-born cells arriving in the OB, the behavioral tests used, and heterogeneous adult-born populations, with each subtype playing a distinct role in an odor behavioral task, may explain the discrepancies (see below). Olfactory enrichment, a process known to enhance the survival of adult-born cells in the OB (Moreno et al., 2009; Rochefort et al., 2002; Rochefort and Lledo, 2005) also has a positive effect on the discrimination ability of rodents that were unable to discriminate between two enantiomers prior to enrichment (Mandairon et al., 2006c; Mandairon et al., 2006d; Moreno et al., 2012; Moreno et al., 2009). This effect on discrimination ability can be counteracted when an anti-mitotic drug is infused during olfactory enrichment (Moreno et al., 2009). Discrimination is also affected in transgenic animals in which the migration of neuroblasts is affected by a deficiency in neural cell adhesion molecule (NCAM) or variant brain-derived neurotrophic factor (Val66Met) (Bath et al., 2008; Gheusi et al., 2000). It should be noted, however, that constitutive gene knock-out and knock-in may affect the development and function of the olfactory system and may lead indirectly to changes in odor behavior. Similarly, olfactory enrichment may also affect sensory neuron turnover and plasticity in the OB (Jones et al., 2008; Watt et al., 2004). When the generation of adult-born neurons is ablated using β-D-arabinofuranoside (AraC), an anti-mitotic drug, no changes in spontaneous odor discrimination are observed (Breton-Provencher et al., 2009). These results show that different approaches for modulating neurogenesis can have different impacts on behavioral outcomes. Furthermore, the use of similar or dissimilar odorants in the discrimination task may also impact the behavioral results since adult-born neurons may be involved in more complex odor discrimination tasks.

Olfactory enrichment is also beneficial for short-term odor memory. Enriched animals displaying increased survival of adult-born neurons are able to recall previously encountered odorants for much longer periods than non-enriched mice

(Rochefort et al., 2002). In line with this, the ablation of adult neurogenesis by AraC infusion impairs short-term odor memory (Breton-Provencher et al., 2009) while the genetic ablation of β2-containing nicotinic acetylcholine receptors, which increases the survival of adult-born cells, improves short-term odor memory (Mechawar et al., 2004).

C. Role of OB interneurons in associative odor-behavior

The role of adult-born neurons in odor-reward conditioning tasks has also been extensively studied. Among those, it is possible to distinguish between non-operant and operant conditioning tasks (***Figure 1.9***). In long-term associative odor memory tasks, a form of non-operant conditioning tasks, partially food-deprived animals are trained for 4 days to discriminate between two odorants presented independently and hidden under clean bedding (Mandairon et al., 2011) (***Figure 1.9***) . A day of training is composed of a session of 4 randomized trials during which one of the two odors is associated with a sugar reward and presented for 2 trials. During the 2 remaining trials, the second odorant is presented alone, without any reward. During the test day, which can be 24 h or several days after the training day, both odorants are presented simultaneously but without a sugar reward. The time spent digging above each odorant is recorded, and if the animals are able to discriminate an odor previously associated with a sugar reward, they dig for a much longer time.

The pharmacological (AraC) or genetic ablation of adult neurogenesis has no effect on long-term associative memory tasks (Breton-Provencher et al., 2009; Imayoshi et al., 2008). Similarly, the suppression of programmed cell death in BAX knock-out mice has no effect on the taste aversion paradigm (Kim et al., 2007). However, it has been also reported that the modulation of neurogenesis has an impact on long-term associative memory (Lazarini et al., 2009; Sultan et al., 2010). It should be noted, however, that Sultan et al. (2010) studied the role of adult-born neurons in long-term memory retention and not in memory acquisition (Sultan et al., 2010). Similar results have been obtained in odor-cued fear conditioning following focal SVZ irradiation (Valley et al., 2009). These findings were further corroborated by another study that took advantage of the tag-and-ablate genetic strategy. Following a treatment with tamoxifen, this model makes it possible to “tag” a large

proportion of Nestin-expressing cells as well as their progeny with the diphtheria toxin receptor. Following a second treatment, this time with diphtheria toxin, the previously tagged population is ablated. This model makes it possible to ablate neurogenesis during specific memory formation phases and has been used to show that adult-born cells are involved in the completion of reward-associated non-operant tasks (Arruda-Carvalho et al., 2014).

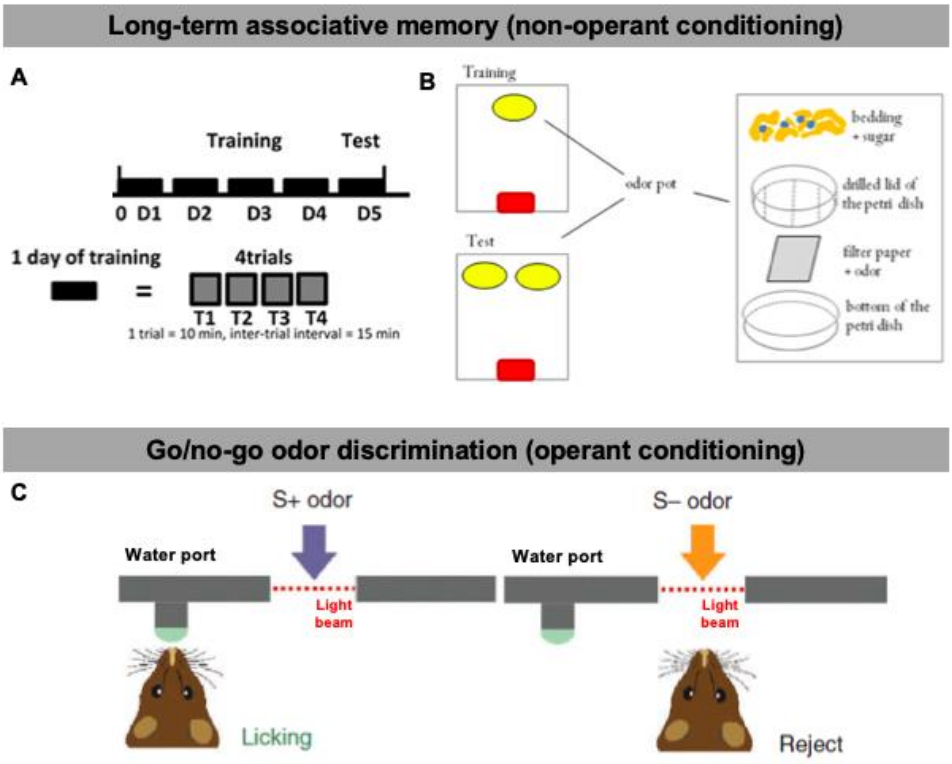

Figure 1.9: The two forms of odor-reward conditioning tasks

A. Experimental procedure for the long-term associative memory task. **B.** Experimental apparatus used for long-term associative memory non-operant conditioning. **C.** Experimental procedure for the go/no-go odor discrimination task. *Adapted from Alonso et al., 2012 and Mandairon et al., 2011.*

During operant conditioning tasks such as go/no-go tasks, partially water-deprived mice have to learn a specific behavior to be able to perform the task (***Figure 1.9***). They learn to self-initiate the task by breaking a light beam while putting their snout into an odor delivery port and licking a water port in response to a certain odorant (the S^+ reinforced stimulus) to receive a water reward. In the meantime, they also learn to retract their snout or not lick the water port in response to another

odorant (the S^- non-reinforced stimulus). Depending on the similarity of the two odorants, the task, and the time taken by the animals to complete it, the test is considered to be more or less difficult and, as such, fine or coarse discrimination can be tested. Operant go/no-go odor discrimination tasks are now widely used to study olfactory processing in the OB and the role played by adult-born neurons in such processing. This relies mostly on the versatility of the test, the resolution in terms of the odor concentrations used for the test, and its adaptability in terms of the difficulty of the task (similar versus dissimilar odorants). The role of adult-born interneurons in the completion and learning of an operant conditioning task has been extensively investigated. Optogenetic activation of GCs in general (i.e., early- and adult-born GCs) and the resulting increase in the inhibitory drive received by principal cells enhance pattern discrimination and accelerate the learning of a discrimination task (Gschwend et al., 2015). On the contrary, a reduction in the inhibition received by MCs through the pharmacogenetic inhibition of GCs decreases pattern separation and disrupts odor discrimination learning (Gschwend et al., 2015). The same type of approach has been used to investigate the role of adult-born interneurons in associative odor learning. The optogenetic activation of $ChR2^+$ adult-born GCs is sufficient to speed up learning in a go/no-go odor discrimination task. However, this effect is observed only when the task involves very similar odorants, suggesting that adult-born neurons play a role in fine odor discrimination (Alonso et al., 2012; Grelat et al., 2018).

4. The heterogeneity of olfactory bulb interneurons: different cells for different functions

Studies which aimed at elucidating the role of adult-born neurons in olfactory behavior have, for a long time, considered these interneurons as a homogenous population of cells. It is conceivable, however, that OB interneurons and, by extension, adult-born interneurons are not as homogeneous as they appear. In line with this, several fate mapping studies have shown that the pool of stem cells in the SVZ is composed of a heterogeneous population and that both early-born and adult-born OB interneurons have distinct temporal origins (Batista-Brito et al., 2008) and

are derived in specific regions along the SVZ and RMS (Merkle et al., 2007). In the following paragraph, I will review recent results with regard to the heterogeneity of OB interneurons and the possible role that each subtype plays in OB network functioning and odor behavior.

A. The heterogeneity of periglomerular cells

Several subtypes of PGs have been described based on their morphology and their expression of non-overlapping histochemical markers (***Figure 1.10***). These include dopamine synthesis enzyme tyrosine hydroxylase-(TH) and calcium-related proteins calretinin$^+$ (CR) and calbindin$^+$ (CB) PGs (Batista-Brito et al., 2008; Kosaka and Kosaka, 2005). The temporal expression and turnover of these PGs varies throughout their lifetimes, each having its own temporal production signature. In fact, CR$^+$ PGs are mainly produced during adulthood while CB$^+$ PGs are mainly produced during the early postnatal period and see their production decreasing with age (Batista-Brito et al., 2008; De Marchis et al., 2007). The temporal profile of TH$^+$ cells is, however, less clear. While genetic fate mapping has indicated that most dopaminergic PGs are produced late during embryonic development (Batista-Brito et al., 2008), another study using fluorogold labelling of the SVZ and homo/heterochronic transplantation has indicated that most TH$^+$ cells are produced during adulthood (De Marchis et al., 2007).

To date, few studies have investigated the roles of PG subtypes. *In vivo* two-photon imaging experiments on adult-born PGs have shown that they maintain high synaptic dynamics long after integration (Mizrahi, 2007). A combination of *in vivo* Ca^{2+} imaging and electrophysiological recordings has revealed that adult-born PGs are sensitive to olfactory stimulation less than 48 h after their arrival in the GL. Moreover, in the second week after their birth, the odor-evoked Ca^{2+} transients, odor sensitivity, and odor-evoked action potentials (APs) of adult-born PGs resemble those of resident PGs (Kovalchuk et al., 2015).

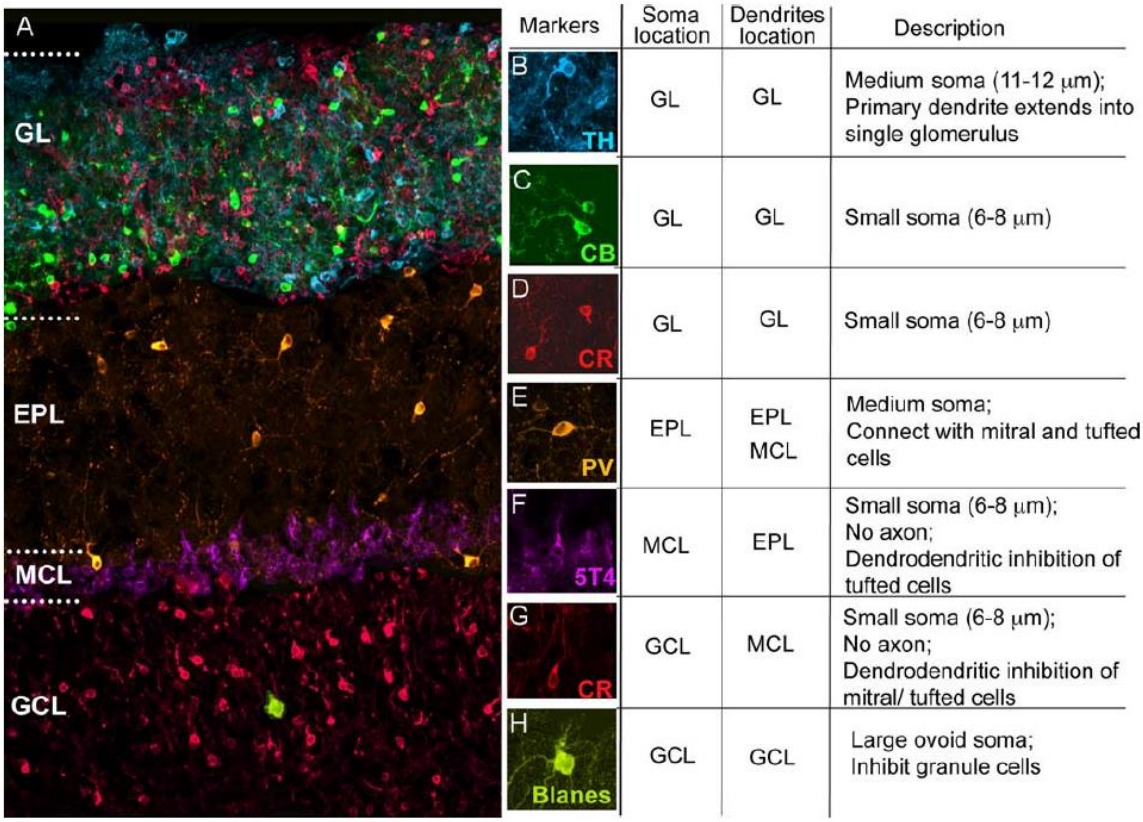

Figure 1.10: Olfactory bulb interneurons diversity

Seven OB interneuron populations based on their position and expression of immunomarkers are distinguishable. **A.** Example section of mouse olfactory bulb. **B.** TH-expressing GL cell (blue). **C.** CB-expressing GL cell (green). **D.** CR-expressing GL cell (red). **E.** Parvalbumin- (PV) expressing EPL cell (orange). **F.** 5T4-expressing MCL granule cell (purple). **G.** CR-expressing GCL granule cell (red). **H.** CB-positive Blanes cell in GCL (green). *Adapted from Batista-Brito et al., 2008.*

PGs can be generally divided into two subtypes: type 1 GABAergic PGs, which receive direct inputs from olfactory nerve terminals, and type 2 GABAergic PGs, which do not receive inputs from the olfactory nerve but are indirectly activated by the dendro-dendritic synapses of principal cells (Kosaka and Kosaka, 2007). The chemical make-ups of these two types of PGs have also been described, and immunohistochemical labelling has revealed that CB^+ and CR^+ cells are type 2 PGs, whereas TH^+ cells are type 1 PGs that receive direct inputs from the olfactory nerve (Kosaka et al., 1995; Kosaka and Kosaka, 2007). It thus appears that TH^+ PGs may be the PG subtype that is most sensitive to the level of olfactory activity. In fact, it is well established that TH immunoreactivity and, as such, its expression markedly decreases following sensory deprivation (Baker et al., 1993; Bastien-Dionne et al.,

2010). The influence of sensory activity on TH levels has also been studied in the context of social olfaction. Shortly after mating, a surge in TH expression occurs in PGs, resulting in increased dopaminergic transmission in the OB and impairment of social odor discrimination by female animals. This increase in dopaminergic activity is required to prevent interruptions of pregnancy shortly after mating in the presence of male urine odors (Serguera et al., 2008). However, the roles of TH^+, CR^+, and CB^+ adult-born interneurons in different odor behavior tasks remain unclear. Further studies are needed to better understand the specific contributions of individual PG subtypes to olfactory bulb functioning and odor behavior.

B. The heterogeneity of granule cells

GCs are the most abundant neuronal population in the OB. *In vivo* two-photon imaging experiments have shown that the odor-evoked Ca^{2+} responses of GCs are spatially and temporally heterogeneous (Wienisch and Murthy, 2016). The heterogeneity of the functional responses of GCs to odor stimulations is likely due to their different molecular signatures and distinct wiring in the OB network (***Figure 1.10***).

CR, Ca^{2+}/calmodulin-dependent protein kinase IIα (CaMKIIα) and IV (CaMKIV), metabotropic glutamate receptor 2 (mGluR2), Cytoplasmic polyadenylation element-binding protein 4 (CPEB4) and oncofetal trophoblast glycoprotein 5T4 GCs have already been identified (Baker et al., 2001; Batista-Brito et al., 2008; Imamura et al., 2006; Jacobowitz and Winsky, 1991; Merkle et al., 2014; Murata et al., 2011; Tseng et al., 2017; Tseng et al., 2019; Zou et al., 2002). These subtypes differ in terms of their location in the GCL, their activation by different odor behavioral tasks, and their roles in the OB network (Baker et al., 2001; Batista-Brito et al., 2008; Imamura et al., 2006; Jacobowitz and Winsky, 1991; Merkle et al., 2014; Murata et al., 2011; Takahashi et al., 2016; Yoshihara et al., 2012; Zou et al., 2002). Of these GC subtypes, CR^+, $5T4^+$ and, to a lesser extent, $mGluR2^+$ cells are renewed during adulthood (Batista-Brito et al., 2008; Merkle et al., 2014; Murata et al., 2011).

CPEB4 is an RNA-binding protein that was shown to be highly expressed in both early-born and adult-born GCs, but its level of expression decreases with OB growth (Tseng et al., 2017; Tseng et al., 2019). Knocking-out the protein in neonatal GCs leads to a reduction in OB size and volume as well as a reduction in the expression of the activity marker cFos, while sparing the process of adult neurogenesis (Tseng et al., 2017). However, reduction in CPEB4 expression has behavioral outcomes. In fact, odor discrimination abilities of mice are altered when this protein is ablated specifically in early-born interneurons, an effect that fails to be compensated by the arrival of adult-born GCs when animal were tested at a later time point (Tseng et al., 2019).

The involvement of the $5T4^+$ GC subtype in olfactory processing and behavior has also been investigated. While the generation of $5T4^+$ cells in the MCL does not change over time (Batista-Brito et al., 2008), sensory activity is important for the maintenance of this subtype of GC. In fact, sensory deprivation results in a decrease in 5T4 expression and in the number of $5T4^+$ cells in the odor-deprived OB (Imamura et al., 2006; Yoshihara et al., 2012). A recent study has also revealed that the depletion of $5T4^+$cells in the OB following 5T4 knockout or knockdown results in an increased odor detection threshold of both neutral and fear-inducing odorants. Performances are also altered in an associative odor discrimination task following the depletion of $5T4^+$ cells (Takahashi et al., 2016).

Other subtypes of GCs have also been identified, but their functional roles are unknown. Notably, four additional subtypes of adult-born GCs have been described based on their morphologies and locations in the GCL (Merkle et al., 2014) (***Figure 1.11***). Type 1 deep-branching GCs display an arborization that generally does not extend beyond the internal plexiform layer and that branches primarily in the GCL. The cell bodies of Type 2 shrub GCs are located in the MCL. These GCs lack basal dendrites and extend a single primary dendrite deep into the EPL that branches extensively with small and spiny secondary dendrites. The cell bodies of type 3 perimitral GCs are confined to the MCL and present multiple thin and mostly spineless processes branching above and below the MCL. Lastly, the cell bodies of

type 4 satellite cells are located in the EPL. Type 4 cells often project radial processes with varicosities but few spines.

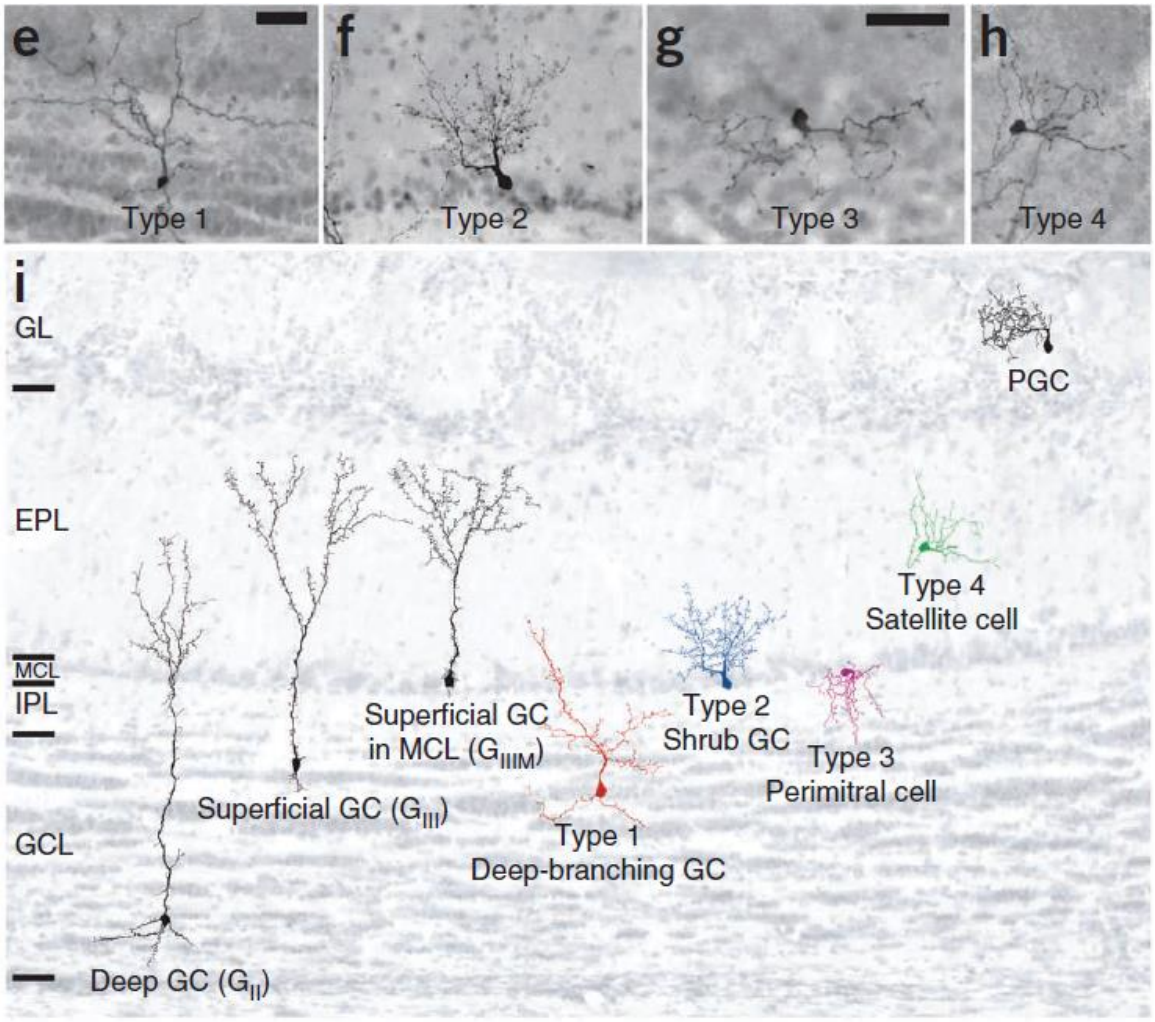

Figure 1.11: The 4 types of adult-born GCs, based on morphological and GCL location characterization

(**A-D**) The 4 types of adult-generated GCs, stained here by diaminobenzidine (DAB). (**E**) Diagram showing camera lucida traces of previously known adult-born OB interneuron types (black) and newly identified cell types (red, blue, magenta, green) superimposed on a photomicrograph of a hematoxylin-stained OB to show their relative positions. Cells are shown to scale, and the pial surface is up. Scale bars represent 25µm for **A-D**. *Adapted from Merkle et al., 2014.*

The findings presented above shed some light on the roles played by the different subpopulations of early-born and adult-born GCs and indicate that each subtype makes a specific contribution to the functioning of the OB network and to odor behavior. My own work contributed to the elucidation of the role played by

different GCs subtypes in the odor behavior, by focusing on CaMKIIα+, CaMKIIα- and CR+ GCs. These data will be discussed in Chapters 1 and 2. However, other subtypes may still be identified, which will add another level of complexity to understanding odor information processing in the OB. It is also conceivable that GCs might express not only one but several markers, which would refine their specific and unique involvement in the network.

C. Another level of heterogeneity: the differential wiring of olfactory bulb interneurons

As discussed above, the population of OB interneurons can be described as a heterogeneous cell population, expressing several neurochemical markers, and each subpopulation potentially contributes in a unique way to OB network functioning. However, it is noteworthy that OB activity is also refined by the inputs sent by other brain regions towards this region. Therefore, it is also conceivable that different assembly of cells in the OB may exist in terms of the inputs that they receive from these other brain regions.

a. Methods for mapping brain connections in vivo

Decades ago, Ramon y Cajal in his precursor work already took advantage of a labelling method to determine the projections of brain structures towards others. In fact, using the silver-based Golgi staining, Cajal was able to visualize neurons in their entirety, therefore creating the first “connectivity maps” of the brain. Since then, tracing methods have evolved and nowadays, new useful viral tools regularly provides new insights towards brain structures connectivity (for review see (Nassi et al., 2015)) (***Figure 1.12***). A first and classical method to virally trace neuronal projection from a brain region to another is to use anterograde viral vectors allowing for the expression of a reporter, or to stimulate the afferents innervating a region of interest. These vectors, once injected in a region of interest, allow to visualize axonal connections made with other brain regions, the virus anterogradely propagating from the cell bodies to the terminals of infected neurons. This also allows, when coupled to an optogenetic approach, to investigate the functional or behavioral impact of synaptic inputs stimulation in different behavioral tasks. In a recent study, a new AAV

serotype was also designed, allowing this time, when injected in a particular region of interest, to retrogradely label neurons projecting to this region (Tervo et al., 2016). However, none of these techniques provide any information towards the neuronal subtypes on which these projections impinge on at the level of the labelled projections.

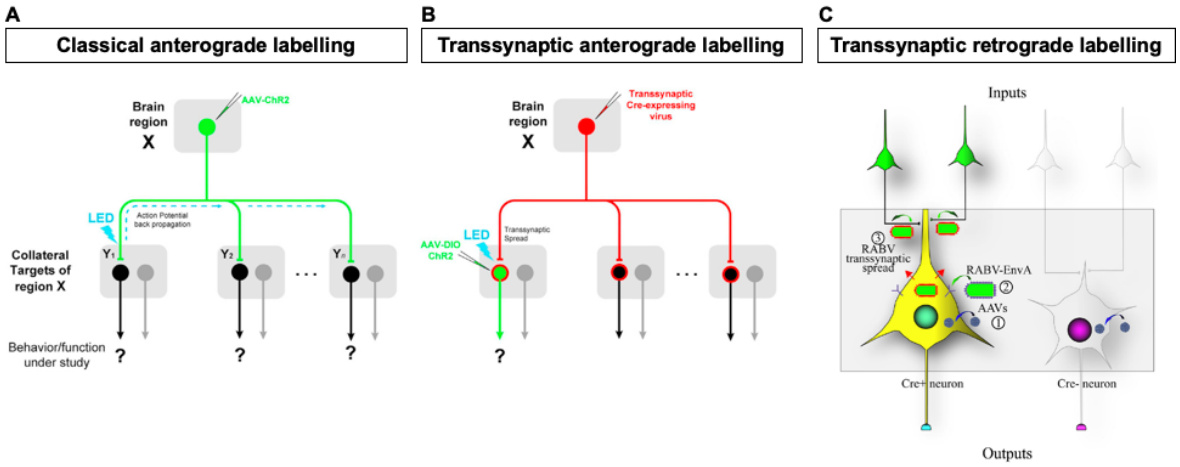

Figure 1.12: Example of strategies for brain connections mapping

A. A brain region ‘‘X’’ is known to mediate a behavior/function of interest. Neurons in X project to multiple target nuclei (‘‘Y’’). To map the relevant downstream circuit, conventional method relies on activation of ChR2-expressing X axon terminals in a given target nucleus. This may result in unwanted activation of collateral targets via antidromic stimulation (marked by dash lines). B. A virus capable of anterograde transsynaptic spread would allow direct activation of postsynaptic cells in a target region that specifically receive input from region X, by enabling Cre-dependent transgene expression (green) in a Y nucleus. C. Design of the rabies viruses (RABV). Expression of the avian tumor virus receptor A (TVA) dictates the types of cells that can be infected. *Adapted from Zingg et al., 2017 and Nassi et al., 2015*.

In the last few years, transsynaptic approaches were also described, allowing for a more precise identification of the neurons receiving inputs from a particular brain region in a region of interest (***Figure 1.12***). These methods can involve different types of viral vectors and act either as an anterograde or retrograde transsynaptic tracer of synaptic connections. Indeed recently it was discovered that some specific adeno-associated viruses serotypes (serotypes 1 and 9) are able to cross synapses, allowing for a anterograde transsynaptic expression of Cre recombinase (Zingg et al., 2017). With this approach, cells from a particular structure and expressing a cre-dependant gene, express this gene after recombination if

receiving synaptic inputs from the structure in which the transsynaptic AAV1 or AAV9 Cre virus was injected. In some cases, it is also of relevance to retrogradely label the presynaptic neurons impinging on a postsynaptic target. For this purpose, retrograde transsynaptic viral tracers were developed, taking for instance the ability of Rabies viruses to diffuse retrogradely (***Figure 1.12***). In this approach, starter cells will first be infected with an AAV allowing for a cre-dependant expression of the avian tumor virus receptor A (TVA). When later a pseudotyped rabies virus will be injected, only TVA-expressing cell will be infected, the rabies virus specifically expressing the EnvA extracellular domain that will target the TVA receptor. The rabies virus can then transsynaptically and retrogradely spread toward cell bodies of neurons (acceptor cells) directly contacting the TVA-expressing starter neuron. However, the use of rabies virus can present some disadvantages. In fact, they can induce a certain level of cytotoxicity, and the synaptic spreading could be in some cases not limited to a single synapse. However, to counteract these drawbacks, a new approach was lastly developed and allows for a non-toxin retrograde transsynaptic labelling, using recombinant AAV viruses combined to a previously described retrograde tracer (Reinert et al., 2019).

b. Towards a differential connectivity of OB interneurons

Although the output information sent by OB principal cells toward higher cortical regions is already largely refined mostly by interneurons' activity (Arevian et al., 2008; Gschwend et al., 2015; Urban, 2002; Yokoi et al., 1995), accumulating data revealed that the OB also receives top-down projections from higher cortical regions. This was confirmed by several tracing experiments that revealed and confirmed that the OB receives projections from several brain regions such as the piriform cortex (PC), the anterior olfactory nucleus (AON), the olfactory tubercle, horizontal limb of diagonal band of Broca (HDB), dorsal raphe nucleus but also the amygdala (Hintiryan et al., 2012; In 't Zandt et al., 2019; Padmanabhan et al., 2016; Wen et al., 2019).

When focusing on the projections impinging mostly in the GCL, data obtained and referenced in the Allen Brain website revealed that the GCL receives projections

from several regions such as the piriform area, the anterior amygdalar area, and the dorsal raphe nucleus, among others (***Figure 1.13***). The examples presented on ***Figure 1.13*** highlight the differential innervation of the granule cell layer, some regions projecting mostly to the deep GCL like the piriform area, while others on the contrary like the anterior amygdalar area projecting all over the GCL. This differential and topographical innervation of the GCL was also confirmed by other tracing studies that used either anterograde or retrograde tracers (Hintiryan et al., 2012; Niedworok et al., 2012; Padmanabhan et al., 2016). Interestingly, Hintiryan and colleagues revealed that the anterior part of the PC projects mainly to the superficial part of the GCL, whereas on the contrary the posterior part projects mostly to the deep GCL (Hintiryan et al., 2012). Considering the preferential location of adult-born GCs in the deeper layers of the GCL (Lemasson et al., 2005), it is conceivable that the posterior PC could send inputs preferentially towards adult-born GCs.

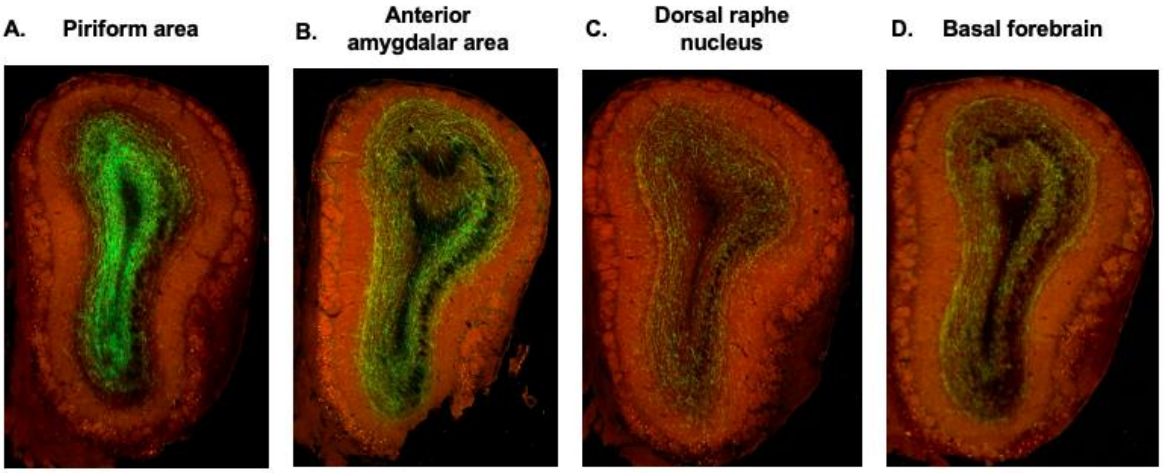

Figure 1.13: GCs receive inputs from different brain regions based on Allen Brain website.

A-D. Injections of an AAV-eGFP reporter in different target regions of the brain were performed in C57Bl/6 animals. eGFP labelling was then investigated at the level of the OB to determine whether it receives projections from the injected area. The pictures presented are examples showing that the olfactory bulb receives projections from the piriform area (**A**), the anterior amygdalar area (**B**), the dorsal raphe nucleus (**C**) and the basal forebrain (**D**). *Images were obtained from the Allen Brain website (http://portal.brain-map.org/).*

The functional implication of these projections on OB processing and behavior has also been investigated. In fact, the OB receives vast centrifugal inputs that result in an important noradrenergic, serotoninergic, GABAergic but also cholinergic

modulation of the OB network (Boyd et al., 2012; Markopoulos et al., 2012; Matsutani and Yamamoto, 2008). Manipulation of these projections' activity was shown to have an impact on OB functioning. For instance, optogenetic activation of piriform cortex projections at the level of the OB increases GC excitability, resulting in an odor-evoked inhibition of OB principal cells (Boyd et al., 2012). Moreover, the GCL receives important GABAergic inputs from the basal forebrain, and more especially from the HDB and the magnocellular preoptic nucleus (MCPO) (Gracia-Llanes et al., 2010; Niedworok et al., 2012). Inhibition of the projections through a chemogenetic approach lead to an alteration of odor discrimination abilities (Nunez-Parra et al., 2013). The basal forebrain also sends important cholinergic projections to the GCL (Gracia-Llanes et al., 2010; Nunez-Parra et al., 2013) and there is some evidence that cholinergic modulation can influence odor decorrelation and olfactory discrimination performances (Chaudhury et al., 2009; Escanilla et al., 2012; Mandairon et al., 2006a), but also learning of an olfactory fear conditioning task (Pavesi et al., 2012; Ross et al., 2019).

Hence, the data discussed above show that the GCL, and so by extension its major resident population the GCs seem to be also heterogeneous in terms of the brain regions from which they receive inputs from. The modulatory drive of centrifugal projections received by the OB can also influence olfactory processing and olfactory behavior. It remains, however, unknown whether there is any cellular specificity of these centrifugal projections, and whether some GCs receive preferential synaptic inputs for some top-down inputs, whereas other GCs are synaptically driven by other centrifugal inputs. Together with the heterogeneous neurochemical makeup of GCs presented earlier in the introduction, this could strengthen, but also complexify the idea of a specific contribution of GCs subtypes to OB functioning.

5. Hypothesis and objectives of the thesis

In the introduction, I discussed the fact that, as opposed to what was believed for a long time, the population of GCs in the OB is not a homogeneous cell population. In fact, in addition of being composed of cells generated at different developmental periods (i.e early post-natal period vs adulthood), already creating a heterogeneity among the entire population of GCs, those cells can also express different immunohistochemical markers and present different morphologies. I therefore hypothesize that this heterogeneity could potentially reflect on the electrophysiological characteristics of each subtype of cells and thus impact on the role and the contribution they will have in the OB network.

Thus, my overarching hypothesis is that ***each GC subpopulation can display unique properties and play its own and particular role in OB network functioning and olfactory behaviors***.

During my PhD, my main objective was to investigate and compare the properties of two subpopulations of GCs: the cells expressing the protein CaMKIIα (CaMKIIα+) and the general population of GCs. Using two-photon *in vivo* calcium imaging, I characterized the calcium dynamics of the two cells population in basal conditions but also following an odor stimulation. I also determined using an immunohistochemistry approach, to reveal the expression of an activity marker, the level of activation of each subpopulation of cells following several behavioral paradigms. Finally, I assessed the impact of an inhibition of CaMKIIα+ cells or GCs in general on animals' ability to complete behavioral tasks.

I also participated in another project aiming at characterizing the morpho-functional properties of early- and adult-born CR+ GCs versus CR- GCs, as well as their involvement in the different olfactory behaviors. Toward that end, I performed behavioral tasks followed by immunohistochemical analysis to assess the activation and thus involvement of these two subtypes of cells (i.e CR+ and CR- cells) in these behavioral tasks.

CHAPTER I : CaMKIIA EXPRESSION DEFINES TWO FUNCTIONALLY DISTINCT POPULATIONS OF GRANULE CELLS INVOLVED IN DIFFERENT TYPES OF ODOR BEHAVIOR.

Sarah Malvaut[1], Simona Gribaudo[2,*], Delphine Hardy[1,*], Linda Suzanne David[1], Laura Daroles[2], Simon Labrecque[1], Marie-Anne Lebel-Cormier[1], Zayna Chaker[3,4,¤], Daniel Coté[1,5], Paul De Koninck[1,5], Martin Holzenberger[4], Alain Trembleau[2], Isabelle Caille[2,3,§], and Armen Saghatelyan[1,6, §,#]

Affiliations

[1] CERVO Brain Research Center, Quebec City, QC, Canada G1J 2G3

[2] Sorbonne Universités, UPMC Université Paris 06, INSERM, CNRS, Institut de Biologie Paris Seine, Neuroscience Paris Seine, F-75005, Paris, France

[3] Université Paris Diderot, Sorbonne Paris Cité, 75013 Paris, France

[4] INSERM and Sorbonne Universités, UPMC, Centre de Recherche Saint-Antoine, Paris, France

[5] Faculté des sciences et de génie, Université Laval, Québec City, QC, Canada G1V 0A6

[6] Department of Psychiatry and Neuroscience, Université Laval, Quebec City, QC, Canada G1V 0A6

*These authors contributed equally to this work

[§]Corresponding authors:

isabelle caille@upmc.fr; armen.saghatelyan@fmed.ulaval.ca

#Lead contact: armen.saghatelyan@fmed.ulaval.ca

¤Present address: ZC, Biozentrum, University of Basel, Basel CH-4056, Switzerland

Current Biology, November 6th 2017, 27(21):3315-3329

1. Résumé

Les cellules granulaires (CGs) du bulbe olfactif (BO) jouent un rôle prépondérant dans le traitement des informations odorantes. Bien que différents sous-types de ces cellules aient été identifiés sur la base de l'expression de différents marqueurs immunohistochimiques, le rôle fonctionnel de chacun de ces sous-types demeure méconnu. Grâce à l'imagerie calcique deux-photons *in vivo*, nous avons pu révéler également l'existence de sous-types de CGs fonctionnellement distincts. Nous montrons que 50% des CGs expriment la protéine CaMKIIα, et que ces cellules sont préférentiellement activées par des stimuli olfactifs. Cette activation préférentielle repose sur un niveau d'inhibition plus faible reçu par les CGs CaMKIIα+, par rapport à leurs homologues CaMKIIα immunonégatifs (CaMKIIα-). En lien avec ces données fonctionnelles, notre analyse immunohistochimique révèle également que 75-90% des CGs exprimant le gène d'induction précoce *cFos* sont également CaMKIIα+ chez des souris naïves ou encore chez des animaux exposés à une nouvelle odeur ou soumis à différentes tâches comportementales de discrimination olfactive spontanée, de conditionnement opérant ou encore de mémoire olfactive à long-terme. A l'inverse une tâche d'apprentissage perceptuel résulte en une activation accrue de cellules CaMKIIα-. L'inhibition par une approche pharmacogénétique des cellules CaMKIIα+ a montré que ce sous-type cellulaire est impliqué au cours de tâches de discrimination olfactive, mais pas lors d'un apprentissage perceptuel. Néanmoins, l'inhibition pharmacogénétique des CGs, indépendamment du sous-type auquel elles appartiennent, affecte l'apprentissage perceptuel. Ainsi nos résultats indiquent que les CGs CaMKIIα+ et CaMKIIα- jouent un rôle distinct lors des différentes tâches olfactives.

Mots-clés: Bulbe olfactif, cellules granulaires, CaMKIIα, imagerie calcique *in vivo*, olfaction, discrimination olfactive, apprentissage perceptuel, pharmacogénétique

2. Abstract

Granule cells (GCs) in the olfactory bulb (OB) play an important role in odor information processing. While they have been classified into various subtypes, the functional roles of these subtypes remain unknown. We used *in vivo* two-photon Ca^{2+} imaging combined with cell type-specific identification of GCs in the mouse OB to reveal functionally distinct GCs subtypes. We showed that half of GCs express Ca^{2+}/calmodulin-dependent protein kinase IIα ($CaMKII\alpha^{+}$) and that these cells are preferentially activated by the sensory input. The higher activity of $CaMKII\alpha^{+}$ cells is due to the weaker inhibitory input that these GCs receive as compared to their CaMKIIα–immunonegative ($CaMKII\alpha^{-}$) counterparts. In line with these functional data, immunohistochemical analyses showed that 75-90% of GCs expressing the immediate early gene *cFos* are $CaMKII\alpha^{+}$ in naïve animals and in mice that had been exposed to a novel odor, long-term associative memory, go/no-go operant conditioning, or spontaneous habituation/dishabituation odor discrimination task. On the other hand, a perceptual learning task resulted in increased activation of $CaMKII\alpha^{-}$ cells. Pharmacogenetic inhibition of $CaMKII\alpha^{+}$ GCs revealed that this subtype is involved in habituation/dishabituation and go/no-go odor discrimination but not in perceptual learning. In contrast, pharmacogenetic inhibition of GCs in a subtype-independent manner affected perceptual learning. Our results indicate that $CaMKII\alpha^{+}$ and $CaMKII\alpha^{-}$ GCs are differentially recruited and play distinct roles during different odor tasks.

Keywords: Olfactory bulb, granule cells, CaMKIIα, *in vivo* Ca^{2+} imaging, olfaction, odor discrimination, perceptual learning, pharmacogenetics

3. Highlights

- CaMKIIα expression defines functionally distinct granule cell subtypes
- CaMKIIα^{+} granule cells in the olfactory bulb receive weaker inhibitory inputs than CaMKIIα^{-} cells
- CaMKIIα^{-} granule cells are activated and are involved in the perceptual learning
- CaMKIIα^{+} cells are activated and are essential for spontaneous and go/no-go odor discrimination

4. eToc Blurb

Malvaut et al. have shown that CaMKIIα expression defines functionally distinct granule cell (GC) subtypes in the olfactory bulb. CaMKIIα^{+} GCs receive weaker inhibitory inputs and are preferentially activated by sensory inputs. CaMKIIα^{+} and CaMKIIα^{-} GCs are differentially recruited and play distinct roles during different odor tasks.

5. Introduction

Granule cells (GCs) are the most abundant neuronal population in the olfactory bulb (OB) and largely outnumber bulbar principal neurons (mitral/tufted cells) (Shepherd et al., 2004). They establish reciprocal dendro-dendritic synapses with the lateral dendrites of principal neurons and play a major role in odor information processing by synchronizing principal cell activity via lateral and recurrent inhibitions (Fukunaga et al., 2014; Urban, 2002). The synchronization of principal neurons by GCs plays an important role in neuronal pattern separation by improving odor discrimination and disambiguating overlapping sensory maps evoked by similar odorants (Gschwend et al., 2015; Nunes and Kuner, 2015). *In vivo* two photon Ca^{2+} imaging revealed, however, that odor responses by GCs are temporally and spatially heterogeneous (Wienisch and Murthy, 2016). The molecular and cellular mechanisms underlying such heterogeneous responses in GCs remain unclear.

Several GC subtypes have been identified based on immunohistochemical markers (Batista-Brito et al., 2008; Gribaudo et al., 2009; Imamura et al., 2006; Neant-Fery et al., 2012; Zou et al., 2002). In addition, up to 15% of GCs are continuously renewed during adulthood (Chaker et al., 2015; Lagace et al., 2007; Ninkovic et al., 2007), which adds another level of complexity. Adult-born neuronal precursors are derived from stem cells in the subventricular zone (SVZ) of the lateral ventricle. Following their migration along the rostral migratory stream (RMS) into the OB, approximately 95% differentiate into GCs (Gengatharan et al., 2016; Ihrie and Alvarez-Buylla, 2011; Lepousez et al., 2015). Little is known about the neurochemical heterogeneity of adult-born GCs and, until now, studies aimed at understanding the roles of adult-born neurons in odor information processing have considered these cells as a homogeneous population (Alonso et al., 2012; Arruda-Carvalho et al., 2014; Breton-Provencher et al., 2009; Imayoshi et al., 2008). However, it is conceivable that different subtypes of both early-born and adult-born GCs may be activated by distinct olfactory tasks and may play specific roles in different odor behaviors (Malvaut and Saghatelyan, 2016). There is thus a need to understand the exact contributions of specific GC subtypes to odor behavior.

In the present study, we used in vivo two-color, two-photon imaging to show that a higher proportion of CaMKIIα-immunopositive (CaMKIIα+) GCs are spontaneously activated under baseline conditions and are more responsive to odor stimulation than CaMKIIα-immunonegative (CaMKIIα-) GCs. In line with our imaging data, our analysis of the expression of the immediate early gene cFos combined with an assessment of CaMKIIα immunolabeling revealed that 75%–90% of cFos-immunoreactive (cFos+) cells belong to the CaMKIIα+ GC subtype in naive mice as well as in mice that have been exposed to a novel odor stimulation, long-term associative odor memory, go/no-go operant conditioning, or spontaneous habituation/dishabituation odor discrimination tasks. This percentage decreased following an olfactory perceptual learning task, indicating that CaMKIIα- GCs had been recruited. CaMKIIα+ GCs make up half of early-born and adult-born GCs and are morphologically indistinguishable from their CaMKIIα- counterparts. In contrast, our electrophysiological recordings revealed that CaMKIIα+ GCs receive weaker inhibitory inputs, which may underlie their higher sensitivity to incoming sensory inputs. Pharmacogenetic inactivation of CaMKIIα+ GCs affected go/no-go and habituation/dishabituation odor discrimination, but not perceptual learning. On the other hand, subtype-independent pharmacogenetic inhibition of GCs impaired perceptual learning. Our results show that CaMKIIα+ GCs play an important role in processing odorant information in the basal state and during spontaneous and go/no-go odor discrimination, but not during perceptual learning, indicating that different subtypes of GCs make distinct functional contributions to specific odor behaviors.

6. Results

A. Functionally heterogeneous populations of GCs in the adult OB

To study the activity of GCs *in vivo*, we injected an AAV encoding the Ca2+ indicator GCaMP6s into the OB. Two to four weeks post-injection, we implanted a cranial window over the dorsal OB and investigated the Ca^{2+} responses of GCs in anesthetized mice under baseline conditions and following odor stimulation (**Figure**

2.1A,B). In line with and extending previous reports (Kato et al., 2012; Wienisch and Murthy, 2016), our *in vivo* Ca^{2+} imaging revealed the presence of functionally distinct subtypes of GCs based on their spontaneous activity. Slightly more than half of the GCs did not show any change in their fluorescence intensity during the 2-min acquisition period (30-Hz sampling rate) (blue arrowhead in **Figure 2.1C**, top trace in **Figure 2.1D**). In contrast, 47.7±2.9% of GCs displayed a clear spontaneous increase in fluorescence intensity (red arrowheads in **Figure 2.1C**, middle and bottom traces in **Figure 2.1D**; n=608 cells from 8 animals, **Figure 2.1E**). To determine whether GC responses are modified by novel odor stimulations, we presented six structurally different odors that are known to activate the dorsal surface of the OB (Breton-Provencher et al., 2016; Livneh et al., 2009; Wienisch and Murthy, 2016). Odor stimulations resulted in an increase in Ca2+ levels in GCs (**Figure 2.1F, SI movie 2.1**). In some GCs, the increase appeared during the 5-s odor presentation period (ON response), while in other GCs, Ca^{2+} levels increased after the end of the odor stimulation (OFF response) (**Figure 2.1F-G; SI movie 2.1**). The percentage of responsive cell-odor pairs for the ON and OFF responses were 40.6±5.4% and 10.5±1.7%, respectively (n=1937 cell-odor pairs from 6 mice; **Figure 2.1H-I**). The peak amplitude of responses (ΔF/F) was 50.2±1.9%, and odor tuning (the number of odors eliciting responses from among the six odors tested) was 1.5±0.09. These results suggest that functionally heterogeneous populations of GCs exist and that some are more prone to activation under both baseline conditions and following odor stimulation.

B. GCs can be divided into two functionally different subtypes based on the expression of CaMKIIα

CaMKIIα plays a major role in different forms of synaptic plasticity and is highly expressed in the adult OB granule cell layer (GCL) (Neant-Fery et al., 2012; Zou et al., 2002). However, it is not known whether all GCs express CaMKIIα, including adult-born GCs, or whether there is a developmental shift in CaMKIIα expression during GC maturation. We thus quantified the percentage of CaMKIIα+ GCs by immunolabeling combined with either DAPI or neuronal marker (NeuN) staining, and observed that 47.8±1.4% of DAPI- and 50.8±2.1% of NeuN-stained cells express

CaMKIIα (**Figure 2.2A-C**). To determine whether CaMKIIα is stably or transiently expressed in GCs, we analyzed CaMKIIα- tdTomato mice and found that the reporter is expressed by 66.5±3.9% of the GC population (**Figure 2.2B,C**), irrespective of the location of the GCs in the GCL **(Figure 2.2D,E)**. In addition, 87.9±2.6% of the tdTomato+ GCs were CaMKIIα+. CaMKIIα was also expressed by nearly 50% of adult-born GCs labeled by the intraperitoneal injection of BrdU, a DNA replication marker (**Figure 2.2F,G**). Since BrdU labels only a small cohort of adult-born neurons, we labeled larger populations of cells by injecting tamoxifen into adult NestinCreERT2::CC-GFP mice. Our results showed that 44.2±3.0% of 4-week-old GFP+ adult-born neurons also express CaMKIIα (**Figure 2.2G**). These findings suggest that GCs can be divided into two equally represented CaMKIIα+ and CaMKIIα− subtypes.

To determine whether these equally represented subtypes of GCs are functionally similar or not, we examined their activity using GCaMP6s and two-color two-photon imaging. To discriminate the two populations, we co-injected GCaMP6s AAV under the ubiquitous CAG promoter with the CaMKIIα-Cre-mCherry and CAG-Flex-tdTomato AAV vectors. To determine the efficiency of viral infection, we quantified the percentage of red fluorescent protein (RFP=mCherry or tdTomato)-expressing GCs that were CaMKIIα+. Our results revealed that 85.1±0.8% of RFP-expressing (RFP+) GCs were CaMKIIα+ (n=350 cells from 3 mice). Since our GCaMP6s vector was under the ubiquitous CAG promoter, we also observed that 48.5±4.8% of GCaMP6s-infected cells were CaMKIIα+. Interestingly, our *in vivo* two-photon imaging data revealed functional differences between RFP+/GCaMP6s+ and RFP-/GCaMP6s+ GCs under baseline conditions. While 59.6±3.3% of RFP+/GCaMP6s+ GCs displayed a clear spontaneous increase in fluorescence intensity under baseline conditions, significantly fewer RFP-/GCaMP6s+ showed changes in the fluorescence intensity (44.3±3.0%, n=133 and n=475 cells from 7 and 8 mice, respectively; $p<0.01$; **Figure 2.2H,I; SI movie 2**). Since RFP-/GCaMP6s+ cells were comprised of both CaMKIIα+ and CaMKIIα− GCs, the observed 15% difference in the percentage of responsive cells is likely an underestimation.

Our *in vivo* Ca^{2+} imaging was, however, restricted to the dorsal surface of the OB and allowed us only to determine the percentage of active GCs among virally infected CaMKIIα+ cells. Furthermore, it has previously been shown that GC activity increases with wakefulness (Kato et al., 2012). We thus determined the percentage of CaMKIIα+ GCs among all activated cells throughout the GCL and whether their activation differed in awake animals. We performed immunolabeling for CaMKIIα and the immediate early gene *cFos,* a commonly used cell activity marker in the OB (Inaki et al., 2002; Mandairon et al., 2008). We found that 77.2±2.8% of the cFos+ GCs located in the GCL were also CaMKIIα+ (**Figure 2.2J-K**). This result was confirmed in CaMKIIα-tdTomato reporter mice (**Figure 2.2J-K**). These findings extend our *in vivo* Ca^{2+} imaging results and suggest that CaMKIIα+ GCs are preferentially activated under baseline conditions throughout the GCL and in awake animals, and that, in addition to being biochemically heterogeneous, GCs in the adult OB are also functionally distinct.

C. The population of CaMKIIα+ GCs is sensitive to olfactory experience

Given that CaMKIIα$_+$ GCs are activated in the basal state, we next investigated the response of this subtype following an acute exposure to a novel odor or to sensory deprivation. We first performed *in vivo* two-photon Ca^{2+} imaging following the individual presentation of a set of six different odors. Odor stimulation resulted in a higher percentage of ON and OFF responsive cell-odor pairs in CaMKIIα$_+$ RFP$_+$/GCaMP6s$_+$ GCs than in RFP$_-$/GCaMP6s$_+$ GCs (60.5±3.0% for RFP$_+$/GCaMP6s$_+$ and 47.3±4.7% for RFP$_-$/GCaMP6s$_+$ GCs, n=414 and n=1522 cell-odor pairs from 6 mice; $p<0.05$, Student's *t*-test; **Figure 2.3A-D).** We also observed differences in odor tuning (1.85±0.16 and 1.2±0.1 for RFP$_+$/GCaMP6s$_+$ GCs and RFP$_-$/GCaMP6s$_+$ GCs, respectively; $p<0.05$, Kolmogorov-Smirnov test; **Figure 2.3E**), indicating once again that there are functional differences between these two GC subtypes. The peak amplitudes of responses (ΔF/F) were, however, not significantly different in RFP$_+$/GCaMP6s$_+$ and RFP$_-$/GCaMP6s$_+$ GCs (54.6±2.3% and 37.0±3.0%, respectively; **Figure 2.3F)**. The temporal dynamics of odor responses in RFP$_+$/GCaMP6s$_+$ and RFP$_-$/GCaMP6s$_+$ GCs were also similar (**Figure 2.3D**). These

data suggest that CaMKIIα+ GCs are more responsive to novel odor stimulations than their CaMKIIα- counterparts.

To ascertain whether the increased responsiveness of CaMKIIα+ GCs to novel odors applies to the entire population of activated cells in the GCL, we immunolabeled for cFos and CaMKIIα following a 1-h exposure of the mice to (+)-limonene and (-)-limonene. As expected, the odor exposure resulted in a significant increase in the total density of activated cFos+ GCs compared to unstimulated control mice (254,340±25,652 cells/mm3 in controls vs. 638,029±79,083 cells/mm3 in odor stimulated mice, $p<0.01$; **Figure 2.4A-B)**. This increase in the density of cFos+ GCs was not accompanied by statistically significant changes in the percentage of cFos+/CaMKIIα+ GCs (68.1±6.3% in controls vs. 80.8±1.1% in odor stimulated mice; **Figure 2.4C**). These results suggest that the presentation of a novel odor predominantly activates CaMKIIα+ GCs. The activation was the consequence of the recruitment of new CaMKIIα+ GCs rather than a shift from a CaMKIIα− to a CaMKIIα+ subtype since no difference in the percentage of DAPI+/CaMKIIα+ GCs was observed (**Figure 2.4D**).

The specific activation of CaMKIIα+ GCs in the basal state and following the presentation of a novel odor indicated that this subtype is more sensitive to incoming sensory inputs. We thus hypothesized that blocking sensory inputs for 24h should decrease the percentage of cFos+/CaMKIIα+ GCs. Sensory deprivation decreased the density of activated cFos+ GCs (92,591±4832 cells/mm3 in the control OB vs. 44,812±3443 cells/mm3 in the occluded OB, $p<0.01$) (**Figure 2.4E-F**) and reduced the percentage of cFos+/CaMKIIα+ GCs (75.4±1.3% in the control OB vs. 59.0±3.4% in the occluded OB, $p<0.05$) (**Figure 2.4G**). No change in the percentage of DAPI+/CaMKIIα+ GCs was observed (**Figure 2.4H**). These results suggest that CaMKIIα+ and CaMKIIα− GCs are functionally distinct and that CaMKIIα+ GCs are more sensitive to incoming sensory inputs.

D. Structuro-functional properties of CaMKIIα+ and CaMKIIα− GCs

To shed light on the cellular mechanisms that underlie the distinct functional responses of CaMKIIα+ and CaMKIIα− GCs, we next performed morphological and electrophysiological analyses of the two subtypes. We observed no differences in the length of the primary dendrites or the total dendritic arborization of GFP-expressing adult-born CaMKIIα+ and CaMKIIα− GCs at 14, 21, and 28 days post-injection (dpi) (**Figure 2.5A-C**). The spine densities on the distal dendrites of the two GC subtypes were also similar (**Figure 2.5D**). We next determined whether there were any morphological differences between early-born CaMKIIα+ and CaMKIIα− GCs and again observed no differences in the length of the primary dendrites, total dendritic arborization, or spine density of the CaMKIIα+ and CaMKIIα− GCs at 18 dpi **(Figure 2.5A-D)**.

We then determined whether CaMKIIα+ and CaMKIIα− GCs had different electrophysiological properties. We used a CaMKIIα-GFP AAV to identify CaMKIIα+ GCs. For the control group, we used an AAV expressing a ubiquitous chicken β-actin (CBA) promoter. To assess the efficiency of these AAVs, we injected the RMS of adult C57Bl/6 mice with one of the two AAVs. Two to three weeks post-infection, CaMKIIα immunolabeling of OB sections showed that 90.2±4.1% of the GCs infected with the CaMKIIα-GFP AAV were CaMKIIα+ (n=150 cells from 3 mice) while 53.2±3.2% of the GFP+ GCs from the control animals injected with the CBA-GFP AAV were CaMKIIα+, which was expected given that the ubiquitous promoter targeted all GCs. Hence, any difference in electrophysiological properties observed using the two AAVs would be an underestimation given that the control group was composed of approximately 50% CaMKIIα+ GCs.

We recorded spontaneous EPSCs and IPSCs from GCs to determine whether CaMKIIα+ GCs receive different excitatory and inhibitory inputs. No differences in the frequencies and amplitudes of spontaneous and miniature EPSCs (sEPSCs and mEPSCs) (**Figure 2.5E-G**) or in the rise-time, decay-time, or charge of mEPSCs (**Figure 2.5H**) were observed. Recordings of spontaneous and miniature IPSCs (sIPSCs and mIPSCs) (**Figure 2.5I-J**) showed that the frequency of these events is

the same for the two groups (**Figure 2.5K**). The amplitudes of the sIPSCs and mIPSCs were, however, significantly lower in CaMKIIα+ GCs (sIPSCs: 48.3±5.2 pA for GCs (n=11) vs. 33.1±2.9 pA for CaMKIIα+ GCs (n=9), $p<0.05$; mIPSCs: 27.6±2.1 pA for GCs (n=10) vs. 21.7±1.5 pA for CaMKIIα+ GCs (n=8), $p<0.05$) (**Figure 2.5L**). We also observed that the rise and decay times of mIPSCs recorded from CaMKIIα+ GCs were faster than those recorded from general population of GCs, which led to smaller charges for inhibitory events in CaMKIIα+ GCs (735±63 pF for GCs (n=10) vs. 557±29 pF for CaMKIIα+ GCs (n=8), $p<0.05$) (**Figure 2.5M**). These results show that CaMKIIα+ GCs receive a lower level of inhibition, which may explain why they are preferentially activated in the basal state and following odor stimulation.

E. Perceptual learning activates CaMKIIα− GCs

Since our *in vivo* Ca^{2+} imaging, electrophysiological, and early immediate gene expression results showed that the GC population is functionally heterogeneous, we wondered whether different GC subpopulations play different roles in distinct olfactory tasks. We first assessed the involvement of CaMKIIα+ and CaMKIIα− GCs in perceptual learning, a non-associative form of odor learning that improves the ability of mice to discriminate between two perceptually similar odors following a passive 10-day exposure to the odors (Daroles et al., 2016; Mandairon et al., 2008). The mice were submitted to odor enrichment with perceptually similar odorants ((+)-limonene and (-)-limonene) daily for 1 h. The day after the end of the olfactory enrichment, the mice were separated into two groups, one of which was again submitted to the two odorants (Learning + Odor re-exposure group) for 1 h, while the other group was not (Learning group) (**Figure 2.6A**). Re-exposing the animals to perceptually similar odors after the learning task resulted in an increase in cFos+ GC density (107,750±7750 cells/mm^3 after re-exposure vs. 78,500±4750 cells/mm^3, n=3, $p<0.001$, **Figure 2.6B-C**). Interestingly, the perceptual learning task reduced the percentage of cFos+/CaMKIIα+ GCs from 77.2±2.8% in the basal state to 49.0±1% (n=3, **Figure 2.6D**), indicating that CaMKIIα− GCs are activated by this task. Re-exposing the animals to the odors after the perceptual learning task recruited CaMKIIα+ GCs (49.0±1.1% of cFos+/CaMKIIα+ GCs for the Learning group

vs. 62.0±1.1% for the Learning + Odor re-exposure group, n=3; p<0.0001; **Figure 2.6D**). No change in the percentage of DAPI+/CaMKIIα+ cells was observed (**Figure 2.6E**). This suggests that olfactory perceptual learning relies on a broader recruitment of CaMKIIα- GCs.

Nevertheless, these experiments did not rule out the involvement of CaMKIIα+ GCs in this odor learning task. To address this issue, we inactivated CaMKIIα+ GCs *in vivo* using an AAV under the CaMKIIα promoter (CaMKIIα-HA-hM4D(G_i)-IRES-mCitrine) based on the DREADD approach (Roth, 2016). The control mice were injected either with a CaMKIIα-GFP or a GFP under a synapsin (Syn) promoter AAV (**Figure 2.6F)**. As expected, AAVs with the CaMKIIα promoter only infected the CaMKIIα+ GCs (87.3±1.2% for the CaMKIIα-GFP AAV and 85.2±1.9% for the CaMKIIα-DREADD AAV), whereas the Syn-GFP AAV infected both subtypes of GCs. To test the efficiency of our pharmacogenetic approach, we administrated CNO, the DREADD-receptor ligand, to both groups of mice and perfused the animals 90 min later. Immunolabelling for cFos and GFP showed that CaMKIIα-DREADD AAV-injected mice contain significantly fewer GFP+/cFos+ GCs (29.0±2.0% in CaMKIIα- GFP infected GCs vs. 16.0±1.6% in CaMKIIα-DREADD infected GCs; n=3 mice; p<0.05; **Figure 2.6G)**. Similarly, Syn-DREADD (Syn-HA-hM4D(G_i)-mCherry) AAV-infected GCs contained significantly fewer mCherry+/cFos+ GCs than Syn-GFP infected GCs (16.8±2.5% in Syn-GFP infected GCs vs. 3.3±1.7% in Syn-DREADD infected GCs; n=3 mice; p=0.01; **Figure 2.6H).** We next determined whether the inhibition of CaMKIIα+ GCs during the learning task (**Figure 2.6I)** affected the discrimination of perceptually similar odors. As reported previously (Daroles et al., 2016; Mandairon et al., 2008), the mice were able to discriminate between two perceptually close odorants after the learning task (post-enrichment test: 162.9±27.7% increase in exploration time for the dishabituation odor vs. 100.0±17.2%, for the habituation odor, n=18 mice, p<0.05), but not before (pre-enrichment test: 75.5±14.9% increase for the dishabituation odor vs. 100.0±17.6% for the habituation odor, n=18 mice, p=0.2; **Figure 2.6J**). Interestingly, the inhibition of CaMKIIα+ GCs during the learning task did not affect the ability of these mice to discriminate between two perceptually similar odors (post-enrichment test:

185.5±61.1% increase for the dishabituation odor vs. 100.0±36.8% for the habituation odor, n=7 mice, $p<0.05$; **Figure 2.6K**). The unaltered perceptual learning following the pharmacogenetic inhibition of CaMKIIα+ GCs may be simply due to the fact that GCs in general are not needed for this type of learning. To test this possibility, we inactivated GCs in a subtype-independent manner using DREADDs under the Syn promoter. This subtype-independent inhibition of GCs during the learning task affected the ability of mice to discriminate between two perceptually similar odors (post-enrichment test: 82.1±32.4% for the dishabituation odor vs. 100.0±25.3% for the habituation odor, n=10 mice; **Figure 2.6L**). These results suggest that while GCs are required for perceptual learning, CaMKIIα+ GCs are not involved in this type of learning, indicating that CaMKIIα- GCs are required for perceptual learning.

F. CaMKIIα+ GCs are essential for spontaneous and go/no-go odor

We next determined whether CaMKIIα+ GCs are involved in other odor discrimination paradigms that, unlike perceptual learning, are based on active odor learning (go/no-go odor discrimination and long-term odor associative memory) or spontaneous habituation/dishabituation tasks. In the long-term associative memory task (**Figure S2.1A**), mice were conditioned to associate one of two chemically similar odors ((+)-carvone) with a sugar reward. We used pseudo-conditioned mice, which received the reward independently of the odor presented ((+)-carvone or (-)-carvone) as a control. During the test, the mice were re-exposed to the two odors, and the exploration time was measured 24 h after a 4-day training period. The conditioned mice spent significantly more time exploring the reward-associated odor, while the pseudo-conditioned mice spent the same amount of time investigating both enantiomers (**Figure S2.1B**). The density of activated cFos+ cells, the percentage of DAPI+ cells expressing CaMKIIα, and the percentage of cFos+/CaMKIIα+ GCs were similar for the conditioned and pseudo-conditioned groups (**Figure S2.1C and F**).

We next used the go/no-go operant conditioning paradigm in which mice are trained to insert their snouts into the odor sampling port of an olfactometer and to

associate a specific odor (0.1% octanal; S+) with a water reward. The mice were able to reach the criterion of 80% correct responses in a few blocks of 20 odor presentation trials. The control group was subjected to the same go/no-go procedure but received the water reward independently of the odor used (S+ or S-). An analysis of the phenotypes of the GCs activated following this task did not reveal any difference in the density of cFos+ GCs (**Figure 2.7A,B**), the percentage of CaMKIIα+/cFos+ GCs (**Figure 2.7C**), or the percentage of CaMKIIα+/DAPI+ GCs (**Figure 2.7D**).

The lack of difference in the percentage of activated CaMKIIα+ GCs following the long-term associative memory and go/no-go odor discrimination learning tasks may reflect the high activation level of this subtype in the basal state. We thus used a pharmacogenetic approach to selectively inhibit CaMKIIα+ GCs **(Figure 2.7E)** and to determine their contribution to the go/no-go odor discrimination task. This made it possible to precisely administer structurally distinct odors as well as complex odor mixtures. The mice injected with both CaMKIIα-GFP and CaMKIIα-DREADDs AAVs were able to discriminate between two structurally distinct odors (0.1% octanal vs. 0.1% decanal) following the application of CNO **(Figure 2.7F).** However, pharmacogenetic inactivation of CaMKIIα+ GCs affected the ability of the mice to discriminate between complex odor mixtures (0.6% (+)-carvone/0.4% (-)-carvone vs. 0.4% (+)-carvone/0.6% (-)-carvone; **Figure 2.7G).** The mice whose CaMKIIα+ GCs were pharmacogenetically inactivated required more blocks to reach the criterion of 80% correct responses (13.1±1.7 blocks for control mice vs. 20.8±1.3 blocks for mice in the experimental group, n=7 and 8 mice, respectively; $p<0.01$; **Figure 2.7G).** These results indicate that CaMKIIα+ GCs are required for go/no-go odor discrimination learning of complex odor mixtures.

We next used a spontaneous habituation/dishabituation odor discrimination task in which the mice were first habituated to (+)-carvone by four consecutive presentations followed by the presentation of a new (dishabituation) odor ((-)-carvone) (**Figure 2.7H**). For the control group, the mice were presented with the same habituation odor during the last odor presentation (habituation/habituation

group; **Figure 2.7H**). As expected, the mice from the two groups became habituated to the first odor. The increase in exploration time observed with the experimental habituation/dishabituation group when the second odor was presented showed that the mice were able to spontaneously discriminate between the two odorants (143.7±24.0% increase in dishabituation odor compared to the last presentation of the habituation odor; n=11, $p<0.05$; **Figure 2.7I**). An analysis of the phenotypes of the GCs activated following the odor discrimination task did not reveal any differences in the density of cFos+ GCs, the percentage of CaMKIIα+/DAPI+ GCs, or the percentage of CaMKIIα+/cFos+ GCs (n=4 mice per group; **Figure 2.7J-M**).

As for long-term associative odor memory and go/no-go odor discrimination learning, we reasoned that the lack of difference in the percentage of activated CaMKIIα+ GCs reflects their high activation level in the basal state. We thus again used a pharmacogenetic approach to selectively inhibit CaMKIIα+ GCs and to determine their contribution to spontaneous odor discrimination (**Figure 2.7N**). While the mice injected with the control CaMKIIα-GFP AAV were able to discriminate between the two enantiomers (158.6±27.1% increase in dishabituation odor compared to the last presentation of the habituation odor, n=9, $p<0.01$) (**Figure 2.7O**), the inhibition of the CaMKIIα+ GCs disrupted the mice's ability to discriminate between two similar odors (82.9±14.0% compared to the last presentation of the habituation odor, n=10, $p=0.3$) (**Figure 2.7O**). These results indicate that CaMKIIα+ GCs in the adult OB are also required for spontaneous odor discrimination of similar odors.

7. Discussion

We showed that there are two functionally distinct subtypes of GC in the OB that fulfill different roles in odor behavior. CaMKIIα+ GCs receive weaker inhibitory inputs, making them more susceptible to activation by olfactory stimuli. This subtype of GC is essential for go/no-go operant conditioning and habituation/dishabituation spontaneous odor discrimination, but not for perceptual learning. On the other hand,

CaMKIIα− GCs are preferentially activated by and are involved in perceptual learning.

One challenge in comprehending odor information processing is understanding the role played by different cell types in the OB. Despite the fact that GCs make up the largest neuronal population in the OB with neurochemically distinct subtypes, little is known about their functional heterogeneity. Studies aimed at addressing their roles in sensory information processing and odor behavior have usually considered them as a homogeneous population of interneurons (Alonso et al., 2012; Gschwend et al., 2015; Nunes and Kuner, 2015). Using *in vivo* two photon imaging of GCaMP6s-infected GCs, we identified two types of GCs based on their level of spontaneous activity and their responses to odor stimulation. We showed that GCs are heterogeneous and that a substantial proportion of them are already active under basal conditions and following odor stimulation. Our study revealed the molecular and cellular mechanisms underlying these heterogeneous responses. In fact, 60-70% of responsive cells belonged to the CaMKIIα+ GC subtype that receives a lower level of inhibition than their CaMKIIα− counterparts. It should be noted, however, that the electrophysiological recordings were performed with adult-born GC populations, and it remains to be shown whether the same differences in the level of inhibition exist in early-born CaMKIIα+ and CaMKIIα− GCs. Our *in vivo* Ca^{2+} imaging data were corroborated by the early immediate gene analysis showing that the vast majority (70-90%) of cFos+ GCs activated in basal conditions or following go/no-go operant conditioning, long-term associative memory, and spontaneous habituation/dishabituation odor discrimination tasks belong to the CaMKIIα+ subtype. In contrast, perceptual learning recruited CaMKIIα− GCs, indicating that these two subtypes of GCs may be differently modulated during distinct olfactory tasks. CaMKIIα+ GCs receive weaker inhibitory inputs and are more prone to activation by sensory stimuli while CaMKIIα− GCs receive stronger inhibitory inputs and require stronger excitatory stimuli to be recruited during particular olfactory tasks. This may occur in perceptual learning tasks that rely on stronger sensory stimuli (1 h/day exposure to undiluted odors for 10 days). Our pharmacogenetic

experiments indicate that GC subtypes are not only differently modulated but also play diverse roles in distinct olfactory tasks.

We showed that the CaMKIIα+ and CaMKIIα− GC subtypes fulfill distinct functional roles in odor information processing. However, other GC subtypes have been identified based on the expression of neurochemical markers such as calretinin, 5T4, neurogranin, and mGluR2 (Batista-Brito et al., 2008; Gribaudo et al., 2009; Imamura et al., 2006; Merkle et al., 2014; Murata et al., 2011). The roles of 5T4-expressing GCs in odor detection and discrimination have recently been described (Takahashi et al., 2016) while the roles of other GC subtypes in odor behavior remain to be determined. The adult OB also constantly receives new neurons that add another level of complexity to deciphering the roles of specific GC subtypes in odor information processing. Many studies have shown that adult-born neurons are involved in different types of odor behavior, including short- and long-term odor memory, odor discrimination, and maternal and social behaviors (Alonso et al., 2012; Arruda-Carvalho et al., 2014; Breton-Provencher et al., 2009; David et al., 2013; Mak et al., 2007; Moreno et al., 2009; Shingo et al., 2003). While these studies have provided new insights into the roles of adult-born neurons in the functioning of the OB neuronal network and the execution of selected olfactory behaviors, we (Breton-Provencher et al., 2009; David et al., 2013) and others (Alonso et al., 2012; Arruda-Carvalho et al., 2014; Mak et al., 2007; Shingo et al., 2003) have considered adult-born GCs as a homogeneous population of cells. However, the results presented here indicate that adult-born GCs are a functionally heterogeneous population of interneurons with distinct electrophysiological properties. This, in turn, implies that, like early-born neurons, the roles of these distinct subtypes of adult-born cells in the functioning of the OB network and odor behavior may be quite different depending on the level of their activation by a given behavioral task and their roles in the OB network.

CaMKIIα is one of the most abundant proteins in the brain, making up 1-2% of the total protein content, with the α subunit being the most prominent in the brain (Lisman et al., 2002). CaMKIIα expression is usually confined to excitatory neurons

(Benson et al., 1992; Jones et al., 1994), but principal cells in the OB lack this enzyme, which is specifically expressed by GCs (Neant-Fery et al., 2012; Zou et al., 2002). Our finding that CaMKIIα^{+} GCs receive weaker inhibitory inputs than their CaMKIIα^{-} counterparts raises an important question as to whether CaMKIIα confers a GC subtype with functional properties distinct from other interneurons. While this question requires further investigation, it is interesting to note that CaMKIIα is a major player in the synaptic development and plasticity of both excitatory and inhibitory synapses. Indeed, CaMKIIα plays an essential role in decoding Ca^{2+} signals in excitatory neurons and modulates the synaptic remodeling and plasticity of these cells (De Koninck and Schulman, 1998; Giese et al., 1998; Lemieux et al., 2012; Lledo et al., 1995). CaMKIIα is also involved in the remodeling and plasticity of inhibitory synapses via trafficking of different $GABA_A$ receptor subunits as well as gephyrin, the main scaffolding protein of inhibitory synapses (Flores et al., 2015; Marsden et al., 2010; Petrini et al., 2014; Saliba et al., 2012). Several $GABA_A$ receptor subunits are highly expressed in the OB (Fritschy and Mohler, 1995), and differences in subunit composition determine the functional characteristics of $GABA_A$ receptors (Farrant and Nusser, 2005). Differences in the amplitudes and kinetics of the inhibitory currents of the two GC subtypes may thus result from a differential expression of $GABA_A$ receptor subunits. It is also possible that different GC subtypes receive inhibitory inputs originating from distinct sources that confer different functions. A number of local and long-ranging GC inhibitory inputs have been identified (Deshpande et al., 2013; Nagayama et al., 2014; Shepherd et al., 2004), but it is not known whether they segregate differently onto distinct GC subtypes. Altogether, our results provide evidence for the existence of functionally distinct GC subtypes in the adult OB and show that they each have a distinct involvement in odor behavior.

8. Star methods

A. Key resource table

Table 2.1: Key resource table

REAGENT or RESOURCE	SOURCE	IDENTIFIER
Antibodies		
Mouse monoclonal anti-CaMKIIα	ThermoFisher Scientific	Cat# MA1-048; RRID: AB_325403
Rabbit polyclonal anti-c-Fos	Santa Cruz Biotechnology	Cat# sc-52; RRID: AB_2106783
Rabbit polyclonal anti-GFP	ThermoFisher Scientific	Cat# A-11122; RRID: AB_221569
Chicken polyclonal anti-GFP	Avès	GFP-1020; RRID:AB_10000240
Rabbit monoclonal anti-NeuN	Cell signaling	Cat# 12943; RRID: AB_2630395
Rabbit polyclonal anti-mCherry	BioVision	Cat # 5993-100; RRID:AB_1975001
Bacterial and Virus Strains		
AAV 2/1-CBA-GFP	Molecular Tool Platform CERVO Brain Research center	Lot # AAV 19
AAV 2/1-CaMKIIα-GFP	Molecular Tool Platform CERVO Brain Research center	Lot # AAV 36
AAV 2/5-CaMKIIα-HA-hM4D(Gi)-IRES-mCitrine	University of North Carolina Vector Core Facility	Lot # AV4617d
AAV 2/5-CAG-GCaMP6s-WPRE-SV40	University of Pennsylvania Vector Core Facility # AV-5-PV2833	Cat #AV-5-PV2833
AAV 2/5-EF1α-DIO-EYFP	University of North Carolina Vector Core Facility	Lot # AV4310J
AAV 2/5-CAG-FLEX-tdTomato	University of North Carolina Vector Core Facility	Lot # AV4599
AAV 2/5-hSyn-EGFP	Addgene	Cat # 50465-AAV5
AAV 2/5-hSyn-HA-hM4D(Gi)-mCherry	Addgene	Cat # 50475-AAV5
AAV 2/5- CaMKIIα-mCherry-Cre	University of North Carolina Vector Core Facility	Lot # AV6448b
LV-EF1α-Cre-mCherry-Puro	SignaGen Laboratories	Cat # SL100281
LV-GFP	Ecole des Neuroscience platform (ENP), Paris	N/A
Chemicals, Peptides, and Recombinant Proteins		

Butyraldehyde	Sigma-Aldrich	538191; CAS: 123-72-8
Ethyl tiglate	Sigma-Aldrich	W246018; CAS: 5837-78-5
Valeric Acid	Sigma-Aldrich	75054; CAS: 109-52-4
Isoamyl acetate	Sigma-Aldrich	W205508; CAS: 123-92-2
(+)-carvone	Sigma-Aldrich	22070; CAS: 2244-16-8
(-)-carvone	Sigma-Aldrich	22060; CAS: 6485-40-1
Decanal	Sigma-Aldrich	59581; CAS: 112-31-2
Octyl aldehyde (octanal)	Sigma-Aldrich	5608; CAS: 124-13-0
(R)-(+)-limonene	Sigma-Aldrich	62118; CAS: 5989-27-5
(S)-(-)-limonene	Sigma-Aldrich	62128; CAS: 5989-54-8
Sunflower seed oil	Sigma-Aldrich	47123; CAS: 8001-21-6
Mineral oil	Sigma-Aldrich	M5904; CAS: 8042-47-5
Paraformaldehyde	Sigma-Aldrich	P6148; CAS: 30525-89-4
Kynurenic acid	Sigma-Aldrich	K3375; CAS: 492-27-3
Biccuculine Methiodine	Abcam	ab120108
Tetrodotoxin	Affix Scientific	AF3015; CAS: 4368-28-9
Clozapine-N-Oxide	Tocris Bioscience	4936; CAS: 34233-69-7
Tamoxifen	Sigma-Aldrich	T5648; CAS: 10540-29-1
Anhydrous ethyl alcohol	Commercial Alcohols	1019C
Experimental Models: Organisms/Strains		
Mouse: NestinCreERT2	(Lagace et al., 2007)	N/A
Mouse: CAG-CAT-EGFP	(Waclaw et al., 2010)	N/A
Mouse: NestinCreERT2::CC-GFP	This paper	N/A
Mouse: CamkCre4	(Mantamadiotis et al., 2002)	N/A
Mouse: B6;129S6-Gt(ROSA)26Sor$^{tm14(CAG-tdTomato)Hze}$/J (CAG-tdTomato)	The Jackson Laboratory	Cat# JAX:007908; RRID:IMSR_JAX:007908
Mouse: CD1	Charles Rivers	Strain code: 022
Mouse: C57BL/6NCRL	Charles Rivers	Strain code: 027
Software and Algorithms		
MATLAB 2016a	Mathworks	https://www.mathworks.com/
MATLAB scripts for Ca^{2+} imaging analysis	This paper	N/A
ImageJ	NIH	https://imagej.net/Welcome
Huygens	Scientific Volume Imaging	https://svi.nl/HuygensSoftware
NeuronStudio	Computational Neurobiology and Imaging center	http://research.mssm.edu/cnic/tools-ns.html
Mini Analysis	Synaptosoft	http://www.synaptosoft.com/
Other		

Polyethylene tubing (PE50, I.D. 0.58 mm, O.D. 0.965 mm)	Becton Dickinson	427517
Vicryl suture (3-0)	Johnson & Johnson	J442H
4-channels olfactometer	Knosys	http://www.knosysknosys.com

B. Contact for reagent and resource sharing

Further information and requests for resources and reagents should be directed to and will be fulfilled by the Lead Contact Armen Saghatelyan (armen.saghatelyan@fmed.ulaval.ca).

C. Experimental model and subject details

Adult (>2-month-old) male C57Bl/6 mice (Charles River) were used for most experiments. NestinCreERT2::CAG-CAT-EGFP (NestinCreERT2::CC-GFP) mice were used to study the expression of CaMKIIα in adult-born neurons. These mice were obtained by crossing NestinCreERT2 mice (Lagace et al., 2007) with CAG-CAT-EGFP mice (Waclaw et al., 2010). They received daily injections of tamoxifen (180 mg/kg, Sigma Aldrich) for 5 days to induce the expression of GFP by stem cells and their progeny. Tamoxifen was diluted in sunflower seed oil (Sigma Aldrich) and 10% anhydrous ethanol. Postnatal day 5 (P5) CD1 mice (Charles River) were used to compare the morphological characteristics of early-born GCs. The experiments were performed in accordance with Canadian Guide for the Care and Use of Laboratory Animals guidelines and were approved by the Animal Protection Committee of Université Laval. The mice were kept in groups of 4-5 on a 12-h light/dark cycle in a temperature-controlled facility (22˚C), with food and water *ad libitum*, except for the mice in go/no-go odor discrimination and long-term associative memory groups, which were partially water- and food-deprived, respectively. Animals that underwent behavioral procedures were individually housed and kept on a reverse light-dark cycle for 7-10 days before beginning the experiments. Animals were randomly assigned to the various experimental groups. To genetically label CaMKIIα+ cells, the CamkCre4 (Mantamadiotis et al., 2002) and CAG-tdTomato (http://jaxmice.jax.org/strain/007908.html) mouse transgenes were backcrossed to

C57BL/6 and 129/SvPas genetic backgrounds, respectively. Hemizygous CamkCre4$^{+/0}$ and CAG-tdTomato$^{+/0}$ mice were then crossed to obtain double transgenic F1 offspring (CaMKIIα-tdTomato). All mice were individually housed in ventilated cages under specific pathogen-free conditions at 22°C and a 12-h light/dark cycle, with food and water *ad libitum*. The experiments were approved by the Charles Darwin University Animal Ethics Committee (approvals Ce5/ 2012/074 and C2EA-05).

9. Method details

A. Stereotaxic injections

We used adeno-associated viral vectors (AAVs) to label neuronal precursors to assess the electrophysiological properties of GCs. The AAVs were produced at the Molecular Tools Platform of the CERVO Research Center. The mice were stereotaxically injected in the RMS with either a control vector (GFP under the chicken β-actin CBA promoter; CBA-GFP) to label neuronal precursors regardless of their molecular characteristics or a CaMKIIα-specific vector (GFP under the CaMKIIα promoter; CaMKIIα-GFP) to infect precursors that differentiate into CaMKIIα$_+$ GCs. The stereotaxic injections were performed under ketamine/xylazine anesthesia (10 mg/mL and 1 mg/mL respectively; 0.1 mL per 10 g of body weight) at the following coordinates (with respect to the bregma): anterior-posterior (AP) 2.55, medio-lateral (ML) 0.82, and dorso-ventral (DV) 3.15. The mice were allowed to recover and were returned to their home cages. For the morphological analyses of adult-born GCs, the SVZs of C57Bl/6 mice were injected with a GFP-expressing lentivirus at the following coordinates AP: 1, ML: 1, DV: 2.1. They were sacrificed 14, 21, and 28 days after the injections (n=4 mice per time-point).

For the morphological analyses of early-born GCs, the OBs of CD1 P5 mice were injected with a mixture of EF1α-Cre-mCherry lentivirus (SignaGen Laboratories, 3.88x10^9 TU/mL) and EF1α-DIO-EYFP AAV (University of North Carolina Vector Core Facility, 6.5x10^{12} TU/mL) at a ratio of 0.2/0.8. The low amount

of Cre virus made it possible to sparsely label GCs and thus to accurately assess their dendritic morphology and spine density.

B. Cranial window surgery and in vivo two-photon calcium imaging

Adult mice were injected with a mixture of three different AAV vectors (at a ratio of 1:1:1) to allow the simultaneous comparison of Ca^{2+} activity in CaMKIIα+ and general population of GCs (composed of CaMKIIα+ and CaMKIIα-). We used AAVCAG- GCaMP6s-WPRE-SV40 (University of Pennsylvania Vector Core Facility, $2.23x10^{13}$ iu/mL), AAV-CAG-FLEX-tdTomato (University of North Carolina Vector Core Facility, $8x10^{12}$ iu/mL), and AAV-CaMKIIα-Cre-mCherry (University of North Carolina Vector Core Facility, $4.8x10^{12}$ iu/mL). Co-injection of the CaMKIIα-Cre-mCherry and CAG-Flex-tdTomato AAV vectors boosted the red fluorescence signal in co-infected CaMKIIα+ GCs. Furthermore, tdTomato is more suitable for multi-photon imaging than mCherry at the excitation wavelength we used (1040 nm) (Drobizhev et al., 2009). The viruses were injected bilaterally in the OB at the following coordinates (with respect to the bregma): AP 5.3, ML 0.5, DV 0.9; and AP 4.6, ML 0.75, DV 1.0. Two to four weeks post-viral infection, cranial window surgery was performed as previously described (Breton-Provencher et al., 2016). The mice were anesthetized with 2-3% isoflurane, and their body temperature was maintained at 37.5°C using an infrared heating blanket (Kent Scientific). After removing the skin, a circular craniotomy centered over the OB was drilled and the bone was removed, leaving the dura mater intact. A 3-mm-diameter glass coverslip was put on the top surface of the OB, and Kwik-Seal (World Precision Instruments) and Metabond cement (Parkell Inc.) were used to fix the coverslip in place. During the procedure, a custom-made head plate was also attached to the skull in order to prevent the animal's head from moving during imaging. At the end of the surgery, the isoflurane concentration was gradually decreased. The mice were kept under ketamine/xylazine anesthesia for the entire imaging session.

A custom-built video-rate two-photon microscope was used to image Ca^{2+} activity in the GC subtypes (Veilleux et al., 2008). The mouse was positioned under the microscope using the head plate on a custom-made stereotaxic frame controlled

by a micromanipulator (MPC 200; Sutter). A 20x water-immersion objective (XLUMPlanFl 20/numerical aperture (NA) 0.95; Olympus) was used to locate the region of interest (ROI). A Ti:Sapphire tunable laser (Mai Tai; Spectra Physics) with a wavelength of 920-940 nm was used to excite GCaMP6s, and a 1040 nm HighQ-2 laser (Spectra Physics) was used to excite tdTomato and reveal the GC subtypes. Ca^{2+} activity in the GCs was imaged using a 60x water immersion objective (LUMPlanFlN 60x/NA 1.0). GCs were identified by their smaller size and their location in the GCL. Several ROIs were selected, and baseline activity was recorded in these regions during 2-min acquisitions at a frame rate of 30-32 Hz. Odor-evoked responses were then recorded in the same ROIs. Odors were delivered for 5 s using a custom-made olfactometer. Odor delivery was preceded by 10-s imaging of baseline fluorescent activity of GCaMP6s-infected cells. Six different odorants (butyraldehyde, methylbenzoate, ethyltiglate, valeric acid, isoamylacetate, (+)-carvone; Sigma Aldrich) were diluted in mineral oil to a final concentration of 1% v/v. These odorants were chosen because they activate the medio-lateral part of the dorsal surface of the OB (Breton-Provencher et al., 2016; Livneh et al., 2009; Wienisch and Murthy, 2016). Each odor was presented three times, with a 1-2 min inter-trial interval. Since it has been shown that mice respond with a higher sniffing rate to the first application of each odor (Kato et al., 2012), only the second and third trials of odor application were retained for analysis. The responses of the second and third trials were averaged. No correction for neuropil fluorescence was applied.

C. Immunohistochemistry

The mice were deeply anesthetized using an intraperitoneal injection of sodium pentobarbital (12 mg/mL; 0.1 mL per 10 g of body weight) and were intracardiacally perfused with 0.9% NaCl followed by 4% paraformaldehyde (PFA). The brains were collected and were post-fixed overnight in 4% PFA. Coronal or horizontal 50 or 100-µm-thick OB sections were cut using a vibratome (Leica) and were incubated with the following primary antibodies: rabbit anti-cFos (SC-52, 1:40,000, 48 h; Santa Cruz), mouse anti-CaMKIIα (MA1-048, 1:500, 48 h; ThermoFisher Scientific), rabbit anti-NeuN (D3S31, 1:500; 24 h, Cell Signaling), rabbit anti-GFP (A-11122, 1:1000,

24 h; ThermoFisher Scientific), chicken anti-GFP (GFP-1020, 1:1000, 24 h; Aves) or rabbit anti-mCherry (5993-100, 1:1000; 24 h; Biovision). The antibodies were diluted in either 0.5% Triton X-100 and 4% milk or 0.3% Triton X- 100 and 10% FBS prepared in PBS. The corresponding secondary antibodies were used. Fluorescence images were acquired using a confocal microscope (FV 1000; Olympus) with 60x (UPlanSApoN 60x/NA 1.42; Olympus) and 40x (UPlanSApoN 40x/NA 0.90; Olympus) oil and air immersion objectives, respectively.

D. Morphological analysis

The morphologies of 14, 21, and 28-d post-injection (dpi) adult-born and 18 dpi early-born neurons were determined as previously described (Daroles et al., 2016; David et al., 2013; Scotto-Lomassese et al., 2011). To distinguish the two GC populations, CaMKIIα immunostaining was performed. Images were acquired with a LSM 700 AxioObserver confocal microscope using 40x objective. For spine density quantification, images were zoomed 4 times.

E. Electrophysiological recordings

Two to three weeks after the stereotaxic injection of either a control CBA-GFP AAV or a CaMKIIα-GFP AAV, the mice were deeply anesthetized and were perfused transcardiacally with ice-cold sucrose-based artificial cerebro-spinal fluid (ACSF) containing the following (in mM): 250 sucrose, 3 KCl, 0.5 $CaCl_2$, 3 $MgCl_2$, 25 $NaHCO_3$, 1.25 NaH_2PO_4, and 10 glucose. The brains were quickly collected and were immersed in ACSF. Horizontal 250-µm-thick OB slices were obtained using a vibrating blade microtome (HM 650V; Thermo Scientific). The slices were transferred into oxygenated ACSF maintained at 32°C containing the following (in mM): 124 NaCl, 3 KCl, 2 $CaCl_2$, 1.3 $MgCl_2$, 25 $NaHCO_3$, 1.25 NaH_2PO_4, and 10 glucose. Inhibitory postsynaptic currents (IPSCs) and excitatory postsynaptic currents (EPSCs) were recorded using a Multiclamp 700A amplifier (Molecular Devices). We opted for recordings from virally labeled CBA-GFP GCs that, unlike recordings from the CaMKIIα-GFP-negative population (not labeled virally), allowed us to select GCs that had preserved dendritic morphology based on the expression of GFP. Patch electrodes with resistances ranging from 7 to 9 MΩ were filled with a CsCl-based

intracellular solution to record inhibitory currents from GFP-labeled GCs. The intracellular solution contained the following (in mM): 135 CsCl, 10 HEPES, 0.2 EGTA, 2 ATP, 0.3 GTP, and 10 glucose (pH≈7.2). The access resistance was continuously monitored, and recordings with a >15% change were discarded. The GCs were kept at -60 mV. Spontaneous IPSCs (sIPSCs) were isolated by bath applying 5 mM kynurenic acid (Kyn) to block glutamatergic activity. Miniature IPSCs (mIPSCs) were isolated by applying 1 μM tetrodotoxin (TTX) to block voltage-sensitive sodium channels in the presence of 5 mM Kyn. To record EPSCs, the patch electrodes were filled with a K-methylsulfate-based intracellular solution containing the following (in mM): 130 K-methylsulfate, 10 HEPES, 6 KCl, 2 ATP, 0.4 GTP, 10 Na-phosphocreatine, and 2 ascorbate (pH≈7.2). Spontaneous EPSCs (sEPSCs) were isolated by bath applying 50 μM biccuculine methiodide (BMI) to block $GABA_A$ receptors. Miniature EPSCs (mEPSCs) were isolated by applying 1 μM TTX to block voltage-sensitive sodium channels in the presence of 50 μM BMI. Spontaneous synaptic events were analyzed during 2 min of continuous recording using the Mini analysis program (Synaptosoft). The analysis was blinded to the experimental group.

F. Novel odor stimulation

The mice were separated into two groups. Each mouse was individually housed in a clean cage and spent 1 h with no odor. The two groups were then presented for 1 h with two tea balls suspended in the cage. For the control group, the tea balls were filled with a filter paper alone, whereas for the experimental group, the tea balls were filled with a filter paper soaked with 100 μl of pure (+)-limonene and (-)-limonene. The tea balls were then removed, and the animals were perfused with 4% PFA 1 h later. The density of $cFos^+$ cells and the percentage of $CaMKII\alpha^+/cFos^+$ and $CaMKII\alpha^+/DAPI^+$ cells were determined blindly to the experimental condition.

G. Sensory deprivation

Occlusion plugs were fabricated using polyethylene tubing (PE50, I.D. 0.58 mm, O.D. 0.965 mm; Becton Dickinson), with the center blocked using a tight-fitting Vicryl suture knot (3-0; Johnson & Johnson). The ~5-mm-long petroleum jelly-coated

plugs were inserted in the left nostrils of four mice under isoflurane anesthesia. The mice were sacrificed by intracardiac perfusion 1 day later.

H. Behavioral procedures

a. Odor discrimination

For the odor discrimination task based on habituation/dishabituation, the odors were presented in glass Pasteur pipettes containing filter paper soaked with 6 µL of 2% odorant in mineral oil. The odor presentations consisted of 5-min sessions separated by 20-min intervals. The mice were first habituated to the glass pipette by presenting it to them twice. They were then subjected to four habituation sessions with a first odor ((+)-carvone; Sigma Aldrich). One group of animals (control group) was subjected to a fifth session with the same habituation odor. A second group of animals (habituation/dishabituation group) was subjected to a second odor (dishabituation odor, (-)-carvone; Sigma Aldrich). The time spent exploring the pipette during each session was recorded. The mice from the two groups were sacrificed 1 h after completing the task by intracardiac perfusion with 4% PFA. Fifty-µm-thick OB coronal slices were cut and were immunolabeled for cFos and CaMKIIα.

b. Perceptual learning

The mice were exposed in their home cages to two tea balls for 1 h per day for 10 consecutive days. One tea ball contained 100 µL of pure (+)-limonene and the other contained 100 µL of pure (-)-limonene. On day 11, the mice were separated into two groups. One group was placed in a clean cage, and the mice were sacrificed after 1 h (Learning group). The second group (Learning + Odor reexposure group) was placed in a clean cage and was exposed to the odorants for 1 h. The mice were then transferred to a clean cage and were sacrificed after 1 h.

c. Go/no-go olfactory discrimination learning

The mice were partially water-deprived until they reached 80-85% of their initial body weight prior to starting the go/no-go training. They underwent training sessions

to habituate them to the cage of the olfactometer and to learn how to get a water reward. The mice were trained using 20 trials, with no exposure to an odor, to insert their snouts into the odor sampling port and to lick the water port to receive a 3-µL water reward. The ports were located side-by-side. The reward-associated odor (0.1% octanal; S+) was then introduced. Inserting the snout into the odor sampling port broke a light beam and opened an odor valve. The duration of the opening was increased gradually from 0.1 to 1 s over several sessions, and the mice with a minimum sampling time of 50 ms were given a water reward. The mice usually completed this training after one or two 30-min sessions. Once they had successfully completed this training step, the mice were subjected a go/no-go odor discrimination test. Prior to being introduced to the odor not associated with a reward (0.1% decanal; S-), the mice underwent an introductory S- session consisting of exposure to S+ for 30 trials. If the success rate was at least 80%, the discrimination task was begun. The mice were then exposed randomly to S+ or S-, and the percentage of correct responses was calculated for each block of 20 trials. If a mouse licked the water port after being exposed to S+ (hit) and did not lick the water port after being exposed to S- (correct rejection), this was recorded as a correct response. A false response was recorded if the mouse licked the water port after being exposed to S- or if it did not lick the water port after being exposed to S+. A mouse was considered successful if it reached the criterion score of 80%. The control group underwent the same go/no-go procedure but received the water reward independently of the odor used (S+ or S-). The mice from the two groups were sacrificed 1 h after completing the task by intracardiac perfusion with 4% PFA. Fifty-µm-thick OB coronal slices were cut and were immunolabeled for cFos and CaMKIIα. The density of $cFos^+$ cells and the percentage of $CaMKII\alpha^+/cFos^+$ and $CaMKII\alpha^+/DAPI^+$ cells were blindly determined.

d. Long-term associative memory

The mice used for this task were deprived of food for four to five days before beginning the test as well as during the learning period to reduce their initial body weight by 15-20%. The test was performed as described previously (Breton-

Provencher et al., 2009; Imayoshi et al., 2008). Briefly, during the first training period, the mice underwent four 10-min sessions a day. For two of the sessions, the first odor (15% (+)-carvone in mineral oil) was presented in association with a sugar reward. For the other two sessions, the second odor (15% (-)-carvone in mineral oil) was presented with no reward. For the control group (pseudo-conditioned mice), the sugar reward was randomly presented with either (+)-carvone or (-)-carvone. Associative memory was assessed 24 h after the last training session. The mice were then re-exposed to both odors with no sugar reward and were allowed to explore them for 5 min. The time spent clawing the bedding above each odor was recorded**.** The density of cFos$_+$ cells and the percentage of CaMKIIα$_+$/cFos$_+$ and CaMKIIα$_+$/DAPI$_+$ cells were blindly determined.

e. Pharmacogenetic inhibition of CaMKIIα$_+$ GCs

We inactivated the GCs using the Designer Receptors Exclusively Activated by Designer Drugs (DREADD) pharmacogenetic approach to investigate the roles of different subtypes of GCs in odor behavior (Roth, 2016)[29]. The mice were separated into different groups and received a stereotaxic injection of either a control (CaMKIIα- GFP or Syn-GFP) or a CaMKIIα-specific DREADD (CaMKIIα-HA-hM4D(G$_i$)-IRES-mCitrine; University of North Carolina Vector Core Facility; 2x10^{12} iu/mL) or a Synapsin-specific DREADD (hSyn-HA-hM4D(G$_i$)-mCherry) AAV (Addgene; 3x10^{12} iu/mL). No differences in the behavioral performances of two control groups injected either with CaMKIIα-GFP or Syn-GFP were observed and the data was thus pooled. The injections were performed bilaterally in the OB at two different sites at the following coordinates (with respect to the bregma): AP 5.3, ML 0.5, DV 0.9; and AP 4.6, ML 0.75, DV 1.0. Three to four weeks post-injection, the mice were tested using the odor discrimination habituation/dishabituation, go/no-go operant conditioning, or perceptual learning task. To investigate the effect of CaMKIIα$_+$ GC activity inhibition on habituation/dishabituation odor discrimination performances, mice from the two groups received an intraperitoneal injection of clozapine-N-oxide (CNO, 2 mg/kg of body weight in 0.9% NaCl; Tocris Bioscience) 30 min before the dishabituation odor was presented. For the go/no-go odor

discrimination learning task, the mice from the two groups received the CNO injection 30 min before the test. No treatment was given during the training period. For the perceptual learning task, the mice received daily injections of CNO during the 10-day odor enrichment period 30 min before being exposed to the odors. No treatment was given on day 11.

For the perceptual learning task, the mice were tested using an odor discrimination task before and after a 10-day enrichment procedure, as previously described (Daroles et al., 2016). After an initial 50-s presentation of mineral oil, the mice underwent four consecutive 50-s presentations of the habituation odor ((+)-limonene) at 5-min intervals. The dishabituation odor ((-)-limonene) was presented for 50 s during the fifth session, and the exploration time was measured. After 10 days of olfactory enrichment and the CNO treatment, the mice were retested using the same task (i.e., post-enrichment test). All pharmacogenetic experiments were performed with the investigator blinded to the experimental condition.

I. Quantification and statistical analysis

Cell morphology was analyzed using the simple neurite tracer and cell counter plugins in ImageJ or with NeuronStudio software. To determine the percentage of CaMKIIα$_+$ or tdTomato$_+$ GCs among the DAPI$^+$ or NeuN$^+$ cells, as well as the density of cFos$_+$ GCs, the counting was performed using images acquired with 63x or 40x objectives with 1-µm-thick optical sections. At least three coronal slices derived from the anterior, medial, and posterior portion of the OB (in the rostro-caudal axis) from each individual animal were used. Images were acquired from the medial, lateral, and ventral portions of the GCL to avoid regional bias in cFos expression. cFos cells in the field were identified, and co-labeling for CaMKIIα or tdTomato was evaluated in consecutive optical sections. The investigator was blinded to the experimental conditions in most immunohistochemical quantifications (novel odor presentation, long-term associative memory, go/no-go olfactory discrimination learning).

Ca^{2+} responses were analyzed using a custom-written script in MATLAB (MathWorks Inc., USA). GCaMP6s and RFP (tdTomato and mCherry) video-rate

image stacks (30 ms/frame) were recorded for the XY positions and were corrected for brain motion using the StackReg ImageJ plugin. The aligned stacks were time-averaged in 1-s bins. To remove out-of-focus frames and quantify GCaMP6s GC activity, we used a custom-written script in MATLAB that allowed us to select the z planes based on the homology between the frames of the RFP channel. The script computed the average normalized cross-correlation peak for the complete image stack. The frames with the highest peak correlation values were considered in focus, whereas the frames with peak correlation values lower than a user-defined threshold (set at 1%) were removed. ROIs in each cell were manually drawn to extract the GCaMP6s fluorescence signal over the entire cell body. The background signal was measured in at least three different regions of the movie and was subtracted from the Ca^{2+} traces in the cells. For experiments assessing Ca^{2+} activity under baseline conditions, all peaks with amplitude greater than 2.5 times that of the mean standard deviation (SD) of each trace were retained. Several thresholds (1xSD, 1.5xSD, 2xSD, 2.5xSD) were empirically tested by visually inspecting Ca^{2+} activity and by determining whether motion-induced negative deflections in the ΔF/F traces could be detected. For the odor stimulation experiments, we calculated the ΔF/F value, and the response threshold was defined as 2.5xSD of the fluorescence intensity of the pre-odor value. If the peak fluorescence intensity during the odor stimulation was higher than the response threshold, the cell was classified as an 'ON' cell. If the peak fluorescence intensity of the post-odor period (occurring up to 5 s after the end of odor stimuli) was higher than the response threshold, the cell was classified as an 'OFF' cell. These periods were chosen based on a previous report showing that the temporal dynamic of mitral cell responses to odors is diverse, spanning the 5-s period of odor presentation and a few seconds after the odor offset (Kato et al., 2012), and the fact that responses recorded in GCs were one synapse away from those recorded in mitral cells. Non-responsive cells were also logged in the analysis to calculate the percentage of ON and OFF responses and odor tuning. Odor tuning responses were analyzed using a custom-written MATLAB script. This algorithm labels all cells in the imaging region and localizes them through different acquisitions of the six odors presented. A template containing all the cells is then created by

summing the binary images of every acquisition. The Ca^{2+} responses of GCs to each individual odor that had been analyzed using the custom-written MATLAB script were compiled in a file by matching the coordinates of cells in the summed and individual binary images, and the odor tuning responses were calculated.

Data are expressed as means ± SEM. When possible, the investigator was blinded to the experimental conditions as specified in Methods details. Statistical significance was determined using a paired or unpaired two-sided Student's *t*-test, or Kolmogorov-Smirnov test depending on the experiment, as indicated in the text and corresponding figure legends. The exact value of n and its representation (cells, animals) is indicated in the text and corresponding figure legends. No statistical methods were used to predetermine the sample size. Equality of variance for the unpaired t-test was verified using the F-test. The levels of significance were as follows: * $p<0.05$, ** $p<0.01$, *** $p<0.001$.

10. References

Alonso, M., Lepousez, G., Sebastien, W., Bardy, C., Gabellec, M.M., Torquet, N., and Lledo, P.M. (2012). Activation of adult-born neurons facilitates learning and memory. Nat Neurosci *15*, 897-904.

Arruda-Carvalho, M., Akers, K.G., Guskjolen, A., Sakaguchi, M., Josselyn, S.A., and Frankland, P.W. (2014). Posttraining ablation of adult-generated olfactory granule cells degrades odor-reward memories. J Neurosci *34*, 15793-15803.

Batista-Brito, R., Close, J., Machold, R., and Fishell, G. (2008). The distinct temporal origins of olfactory bulb interneuron subtypes. J Neurosci *28*, 3966-3975.

Benson, D.L., Isackson, P.J., Gall, C.M., and Jones, E.G. (1992). Contrasting patterns in the localization of glutamic acid decarboxylase and Ca2+/calmodulin protein kinase gene expression in the rat central nervous system. Neuroscience *46*, 825-849.

Breton-Provencher, V., Bakhshetyan, K., Hardy, D., Bammann, R.R., Cavarretta, F., Snapyan, M., Cote, D., Migliore, M., and Saghatelyan, A. (2016). Principal cell activity induces spine relocation of adult-born interneurons in the olfactory bulb. Nature Communications *7*, 12659.

Breton-Provencher, V., Lemasson, M., Peralta, M.R., 3rd, and Saghatelyan, A. (2009). Interneurons produced in adulthood are required for the normal functioning of the olfactory bulb network and for the execution of selected olfactory behaviors. J Neurosci *29*, 15245-15257.

Chaker, Z., Aid, S., Berry, H., and Holzenberger, M. (2015). Suppression of IGF-I signals in neural stem cells enhances neurogenesis and olfactory function during aging. Aging Cell *14*, 847-856.

Daroles, L., Gribaudo, S., Doulazmi, M., Scotto-Lomassese, S., Dubacq, C., Mandairon, N., Greer, C.A., Didier, A., Trembleau, A., and Caille, I. (2016). Fragile X Mental Retardation Protein and Dendritic Local Translation of the Alpha Subunit of the Calcium/Calmodulin-Dependent Kinase II Messenger RNA Are Required for the Structural Plasticity Underlying Olfactory Learning. Biol Psychiatry *80*, 149-159.

David, L.S., Schachner, M., and Saghatelyan, A. (2013). The extracellular matrix glycoprotein tenascin-R affects adult but not developmental neurogenesis in the olfactory bulb. J Neurosci *33*, 10324-10339.

De Koninck, P., and Schulman, H. (1998). Sensitivity of CaM kinase II to the frequency of Ca2+ oscillations. Science *279*, 227-230.

Deshpande, A., Bergami, M., Ghanem, A., Conzelmann, K.K., Lepier, A., Gotz, M., and Berninger, B. (2013). Retrograde monosynaptic tracing reveals the temporal evolution of inputs onto new neurons in the adult dentate gyrus and olfactory bulb. Proc Natl Acad Sci U S A *110*, E1152-1161.

Drobizhev, M., Tillo, S., Makarov, N.S., Hughes, T.E., and Rebane, A. (2009). Absolute two-photon absorption spectra and two-photon brightness of orange and red fluorescent proteins. J Phys Chem B *113*, 855-859.

Farrant, M., and Nusser, Z. (2005). Variations on an inhibitory theme: phasic and tonic activation of GABA(A) receptors. Nat Rev Neurosci *6*, 215-229.

Flores, C.E., Nikonenko, I., Mendez, P., Fritschy, J.M., Tyagarajan, S.K., and Muller, D. (2015). Activity-dependent inhibitory synapse remodeling through gephyrin phosphorylation. Proc Natl Acad Sci U S A *112*, E65-72.

Fritschy, J.M., and Mohler, H. (1995). GABAA-receptor heterogeneity in the adult rat brain: differential regional and cellular distribution of seven major subunits. J Comp Neurol *359*, 154-194.

Fukunaga, I., Herb, J.T., Kollo, M., Boyden, E.S., and Schaefer, A.T. (2014). Independent control of gamma and theta activity by distinct interneuron networks in the olfactory bulb. Nat Neurosci *17*, 1208-1216.

Gengatharan, A., Bammann, R.R., and Saghatelyan, A. (2016). The Role of Astrocytes in the Generation, Migration, and Integration of New Neurons in the Adult Olfactory Bulb. Front Neuroscience *10*, 149.

Giese, K.P., Fedorov, N.B., Filipkowski, R.K., and Silva, A.J. (1998). Autophosphorylation at Thr286 of the alpha calcium-calmodulin kinase II in LTP and learning. Science *279*, 870-873.

Gribaudo, S., Bovetti, S., Garzotto, D., Fasolo, A., and De Marchis, S. (2009). Expression and localization of the calmodulin-binding protein neurogranin in the adult mouse olfactory bulb. J Comp Neurol *517*, 683-694.

Gschwend, O., Abraham, N.M., Lagier, S., Begnaud, F., Rodriguez, I., and Carleton, A. (2015). Neuronal pattern separation in the olfactory bulb improves odor discrimination learning. Nat Neurosci *18*, 1474-1482.

Ihrie, R.A., and Alvarez-Buylla, A. (2011). Lake-front property: a unique germinal niche by the lateral ventricles of the adult brain. Neuron *70*, 674-686.

Imamura, F., Nagao, H., Naritsuka, H., Murata, Y., Taniguchi, H., and Mori, K. (2006). A leucine-rich repeat membrane protein, 5T4, is expressed by a subtype of granule cells with dendritic arbors in specific strata of the mouse olfactory bulb. J Comp Neurol *495*, 754-768.

Imayoshi, I., Sakamoto, M., Ohtsuka, T., Takao, K., Miyakawa, T., Yamaguchi, M., Mori, K., Ikeda, T., Itohara, S., and Kageyama, R. (2008). Roles of continuous neurogenesis in the structural and functional integrity of the adult forebrain. Nat Neurosci *11*, 1153-1161.

Inaki, K., Takahashi, Y.K., Nagayama, S., and Mori, K. (2002). Molecular-feature domains with posterodorsal-anteroventral polarity in the symmetrical sensory maps of the mouse olfactory bulb: mapping of odourant-induced Zif268 expression. Eur J Neurosci *15*, 1563-1574.

Jones, E.G., Huntley, G.W., and Benson, D.L. (1994). Alpha calcium/calmodulin-dependent protein kinase II selectively expressed in a subpopulation of excitatory neurons in monkey sensory-motor cortex: comparison with GAD-67 expression. J Neurosci *14*, 611-629.

Kato, H.K., Chu, M.W., Isaacson, J.S., and Komiyama, T. (2012). Dynamic sensory representations in the olfactory bulb: modulation by wakefulness and experience. Neuron *76*, 962-975.

Lagace, D.C., Whitman, M.C., Noonan, M.A., Ables, J.L., DeCarolis, N.A., Arguello, A.A., Donovan, M.H., Fischer, S.J., Farnbauch, L.A., Beech, R.D*., et al.* (2007). Dynamic contribution of nestin-expressing stem cells to adult neurogenesis. J Neurosci *27*, 12623-12629.

Lemieux, M., Labrecque, S., Tardif, C., Labrie-Dion, E., Lebel, E., and De Koninck, P. (2012). Translocation of CaMKII to dendritic microtubules supports the plasticity of local synapses. J Cell Biol *198*, 1055-1073.

Lepousez, G., Nissant, A., and Lledo, P.M. (2015). Adult neurogenesis and the future of the rejuvenating brain circuits. Neuron *86*, 387-401.

Lisman, J., Schulman, H., and Cline, H. (2002). The molecular basis of CaMKII function in synaptic and behavioural memory. Nat Rev Neurosci *3*, 175-190.

Livneh, Y., Feinstein, N., Klein, M., and Mizrahi, A. (2009). Sensory input enhances synaptogenesis of adult-born neurons. J Neurosci *29*, 86-97.

Lledo, P.M., Hjelmstad, G.O., Mukherji, S., Soderling, T.R., Malenka, R.C., and Nicoll, R.A. (1995). Calcium/calmodulin-dependent kinase II and long-term potentiation enhance synaptic transmission by the same mechanism. Proc Natl Acad Sci U S A *92*, 11175-11179.

Mak, G.K., Enwere, E.K., Gregg, C., Pakarainen, T., Poutanen, M., Huhtaniemi, I., and Weiss, S. (2007). Male pheromone–stimulated neurogenesis in the adult female brain: possible role in mating behavior. Nature Neuroscience *10*, 1003.

Malvaut, S., and Saghatelyan, A. (2016). The Role of Adult-Born Neurons in the Constantly Changing Olfactory Bulb Network. Neural Plast *2016*, 1614329.

Mandairon, N., Didier, A., and Linster, C. (2008). Odor enrichment increases interneurons responsiveness in spatially defined regions of the olfactory bulb correlated with perception. Neurobiol Learn Mem *90*, 178-184.

Mantamadiotis, T., Lemberger, T., Bleckmann, S.C., Kern, H., Kretz, O., Martin Villalba, A., Tronche, F., Kellendonk, C., Gau, D., Kapfhammer, J.*, et al.* (2002). Disruption of CREB function in brain leads to neurodegeneration. Nat Genet *31*, 47-54.

Marsden, K.C., Shemesh, A., Bayer, K.U., and Carroll, R.C. (2010). Selective translocation of Ca2+/calmodulin protein kinase IIalpha (CaMKIIalpha) to inhibitory synapses. Proc Natl Acad Sci U S A *107*, 20559-20564.

Merkle, F.T., Fuentealba, L.C., Sanders, T.A., Magno, L., Kessaris, N., and Alvarez-Buylla, A. (2014). Adult neural stem cells in distinct microdomains generate previously unknown interneuron types. Nat Neurosci *17*, 207-214.

Moreno, M.M., Linster, C., Escanilla, O., Sacquet, J., Didier, A., and Mandairon, N. (2009). Olfactory perceptual learning requires adult neurogenesis. Proc Natl Acad Sci U S A *106*, 17980-17985.

Murata, K., Imai, M., Nakanishi, S., Watanabe, D., Pastan, I., Kobayashi, K., Nihira, T., Mochizuki, H., Yamada, S., Mori, K.*, et al.* (2011). Compensation of depleted neuronal subsets by new neurons in a local area of the adult olfactory bulb. J Neurosci *31*, 10540-10557.

Nagayama, S., Homma, R., and Imamura, F. (2014). Neuronal organization of olfactory bulb circuits. Front Neural Circuits *8*, 98.

Neant-Fery, M., Peres, E., Nasrallah, C., Kessner, M., Gribaudo, S., Greer, C., Didier, A., Trembleau, A., and Caille, I. (2012). A role for dendritic translation of CaMKIIalpha mRNA in olfactory plasticity. PLoS One *7*, e40133.

Ninkovic, J., Mori, T., and Gotz, M. (2007). Distinct modes of neuron addition in adult mouse neurogenesis. J Neurosci *27*, 10906-10911.

Nunes, D., and Kuner, T. (2015). Disinhibition of olfactory bulb granule cells accelerates odour discrimination in mice. Nat Commun *6*, 8950.

Petrini, E.M., Ravasenga, T., Hausrat, T.J., Iurilli, G., Olcese, U., Racine, V., Sibarita, J.B., Jacob, T.C., Moss, S.J., Benfenati, F.*, et al.* (2014). Synaptic recruitment of gephyrin regulates surface GABAA receptor dynamics for the expression of inhibitory LTP. Nat Commun *5*, 3921.

Roth, B.L. (2016). DREADDs for Neuroscientists. Neuron *89*, 683-694.

Saliba, R.S., Kretschmannova, K., and Moss, S.J. (2012). Activity-dependent phosphorylation of GABAA receptors regulates receptor insertion and tonic current. EMBO J *31*, 2937-2951.

Scotto-Lomassese, S., Nissant, A., Mota, T., Neant-Fery, M., Oostra, B.A., Greer, C.A., Lledo, P.M., Trembleau, A., and Caille, I. (2011). Fragile X mental retardation protein regulates new neuron differentiation in the adult olfactory bulb. J Neurosci *31*, 2205-2215.

Shepherd, G.M., Chen, W.R., and Greer, C.A. (2004). Olfactory Bulb. In The Synaptic Organization of the Brain, G.M. Shepherd, ed., pp. 165–216.

Shingo, T., Gregg, C., Enwere, E., Fujikawa, H., Hassam, R., Geary, C., Cross, J.C., and Weiss, S. (2003). Pregnancy-stimulated neurogenesis in the adult female forebrain mediated by prolactin. Science *299*, 117-120.

Takahashi, H., Ogawa, Y., Yoshihara, S., Asahina, R., Kinoshita, M., Kitano, T., Kitsuki, M., Tatsumi, K., Okuda, M., Tatsumi, K.*, et al.* (2016). A Subtype of Olfactory Bulb Interneurons Is Required for Odor Detection and Discrimination Behaviors. J Neurosci *36*, 8210-8227.

Urban, N.N. (2002). Lateral inhibition in the olfactory bulb and in olfaction. Physiol Behav *77*, 607-612.

Veilleux, I., Spencer, J.A., Biss, D.P., Cote, D., and Lin, C.P. (2008). In Vivo Cell Tracking With Video Rate Multimodality Laser Scanning Microscopy. IEEE Journal of selected topics in quantum electronics *14*.

Waclaw, R.R., Ehrman, L.A., Pierani, A., and Campbell, K. (2010). Developmental origin of the neuronal subtypes that comprise the amygdalar fear circuit in the mouse. J Neurosci *30*, 6944-6953.

Wienisch, M., and Murthy, V.N. (2016). Population imaging at subcellular resolution supports specific and local inhibition by granule cells in the olfactory bulb. Sci Rep *6*, 29308.

Zou, D.J., Greer, C.A., and Firestein, S. (2002). Expression pattern of alpha CaMKII in the mouse main olfactory bulb. J Comp Neurol *443*, 226-236.

11. Figures

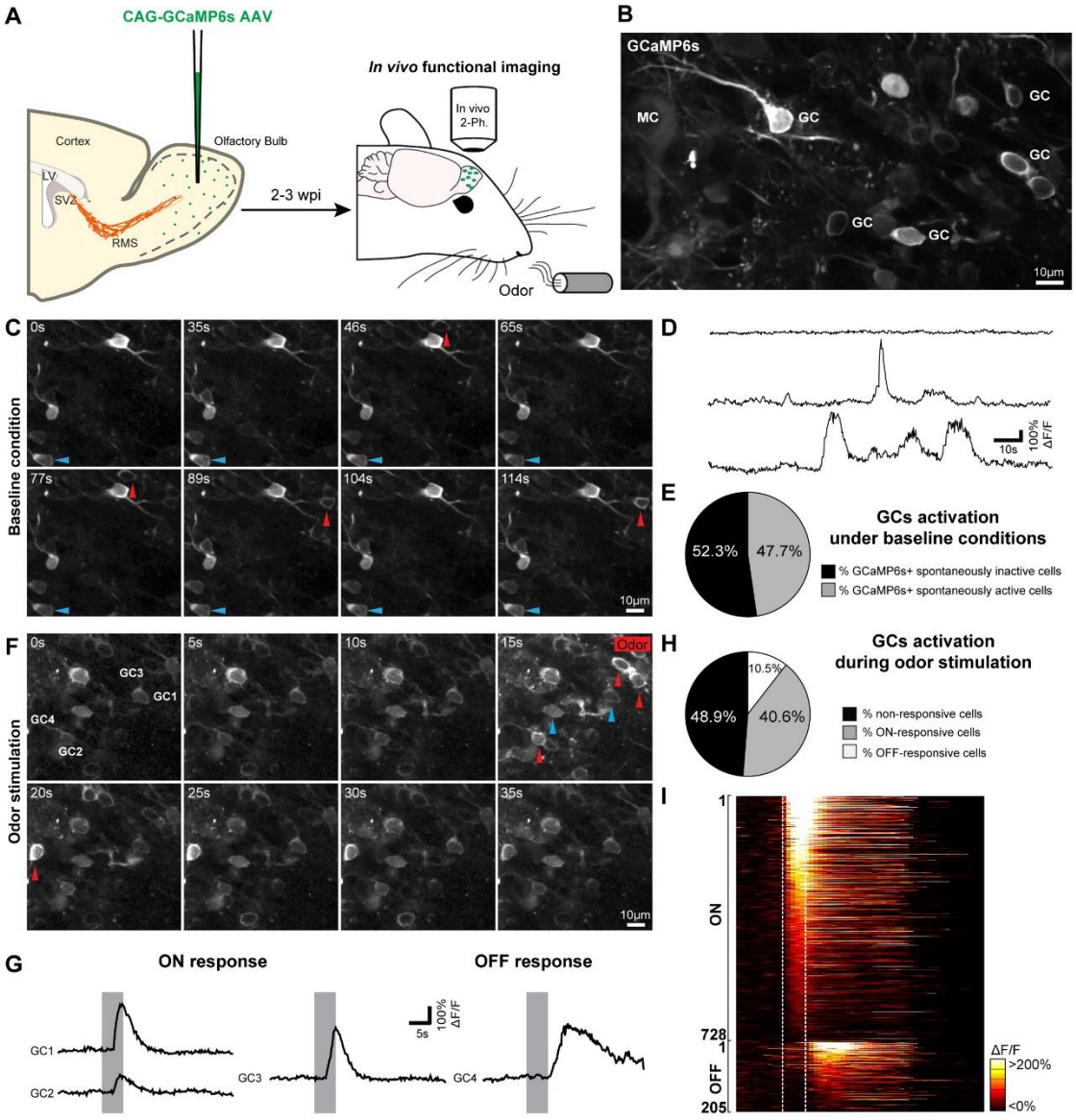

Figure 2.1: In vivo Ca^{2+} imaging of GC activity under baseline and odor stimulation conditions.

A-B. Schematic representation and representative two-photon image of *in vivo* Ca^{2+} imaging 2 to 4 weeks after GCaMP6s-expressing AAV injection. **C.** Two-photon *in vivo* recordings of GC activity under baseline conditions. Red and blue arrowheads indicate cells with high and low baseline activity, respectively. **D-E**. Quantification and sample traces of cells recorded under baseline conditions. **F.** Representative images of *in vivo* Ca^{2+} imaging of GC activity during an odorant stimulation. The time is indicated in the upper left corner. The odor application interval is indicated in the upper right corner. ON or OFF responsive GCs are indicated by red arrowheads, whereas non-responsive cells are indicated by blue arrowheads. **G.** Sample traces of ON and OFF responsive GCs. Odor application (5s) is indicated by the gray box. **H.** GC activation following odor presentation, with the percentage of ON, OFF, and non-responsive cell-odor pairs. **I.** Pseudo-colored heatmaps of ON and OFF responsive GCs are shown. Cell-odor pairs are sorted according to the amplitude of their responses.

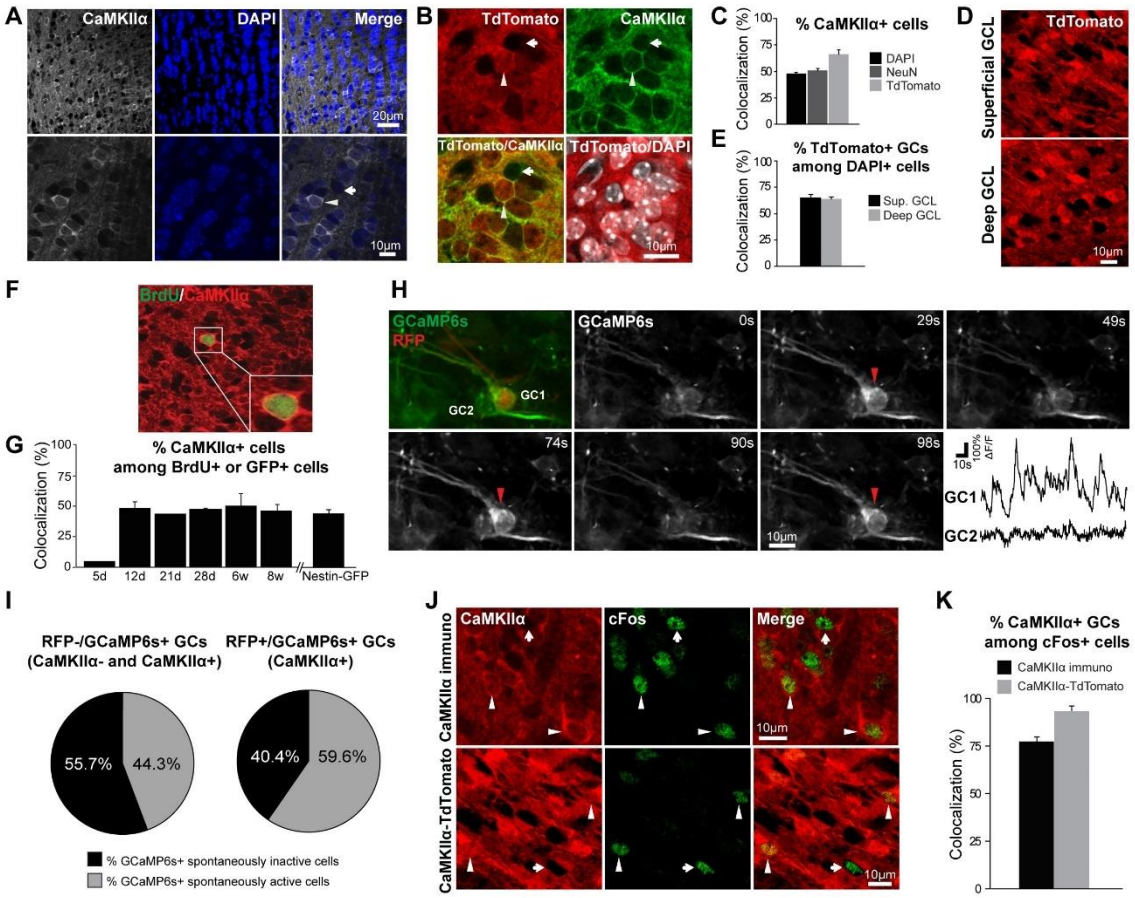

Figure 2.2: Expression of CaMKIIα in the adult olfactory bulb

A. Confocal images of CaMKIIα immunolabeling (white) and DAPI staining (blue) in the GCL. The bottom panel shows a higher magnification of the images in the upper panel. The arrow and arrowhead indicate CaMKIIα− and CaMKIIα+ GCs, respectively. **B.** Confocal images of CaMKIIα-tdTomato-expressing cells (red), CaMKIIα immunolabeling (green), and DAPI staining (white) in the GCL. The arrow and arrowhead indicate CaMKIIα− and CaMKIIα+ GCs, respectively. **C.** Quantification of the percentage of CaMKIIα+ GCs among DAPI+ (black) and NeuN+ (dark gray) cells in C57Bl/6 mice and tdTomato+ GCs among DAPI+ (light gray) cells in CaMKIIα-tdTomato reporter mice. **D-E.** Confocal images and quantification of deep and superficial tdTomato+ GCs in CaMKIIα-tdTomato reporter mice. **F.** Confocal images of a 21-day-old BrdU+ GC (green) that also expresses CaMKIIα (red). **G.** Quantification of the percentages of adult-born CaMKIIα+ GCs. **H.** *In vivo* two-photon Ca^{2+} imaging of RFP+ (CaMKIIα+) and RFP- GCs expressing GCaMP6s (green). Note the spontaneous Ca^{2+} events in RFP+ (CaMKIIα+) GCs but not RFP- GCs. **I.** GC activation under baseline conditions. **J.** Representative confocal images of cFos+ GCs (green) following CaMKIIα immunolabeling (top panel, red) and in CaMKIIα-tdTomato reporter mice (bottom panel, red). The arrows indicate CaMKIIα− GCs. The arrowheads indicate CaMKIIα+ GCs. **K.** Quantification of the percentage of cFos/CaMKIIα+ and cFos+/tdTomato+ GCs.

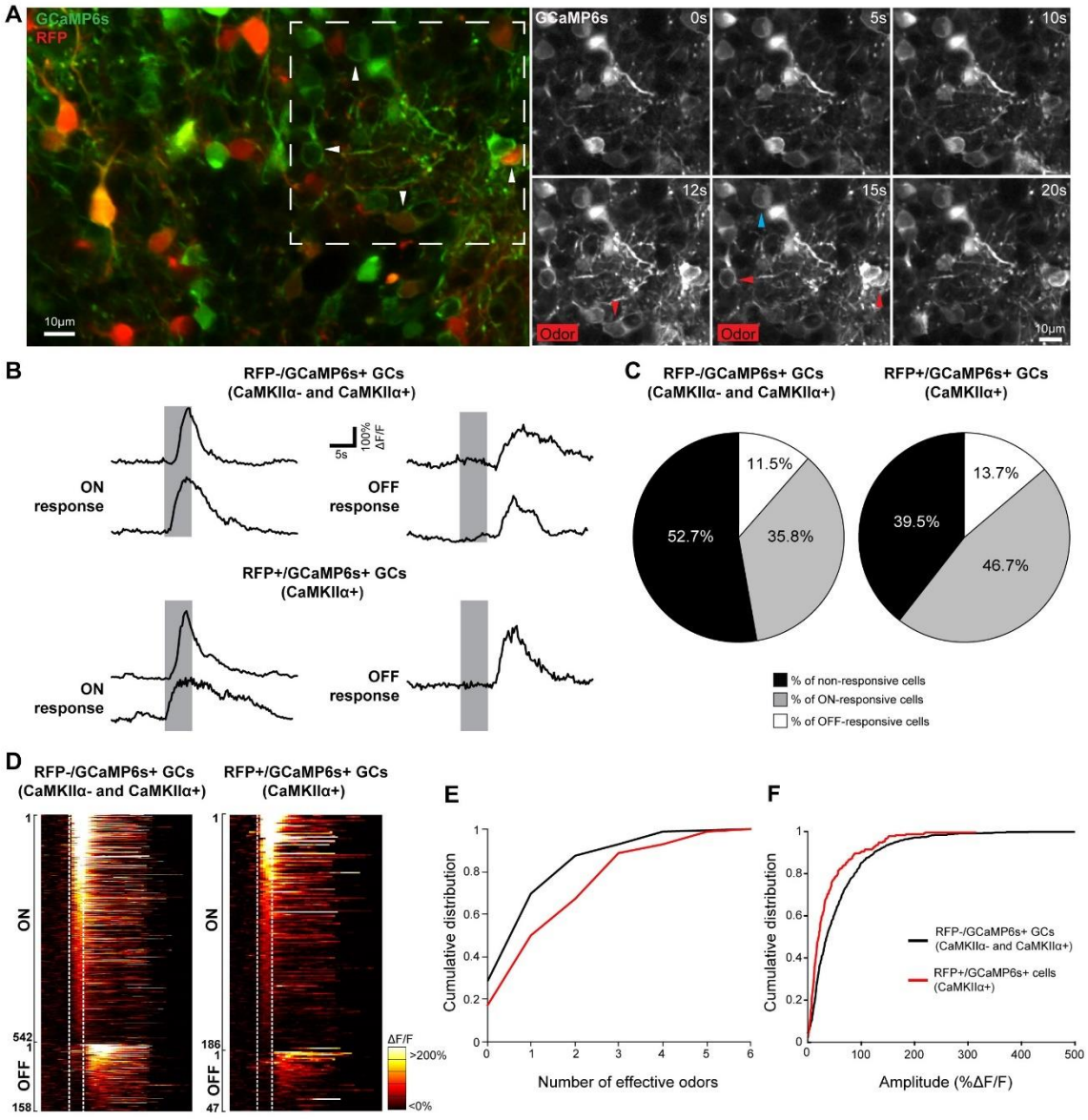

Figure 2.3: Sensory stimulation induces higher Ca^{2+} activity in CaMKIIα+ GCs.

A. *In vivo* two-photon Ca^{2+} imaging of RFP+/GCaMP6s+ (CaMKIIα+) and RFP-/GCaMP6s+ GCs following a 5-s odor stimulation with six structurally different odors. The odor application interval is indicated in the upper right corner. Arrowheads indicate responsive (red) and non-responsive (blue) cells. **B-C.** Sample traces and quantification of ON and OFF responsive and non-responsive GCs for both populations. Odor application is indicated by the gray box. **D.** Pseudo-colored heatmaps of ON and OFF responsive GCs for RFP-/GCaMP6s+ and RFP+/GCaMP6s+ are shown. Cell-odor pairs are sorted according to the amplitude of their responses. **E-F.** Cumulative distributions of odor tuning and ΔF/F responses of RFP-/GCaMP6s+ and RFP+/GCaMP6s+ (CaMKIIα+) GCs.

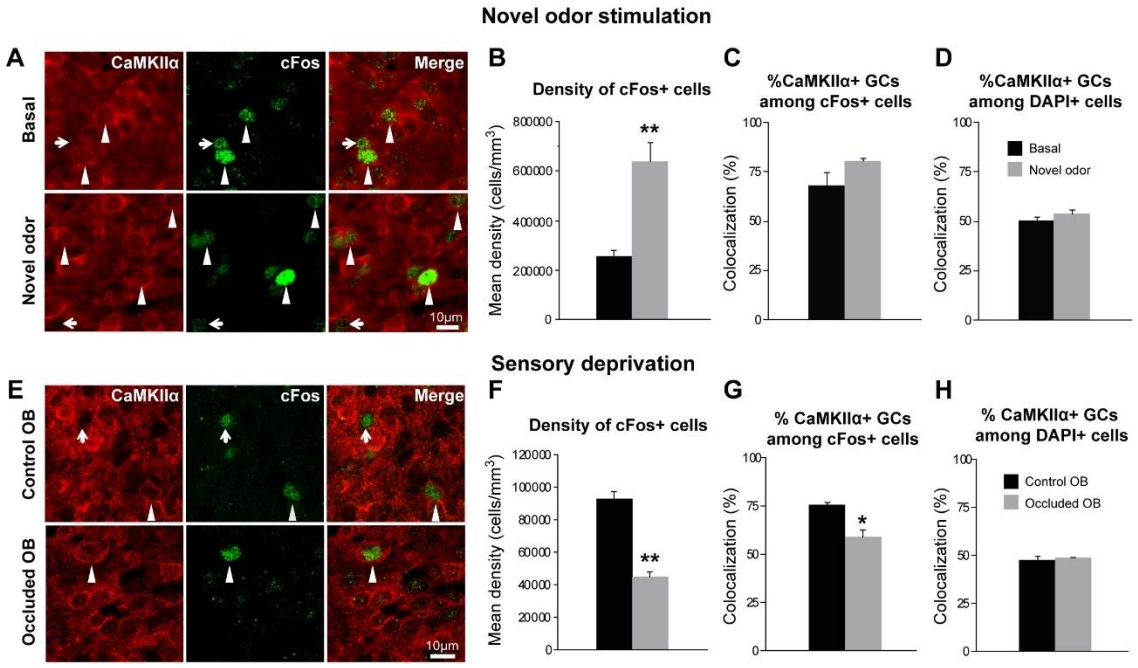

Figure 2.4: CaMKIIα+ cells are more responsive to sensory activity

A. Representative images of activated cFos+ GCs (green) also expressing CaMKIIα (red) in the basal state (top panel) and following an acute odor stimulation (bottom panel). **B.** The total density of cFos+ cells in the GCL increased after the acute odor exposure. **C-D**. Percentage of cFos+ (basal: n=190 cells; acute exposure: n=342 cells, n=3 mice, **C**) and DAPI+ (basal: n=1940 cells; acute exposure: n=2012 cells, n=3 mice; **D**) GCs co-expressing CaMKIIα in the basal state and following an acute odor stimulation. ***p*<0.01 Student's *t*-test. **E-H**. Effect of sensory deprivation on CaMKIIα+ GC activation. **E.** CaMKIIα and cFos immunolabeling in control (top panel) and odor-deprived (bottom panel) OBs 24 h after unilateral nostril occlusion. The arrows and arrowheads indicate CaMKIIα−/cFos+ and CaMKIIα+/cFos+ GCs, respectively. **F.** Mean density of activated cFos+ GCs in the GCL of control and odor-deprived OBs. **G.** The percentage of cFos+/CaMKIIα+ GCs was significantly lower in the occluded OB (gray) following the 24-h sensory deprivation (control OB: n=222 cells; occluded OB: n=79 cells, n=3 mice). **H.** Percentage of CaMKIIα+/DAPI+ GCs (control OB: n=616 cells; occluded OB: n=560 cells, n=3 mice). *p<0.05, **p<0.01 paired Student's *t*-test.

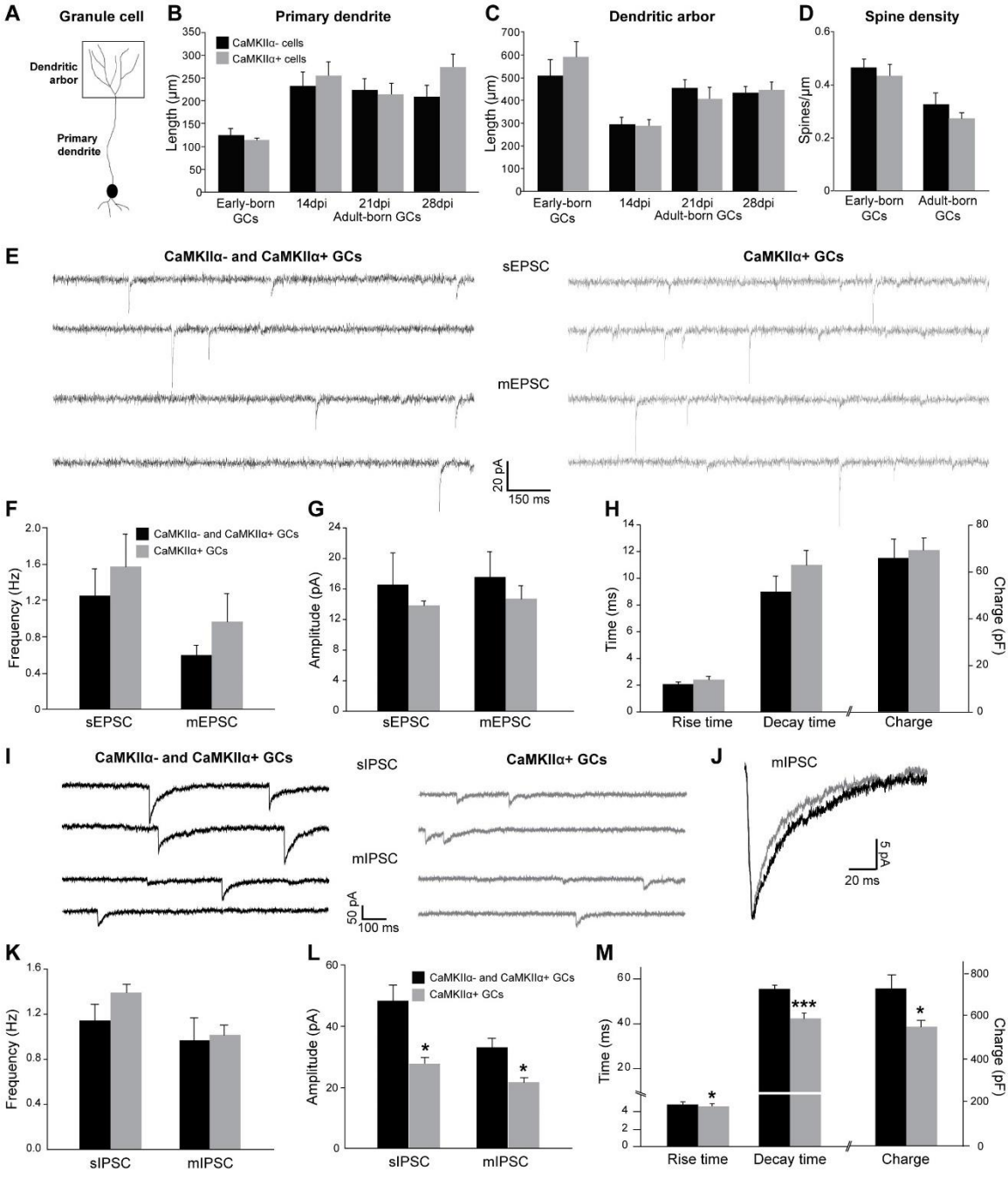

Figure 2.5: Morphological and functional characteristics of CaMKIIα+ and CaMKIIα- GCs

A. Schematic representation of GC morphology. **B-D.** Morphological analysis of early-born and adult-born CaMKIIα+ and CaMKIIα- GCs. The lengths of the primary dendrites (**B**), dendritic arborizations (**C**), and spine densities (**D**) were similar for both GC subtypes. **E.** sEPSCs and mEPSCs were recorded from CaMKIIα-GFP (gray traces) and CBA-GFP (black traces) AAV infected GCs. **F-H.** The frequencies (**F**) and amplitudes (**G**) of sEPSCs and mEPSCs, as well as the rise times, decay times, and charges (**H**) of mEPSCs from the two GC populations were indistinguishable. sEPSCs: GCs (n=9), CaMKIIα+ GCs (n=7); mEPSCs: GCs (n=7), CaMKIIα+ GCs (n=7). **I.** Examples of sIPSCs and

mIPSCs recorded from CaMKIIα-GFP− (gray traces) or CBAGFP- (black traces) infected GCs. **J.** Scaled mIPSCs recorded in a CaMKIIα+ GC (gray trace) and the general population of GCs (black trace). **K-L.** The frequencies of the sIPSCs and mIPSCs of the two GC populations were the same (**K**), whereas the amplitude was significantly lower in CaMKIIα+ GCs (**L**). **M.** The rise times, decay times, and charges of mIPSCs from CaMKIIα+ GCs were also significantly different from those from the general population of GCs. sIPSCs: n=11 GCs, CaMKIIα+ GCs (n=9); mIPSCs: GCs (n=10), CaMKIIα+ GCs (n=8), **p*<0.05, ****p*<0.001 Student's *t*-test.

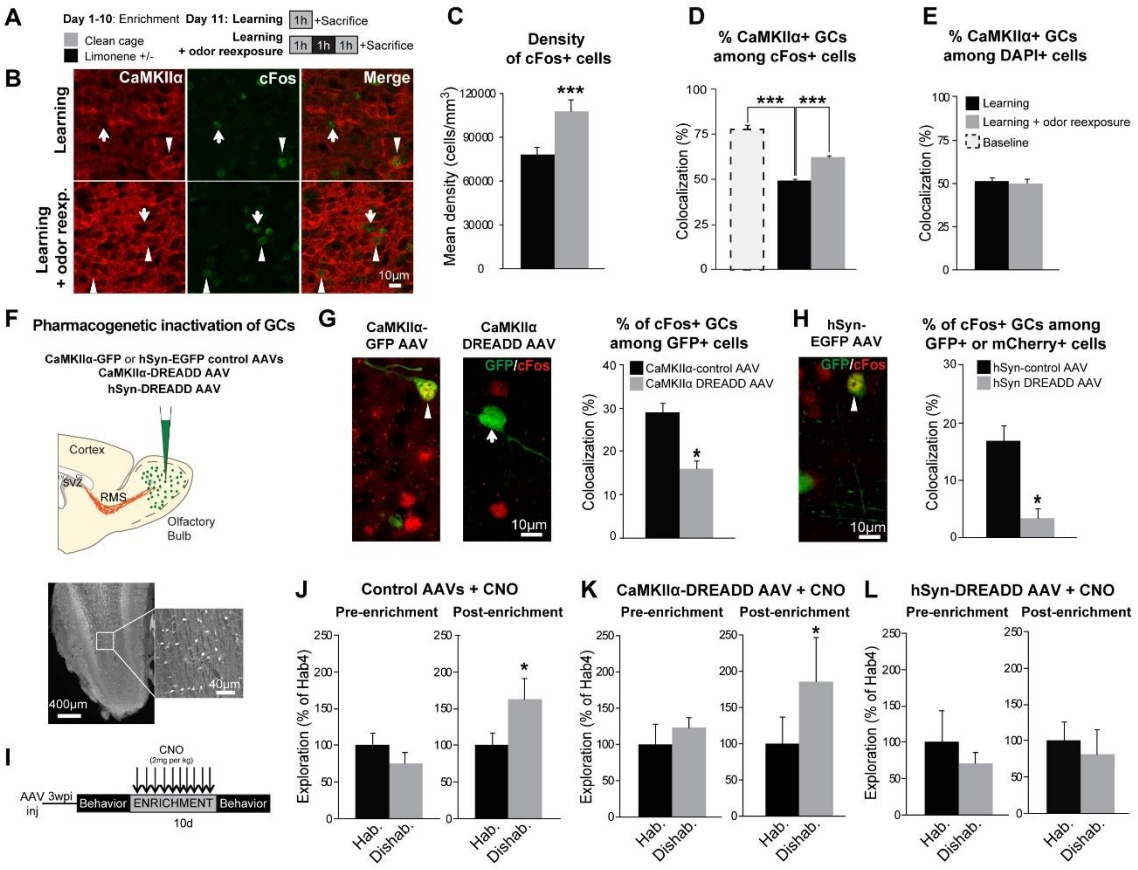

Figure 2.6: CaMKIIα+ GCs are not required for perceptual learning

A. Experimental procedure for the perceptual learning task. **B.** Representative images of cFos and CaMKIIα immunolabeling after learning (Learning) and learning followed by odor re-exposure (Learning + Odor re-exposure). **C.** Density of cFos+ cells following the perceptual learning task. **D.** Percentage of cFos+/CaMKIIα+ GCs following the perceptual learning task. For comparison purposes, the percentage of cFos+/CaMKIIα+ GCs observed in baseline conditions (**Figure 2.2I**) is plotted (dashed bar). **E.** Percentage of DAPI+/CaMKIIα+ GCs. **F.** Schematic representation and photomicrograph of AAV injections in the OB to pharmacogenetically modulate GC subtypes activity. **G.** Confocal image of a coronal OB section and quantification of GFP+/cFos+ GCs following CNO injection. Representative images of GCL injected with a control (left panel) or a CaMKIIα- DREADD-expressing AAV (right panel), labeled with GFP, are shown. **p*<0.05 paired Student's *t*-test. H. Confocal image and quantification of GFP+/cFos+ in Syn-GFP and mCherry+/cFos+ in Syn-DREADD GCs following CNO injection. **p*<0.05 Student's *t*-test. **I.** Experimental protocol used to inactivate CaMKIIα+ GCs during the perceptual learning task. **J-L.** Mean exploration time, expressed as the percentage of increase during the presentations of dishabituation *vs.* habituation odors, of control CaMKIIα-GFP or Syn-GFP AAV (**J**), CaMKIIα-DREADD (**K**), and Syn-DREADD (**L**) AAV-injected mice before and 10 days after the enrichment period. **p*<0.05 paired Student's *t*-test. n=18, 7, and 10 mice for the control, CaMKIIα-DREADD, and Syn-DREADD groups, respectively.

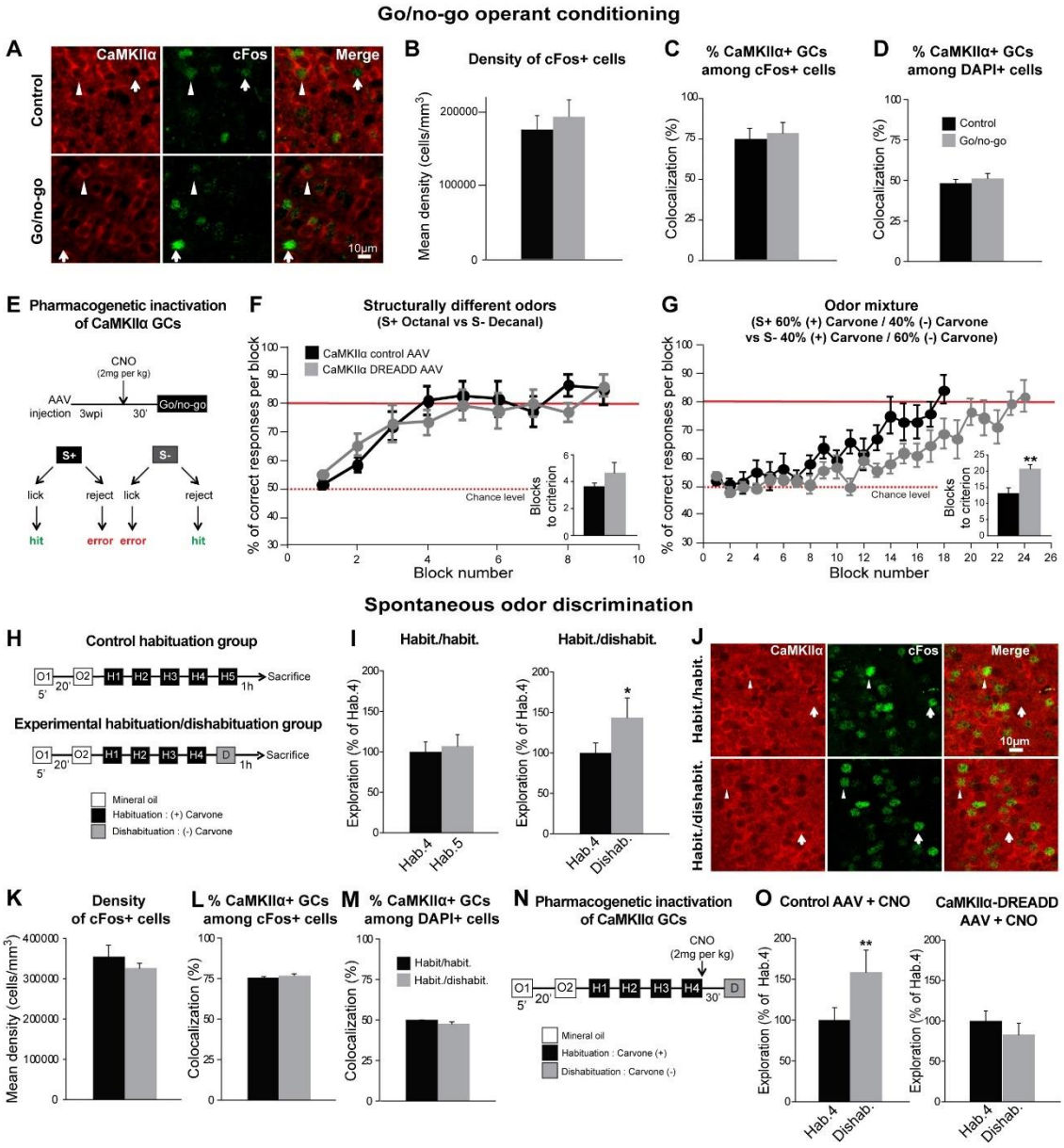

Figure 2.7: CaMKIIα+ GCs are required for go/no-go odor discrimination learning and spontaneous odor discrimination

A. CaMKIIα (red) and cFos (green) immunolabeling in the control (top panel) and experimental (bottom panel) groups following a go/no-go odor discrimination task. The arrows and arrowheads indicate CaMKIIα− and CaMKIIα+ GCs, respectively. **B.** The density of cFos-immunolabeled cells did not change following the go/no-go task (n=3 mice per group). **C.** Percentage of cFos+/CaMKIIα+ cells (n=847 and 766 cells from 3 mice for the control and experimental groups, respectively). **D.** Percentage of CaMKIIα+/DAPI+ GCs (n=4500 and 5278 cells from 3 mice for control and experimental groups, respectively). **E.** Experimental design for the pharmacogenetic inhibition of CaMKIIα+ GCs during the go/no-go odor discrimination task. **F-G.** Pharmacogenetic inhibition of CaMKIIα+ GCs affected complex odor mixture discrimination (**G**) but spared that of structurally distinct odors (**F**). ***p*<0.01, Student's *t*-test. n=7 and 8 mice for the control and CaMKIIα-DREADD groups, respectively.

H. Schematic representation of the spontaneous odor discrimination task. **I.** Mean exploration time of mice in the experimental and control groups exposed to either a new dishabituation odor or the same habituation odor, respectively (n=11 and 8 mice respectively). *p<0.05, paired Student's t-test. **J.** Confocal images of cFos- and CaMKIIα-immunolabeled GCs in the control habituation (top panel) and experimental habituation/dishabituation groups (bottom panel). The arrows and arrowheads indicate CaMKIIα− and CaMKIIα+ GCs, respectively. **K.** The density of cFos-immunolabeled cells did not change following the discrimination task (n=4 mice per group). **L.** Percentage of cFos+/CaMKIIα+ cells in the two groups (n=484 and 587 cells from 4 mice for the habituation and habituation/dishabituation groups, respectively). **M.** Percentage of CaMKIIα+/DAPI+ GCs (n=891 and 1035 cells from 4 mice from the habituation and habituation/dishabituation groups, respectively). **N.** Experimental protocol for the pharmacogenetic inhibition of CaMKIIα+ GCs during the odor discrimination task. **O.** While administering CNO to control CaMKIIα-GFP mice did not affect discrimination (left histogram), administering CNO resulted in a complete block of odor discrimination in CaMKIIα-DREADD mice (right histogram). **p<0.01 paired Student's t-test. n=9 and 10 mice for the control and CaMKIIα-DREADD groups, respectively. See also **Figure S2.1.**

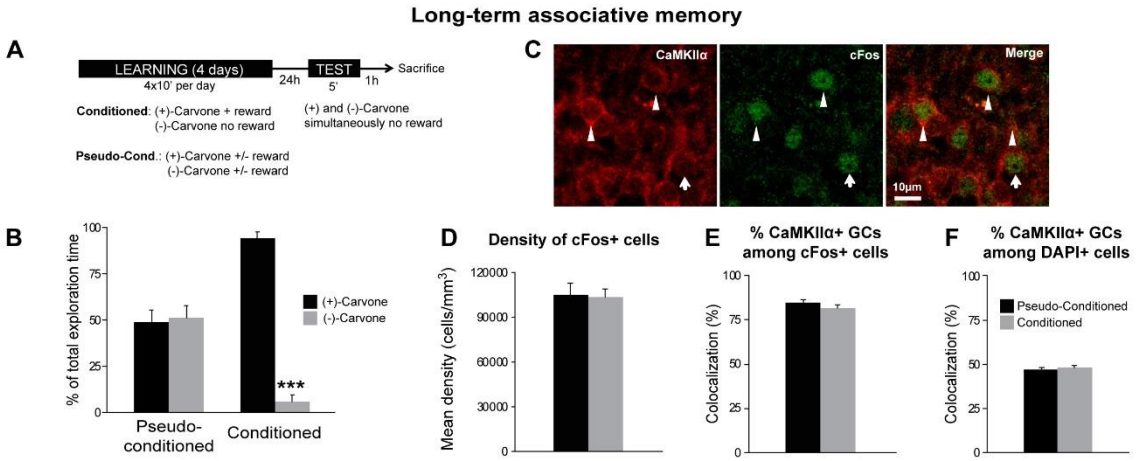

Figure S2.1: GCs subtypes activation during long-term associative memory.

Related to Figure 2.7. A. Experimental design of the long-term associative memory task. **B.** Long-term associative memory behavioral results after the 24-h task. Mice from the pseudo-conditioned group (n=5) spent the same percentage of time exploring both odorants. Conditioned mice (n=10) expressed a clear preference for the odorant previously associated with the odor reward. ***p<0.001 paired Student's t-test. **C.** CaMKIIα (red) and cFos (green) immunolabeling. The arrows indicate a CaMKIIα- GC. The arrowheads indicate a CaMKIIα+ GC. **D.** No difference in the density of cFos+ GCs was observed between the two groups. **E**. No change in the percentage of cFos+/CaMKIIα+ GCs was observed after the long-term associative learning task (pseudo-conditioned: n=291 cells, n=3 mice; conditioned: n=397 cells, n=4 mice). **F.** Percentage of DAPI+/CaMKIIα+ GCs (pseudo-conditioned: n=841 cells, n=3 mice; conditioned: n=1587 cells, n=5 mice).

12. Acknowledgments

This work was funded by an operating grant from the National Science and Engineering Research Council of Canada (NSERC) and a grant from the Canadian Institutes of Health Research (CIHR; MOP 105859) to A.S., CIHR and Brain Canada grants to P.D.K., and CNRS, INSERM, Université Pierre et Marie Curie (UPMC), and Fondation Lejeune grants to A.T. and I.C. The Development and Plasticity of Neural Networks team is affiliated with the Bio-Psy Laboratory of Excellence. This work was also supported in part by the *Investissements d'Avenir* program managed by the Agence Nationale de la Recherche under reference ANR-11-IDEX-0004-02 and L.D. benefited from an extension of her doctoral fellowship from the Bio-Psy Laboratory of Excellence. S.G. benefited from a postdoctoral fellowship from Region Île de France (DIM NerF). We thank Erik Belanger and Feng Wang for help with the two-photon imaging software. A.T and I.C. thank the Institut de Biologie Paris Seine for the imaging and animal facilities. A.S. holds a Canada Research Chair in postnatal neurogenesis.

13. Supplementary movie legends

Movie 2.1: In vivo Ca^{2+} imaging of GCs during odor stimulation, Related to Figure 2.1

Le fichier vidéo a été déposé séparément.

Ca^{2+} activity and ΔF/F quantification in GCaMP6s-expressing GCs during an odor stimulation with valeric acid. The time is indicated in the upper left corner. The odor application interval is indicated by the red box on ΔF/F quantification graph. Note ON-, OFF-, and non-responsive GCs.

Movie 3.2: In vivo Ca^{2+} imaging of two populations of GCs under baseline conditions, Related to Figure 2.2

Le fichier vidéo a été déposé séparément.

Two-minute movie showing Ca2+ fluctuations in GCaMP6s-expressing GCs under baseline conditions. Changes in fluorescence levels were clearly identifiable in the RFP+/GCaMP6s+ GC soma (CaMKIIα+) but not the RFP-/GCaMP6s+ GC soma during the 2-min acquisition period. The time is indicated in the upper left corner.

CHAPTER II : THE ROLE OF CALRETININ-EXPRESSING GRANULE CELLS IN OLFACTORY BULB FUNCTIONS AND ODOR BEHAVIOR

1. Résumé

Chez la souris adulte, le bulbe olfactif reçoit quotidiennement de nouveaux neurones qui se différencient principalement en cellules granulaires (CGs). Bien que différents sous-types de CGs nouvellement générées aient pu clairement être identifiés, le rôle joué par chacun de ces sous-types dans le fonctionnement du réseau bulbaire ainsi que dans les différents comportements olfactifs demeurent méconnus. De plus, il reste à déterminer si au sein d'une même sous-population il existe des différences morpho-fonctionnelles selon que les cellules aient été générées au cours du développement post-natal ou à l'âge adulte. Nous montrons ici que les cellules nouvellement générées exprimant ou non la calrétinine (cellules CR+ ou CR- respectivement), ainsi que les CGs CR+ générées au cours du développement post-natal diffèrent quant aux entrées inhibitrices qu'elles reçoivent, mais présentent des entrées excitatrices et des caractéristiques morphologiques similaires. En effet, la fréquence des courants inhibiteurs post-synaptiques ainsi que l'expression de la protéine gephyrin sont inférieurs chez les cellules CR+, par rapport aux cellules CR- nouvellement générées. De plus, les CGs CR+ présentent également une activation plus importante à la suite de tests comportementaux de discrimination olfactive, comme le révèle notre analyse de l'expression de gènes d'induction précoce. Ce résultat fut confirmé également suite à l'inhibition pharmacogénétique des CGs CR+, entrainant une altération des capacités de discrimination fine. Ainsi, nos résultats montrent que les CGs CR+ et CR- nouvellement générées présentent des propriétés morpho-fonctionnelles différentes, mais que ces propriétés sont similaires au sein même de la population de cellules CR+, indépendamment de leur période de développement. Finalement, nous montrons que les cellules CR+ jouent un rôle dans la discrimination olfactive fine.

2. Abstract

The adult mouse olfactory bulb is continuously supplied with new neurons that mostly differentiate into granule cells (GCs). Different subtypes of adult-born GCs have been identified, but their maturational profiles and their roles in bulbar network functioning and odor behavior remain elusive. It is also not known whether the same subpopulations of GCs born during early postnatal life (early-born) or during adulthood (adult-born) differ in their morpho-functional properties. Here, we show that adult-born calretinin-expressing (CR+) and non-expressing (CR−) GCs, as well as early-born CR+ GCs, display distinct inhibitory inputs but indistinguishable excitatory inputs and similar morphological characteristics. The frequencies of inhibitory post-synaptic currents were lower in early-born and adult-born CR^+ GCs than in adult-born CR− neurons. These findings were corroborated by the reduced density of $gephyrin^+$ puncta on CR+ GCs. CR+ GCs displayed a higher level of activation following olfactory tasks based on odor discrimination, as determined by an immediate early gene expression analysis. Pharmacogenetic inhibition of CR+ GCs diminished the ability of the mice to discriminate complex odor mixtures. Altogether, our results indicate that distinct inhibitory inputs are received by adult-born CR+ and CR− GCs, that early- and adult-born CR+ neurons have similar morpho-functional properties, and that CR+ GCs are involved in complex odor discrimination tasks.

3. Introduction

Granule cells (GCs) are the most abundant neuronal population in the olfactory bulb (OB). They make reciprocal dendro-dendritic synapses with mitral cells (MCs) and tufted cells (TCs) (Isaacson and Strowbridge, 1998) and are involved in the fine spatio-temporal tuning of the responses of these principal OB neurons to odors (Fukunaga et al., 2014; Lagier et al., 2004; Lagier et al., 2007). GCs receive glutamatergic inputs from MC/TCs and top-down fibers (Lepousez et al., 2014; Whitman and Greer, 2007) and inhibitory inputs from short-axon and Blanes cells (Pressler and Strowbridge, 2006; Ravi et al., 2017). The disinhibition of GCs (Nunes and Kuner, 2015) and the pharmacogenetic and/or optogenetic manipulation of their activity (Grelat et al., 2018; Gschwend et al., 2015) affects the ability of mice to discriminate chemically similar odors and odor mixtures.

GCs are continuously renewed throughout life. During adulthood, neuronal precursors born in the subventricular zone (SVZ) of the lateral ventricle migrate along the rostral migratory stream (RMS) and, once in the OB, differentiate into inhibitory interneurons and integrate into the already functioning bulbar network (Belluzzi et al., 2003; Carleton et al., 2003; Petreanu and Alvarez-Buylla, 2002). Adult-born GC-mediated inhibition is required for the maintenance of the synchronized activity of MCs (Breton-Provencher et al., 2009). Environmental, pharmacological, optogenetic, and genetic manipulations that affect the number or activity of adult-born neurons modulate short-term odor memory (Breton-Provencher et al., 2009; Rochefort et al., 2002), olfactory perceptual learning(Moreno et al., 2009), fine olfactory discrimination (Alonso et al., 2012; Enwere et al., 2004), and innate olfactory responses (Sakamoto et al., 2011). While these studies have considered GCs as a homogenous population of neurons, different GC subtypes have been identified based on their localization pattern and their expression of calretinin (CR) (Batista-Brito et al., 2008), metabotropic glutamate receptor 2 (mGluR2) (Murata et al., 2011), Ca^{2+}/calmodulin-dependent protein kinase II α (CaMKIIα) and IV (CaMKIV) (Zou et al., 2002), and glycoprotein 5T4 (Takahashi et al., 2016). The roles of these distinct GC subpopulations in OB network functioning

and odor behavior may be quite different, depending on the level of activation of the cells by a given behavioral paradigm and their roles in the bulbar network. It is also unclear whether there are any morpho-functional differences between the same subpopulation of GCs born during early postnatal life or during adulthood. To start addressing these issues, we studied the integration and functional roles of CR-expressing and non-expressing (CR^+ and CR^-, respectively) adult-born and CR^+ early-born GCs in the OB.

We showed that early-born CR^+ and adult-born CR^+ and CR^- GCs display similar dendritic arborization and spine density on secondary dendrites, and receive the same excitatory inputs. However, the frequencies of inhibitory post-synaptic currents were lower in both early-born and adult-born CR^+ GCs than in adult-born CR^- GCs. In agreement with these functional results, an immunohistochemical analysis showed that there are fewer gephyrin$^+$ puncta on the primary dendrites of adult-born CR^+ GCs. We then assessed the involvement of CR^+ GCs in different odor behavior tasks by co-immunolabeling for CR and the immediate early genes *cFos* and *Zif268*. Our results showed that CR^+ GCs are involved in olfactory behaviors based on odor discrimination and that the pharmacogenetic inhibition of CR^+ GCs results in a significant decrease in the fine odor discrimination ability of mice. Our results, thus, show that distinct inhibitory inputs impinge on adult-born CR^+ and CR^- GCs, that early-born and adult-born CR^+ GCs have similar morpho-functional properties, and that the CR^+ GC subtype makes an important contribution to fine odor discrimination.

4. Results

A. CR^+ and CR^- GCs display similar morphological characteristics

Two different approaches were used to assess the morphological properties of adult-born CR^+ and CR^- GCs. First, a GFP-encoding lentivirus was injected into the RMS of adult C57Bl/6 mice, and OB sections were immunolabeled for CR at three and five weeks post-injection (wpi) (**Figure 3.1a, b)**. The pattern of localization of CR^+ GCs in the granule cell layer (GCL) was not uniform and displayed a higher

density in the superficial part of the GCL, which is why we decided to focus our study on GCs in that region (up to 200 µm from the mitral cell layer (MCL)). The mean lengths of the primary, secondary, and basal dendrites were then measured, and the average spine densities of the secondary dendrites of CR+ and CR- virally labeled GCs in the superficial GCL were determined (**Figure 3.1c–f**). No differences in these parameters were observed between the two subtypes of GCs at three and five wpi (**Figure 3.1b–f; Table 3.1).** At three wpi, the CR+ and CR- adult-born GCs had fully developed primary and secondary dendrites that did not grow any further (**Figure 3.1c, d; Table 3.1**). This was in line with our previous observations that GCs reach maturity at three wpi following the injection of viral vectors into the RMS (Breton-Provencher et al., 2016). There was also no significant difference in the mean length of the basal dendrites, although a tendency towards higher values in CR- GCs was observed at both three and five wpi (**Figure 3.1e; Table 3.1**). The spine densities of the secondary dendrites of the adult-born CR+ and CR- GCs were also indistinguishable at three and five wpi (**Figure 3.1f; Table 3.1**).

While this approach makes it possible to compare the structural properties of adult-born CR+ and CR- GCs in fixed brain samples, it cannot be used to identify and functionally characterize these two subtypes in acute brain slices. We thus used a second approach to characterize the morpho-functional properties of CR+ and CR- GCs. A mixture of Cre-dependent and Cre-independent AAVs driving GFP and tdTomato expression, respectively, were co-injected into the RMS of adult Calretinin-Cre (CR-Cre) mice (**Figure 3.1g)**. The maturational profiles of these cells at one, three, and five wpi were first analyzed. No differences in the mean lengths of the primary, secondary, and basal dendrites, or the average spine densities of the secondary dendrites of adult-born CR+ and CR- GCs in the superficial GCL at one, three, or five wpi, were observed (**Figure 3.1h–m; Table 3.1**). Adult-born CR+ and CR- GCs displayed an immature morphology, with short secondary dendrites and few spines at one wpi (**Figure 3.1h, k and m; Table 3.1**). They had, however, fully formed primary dendrites that had not grown any further at three wpi and five wpi (**Figure 3.1h–j; Table 3.1**). This is consistent with observations that basal and primary dendrites start to develop rapidly as soon as adult-born GCs reach the GCL

and that developing GCs receive their first synaptic inputs on their basal dendrites (Carleton et al., 2003; Whitman and Greer, 2007). The main changes in the maturational profiles of adult-born CR+ and CR- GCs occurred between one and three wpi and manifested as a two–fold increase in the length of the secondary dendrites ([F(2,6) = 15.5, p = 0.04, one-way ANOVA followed by a Bonferroni post-hoc test for CR+ GCs, p = 0.02; F(2,6) = 46.3, p = 0.0002, one-way ANOVA followed by a Bonferroni post hoc test for CR- GCs, p = 0.0004]; **Figure 3.1k; Table 3.1**) and in spine densities ([F(2,6) = 19.8, p = 0.01, one-way ANOVA followed by a Bonferroni post hoc test for CR+ GCs, p = 0.01; F(2,6) = 30.6, p = 0.0007, one-way ANOVA followed by a Bonferroni post hoc test for CR- GCs, p = 0.0009]; **Figure 3.1m; Table 3.1**). These changes were not, however, subtype-specific and were the same for CR+ and CR- GCs. CR+ and CR- GCs already had a mature morphology at three wpi that was very similar to that observed at five wpi in terms of the lengths of their primary and secondary dendrites and their spine densities (**Figure 3.1; Table 3.1**). Two different approaches thus show that the maturational profiles of adult-born CR+ and CR- GCs are indistinguishable.

To determine whether the structural properties of CR+ GCs differ depending on the developmental period during which they are generated, the primary, secondary, and basal dendrites as well as the spine densities of CR+ early-born and adult-born GCs were measured at five wpi. To compare the properties of fully mature early-born CR+ GCs with those of adult-born CR+ neurons, the Cre-dependent AAV was injected into the RMS of P12 CR-Cre mice, and their morphologies in the OB were examined at five wpi (**Figure 3.1g**). No differences in their morphological parameters were observed (**Figure 3.1i–m; Table 3.1).**

These results suggest that superficial GCs have the same morphological characteristics independently of their phenotype (CR+ *vs*. CR-) and the developmental period during which they are generated (early-born CR+ *vs.* adult-born CR+ GCs).

B. CR+ and CR– GCs receive similar excitatory but different inhibitory inputs

We next determined whether CR+ and CR– GCs are functionally distinct and have different passive and/or active membrane properties or receive different excitatory and/or inhibitory inputs. The same labeling strategy described above (co-injection of Cre-dependent and Cre-independent GFP and tdTomato AAVs into CR-Cre mice) was used to compare postsynaptic currents in adult-born CR+ and CR– GCs. Whole-cell patch-clamp recordings were taken at three and five wpi in acute OB slices. To target early-born CR+ GCs, another transgenic mouse line obtained from the cross-breeding of CR-Cre mice with GFP reporter mice (CAG-CAT-GFP), in which all CR+ cells express GFP, was used (**Figure 3.2a**). It has been previously shown that adult-born neurons make up only 10-15% of the entire populations of GCs (Lagace et al., 2007; Ninkovic et al., 2007). As such, the vast majority of GFP+ cells in this mouse line are early-born CR+ GCs.

We first measured intrinsic membrane properties of adult-born CR+ and CR– GCs at three and five wpi, as well as early-born CR+ GCs. No differences in the resting membrane potential (Vm), the membrane resistance (Rm), the capacitance (Cm), as well as the activation threshold of voltage-gated Na^+ current (I_{Na+}) and its peak amplitude were observed (**Table 3.2**). We next recorded action potential dependent and independent spontaneous excitatory and inhibitory events from adult-born CR+ and CR– GCs at three and five wpi, as well as early-born CR+ GCs. GCs receive excitatory inputs from MC/TCs and centrifugal fibers (Didier et al., 2001; Whitman and Greer, 2007) and inhibitory inputs from short-axon and Blanes cells (Pressler and Strowbridge, 2006). To record spontaneous excitatory postsynaptic currents (sEPSCs), $GABA_A$ receptors were blocked by the bath application of bicuculline methochlorine (BMI). No differences in sEPSC amplitudes or frequencies were observed between adult-born CR+ and CR– GCs at three wpi (**Figure 3.2b–d; Table 3.3**). An analysis of action potential-independent miniature EPSCs (mEPSCs) isolated by the application of tetrodotoxin (TTX) also showed that the two sub-populations of adult-born GCs have similar mEPSC amplitudes and frequencies (**Figure 3.2b–d; Table 3.3**). To determine whether functional differences between

adult-born CR+ and CR- GCs may arise at later time-points, patch-clamp recordings were also performed at five wpi. Again, no differences between CR+ and CR- adult-born GCs were observed in terms of the amplitudes and frequencies of their sEPSCs and mEPSCs (**Figure 3.2b–d; Table 3.3**). These results suggest that excitatory inputs impinging on CR+ and CR- GCs are indistinguishable. To determine whether there are any differences in the same population of GCs that are generated during different stages of life, sEPSCs and mEPSCs were also recorded from early-born CR+ GCs and were compared to those recorded from adult-born CR+ neurons. sEPSCs recorded from early-born CR+ GCs were similar to those of adult-born CR+ cells at five wpi, although a difference, albeit not significant, was observed in the frequencies of sEPSCs (**Figure 3.2b–d; Table 3.3**). Similarly, the mEPSC amplitudes and frequencies of early-born and adult-born CR+ GCs were comparable **(Figure 3.2b–d; Table 3.3**). These electrophysiological results are in line with the similar spine densities of the secondary dendrites observed with adult-born CR+ and CR- GCs and early-born CR+ neurons (**Figure 3.1**).

Inhibitory postsynaptic currents (IPSCs) isolated by the bath application of kynurenic acid (Kyn) were also recorded. As with EPSCs, no differences in the amplitudes of sIPSCs and mIPSCs were noted between adult-born CR+ and CR- GCs at three and five wpi (**Figure 3.3a, b; Table 3.4**). In contrast, we observed that the frequencies of sIPSCs and mIPSCs in CR+ GCs are lower than those in CR- GCs at both three and five wpi (three wpi, sIPSCs: 0.56 ± 0.07 Hz *vs*. 0.94 ± 0.11 Hz for CR+ and CR- GCs, respectively, $p = 0.008$, Mann-Whitney *U* test; three wpi, mIPSCs 0.38 ± 0.05 Hz *vs.* 0.76 ± 0.11 Hz for CR+ and CR- GCs, respectively, $p = 0.002$, Mann-Whitney *U* test; five wpi, sIPSCs 0.28 ± 0.06 Hz *vs*. 0.67 ± 0.11 Hz for CR+ and CR- GCs, respectively, $p = 0.007$, Mann-Whitney *U* test; and five wpi, mIPSCs 0.24 ± 0.07 *vs*. 0.47 ± 0.07 for CR+ and CR- GCs, respectively, $p = 0.02$, Mann-Whitney *U* test **Figure 3.3a–c; Table 3.4).**

To provide further evidence that adult-born CR+ and CR- GCs receive distinct inhibitory inputs, we performed gephyrin immunolabeling and determined the densities of gephyrin+ puncta on cell bodies, the proximal part of primary dendrites

(up to 50 µm), and the basal dendrites of adult-born CR+ and CR- GCs in the superficial GCL. While no differences in gephyrin puncta density on the cell bodies and basal dendrites of these two subtypes of GCs were observed, the density of gephyrin+ puncta on CR- GC primary dendrites was higher than those of CR+ GCs (0.37 ± 0.04 and 0.51 ± 0.04 mean ± SE for CR+ and CR- GCs respectively, [$t(4) = 10.1$, $p = 0.01$, paired t-test]; **Figure 3.3d, e; Table 3.4**). These results are in line with the electrophysiological results and show that CR+ GCs have fewer inhibitory synapses on their primary dendrites than CR- neurons, resulting in a lower level of inhibition.

To determine whether adult-born CR+ GCs receive different inhibitory inputs than their early-born counterparts, sIPSCs and mIPSCs were also recorded from early-born CR+ GCs. As with EPSCs, there were no differences in the amplitudes and frequencies of sIPSCs and mIPSCs recorded from early- and adult-born CR+ GCs at five wpi (**Figure 3.3a–c; Table 3.4**). However, the frequencies of mIPSCs recorded from early-born CR+ GCs were significantly lower than those recorded from adult-born CR- GCs at five wpi (0.27 ± 0.04 Hz *vs.* 0.47 ± 0.07 Hz for early-born CR+ and adult-born CR- at five wpi, respectively, p = 0.043, Mann-Whitney *U* test]; **Figure 3.3a, c; Table 3.4**)**.** Altogether, these results show that although early- and adult-born CR+ GCs receive similar excitatory and inhibitory inputs, adult-born CR+ and CR- GCs in the superficial GCL receive similar excitatory but different inhibitory inputs.

C. Spontaneous odor discrimination increases the activation of CR+ GCs

To understand the involvement of CR+ GCs in olfactory behavioral tasks, the cells were immunolabeled for CR as well as the immediate early genes (IEG) *cFos* and *Zif268,* which are commonly used as cell activity markers (Guthrie et al., 1993; Sagar et al., 1988; Sultan et al., 2011). The involvement of CR+ GCs in odor discrimination tasks was tested as superficial GCs may preferentially contact TCs (Greer, 1987; Orona et al., 1983; Shepherd et al., 2004), which have been shown to synchronize the activity of iso-functional glomeruli and thus the odor discrimination ability of animals (Zhou and Belluscio, 2008). Given that no morphological or

electrophysiological differences were observed between early-born and adult-born CR+ GCs, the analysis was performed on the total population of CR+ GCs, regardless of whether they were produced during early development or adulthood.

We first used a spontaneous odor habituation/dishabituation task. As expected, the mice in the habituation/dishabituation group spent more time exploring the novel dishabituating odor than during the 4th habituation session (mean exploration time: 4.1 ± 0.5 s for the last habituation session (H4) and 5.9 ± 1.0 s for the dishabituation (D) odor, n = 10 mice, $t(10) = -2.5$, $p = 0.03$, paired t-test; **Figure 3.4a**). This increase was not observed in the habituation/habituation group, where the mice were not dishabituated (mean exploration time: 4.0 ± 0.5 s for H4 *vs.* 4.3 ± 0.6 s for H5, n = 8 mice, **Figure 3.4a**). An analysis of the densities of cFos$^+$ and Zif268$^+$ GCs in the superficial GCL did not reveal any differences between the two groups (306,855 ± 23,485 cells/mm^3 and 243,407 ± 18,507 cells/mm^3 for cFos$^+$ and 528,287 ± 77,365 cells/mm^3 and 403,618 ± 47,760 cells/mm^3 for Zif268$^+$, for the habituation and dishabituation groups, respectively), suggesting that superficial GCs undergo a similar level of activation (**Figure 3.4b, c**). We next determined whether the spontaneous odor discrimination task induces the activation of CR+ GCs by analyzing the percentage of cFos+ and Zif268+ cells among CR+ GCs (**Figure 3.4d**), and assessed whether the level of activation of CR+ and CR− GCs differs by analyzing the percentage of CR+ and CR− GCs among the cFos+ and Zif268+ cells (**Figure 3.4e**). An analysis of cFos+ cells among the CR+ GCs revealed that the odor dishabituation task induced a higher activation of CR+ GCs (% cFos+ among CR+ GCs was 26.1 ± 0.2 %, n = 634 CR+ cells) than the odor habituation task (% cFos+ cells among CR+ GCs was 20.6 ± 1.9 %, n = 713 CR+ cells) [$t(4) = 2.8$, $p = 0.04$, unpaired t-test] (**Figure 3.4b, d**). The same results were obtained with Zif268 (22.6 ± 0.8 % *vs*. 15.8 ± 0.5 % for Zif268+ cells among CR+ cells following the odor dishabituation and habituation tasks, respectively, n = 1270 and 904 CR+ GCs,) [$t(6) = -6.7$, $p = 0.0005$, unpaired t-test] (**Figure 3.4d**). Although these results indicated that CR+ GCs are activated by the spontaneous odor discrimination task, they do not show whether the activation is higher in the CR+ subtype or whether it occurs in all superficial GCs, including CR− GCs. We thus determined the percentage of CR+

GCs (and by consequence CR– GCs) among cFos+ and Zif268+ cells. The percentage of CR+ GCs among cFos+ and Zif268+ cells also increased (14.2 ± 1.1 % *vs*. 10.1 ± 1.0 % for CR+ GCs among cFos+ GCs, n = 1228 and 1443 cFos+ cells for the dishabituation and habituation groups, respectively) [$t(4) = 2.8$, $p = 0.04$, unpaired *t*-test]; (12.4 ± 1.3 % *vs*. 8.8 ± 0.4 % for CR+ GCs among Zif268+ GCs, n = 2553 and 1653 Zif268+ cells) [$t(6) = -2.47$, $p = 0.04$, unpaired *t*-test] (**Figure 3.4e**). These results show that there is greater CR+-specific activation of GCs following the spontaneous odor discrimination task.

D. The go/no-go olfactory learning task induces the activation of CR+ GCs

Since the spontaneous discrimination task caused a significant increase in CR+ GC recruitment, we hypothesized that this subtype would be also activated by an operant go/no-go odor discrimination task. An olfactometer was used to train the mice to associate a stimulus odor (octanal: S+) with a water reward. When the S+ odor is presented, the mice should lick the water port and when a non-reward associated odor (decanal: S−) is presented, the animals should not lick the water port. We considered that the mice were able to discriminate correctly between the two odors when they reached the 85 % criterion of correct responses. For the control group, the water was presented independently of the S+ or S− odor. As expected, the control group reached the 85 % criterion very rapidly (one block) whereas the experimental group needed more blocks to reach the criterion (mean of 4.8 blocks) (**Figure 3.5a**). To avoid bias in the activation of GCs because of different levels of exposure of the control and experimental groups to the odors, the mice in the control group, like the mice in the experimental group (go/no-go), had to complete five blocks. No differences in the densities of cFos+ and Zif268+ GCs were observed between the two groups (for cFos: 473,883 ± 47,932 cells/mm^3 and 410,158 ± 24,965 cells/mm^3, go/no-go and control groups, respectively; and for Zif268: 630,814 ± 59,064 cells/mm^3 and 570,921 ± 44,985 cells/mm^3 for the go/no-go and control groups, respectively; **Figure 3.5b, c**). However, the percentage of activated cFos/CR+ GCs was higher after the go/no-go odor discrimination task. The mean percentages of cFos+ cells among CR+ GCs were 30.7 ± 1.7 % *vs*. 23.5 ± 0.8 % for

the go/no-go and control groups, n = 1590 and 1167 cells, respectively, ([t(6) = –2.9, p = 0.02, unpaired t-test] **Figure 3.5d**). The activation was higher for the CR+ sub-population of GCs since the percentage of CR+ GCs among cFos+ cells was significantly higher following go/no-go odor discrimination task, suggesting that there is a decrease in the percentage of CR– GCs among cFos+ (the mean percentage of CR+ GCs among cFos+ cells was 19.7 ± 1.7 % *vs.* 12.1 ± 0.4 %, go/no-go and control groups, n = 2732 and 2255 cells, respectively; ([t(6) = −3.1, p = 0.02, unpaired t-test]; **Figure 3.5e**). The same results were observed with Zif268. The mean percentages of Zif268+/CR+ GCs were 27.4 ± 2.1 % *vs*. 19.7 ± 0.9 %, n = 897 and 941 cells for the go/no-go and control groups, respectively; [t(6) = −2.6, p = 0.03, unpaired t-test]), and the mean percentages of CR+ GCs among Zif268+ GCs were 12.6 ± 0.4 % *vs.* 10.2 ± 0.7 % for the go/no-go and control groups, n = 1809 and 1820 cells, respectively ([t(6) = −3.2, p = 0.01, unpaired t-test]; **Figure 3.5d, e**). These results suggest that CR+ GCs are recruited following the go/no-go odor discrimination task.

E. The pharmacogenetic inhibition of CR+ GCs diminishes the fine olfactory discrimination ability of mice

Double immunolabeling for CR and Zif268 or cFos showed that CR+ GCs are activated by the odor discrimination task. To determine whether CR+ GCs are required for accomplishment of the odor discrimination task, we used pharmacogenetic tools that specifically inhibit CR+ GCs and subjected the mice to the go/no-go odor discrimination task (**Figure 3.6a**). The Cre-dependent designer receptors exclusively activated by designer drugs (DREADDs) coupled with a G_i protein AAV was injected into the GCL of the CR-Cre OB two weeks before beginning the behavioral task (**Figure 3.6a**). DREADDs-G_i activation by CNO leads to GIRK-mediated K^+ ion extrusion (Rogan and Roth, 2011) and hyperpolarization of the cell. The control group of mice was injected with AAV-GFP, and the two groups received an injection of clozapine-N-oxide (CNO) 30 min prior the task. The percentage of infected cells among the CR+ GCs at the site of injection was 45.0 ± 11.0 % (n = 403 cells from three mice), and we estimate that DREADDs-infected GCs represent about 8 % (n = three mice) of the bulbar CR+ GCs. Essentially all the

DREADDs-infected cells were CR+ (92.8 ± 0.9 %, *n* = 178 cells from three mice) and no infected CR+ periglomerular cells were observed (3.6 ± 2.0 %, *n* = 1731 cells from six mice). To test the efficiency of the pharmacogenetic inhibition, we analyzed the percentage of colocalization of reporter+ cells (GFP or mCherry) and cFos+ cells in the control (EF1α-DIO-EYFP) and DREADDs (EF1α-DIO-hM4D(G_i)-mCherry) AAV-injected CR-Cre mice at three wpi. Significantly lower percentages of reporter+/cFos+ (thus CR+/cFos+) GCs were observed 90 min following the pharmacogenetic inhibition of the CR+ GCs (4.2 ± 0.8 % *vs*. 16.0 ± 2.2 % in the DREADDs-injected and control mice, *n* = 177 and 305 cells, respectively, [$t(6) = -4.5$, $p = 0.02$, paired *t*-test]; **Figure 3.6c**). We next subjected mice to go/no-go odor discrimination task using different odor combinations that progressively increased the difficulty of the task from mixture one (**Figure 3.6d**) to mixture three (**Figure 3.6f**). As expected, the number of blocks needed to reach the criterion of 85 % of correct responses increased with the difficulty of the discrimination task for both the control and DREADDs groups. There were no differences between the mice in the two groups that were exposed to mixture one, and the two groups were equally successful in reaching the 85 % criterion in one day (the mean number of blocks to reach the 85 % criterion was 3.5 for the control group and 3.6 for the DREADDs group; *n* = 9 and 10 mice, respectively; **Figure 3.6d**). When the discrimination task became more difficult (mixture two), the mice in the DREADDs group were less successful at discriminating between the odors. Although there were no significant differences in individual blocks between the two groups, the mean number of blocks required to reach the 85 % criterion was significantly higher for the DREADDs group than for the control group (the mean number of blocks to reach the 85 % criterion was 13.6 for the DREADDs group and 10.1 for the control group, *n* = 9 and 10 mice, respectively; [$t(17) = 2.9$, $p = 0.01$, unpaired *t*-test]; **Figure 3.6e**). The difference became even more striking when the difficulty of the task was further increased with mixture three (**Figure 3.6f**). The ability of the mice in the DREADDs group to discriminate the odors in the mixture was significantly lower than that of the mice in the control group. The number of blocks needed to reach the 85 % criterion was significantly higher for the mice in the DREADDs group (the mean number of blocks

to reach the 85 % criterion was 16.3 and was obtained in a mean of 2.7 ± 0.2 days for the DREADDs group and 11.8 obtained in a mean of 2.2 ± 0.1 days for the control group, n = 10 and nine mice, respectively; [$t(18) = 3.3$, $p = 0.01$, unpaired t-test]; **Figure 3.6f**), and significant differences in individual blocks were observed beginning from block 10 (**Figure 3.6f**). These results show that CR+ GCs are involved in fine odor discrimination.

5. Discussion

We morphologically and functionally characterized CR+ and CR- GCs born at different developmental stages and used two different methods to show that CR+ neurons are involved in odor discrimination. First, an analysis of the expression of IEGs, *cFos*, and *Zif268* following spontaneous and learned odor discrimination tasks showed that CR+ GCs are activated by these tasks. Second, the pharmacogenetic inhibition of CR+ CGs reduced the ability of the mice to discriminate between two similar odor mixtures. Our morpho-functional analysis of CR+ and CR− GCs showed that there are fewer inhibitory synapses on the primary dendrites of CR+ GCs, which was corroborated by the lower frequencies of mIPSCs and sIPSCs recorded from this neuronal subtype. The reduced inhibition received by CR+ GCs may underlie the higher level of activation of this subtype following different odor discrimination tasks.

The inhibition provided by GCs in the OB synchronizes the activity of principal neurons, which is crucial for accomplishing different odor behaviors (Lepousez and Lledo, 2013). The involvement of CR+ GCs in odor discrimination remains unknown. Our observations showed that the pharmacogenetic inhibition of CR+ GCs reduces the fine discriminatory abilities of mice. It should be noted, however, that while the pharmacogenetic inhibition of CR+ GCs significantly reduced the ability of mice to discriminate between two similar odor mixtures, it did not abolish this ability completely. This can be explained by the fact that other GC subtypes also play a role in odor discrimination. For example, we recently showed that CaMKIIα+ GCs are involved in both spontaneous and go/no-go odor discrimination (Malvaut et al., 2017). In addition, we estimate that about 8 % of all CR+ GCs were infected with

DREADDs, which may also explain why the odor discrimination ability was not abolished completely. Our findings are in line with a previous study showing that the optogenetic activation of comparable number of GCs is sufficient to affect odor discrimination (Alonso et al., 2012)**.** Our results also do not rule out the involvement of CR- GCs in odor discrimination despite the fact that this subtype is less prone to activation during spontaneous and learned odor discrimination tasks. The use of pharmacogenetic or optogenetic approaches by injecting Cre-Off viral constructs into CR-Cre mice may help address this issue. CR is also expressed in the subpopulation of periglomerular interneurons (Belluzzi et al., 2003; Fogli Iseppe et al., 2016). However, our stereotaxic injections to pharmacogenetically inhibit CR+ cells in the OB were targeted to the GCL and resulted in very few virally-labeled CR+ periglomerular cells. It has been reported that periglomerular cells are involved in regulating theta, but not gamma, rhythms in the OB (Fukunaga et al., 2014), and that the odor discrimination abilities of mice depend on gamma oscillations (Lepousez and Lledo, 2013). These results suggest that the behavioral phenotypes observed following pharmacogenetic inhibition can be attributed to CR+ GCs but not CR+ periglomerular cells.

Our electrophysiological recordings showed that adult-born CR+ and CR− GCs display similar sEPSC and mEPSC amplitudes and frequencies but distinct IPSC frequencies. The frequencies of sIPSCs and mIPSCs received by adult-born CR+ GCs were comparable to those of early-born CR+ GCs but lower than those of adult-born CR− neurons at three and five wpi. Our results showing that there are fewer gephyrin+ puncta on CR+ GCs are in line with our electrophysiological results. The density of gephyrin+ puncta was lower on primary dendrites, but not on basal dendrites and cell soma, which are also targeted by inhibitory synapses in GCs (Deprez et al., 2015; Pallotto et al., 2012; Panzanelli et al., 2009). Interestingly, olfactory learning affects the density of gephyrin+ puncta on the primary dendrites of adult-born GCs but not on basal dendrites or cell soma (Lepousez et al., 2014). This indicates that inhibitory inputs to the primary dendrites of GCs may be particularly plastic and may be modified in response to the distinct sensory experiences of animals (olfactory learning) or different postsynaptic targets (CR+ or CR− GCs).

These results also suggest that CR− and CR+ GCs may display different levels of inhibitory synapse plasticity following olfactory learning. It also remains to be determined whether these two subtypes of GCs receive inhibitory inputs originating from different sources or whether the presence of CR underlies the differences in the target cell-specific formation of inhibitory synapses.

Several studies have shown that early-born and adult-born GCs have different maturational profiles and undergo distinct odor experience-modulations (Kelsch et al., 2008; Lemasson et al., 2005; Magavi et al., 2005). Surprisingly, we observed no differences in the morphological or electrophysiological profiles of early- and adult-born CR+ GCs. It should be noted that comparisons of the morpho-functional properties of GCs born at different developmental stages have, until now, been performed on the entire GC population, without distinguishing between specific neurochemical subtypes (Kelsch et al., 2008; Lemasson et al., 2005; Magavi et al., 2005). However, GCs can be sub-divided into different subtypes with distinct temporal and spatial origins (Batista-Brito et al., 2008; Lledo et al., 2008; Merkle et al., 2014; Young et al., 2007). For example, very few CR+ GCs are produced during embryogenesis, and their production in the OB peaks at P30 (Batista-Brito et al., 2008), indicating that CR+ GCs make different contributions to the overall populations of early-born and adult-born neurons. Furthermore, early-born and adult-born GCs are preferentially located in the superficial and deep GCL, respectively (Imayoshi et al., 2008; Lemasson et al., 2005), and may thus display different synaptic input/output properties. It is thus possible that comparisons of the morpho-functional properties of the entire populations of early-born and adult-born GCs over-estimate differences due to different compositions of distinct neuronal subtypes in the populations of early-born and adult-born GCs and their localization in the GCL. Further studies will be required to determine whether and how early-born and adult-born GCs belonging to the same neuronal subtype differ in their morpho-functional properties and whether they are differentially involved in odor information processing. It has been also shown that among the adult-born population, the immature adult-born GCs are more prone to activation in response to the sensory input and display transient form of long-term potentiation at their

proximal glutamatergic synapses (Magavi et al., 2005; Nissant et al., 2009). It remains to be shown weather immature and mature adult-born CR+ GCs undergo distinct level of activation following habituation/dishabituation and go/no-go odor discrimination tasks.

Lastly, it should be noted that, in addition to CR+ GCs, several other GC subtypes have been identified based on the expression of mGluR2, CaMKIIα, CaMKIV, or glycoprotein 5T4 (Murata et al., 2011; Takahashi et al., 2016; Zou et al., 2002). We (Malvaut et al., 2017) and others (Takahashi et al., 2016) have described the roles played by CaMKIIα- and 5T4-expressing GCs in different odor behaviors. A deficiency in 5T4 affects the input/output properties of this subtype of GC, which has an impact on the odor detection threshold and on odor discrimination (Takahashi et al., 2016). On the other hand, the expression of CaMKIIα defines functionally distinct subtypes of GCs involved in different odor behaviors. While CaMKIIα-expressing GCs are activated and are involved in the spontaneous and learned odor discrimination of structurally similar odors or odor mixtures, CaMKIIα-immuno-negative GCs that receive higher levels of inhibition are involved in perceptual learning (Malvaut et al., 2017). These studies, together with the results presented here, suggest that distinct GCs subtypes may be activated and involved in different odor tasks. Further studies will be required to determine the contributions of other GC subtypes to odor behavior.

Altogether, our results show that while the morpho-functional properties of early-born and adult-born CR+ GCs are indistinguishable, they receive lower levels of inhibition than adult-born CR− neurons and are involved in the odor discrimination of chemically similar odors or odor mixtures.

6. Material and methods

A. Animals

Experiments were performed using two- to four-month-old adult mice and postnatal 10-12-day-old (P10-P12) pups. The CalretininCre (CR-Cre; B6(Cg)-

Calb2$^{tm1(cre)Zjh}$/J; RRID:IMSR_JAX:010774) (Camillo et al., 2014; Taniguchi et al., 2011) mouse line and the CalretininCre::CAG-CAT-GFP line obtained by cross-breeding CR-Cre and CAGCAT- EGFP mice (FVB.B6-Tg(CAG-CAT-EGFP)1Rbns/KrnzJ; RRID:IMSR_JAX:024636) (Nakamura et al., 2006) were used. Only hemizygous mice were used. The experimental procedures were in accordance with the guidelines of Canadian Council on Animal Care (CCAC), and all animal experiments were approved by the Université Laval animal protection committee. One to four mice per cage were kept on a 12-h light/dark cycle at a constant temperature (22°C) with food and water *ad libitum,* except for the behavior experiments.

B. Stereotaxic injections

The mice were anesthetized with an intraperitoneal injection of ketamine/xylazine (10 mg/mL and 1 mg/mL respectively; 0.1 mL per 10 g of body weight) and were kept on a heating pad during the surgery. Adeno-associated or lentiviral viral vectors (AAV and LV, respectively) were stereotaxically injected into the RMS or into the granule cell layer (GCL) of the OB. The following coordinates (with respect to the bregma) were used for the RMS injections in adult mice: anterior-posterior (AP) 2.55 mm, medio-lateral (ML) 0.82 mm, and dorso-ventral (DV) 3.15 mm; and for GCL injections: AP 4.6 mm, ML 0.75 mm, DV 1 mm and AP 5.3 mm, ML 0.5 mm, DV 0.9 mm. For injections in the RMS of CR-Cre pups, the following coordinates were used: AP 2.05 mm, ML 0.65 mm, and DV 2.7 mm. The following Cre-dependent viruses were used: rAAV 2/5 CAG-Flex-GFP (200 nL; $4x10^{12}$ iu/mL; Vector Core Facility, University of North Carolina), AAV 2/5-EF1α-DIO-EYFP (200nL; $6.5x10^{12}$ iu/mL; Vector Core Facility, University of North Carolina), rAAV 2/8 EF1α-DIO-hM4D(G_i)-mCherry (500 nL; $4x10^{12}$ iu/mL; University of North Carolina Vector Core Facility), and Cre-independent: AAV 2/5 miniCBA-Td-tomato (200 nL; $1.6x10^{12}$ GC/mL; Molecular Tools Platform, CERVO Brain Research Center), rAAV 2/5 CAG-GFP (100 nL; $4x10^{12}$ iu/mL; University of North Carolina Vector Core Facility), and lentiviral vectors encoding GFP expression (LV-GFP; 200 nL; $1.75x10^{8}$ tu/mL; University of North Carolina Vector Core Facility).

C. Immunohistochemistry

The mice were given an overdose of pentobarbital (12 mg/mL; 0.1 mL per 10 g of body weight) and were perfused transcardiacally with 0.9 % NaCl followed by 4 % PFA. The OBs were resected and were post-fixed in 4 % PFA at 4 °C. Horizontal sections (30- or 100-μm-thick) or coronal sections (40-μm-thick) were cut using a vibratome (Leica VT1000S) and were incubated with the following primary antibodies: mouse anti-GFP (48 h, 1:500, Invitrogen, Cat# A-11120, RRID:AB_221568), rabbit anti-mCherry (24 h, 1:1000, Biovision, Cat# 5993-100, RRID:AB_1975001), goat anti-calretinin (24 h, 1:1000, Millipore, Cat# AB 1550, RRID:AB_90764), rabbit anti-cFos (48h, 1:40,000, Santa Cruz, Cat# Sc-52, RRID:AB_2106783), rabbit anti-Egr-1 (Zif268) (48 h, 1:150,000, Santa Cruz, Cat# Sc-110, RRID:AB_2097174), and anti-gephyrin fluorescently labeled with oyster-550 (24h, 1:1000, Synaptic Systems, Cat# 147 011C3, RRID:AB_887716). The corresponding secondary antibodies were used. Fluorescent images were captured using a confocal microscope (FV 1000; Olympus) with 60x (UPlanSApoN 60x/NA 1.40 oil; Olympus) and 40x (UPlanSApoN 40x/NA 0.90; Olympus) objectives. Gephyrin images were captured using an LSM 700 AxioObserver microscope with a 63x objective (Plan-Apochromat 63x/NA 1.40 oil DIC M27, Zeiss). The images were captured from the GCs localized in the superficial GCL of the OB (up to 200 μm from the mitral cell layer). Coronal slices derived from the anterior, medial, and posterior OB were used for the IEG analysis, and horizontal slices derived from the dorsal, medial, and ventral OB were used for the morphological analysis. For the cFos analysis, three mice were used for both the habituation and dishabituation groups (spontaneous olfactory discrimination task), and three and five mice were used for the control and go/no-go groups, respectively. For the Zif268 analysis, four mice for used for both the habituation and dishabituation groups (spontaneous olfactory discrimination task), and three and five mice were used for the control and go/no-go groups, respectively.

D. Patch-clamp recordings

Three to five weeks after the stereotaxic injections, the deeply anesthetized mice were transcardiacally perfused with modified oxygenated artificial cerebro-spinal fluid (ACSF) containing the following (in mM): 210.3 sucrose, 3 KCl, 2 $CaCl_2.2H_2O$, 1.3 $MgCl_2.6H_2O$, 26 $NaHCO_3$, 1.25 $NaH_2PO_4.H_2O$, and 20 glucose. The OBs were then quickly removed and were placed in oxygenated ACSF containing the following (in mM): 125 NaCl, 3 KCl, 2 $CaCl_2.2H_2O$, 1.3 $MgCl_2.6H_2O$, 26 $NaHCO_3$, 1.25 $NaH_2PO_4.H_2O$, and 20 glucose. Horizontal slices (250-µm-thick) were obtained using a vibratome (HM 650V; Thermo Scientific). The slices were superfused with oxygenated ACSF at a rate of 2 mL/min during the electrophysiological experiments. Recordings were amplified using a Multiclamp 700B amplifier (Molecular Devices) and digitized using a Digidata 1440A (Molecular Devices).

Patch electrodes (ranging from 6 to 9 MΩ) were filled with intracellular solution containing the following (in mM): 135 CsCl, 10 HEPES, 0.2 EGTA, 2 ATP, 0.3 GTP, and 10 glucose for spontaneous inhibitory postsynaptic current (sIPSC) recordings or 130 K-methylsulfate, 10 HEPES, 6 KCl, 2 MgATP, 0.4 NaGTP, 10 Na-phosphocreatine, and 2 ascorbate for spontaneous excitatory postsynaptic current (EPSC) recordings. The intracellular solutions were also supplemented with 5 µM Alexa-Fluor 488 (Life Technology, A10436) or Alexa-Fluor 569 (Life Technology, A10438) to ensure that the recordings were taken from GFP or td-Tomato-infected cells.

sIPSCs were isolated by the bath application of kynurenic acid (5 mM Kyn; Sigma-Aldrich, Cat# K3375) to block glutamatergic activity. (−)-Bicuculline methochloride (50 µM BMI; Abcam Cat# AB120108), a $GABA_A$ receptor antagonist, was used to isolate sEPSCs. Miniature IPSCs or EPSCs (mIPSCs or mEPSCs) were isolated by the application of tetrodotoxin (1 µM TTX; Affix Scientific, Cat# AF3015) in the presence of Kyn or BMI to block voltage-dependent sodium channels. Synaptic responses were analyzed using the MiniAnalysis program (Synaptosoft).

For electrophysiological recordings of CR+ GCs, two different Cre-dependent viruses (rAAV 2/5 CAG-Flex-GFP and AAV 2/5-EF1α-DIO-EYFP) were used. As expected, injection of these viral vectors into wild-type C57Bl/6 mice did not result in GFP expression. Surprisingly, however, CR immunostaining three weeks post-injection (wpi) of these AAVs in the RMS of CR-Cre mice revealed different levels of co-labeling for GFP and CR. While 98.0 % of superficial GFP+ GCs were colabelled for CR+ following the injection of AAV 2/5-EF1α-DIO-EYFP, only 48.6 % of GFP+ GCs were labeled for CR following the injection of rAAV 2/5 CAG-Flex-GFP. The reason for the low percentage of GFP+/CR+ GC labeling following the injection of rAAV 2/5 CAG-Flex-GFP is unclear, but is likely related to different activities of the CAG and EF1α promoters during the maturation of neuronal precursors (Jakobsson et al., 2003; Qin et al., 2010; Tsuchiya et al., 2002). CR is transiently expressed during hippocampal and cortical development (Camillo et al., 2014; Jiang and Swann, 1997) and in adult-born neuronal precursors in the dentate gyrus (Brandt et al., 2003). It is thus possible that the transient expression of CR in neuroblasts combined with the different levels of activities of the CAG and EF1α promoters drives GFP expression in a higher number of cells containing the CAG promoter than in cells containing the EF1α promoter. The same observations have been reported for the visual cortex, where cross-breeding CR-Cre mice with Cre-dependent CAG-tdTomato reporter mice results in the expression of tdTomato in cells that do not immunolabel for CR (Camillo et al., 2014). The functional responses of tdTomato+/CR+ and tdTomato+/CR- neurons in the visual cortex were, however, indistinguishable (Camillo et al., 2014). In line with this, we did not observe any differences in the electrophysiological parameters of GCs infected with either the CAG-Flex-GFP or EF1α-DIO-EYFP viral vector and thus pooled the data.

To characterize the morpho-functional properties of CR+ and CR- GCs, a mixture of Cre-dependent and Cre-independent AAVs driving GFP and TdTomato expression, respectively, were co-injected into the RMS of adult CR-Cre mice. To determine the specificity of CR- GC infection by Cre-independent AAV, we quantified the percentage of tdTomato+/GFP- GCs that were immunolabeled for CR. Our results revealed that 18.2 ± 1.5% of tdTomato+/GFP- GCs were CR+. Hence, any

difference in the morpho-functional properties observed using the two AAVs would be an underestimation given that CR− GCs group was composed of approximately 20% CR+ GCs.

E. Morphological analysis

The mice were sacrificed one, three, or five weeks after the viral vector injections into the RMS. Horizontal sections (100-µm-thick) of the OB were immunostained to reveal the presence of GFP, mCherry, and CR. Images were captured as described above. The images were zoomed four times for the spine analyses. The lengths of the primary dendrites were measured from the soma to the first branching point. The total lengths of the secondary dendrites were obtained by adding the lengths of all the individual secondary dendrites of a given cell. Basal dendrites were defined as dendrites beginning at the cell soma and extending in the opposite direction of the primary dendrite. The sum of all the basal dendrites was calculated for a given cell. Spine density was calculated by dividing the number of spines by the length of the section of the secondary dendrite. Adult-born CR+ and CR− GC morphologies at the same wpi were obtained from the same slices, allowing for paired *t*-test comparisons.

F. Analysis of gephyrin immunolabeling

The RMS of C57Bl/6 mice were injected with an AAV-GFP. The mice were sacrificed at three wpi. Horizontal slices (30-µm-thick) were obtained as described above and were immunolabeled for CR and gephyrin. Consecutive 0.35-µm-thick optical sections were analyzed using Fiji software. Median 3D filtering set at two was applied to the images. Gephyrin+ puncta were counted manually using the Cell Counter plug-in in Fiji. The dendritic length and the soma volume were measured using the Simple Neurite Tracer and 3D Object Counter plug-ins, respectively. The densities of gephyrin for CR+ and CR− GCs were obtained from the same slices, allowing for paired t-test comparisons.

G. Behavioral procedures

Seven to ten days before the behavioral experiments, individually housed male mice were put on a 12 h reverse light/dark cycle, with food and water *ad libitum*. The mice were sacrificed 1 h after the completion of each task to analyze the expression of cFos and Zif268 in the OB. The odors used were (−)-carvone (Sigma Aldrich, Cat# 22060), (+)-carvone (Sigma Aldrich, Cat# 22070), (+)-limonene (Sigma-Aldrich, Cat# 62118), (−)-limonene (Sigma-Aldrich, Cat# 62128), octyl aldehyde (octanal) (Sigma-Aldrich, Cat# 5608), and decanal (Sigma-Aldrich, Cat# 59581).

a. Odor discrimination

For the habituation/dishabituation odor discrimination task, the odors were presented in glass Pasteur pipettes containing filter paper soaked with 6 µL of 2 % odorant in mineral oil. The odor presentations consisted of five min sessions at 20 min intervals. The mice were first accustomed to the glass pipette by presenting it to them twice. The mice were then subjected to four habituation sessions with a first odor ((+)-carvone). On the fifth session, one group of animals (control group) was subjected to the habituation odor, whereas a different group of animals (habituation/dishabituation group) was subjected to a new odor (dishabituation odor, (−)-carvone). The time spent exploring the pipette during each session was recorded.

b. Go/no-go olfactory discrimination learning

The mice were partially water-deprived until they reached 80 to 85 % of their initial body weight before starting the go/no-go training. The animals were first trained to insert their snouts into the odor sampling port and to lick the water port to receive a 3 µl water reward. The reward-associated odor (S+) was then introduced. The mice initiated each trial by breaking the light beam across the odor sampling port, which opened an odor valve. The duration of the opening was increased progressively from 0.1 to 1 s. The mice with a minimum sampling time of 50 ms received a water reward. The mice usually successfully completed the training in one-two sessions. Following the training procedure, the mice were subjected to the

go/no-go odor discrimination task. To ensure that the mice successfully learned the task, the first session consisted of 30 trials during which only the S+ odor was presented. Mice that reached at least an 80 % success rate were then exposed randomly to a reward-associated odor (S+) or to a no reward-associated odor (S−) for several blocks of 20 trials each (random exposure to 10 S+ and 10 S−). Correct responses consisted of correct hits (mouse licking the water port after the S+ exposure) and correct rejections (mouse not licking the water port after the S− exposure). False responses consisted of the mouse licking the water port after the S− exposure or not licking the water port after the S+ exposure. The percentage of correct responses for each block of 20 trials was calculated. The mice were considered to have successfully completed the go/no-go olfactory discrimination task if they reached ≥ 85 % of correct responses. The sessions lasted for one to five days, depending on the odorant pairs. The following odor pairs and mixtures were used: 0.1 % octanal diluted in 99.9 % of mineral oil *vs.* 0.1 % decanal diluted in 99.9 % of mineral oil (mixture one); 0.6 % (+)-limonene + 0.4 % (−)-limonene diluted in 99 % of mineral oil *vs.* 0.4 % (+)-limonene + 0.6 % (−)-limonene diluted in 99 % of mineral oil (mixture two); 0.48 % (+)-limonene + 0.52 % (−)-limonene diluted in 99 % of mineral oil *vs.* 0.52 % (+)-limonene + 0.48 % (−)-limonene diluted in 99 % of mineral oil (mixture three). When the go/no-go olfactory discrimination task was coupled with the pharmacogenetic inhibition of CR_+ GCs, the control and experimental groups were both subjected to the same behavioral protocol, with the same exposure to the S+ and S− odors. The only difference was that control group was injected with an AAV-GFP virus whereas the experimental group was injected with a DREADDs virus. To determine whether the go/no-go odor discrimination learning task induced subtype-specific activation of GCs, the mice in the experimental group were subjected to the protocol described above, whereas the mice in the control group were exposed equally and randomly to the two odors but received the water reward independently of the S+ or S− odor. The mice in the control group mice did not thus discriminate the odors. All the mice were sacrificed 1 h after completing the task and were immunolabeled for CR and *cFos* (or *Zif268*).

c. Pharmacogenetic inactivation of CR-expressing GCs

To study the role of CR_+ GCs in the go/no-go olfactory discrimination task, we inactivated the CR_+ GCs using the Designer Receptors Exclusively Activated by Designer Drugs (DREADDs) pharmacogenetic approach. We stereotaxically injected the Cre-dependent rAAV 2/8 EF1α-DIO-hM4D(G_i)-mCherry viral vector bilaterally into the OB of CR-Cre mice and subjected them to go/no-go olfactory discrimination training two weeks after the injection. Following its expression, an evolved human M4 muscarinic receptor with two-point mutations was activated by clozapine-N-oxide (CNO, 2 mg/kg, Tocris, Cat# 4936). This resulted in membrane hyperpolarization by the activation of an outward K_+ current (Rogan and Roth, 2011). The control mice were injected with the rAAV 2/5 CAG-GFP viral vector. It has been shown *in vitro* and *in vivo* that the peak of CNO efficiency occurs after 20 min and last up to 180 min (Alexander et al., 2009; Roth, 2016). To estimate the efficacy of DREADDs virus, we injected Cre-dependent rAAV 2/8 EF1α-DIO-hM4D(G_i)-mCherry virus (DREADDs group) and EF1α-DIOEYFP virus injected (control group) into CR-Cre OB mice (*n* = three for each group). Two weeks after injection, animals received an intraperitoneal dose of CNO and were placed into clean individual cages for 90 min, followed by perfusion with 4 % PFA. 40-µm-thick slices were cut and subjected to immunostainings against mCherry, GFP and cFos. The percentage of colocalization cFos+/DREADDs+ (DREADDs group) and cFos+/GFP+ (control group) were estimated. Our results demonstrate that $DREADDs_+$ GCs are still inhibited at 90 min after CNO injection. For behavioral experiments, the two groups of mice received an intra-peritoneal injection of CNO every day, 25–30 min before starting the go/no-go task, which lasted approximately 45 min for each animal. No CNO was given during the training.

To estimate the percentage of DREADDs-infected CR+ GCs among the entire CR+ GC population, we first calculated the density of CR+ GCs in the GCL. Given that the viral vectors were injected into two sites of the GCL that covered the entire rostro-caudal portion of the dorsal OB, which makes up 50.0 % of the entire GCL, and that 45.0 % of CR+ GCs in the infected area were DREADDs+, we estimate that

the percentage of DREADDs-infected CR+ GCs among the entire CR+ GC at approximately 8 %.

H. Statistical analysis

Male and female mice were used for all the experiments, except the behavior experiments, which were performed only with males. Data are expressed as means ± SE. Statistical significance was determined using a one-way ANOVA test followed by a Bonferroni post hoc test or a paired or unpaired two-sided Student's *t*-test, depending on the experiment, or a non-parametric Mann-Whitney *U* test as indicated in the text and tables. For the morphometric and gephyrin immunolabelling experiments, we first analyzed 7–12 CR+ and CR− GCs in the same animal to obtain the average values for these two subtypes. We then used an ANOVA or paired Student's *t*-test to assess the level of significance across the animals. The exact value of *n* and its representation (cells, animals) is indicated in the text and corresponding tables. No statistical methods were used to predetermine the sample size. Equality of variance for the unpaired *t*-test was verified using the F-test. The levels of significance were as follows: * $p < 0.05$, ** $p < 0.01$, *** $p < 0.001$. When possible, the investigator was blinded to the experimental conditions (all the IEG experiments and gephyrin analysis). The data that support the findings of this study are available upon request.

7. References

Alexander, G.M., Rogan, S.C., Abbas, A.I., Armbruster, B.N., Pei, Y., Allen, J.A., Nonneman, R.J., Hartmann, J., Moy, S.S., Nicolelis, M.A.*, et al.* (2009). Remote control of neuronal activity in transgenic mice expressing evolved G protein-coupled receptors. Neuron *63*, 27-39.

Alonso, M., Lepousez, G., Sebastien, W., Bardy, C., Gabellec, M.M., Torquet, N., and Lledo, P.M. (2012). Activation of adult-born neurons facilitates learning and memory. Nat Neurosci *15*, 897-904.

Batista-Brito, R., Close, J., Machold, R., and Fishell, G. (2008). The distinct temporal origins of olfactory bulb interneuron subtypes. J Neurosci *28*, 3966-3975.

Belluzzi, O., Benedusi, M., Ackman, J., and LoTurco, J.J. (2003). Electrophysiological differentiation of new neurons in the olfactory bulb. J Neurosci *23*, 10411-10418.

Brandt, M.D., Jessberger, S., Steiner, B., Kronenberg, G., Reuter, K., Bick-Sander, A., von der Behrens, W., and Kempermann, G. (2003). Transient calretinin expression defines early postmitotic

step of neuronal differentiation in adult hippocampal neurogenesis of mice. Mol Cell Neurosci *24*, 603-613.

Breton-Provencher, V., Bakhshetyan, K., Hardy, D., Bammann, R.R., Cavarretta, F., Snapyan, M., Cote, D., Migliore, M., and Saghatelyan, A. (2016). Principal cell activity induces spine relocation of adult-born interneurons in the olfactory bulb. Nature Communications *7*, 12659.

Breton-Provencher, V., Lemasson, M., Peralta, M.R., 3rd, and Saghatelyan, A. (2009). Interneurons produced in adulthood are required for the normal functioning of the olfactory bulb network and for the execution of selected olfactory behaviors. J Neurosci *29*, 15245-15257.

Camillo, D., Levelt, C.N., and Heimel, J.A. (2014). Lack of functional specialization of neurons in the mouse primary visual cortex that have expressed calretinin. Front Neuroanat *8*, 89.

Carleton, A., Petreanu, L.T., Lansford, R., Alvarez-Buylla, A., and Lledo, P.M. (2003). Becoming a new neuron in the adult olfactory bulb. Nat Neurosci *6*, 507-518.

Deprez, F., Pallotto, M., Vogt, F., Grabiec, M., Virtanen, M.A., Tyagarajan, S.K., Panzanelli, P., and Fritschy, J.M. (2015). Postsynaptic gephyrin clustering controls the development of adult-born granule cells in the olfactory bulb. J Comp Neurol *523*, 1998-2016.

Didier, A., Carleton, A., Bjaalie, J.G., Vincent, J.D., Ottersen, O.P., Storm-Mathisen, J., and Lledo, P.M. (2001). A dendrodendritic reciprocal synapse provides a recurrent excitatory connection in the olfactory bulb. Proc Natl Acad Sci U S A *98*, 6441-6446.

Enwere, E., Shingo, T., Gregg, C., Fujikawa, H., Ohta, S., and Weiss, S. (2004). Aging results in reduced epidermal growth factor receptor signaling, diminished olfactory neurogenesis, and deficits in fine olfactory discrimination. J Neurosci *24*, 8354-8365.

Fogli Iseppe, A., Pignatelli, A., and Belluzzi, O. (2016). Calretinin-Periglomerular Interneurons in Mice Olfactory Bulb: Cells of Few Words. Front Cell Neurosci *10*, 231.

Fukunaga, I., Herb, J.T., Kollo, M., Boyden, E.S., and Schaefer, A.T. (2014). Independent control of gamma and theta activity by distinct interneuron networks in the olfactory bulb. Nat Neurosci *17*, 1208-1216.

Greer, C.A. (1987). Golgi analyses of dendritic organization among denervated olfactory bulb granule cells. J Comp Neurol *257*, 442-452.

Grelat, A., Benoit, L., Wagner, S., Moigneu, C., Lledo, P.M., and Alonso, M. (2018). Adult-born neurons boost odor-reward association. Proc Natl Acad Sci U S A *115*, 2514-2519.

Gschwend, O., Abraham, N.M., Lagier, S., Begnaud, F., Rodriguez, I., and Carleton, A. (2015). Neuronal pattern separation in the olfactory bulb improves odor discrimination learning. Nat Neurosci *18*, 1474-1482.

Guthrie, K.M., Anderson, A.J., Leon, M., and Gall, C. (1993). Odor-induced increases in c-fos mRNA expression reveal an anatomical "unit" for odor processing in olfactory bulb. Proc Natl Acad Sci U S A *90*, 3329-3333.

Imayoshi, I., Sakamoto, M., Ohtsuka, T., Takao, K., Miyakawa, T., Yamaguchi, M., Mori, K., Ikeda, T., Itohara, S., and Kageyama, R. (2008). Roles of continuous neurogenesis in the structural and functional integrity of the adult forebrain. Nat Neurosci *11*, 1153-1161.

Isaacson, J.S., and Strowbridge, B.W. (1998). Olfactory reciprocal synapses: dendritic signaling in the CNS. Neuron *20*, 749-761.

Jakobsson, J., Ericson, C., Jansson, M., Bjork, E., and Lundberg, C. (2003). Targeted transgene expression in rat brain using lentiviral vectors. J Neurosci Res *73*, 876-885.

Jiang, M., and Swann, J.W. (1997). Expression of calretinin in diverse neuronal populations during development of rat hippocampus. Neuroscience *81*, 1137-1154.

Kelsch, W., Lin, C.W., and Lois, C. (2008). Sequential development of synapses in dendritic domains during adult neurogenesis. Proc Natl Acad Sci U S A *105*, 16803-16808.

Lagace, D.C., Whitman, M.C., Noonan, M.A., Ables, J.L., DeCarolis, N.A., Arguello, A.A., Donovan, M.H., Fischer, S.J., Farnbauch, L.A., Beech, R.D*., et al.* (2007). Dynamic contribution of nestin-expressing stem cells to adult neurogenesis. J Neurosci *27*, 12623-12629.

Lagier, S., Carleton, A., and Lledo, P.M. (2004). Interplay between local GABAergic interneurons and relay neurons generates gamma oscillations in the rat olfactory bulb. J Neurosci *24*, 4382-4392.

Lagier, S., Panzanelli, P., Russo, R.E., Nissant, A., Bathellier, B., Sassoe-Pognetto, M., Fritschy, J.M., and Lledo, P.M. (2007). GABAergic inhibition at dendrodendritic synapses tunes gamma oscillations in the olfactory bulb. Proc Natl Acad Sci U S A *104*, 7259-7264.

Lemasson, M., Saghatelyan, A., Olivo-Marin, J.C., and Lledo, P.M. (2005). Neonatal and adult neurogenesis provide two distinct populations of newborn neurons to the mouse olfactory bulb. J Neurosci *25*, 6816-6825.

Lepousez, G., and Lledo, P.M. (2013). Odor discrimination requires proper olfactory fast oscillations in awake mice. Neuron *80*, 1010-1024.

Lepousez, G., Nissant, A., Bryant, A.K., Gheusi, G., Greer, C.A., and Lledo, P.M. (2014). Olfactory learning promotes input-specific synaptic plasticity in adult-born neurons. Proc Natl Acad Sci U S A *111*, 13984-13989.

Lledo, P.M., Merkle, F.T., and Alvarez-Buylla, A. (2008). Origin and function of olfactory bulb interneuron diversity. Trends Neurosci *31*, 392-400.

Magavi, S.S., Mitchell, B.D., Szentirmai, O., Carter, B.S., and Macklis, J.D. (2005). Adult-born and preexisting olfactory granule neurons undergo distinct experience-dependent modifications of their olfactory responses in vivo. J Neurosci *25*, 10729-10739.

Malvaut, S., Gribaudo, S., Hardy, D., David, L.S., Daroles, L., Labrecque, S., Lebel-Cormier, M.A., Chaker, Z., Cote, D., De Koninck, P*., et al.* (2017). CaMKIIalpha Expression Defines Two Functionally Distinct Populations of Granule Cells Involved in Different Types of Odor Behavior. Curr Biol *27*, 3315-3329 e3316.

Merkle, F.T., Fuentealba, L.C., Sanders, T.A., Magno, L., Kessaris, N., and Alvarez-Buylla, A. (2014). Adult neural stem cells in distinct microdomains generate previously unknown interneuron types. Nat Neurosci *17*, 207-214.

Moreno, M.M., Linster, C., Escanilla, O., Sacquet, J., Didier, A., and Mandairon, N. (2009). Olfactory perceptual learning requires adult neurogenesis. Proc Natl Acad Sci U S A *106*, 17980-17985.

Murata, K., Imai, M., Nakanishi, S., Watanabe, D., Pastan, I., Kobayashi, K., Nihira, T., Mochizuki, H., Yamada, S., Mori, K.*, et al.* (2011). Compensation of depleted neuronal subsets by new neurons in a local area of the adult olfactory bulb. J Neurosci *31*, 10540-10557.

Nakamura, T., Colbert, M.C., and Robbins, J. (2006). Neural crest cells retain multipotential characteristics in the developing valves and label the cardiac conduction system. Circ Res *98*, 1547-1554.

Ninkovic, J., Mori, T., and Gotz, M. (2007). Distinct modes of neuron addition in adult mouse neurogenesis. J Neurosci *27*, 10906-10911.

Nissant, A., Bardy, C., Katagiri, H., Murray, K., and Lledo, P.M. (2009). Adult neurogenesis promotes synaptic plasticity in the olfactory bulb. Nat Neurosci *12*, 728-730.

Nunes, D., and Kuner, T. (2015). Disinhibition of olfactory bulb granule cells accelerates odour discrimination in mice. Nat Commun *6*, 8950.

Orona, E., Scott, J.W., and Rainer, E.C. (1983). Different granule cell populations innervate superficial and deep regions of the external plexiform layer in rat olfactory bulb. J Comp Neurol *217*, 227-237.

Pallotto, M., Nissant, A., Fritschy, J.M., Rudolph, U., Sassoe-Pognetto, M., Panzanelli, P., and Lledo, P.M. (2012). Early formation of GABAergic synapses governs the development of adult-born neurons in the olfactory bulb. J Neurosci *32*, 9103-9115.

Panzanelli, P., Bardy, C., Nissant, A., Pallotto, M., Sassoe-Pognetto, M., Lledo, P.M., and Fritschy, J.M. (2009). Early synapse formation in developing interneurons of the adult olfactory bulb. J Neurosci *29*, 15039-15052.

Petreanu, L., and Alvarez-Buylla, A. (2002). Maturation and death of adult-born olfactory bulb granule neurons: role of olfaction. J Neurosci *22*, 6106-6113.

Pressler, R.T., and Strowbridge, B.W. (2006). Blanes cells mediate persistent feedforward inhibition onto granule cells in the olfactory bulb. Neuron *49*, 889-904.

Qin, J.Y., Zhang, L., Clift, K.L., Hulur, I., Xiang, A.P., Ren, B.Z., and Lahn, B.T. (2010). Systematic comparison of constitutive promoters and the doxycycline-inducible promoter. PLoS One *5*, e10611.

Ravi, N., Sanchez-Guardado, L., Lois, C., and Kelsch, W. (2017). Determination of the connectivity of newborn neurons in mammalian olfactory circuits. Cell Mol Life Sci *74*, 849-867.

Rochefort, C., Gheusi, G., Vincent, J.D., and Lledo, P.M. (2002). Enriched odor exposure increases the number of newborn neurons in the adult olfactory bulb and improves odor memory. J Neurosci *22*, 2679-2689.

Rogan, S.C., and Roth, B.L. (2011). Remote control of neuronal signaling. Pharmacol Rev *63*, 291-315.

Roth, B.L. (2016). DREADDs for Neuroscientists. Neuron *89*, 683-694.

Sagar, S.M., Sharp, F.R., and Curran, T. (1988). Expression of c-fos protein in brain: metabolic mapping at the cellular level. Science *240*, 1328-1331.

Sakamoto, M., Imayoshi, I., Ohtsuka, T., Yamaguchi, M., Mori, K., and Kageyama, R. (2011). Continuous neurogenesis in the adult forebrain is required for innate olfactory responses. Proceedings of the National Academy of Sciences.

Shepherd, G.M., Chen, W.R., and Greer, C.A. (2004). Olfactory Bulb. In The Synaptic Organization of the Brain, G.M. Shepherd, ed., pp. 165–216.

Sultan, S., Rey, N., Sacquet, J., Mandairon, N., and Didier, A. (2011). Newborn neurons in the olfactory bulb selected for long-term survival through olfactory learning are prematurely suppressed when the olfactory memory is erased. J Neurosci *31*, 14893-14898.

Takahashi, H., Ogawa, Y., Yoshihara, S., Asahina, R., Kinoshita, M., Kitano, T., Kitsuki, M., Tatsumi, K., Okuda, M., Tatsumi, K.*, et al.* (2016). A Subtype of Olfactory Bulb Interneurons Is Required for Odor Detection and Discrimination Behaviors. J Neurosci *36*, 8210-8227.

Taniguchi, H., He, M., Wu, P., Kim, S., Paik, R., Sugino, K., Kvitsiani, D., Fu, Y., Lu, J., Lin, Y.*, et al.* (2011). A resource of Cre driver lines for genetic targeting of GABAergic neurons in cerebral cortex. Neuron *71*, 995-1013.

Tsuchiya, R., Yoshiki, F., Kudo, Y., and Morita, M. (2002). Cell type-selective expression of green fluorescent protein and the calcium indicating protein, yellow cameleon, in rat cortical primary cultures. Brain Res *956*, 221-229.

Whitman, M.C., and Greer, C.A. (2007). Synaptic integration of adult-generated olfactory bulb granule cells: basal axodendritic centrifugal input precedes apical dendrodendritic local circuits. J Neurosci *27*, 9951-9961.

Young, K.M., Fogarty, M., Kessaris, N., and Richardson, W.D. (2007). Subventricular zone stem cells are heterogeneous with respect to their embryonic origins and neurogenic fates in the adult olfactory bulb. J Neurosci *27*, 8286-8296.

Zhou, Z., and Belluscio, L. (2008). Intrabulbar projecting external tufted cells mediate a timing-based mechanism that dynamically gates olfactory bulb output. J Neurosci *28*, 9920-9928.

Zou, D.J., Greer, C.A., and Firestein, S. (2002). Expression pattern of alpha CaMKII in the mouse main olfactory bulb. J Comp Neurol *443*, 226-236.

8. Figures

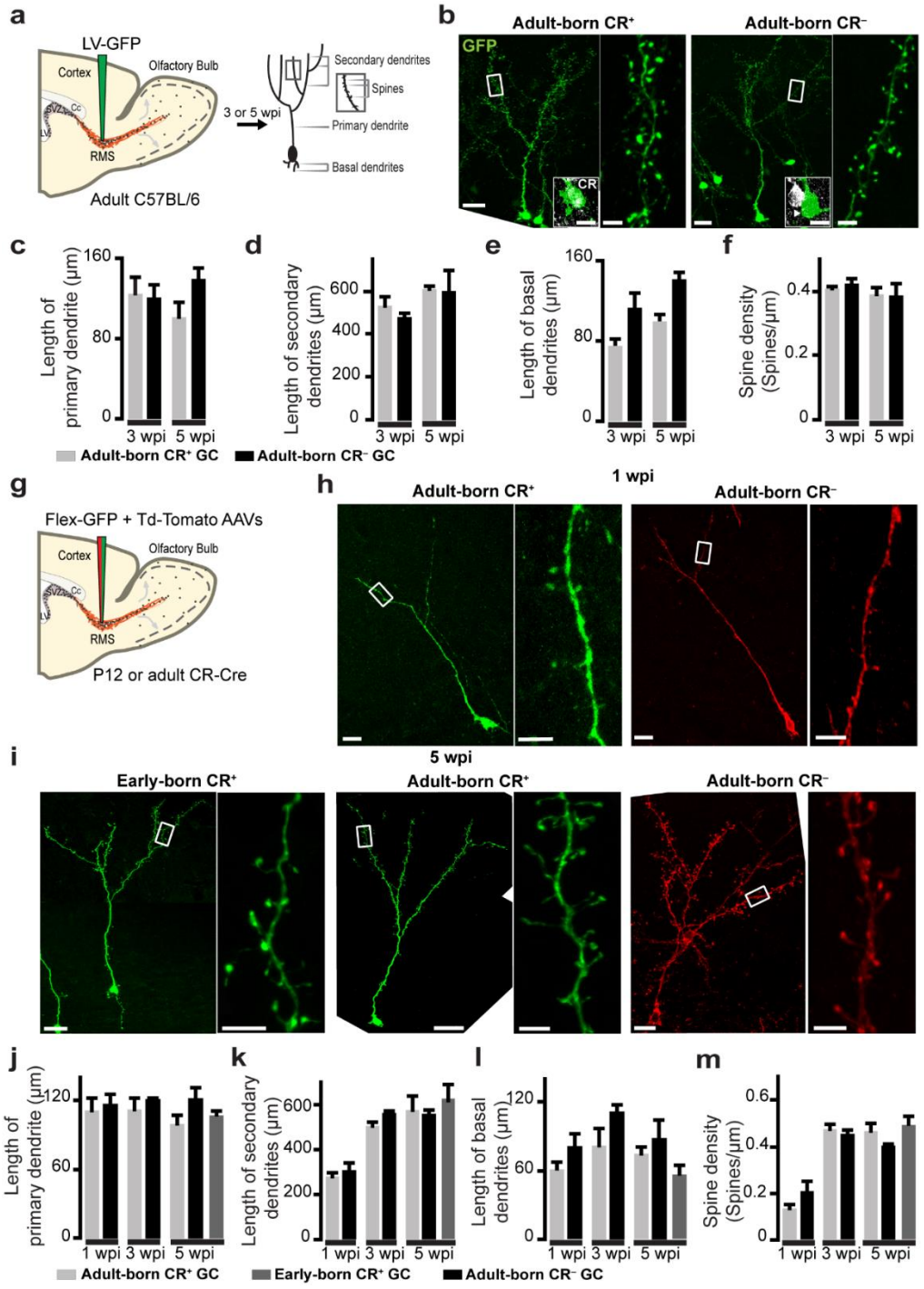

Figure 3.1: Morphological characterization of early-born and adult-born CR+ GCs and adultborn CR− GCs

a. Schematic diagram showing the injection of GFP-encoding lentivirus into the RMS of adult mice and the morphometric parameters used to analyze the structural properties of CR+ and CR- GCs. **b.**

Representative images of CR+ and CR− GCs at three wpi. Insets show CR immunolabeling (white). Scale bars: 20 μm (left image), 4 μm (right image), and 10 μm (inset). **c–f.** The mean lengths of the primary dendrite (**c**), secondary dendrites (**d**), and basal dendrites (**e**), and the spine densities (**f**) of adult-born CR+ and CR− GCs at three and five wpi. **g.** Schematic diagram showing the co-injection of the Flex-GFP and Tdtomato AAVs into the RMS of adult and P12 CR-Cre mice. **h.** Example of adult-born CR+ and CR− GCs at one wpi. **i.** Examples of early-born and adult-born CR+ GCs and adult-born CR− GCs at five wpi. Scale bars: 20 μm (left image) and 2 μm (right image). **j–m.** The mean lengths of the primary dendrites (**j**), secondary dendrites (**k**), basal dendrites (**l**), and spine densities (**m**) of early-born and adult-born CR+ and adult-born CR− GCs at one, three and five wpi. See **Table 3.1**.

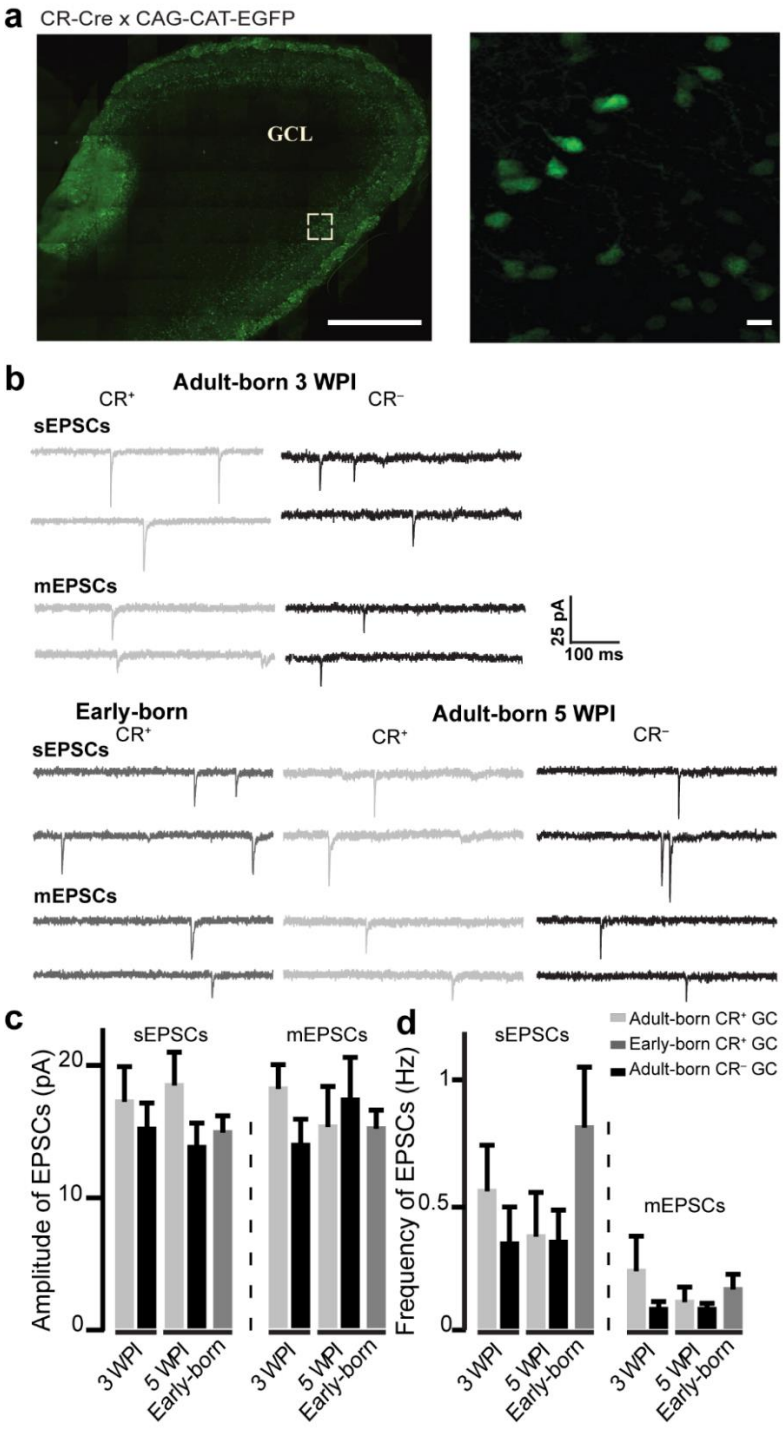

Figure 3.2: The excitatory postsynaptic inputs of CR+ and CR− GCs are indistinguishable

a. Labeling of early-born CR+ GCs in CR-Cre::CAG-CAT-GFP mice. The inset shows a higher magnification of GFP+ GCs in the GCL. Scale bars: 500 µm (left image) and 10 µm (right image). **b.** Examples of sEPSC and mEPSC events recorded from early-born CR+ GCs, adult-born CR+ GCs, and CR- GCs. **c–d.** The mean amplitudes (**c**) and frequencies (**d**) of sEPSCs and mEPSCs recorded from early and adult-born CR+ GCs and adult-born CR- GCs are indistinguishable. See **Table 3.3.**

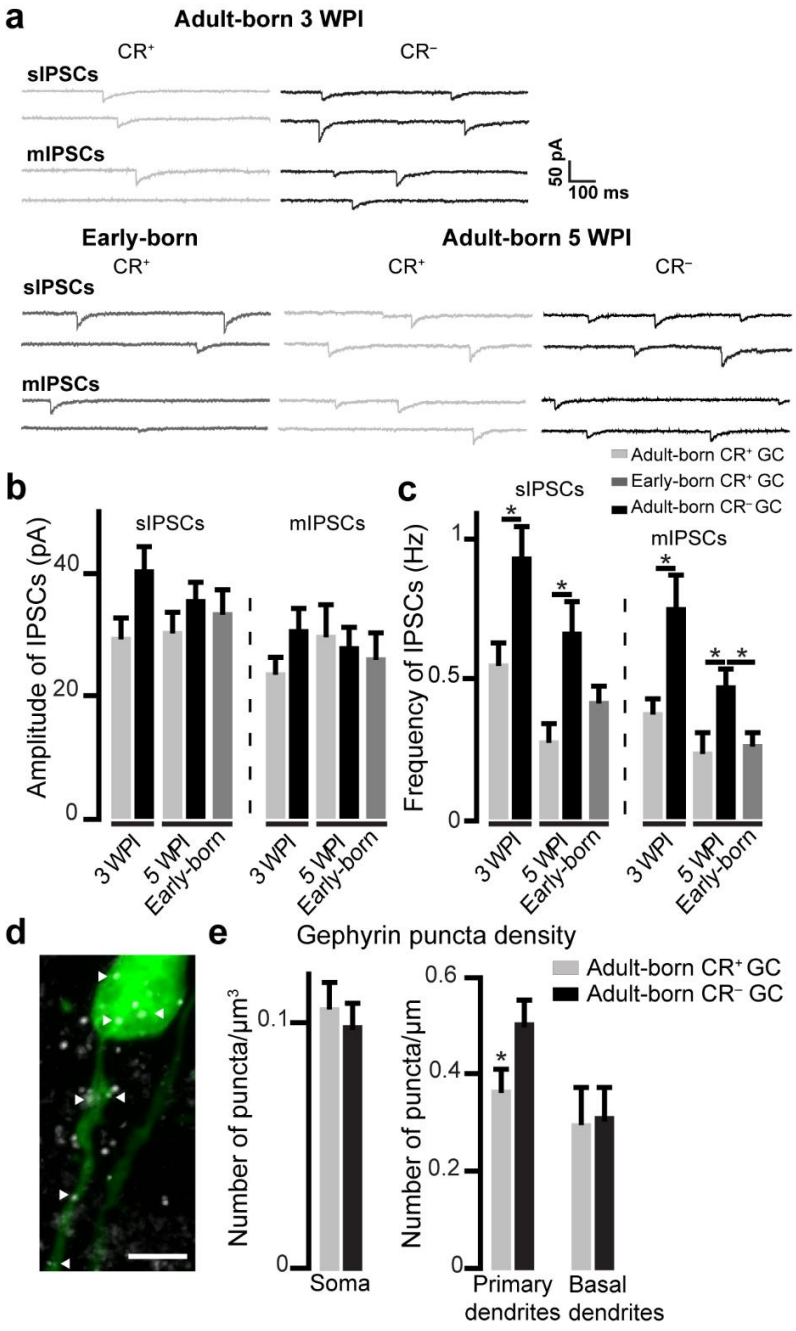

Figure 3.3: CR+ GCs receive weaker inhibitory inputs than CR- GCs and have fewer gephyrin+ puncta on their primary dendrites

a. Examples of sIPSCs and mIPSCs recorded from early-born CR+ GCs, and adult-born CR+ and CR- CGs. b, c. Mean amplitudes (**b**) and frequencies (**c**) of sIPSCs and mIPSCs recorded from early and adult-born CR+ GCs and adult-born CR- GCs. See Table 2.4. **d.** Representative image of virally labeled GCs (green) that have also been labeled for gephyrin (white). Arrowheads indicate gephyrin+ puncta. Scale bars: 10 µm. **e.** Mean densities of gephyrin+ puncta on the primary and basal dendrites and cell soma of CR+ and CR- adult-born GCs at three wpi. See **Table 3.4.** *$p < 0.05$ Mann-Whitney *U*-test for IPSCs frequencies and paired *t*-test for gephyrin analysis.

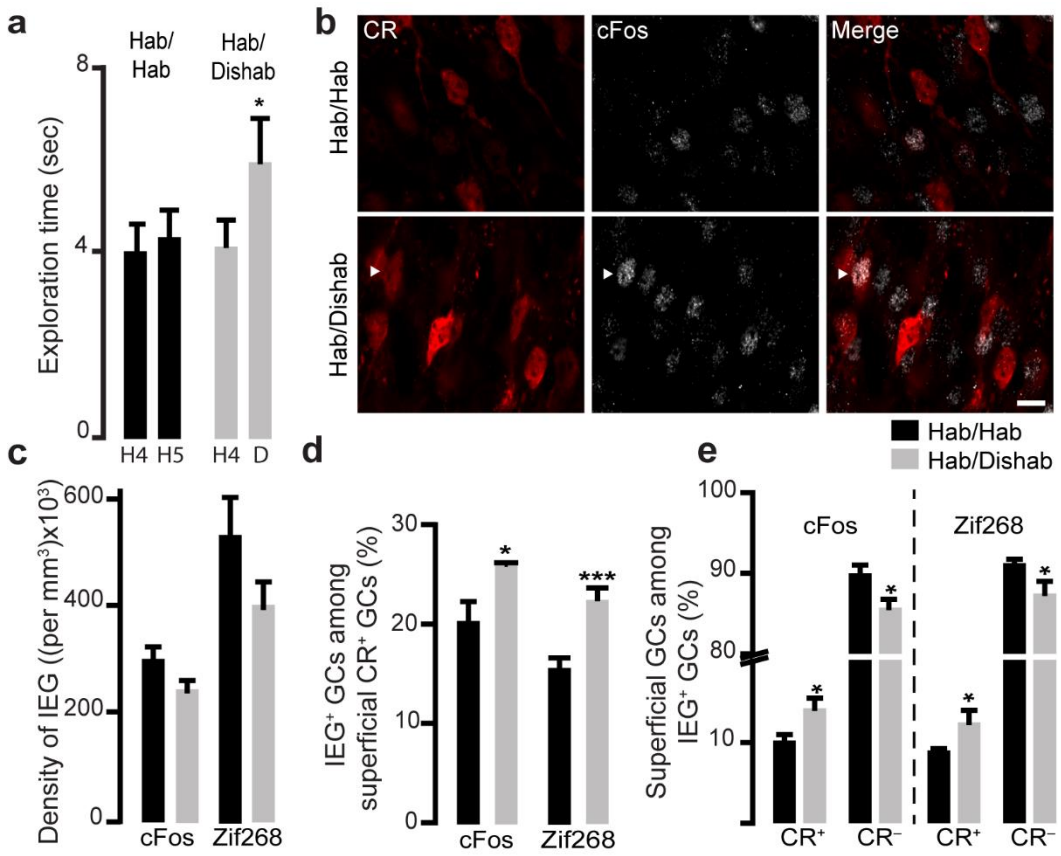

Figure 3.4: Spontaneous odor discrimination induces the activation of CR+ GCs

a. Spontaneous odor discrimination task based on odor habituation/dishabituation (hab/dishab). C57Bl/6 mice were habituated to the presence of a first odor (the habituation odor ((+)-carvone)), which was presented four times. Their ability to discriminate between two similar odors was then investigated by the presentation of a second odor (the dishabituation odor ((−)-carvone)), which was chemically similar to the habituation odor. As expected, mice correctly discriminated between the two odors as shown by the increase in exploration time when the dishabituation odor was presented compared to the fourth presentation of the habituation odor (**a**, right panel). We used mice that were not dishabituated and that received the habituation odor ((+)-carvone) during the last presentation (hab/hab) as a control (**a**, left panel). **b.** Examples of CR and cFos immunolabeling in mice from the control and odor discrimination groups. Arrowheads indicate cFos+/CR+ GCs. Scale bar: 10 µm. **c–e.** Quantification of the density of cFos+ and Zif268+ GCs (**c**), the percentages of cFos+ and Zif268+ GCs among CR+ GCs (**d**), and the percentage of CR+ (left panel) and CR- (right panel) GCs among cFos+ and Zif268+ GCs (**e**). **p* < 0.05, ****p* < 0.001 paired *t*-test for behavioral task and unpaired *t*-test for IEG analysis.

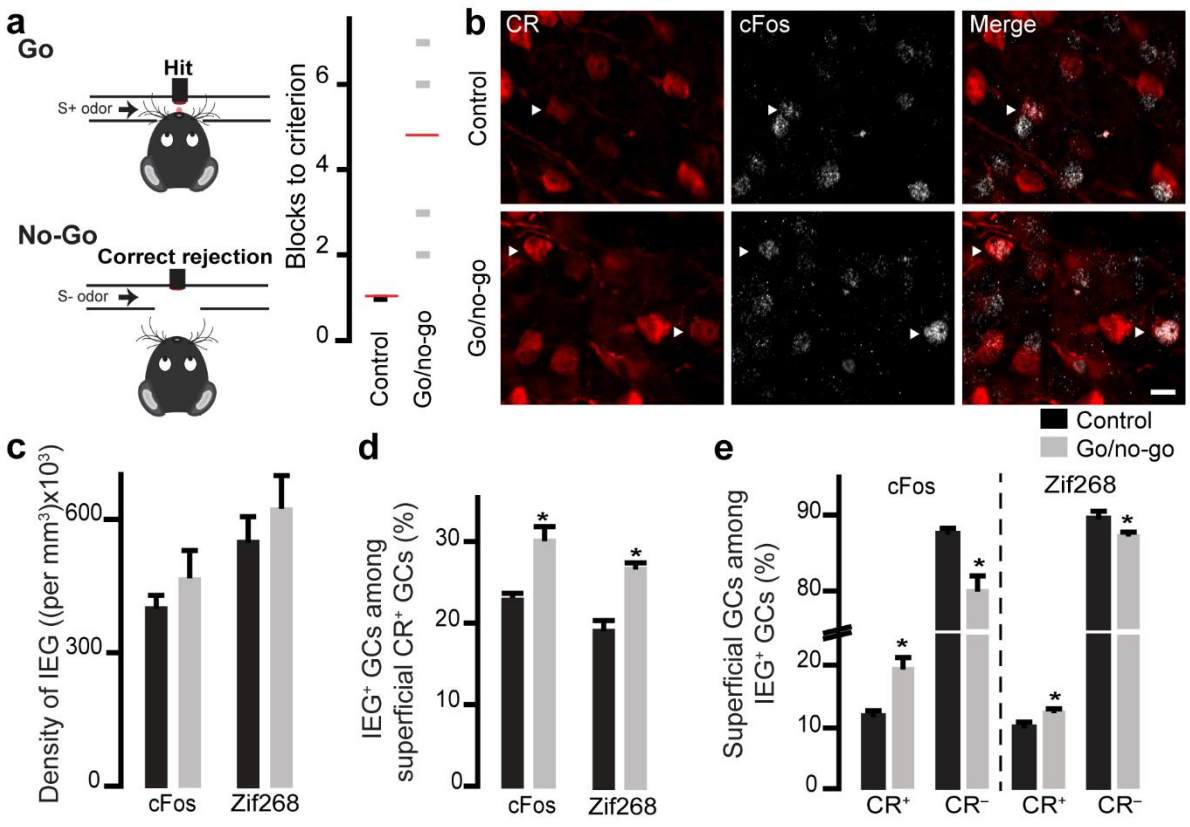

Figure 3.5: Odor discrimination learning activates CR+ GCs

a. Water-restricted C57Bl/6 male mice were tested using the go/no-go odor discrimination task. Mice were randomly exposed to reward-associated and non-reward-associated odors (S+ and S−, respectively), and the percentage of correct responses (hits + correct rejections) was calculated for every 20 trials. The mice were considered to have successfully discriminated between the two odors if they reached the 85 % criterion of correct responses. The odors used were 0.1 % octanal and 0.1 % decanal (mixture one). Number of blocks needed in each group to reach the 85 % criterion (right panel). For mice in the control group, the water was given independently of the odor. **b.** Examples of immunolabeling for CR and cFos on OB slices after the go/no-go odor discrimination task. Arrowheads indicate cFos+/CR+ GCs. Scale bar: 10 µm. **c-e.** Quantification of the densities of cFos+ and Zif268+ GCs (**c**), the percentages of cFos+ and Zif268+ GCs among CR+ GCs (**d**), and the percentages of CR+ (left panel) and CR- (right panel) GCs among cFos+ and Zif268+ GCs (**e**). Note the higher percentages of CR+/cFos+ and CR+/Zif268+ GCs, indicating that CR+ GCs are specifically involved in odor discrimination. *$p < 0.05$ unpaired *t*-test.

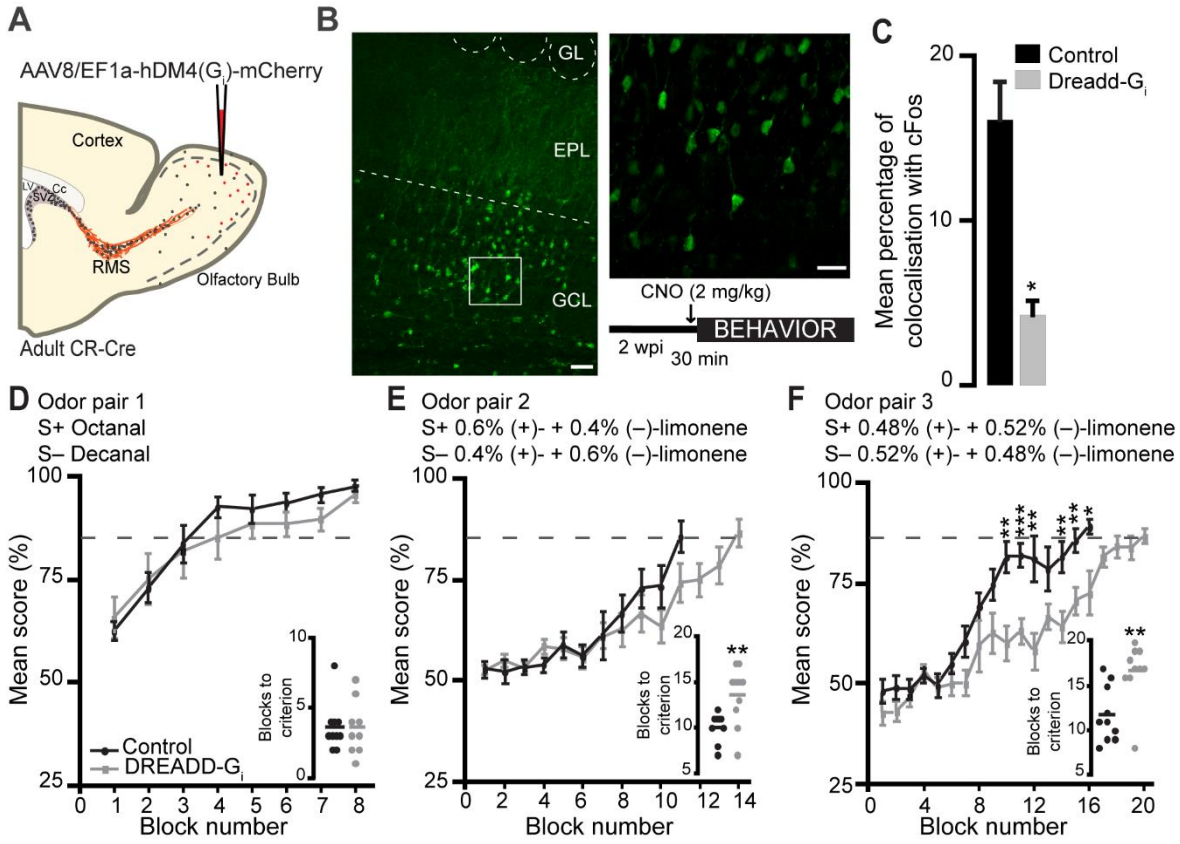

Figure 3.6: The pharmacogenetic inhibition of CR+ GCs reduces the olfactory discriminatory ability of mice

a. The EF1α-DIO-hM4D(G_i)-mCherry AAV was injected into the OB of CR-Cre mice, inducing the expression of the G_i-coupled DREADDs receptor by CR_+ GCs. Control mice were injected with a Cre-independent GFP-encoding AAV, which labeled all GCs. The behavior experiments started at two wpi, and the mice in the two groups were given an intraperitoneal injection of 2 mg/kg of CNO 30 min prior undertaking the behavior task. **b.** Example of the injection of the AAV in the OB. Scale bar: 50 µm. The inset shows a higher magnification image of DREADD-G_i infected cells. Scale bar: 10 µm. **c.** Quantification of the percentages of $reporter_+$ (GFP or mCherry) and $cFos_+$ GCs following the CNO injections in mice previously injected with the control (EF1α-DIO-EYFP) or the DREADDs (EF1a-DIO-hM4D(G_i)-mCherry) AAV. Note the effective pharmacogenetic inhibition of CR_+ GCs (*$p < 0.05$ paired *t*-test). **d–f.** The mean scores in percentages for each block of 20 trials obtained from the control and DREADDs AAV-injected mice for the go/no-go odor discrimination task using odor mixtures of different complexity. The odor pairs used were 0.1 % octanal and 0.1 % decanal (mixture one), n = 10 and nine mice for the control and DREADDs groups, respectively (**d**), 0.6 % (+)-limonene + 0.4 % (−)-limonene and 0.4 % (+)-limonene + 0.6 % (−)-limonene (mixture two), n = 9 and 10 mice for the control and DREADDs groups, respectively (**e**), and 0.48 % (+)-limonene + 0.52 % (−)-limonene and 0.52 % (+)-limonene + 0.48 % (−)-limonene (mixture three), n = 10 mice for the control and DREADDs groups, respectively (**f**). The dashed lines represent the 85 % criterion score. Insets show the mean values for each group to reach the criterion of 85 % correct responses (*$p < 0.05$; **$p < 0.01$ unpaired *t*-test).

9. Tables

Table 3.1: Morphological properties of CR^+ and CR^- GCs

	Adult-born										Early-born
	C57BL/6 (LV-GFP + CR immunostaining)				CR-Cre + AAVs (Flex-GFP + Td-Tomato)						
	Three wpi		Five wpi		One wpi		Three wpi		Five wpi		
	CR^+	CR^-	CR^+	CR^-	CR^+	CR^-	CR^+	CR^-	CR^+	CR^-	CR^+
Primary dendrites (µm)	124.70 ± 17.32	120.66 ± 12.82	101.26 ± 14.21	139.29 ± 10.98	112.24 ± 10.27	117.62 ± 8.51	113.00 ± 9.60	122.22 ± 1.00	100.61 ± 5.60	122.90 ± 9.52	108.03 ± 3.58
Secondary dendrites (µm)	531.46 ± 44.85	505.38 ± 22.33	611.31 ± 14.33	601.90 ± 96.42	276.80 ± 18.80	306.33 ± 30.90	507.23 ± 18.67	560.20 ± 9.87	572.03 ± 62.93	556.90 ± 17.90	625.22 ± 69.72
Basal dendrites (µm)	74.51 ± 7.68	112.65 ± 15.24	99.00 ± 6.70	141.22 ± 6.54	61.31 ± 6.36	81.56 ± 10.97	82.02 ± 15.21	112.50 ± 5.63	74.77 ± 5.85	88.95 ± 15.55	56.60 ± 7.26
	paired $t(2) = -3.56$, $p = 0.07$		paired $t(2) = -0.55$, $p = 0.25$		paired $t(2) = -2.01$, $p = 0.18$		paired $t(2) = -2.65$, $p = 0.11$		paired $t(4) = 0.88$, $p = 0.13$		
									unpaired $t(4) = 1.95$, $p = 0.12$		
Spine density (no. of spines/µm)	0.40 ± 0.01	0.44 ± 0.01	0.39 ± 0.02	0.39 ± 0.04	0.13 ± 0.02	0.21 ± 0.04	0.47 ± 0.02	0.45 ± 0.02	0.46 ± 0.03	0.40 ± 0.00	0.49 ± 0.03
					paired $t(2) = -1.50$, $p = 0.27$					paired $t(4) = 3.15$ $p = 0.08$	
Number of cells/animal	20/3	38/3	22/3	32/3	43/3	41/3	40/3	35/3	41/3	39/3	42/3

Table 3.2: Intrinsic electrophysiological properties of early- and adult-born CR_+ GCs and adult-born CR_- GCs.

	Adult-born				Early-born
	Three wpi		Five wpi		
	CR^+	CR^-	CR^+	CR^-	CR^+
Vm (mV)	−64.78 ± 1.73	−65.38 ± 2.69	−62.25 ± 3.90	−64.67 ± 2.72	−63.50 ± 2.65
Rm (GΩ)	1.14 ± 0.06	1.16 ± 0.09	1.06 ± 0.09	0.97 ± 0.10	1.10 ± 0.15
Cm (pF)	9.29 ± 1.53	11.48 ± 1.34	10.38 ± 1.28	10.11 ± 0.77	8.15 ± 0.59
I_{Na}^+ threshold (mV)	−35.56 ± 4.75	−38.89 ± 2.00	−32.50 ± 10.13	−38.75 ± 2.27	−37.78 ± 1.47
I_{Na}^+ peak of amplitude (nA)	0.731 ± 0.093	1.135 ± 0.155	0.961 ± 0.212	1.091 ± 0.196	0.813 ± 0.046
	$U(16) = 17$, $p = 0.07$				
Number of cells/animal	10/7	9/6	8/6	9/5	11/6

Table 3.3: EPSC amplitudes and frequencies of early-born and adult-born CR+ GCs and adult-born CR- GCs

		Adult-born				Early-born
		Three wpi		Five wpi		
		CR^+	CR^-	CR^+	CR^-	CR^+
sEPSCs	Amplitude (pA)	17.33 ± 2.50	15.23 ± 1.85	18.60 ± 2.33	13.83 ± 1.74	14.98 ± 1.11
				$U(15) = 21$, $p = 0.16$		
	Frequency (Hz)	0.56 ± 0.18	0.35 ± 0.14	0.38 ± 0.17	0.36 ±0.14	0.82 ±0.23
		$U(17) = 35$, $p = 0.43$			$U(18) = 23.5$, $p = 0.052$	
				$U(17) = 25.5$, $p = 0.13$		
	Number of cells/animal	10/7	9/6	8/6	8/5	11/6
mEPSCs	Amplitude (pA)	18.32 ± 1.62	13.98 ± 1.80	15.40 ± 2.92	17.51 ± 2.98	15.27 ± 1.18
		$U(15) = 19$, $p = 0.11$				
	Frequency (Hz)	0.24 ± 0.13	0.09 ± 0.02	0.12 ± 0.05	0.09 ± 0.03	0.17 ± 0.05
		$U(15) = 32$, p=0.72				
	Number of cells /animals	8/7	9/6	8/6	9/6	10/5

Table 3.4: IPSC amplitudes and frequencies of early- and adult-born CR+ GCs and adult-born CR- GCs, and number of gephyrin immunopuncta on adult-born CR+ and CR- GCs

		Adult-born				Early-born
		Three wpi		Five wpi		
		CR^+	CR^-	CR^+	CR^-	CR^+
sIPSCs	Amplitude (pA)	29.52 ± 3.15	40.60 ± 3.73	30.41 ± 3.15	35.56 ± 2.97	33.40 ± 3.92
		$U(22) = 39.5$, $p = 0.06$				
	Frequency (Hz)	0.56 ± 0.07	0.94 ± 0.11	0.28 ± 0.06	0.67 ± 0.11	0.42 ± 0.06
		*$U(22) = 27.5$, $p = 0.008$		*$U(19) = 18$, $p = 0.007$		
					$U(18) = 27$, $p = 0.09$	
				$U(19) = 31$, $p = 0.09$		
	Number of cells/animal	13/8	11/5	11/6	10/5	10/4
mIPSCs	Amplitude (pA)	23.83 ± 2.51	30.86 ± 3.24	29.96 ± 4.77	28.08 ± 3.10	26.25 ± 3.90
		$U(20) = 40$, $p = 0.23$				
	Frequency (Hz)	0.38 ± 0.05	0.76 ± 0.11	0.24 ± 0.07	0.47 ± 0.07	0.27 ± 0.04
		*$U(20) = 15$, $p = 0.002$		*$U(17) = 17$, $p = 0.02$		
					*$U(18) = 23$, $p = 0.04$	
	Number of cells/animal	13/8	9/4	9/5	10/5	10/4
Gephyrin immunopuncta density	Soma (nb. of puncta/µm³)	0.11 ± 0.01	0.10 ± 0.01			
	Basal (nb. of puncta/µm²)	0.30 ± 0.07	0.31 ± 0.06			
	Primary (nb. of puncta/µm²)	0.37 ± 0.04	0.51 ± 0.04			
		*paired $t(2) = 10.1$, $p = 0.01$				

10. Acknowledgements

This work was supported by operating grants from the Canadian Institutes of Health Research (CIHR; MOP 105859) and the National Science and Engineering Research Council of Canada (NSERC) to Armen Saghatelyan.

DISCUSSION AND FUTURE DIRECTIONS

The work presented in this thesis provides new insights with regard to the role played by GCs in the adult OB. Although being the most numerous resident cell population in this structure, the precise role played by GCs in olfactory processing and OB functioning is still poorly understood. Our data are in line with the current idea that GCs should no longer be considered as being a homogenous neuronal population but rather a very heterogeneous one. In fact, GCs were shown to express several different neurochemical markers such as CR, CaMKIIα, CaMKIV, mGluR2, CPEB4 and 5T4 (Baker et al., 2001; Batista-Brito et al., 2008; Imamura et al., 2006; Jacobowitz and Winsky, 1991; Merkle et al., 2014; Murata et al., 2011; Tseng et al., 2017; Tseng et al., 2019; Zou et al., 2002) but to date, only a few have investigated the precise functional role of these GC subpopulations.

In the first part of the study, I presented the work we published and in which we investigated the role of CaMKIIα-expressing GCs. Using an *in vivo* Ca^{2+} imaging approach, we revealed that already in basal conditions, GCs are functionally heterogeneous, some being spontaneously active, whereas the others were inactive. We observed the same disparity in calcium responses in a context of odor stimulation. Interestingly, we show that half of the entire population of GCs express CaMKIIα. When we used our calcium imaging approach combined to a viral strategy to specifically label the population of CaMKIIα+ cells, we observed that this neuronal subtype was overall more active than the general population of GCs. An electrophysiological characterization of the two subpopulations of GCs of interest revealed that this higher level of activity of adult-born CaMKIIα+ GCs could be explained by the lower level of inhibition that they receive. In fact CaMKIIα+ GCs are characterized by a decreased amplitude of miniature and spontaneous IPSCs, which make them more prone to activation by incoming olfactory inputs. To explore further the functional involvement of GCs subtypes, we used both an immunohistochemical and a pharmacogenetic approaches to specifically inhibit either CaMKIIα+ cells or GCs irrespective or their chemical phenotype, during different olfactory tasks. We revealed that CaMKIIα+ GCs activation is indispensable for fine odor discrimination.

On the contrary tasks such as perceptual learning of similar odorants results in a greater activation of CaMKIIα negative cells, inhibition of GCs in a subtype-independent manner altering mice ability to perform the task.

In the second part of the work I presented here, we decided to focus on another population of GCs, comparing this time CR+ cells to CR- ones, taking also into account the population of early- versus adult-born CR-expressing GCs. We show that once again the different subpopulations although presenting similar morphological properties, displayed however different electrophysiological characteristics. CR+ cells receive a lower level inhibition than CR- ones, a reduction characterized for this GC subtype by a decrease in the frequencies of inhibitory post-synaptic currents. However, such a difference was not observed when adult-born CR+ GCs were compared to their early-born homologues. Moreover, when their involvement in several odor behaviors was assessed, we observed that CR-expressing GCs are required for completion of odor discrimination tasks involving similar odors. Inhibiting CR-expressing GCs during an operant-conditioning odor discrimination task with similar odors slowed down animals' learning to perform the task.

Although our data provides more information towards a functional heterogeneity of the interneuronal population in the adult OB, the specific role played by GCs subtypes in OB network functioning and the processing of incoming odorant inputs still remains to be fully described. Below, I propose and discuss new experiments that could help further investigate and add some knowledge to the understanding of GCs functional heterogeneity.

1. The complex functional heterogeneity of GCs in the adult OB

A. The birthdate as a factor of GCs heterogeneity

As already presented above, it is possible to differentiate between different subpopulations of GCs in the adult OB, and this based on different parameters.

Notably, the OB is one of the rare brain regions where newborn immature neurons are constantly entering and integrating the OB network. Therefore, two different populations of interneurons are coexisting in permanence at this level: adult-born GCs and early-born or pre-existing GCs. For long, adult-born cells were considered as a replacement for the loss of pre-existing cells, encouraging the idea of a constant turnover of the interneuronal pool. This was supported by data reporting a shorter lifetime of adult neurons as compared to postnatally born cells (Lemasson et al., 2005; Petreanu and Alvarez-Buylla, 2002). Although this idea was largely accepted for the last years, it was recently questioned. A two-photon based long-term imaging of adult-born cells revealed that only a low percentage of newborn neurons is lost in the first year of mice' life. These data would then support the idea that the OB network could be constantly expanding across an animal's lifetime, as opposed to the previous thought of a replacement of pre-existing neurons by adult-born ones (Platel et al., 2019). Therefore, adult-born neurons could provide an advantage to the OB, allowing it to adapt to an environment in constant remodelling, new odorants being encountered every day. Moreover, it is likely that adult-born and early-born cells in the OB present different functional characteristic, each of them contributing in a specific manner to olfactory processing. In line with this are data revealing the importance of a constant supply in newborn neurons in the normal processing in the OB, these cells display unique electrophysiological properties and influence the activity of OB principal cells in an exquisite way (Breton-Provencher et al., 2009; Carleton et al., 2003; Nissant et al., 2009). Moreover, responsiveness of early- and adult-born cells to incoming olfactory inputs is also different, the latest being more active following an odor stimulation (Livneh et al., 2014; Magavi et al., 2005) and presenting a form a plasticity unique to them allowing for a rapid adaptation to new incoming olfactory stimuli (Breton-Provencher et al., 2016). Several studies aimed at unravelling the involvement of adult-born cells in the different olfactory behaviors, giving rise sometimes to conflicting data and rarely comparing it with the involvement of their early-born homologues.

Several recent studies now take into account both populations of pre-existing and adult generated cells to investigate the role of GCs in olfactory processing and olfactory behavior. Indeed, reward-associated olfactory tasks could specifically activate adult-born cells, modulating their activity through an optogenetic activation or a pharmacogenetic inhibition influencing animals performances during the task (Grelat et al., 2018; Muthusamy et al., 2017). The same results were however not obtained when early-born GCs' activity was modulated (Grelat et al., 2018; Muthusamy et al., 2017). This differential involvement or early- and adult-born GCs was also observed in a context of a spontaneous odor behavior. In fact, an optogenetic inhibition of adult-born neurons prevented animals from discriminating during a perceptual learning task, both in a simple or more complex versions of the task involving similar odorants. On the other hand, early-born GCs inhibition only disrupted mice discrimination abilities during complex perceptual learning (Forest et al., 2019). The results presented above emphasize the fact that to fully understand what is happening during odor processing, one need to consider GCs as a heterogeneous population in term of the age and period of development of the cells. More studies would be needed, especially in a context of spontaneous odor behavior (such as spontaneous odor discrimination or short-term odor memory), to assess the specific contribution of adult- and early-born GCs.

We and others observed an heterogeneity in the calcium responses of GCs both in basal conditions but also in a context of odorant stimulation (Malvaut et al., 2017; Wienisch and Murthy, 2016). However, it is still unknown whether there are differences in the spontaneous and odor-evoked responses of early- and adult-born GCs *in vivo*. A possible experiment directed toward that end could be to inject two different calcium indicators (a GCaMP indicator and a RCaMP indicator for instance), in the RMS of the animals, one during the first postnatal week, and the other once the animal is adult (around postnatal day 60). This would allow to perform dual-color two-photon *in vivo* calcium imaging and compare in the same animals both populations of GCs.

B. The chemical makeup as a factor of GCs functional heterogeneity

As already discussed in the introduction, GCs can express different neurochemical markers. To date, the subpopulations of GCs expressing CR, CaMKIIα, CaMKIV, mGluR2, CPEB4 and 5T4 were described (Baker et al., 2001; Batista-Brito et al., 2008; Imamura et al., 2006; Jacobowitz and Winsky, 1991; Merkle et al., 2014; Murata et al., 2011; Tseng et al., 2017; Tseng et al., 2019; Zou et al., 2002). As presented in the two chapters of this thesis, we provided some insights towards the specific properties and involvement of two of these populations: the populations of CR+ and CaMKIIα+ cells. We showed that when it comes to their morphology, both subtypes are not different from the general population of GCs or to their negative counterparts. However, while both subtypes express a lower level of inhibition, the CR+ cells had decreased frequency of IPSCs associated to the decrease in the number of gephyrin puncta on their primary dendrites, while CaMKIIα+ GCs were characterized with a decreased amplitude and kinetics of the events. The decrease in the amplitude and kinetics could be linked to a differential composition in the subunits of ionotropic $GABA_A$ receptors since this composition determines the functional characteristics of the receptors (Farrant and Nusser, 2005). The different layers of the OB were shown to express different levels of several $GABA_A$ receptors and the GCL was shown for instance to express relatively high levels of the α2, α5, ß2, ß3 subunits, but also express γ2 subunit (Fritschy and Mohler, 1995; Laurie et al., 1992; Nunes and Kuner, 2015; Panzanelli et al., 2009) (***Figure 4.1***). Interestingly, a complete knock-out of the ß3 subunit resulted in an alteration of OB general oscillatory activity, leading to a deficit in odor discrimination (Nusser et al., 2001). However, when this subunit was deleted specifically in the GCL, it resulted in an increased inhibition of MCs and a concomitant acceleration in the learning of a go/no-go odor discrimination task (Nunes and Kuner, 2015). Therefore, investigating potential differences in the expression of some of the $GABA_A$ receptors between the subpopulations of CaMKIIα+ GCs and compare it to the general population of GCs could further precise the molecular basis underlying the electrophysiological differences we observed in two studies presented here. Some of our preliminary immunohistochemistry experiments already showed that

CaMKIIα+ cells express the α5 subunit, whereas the GCL seem to be devoid of a strong α1 labelling (***Figure 4.1***). If differences in the end are observed between our different GC subpopulations of interest, it would be interesting to knock-out or knock down the expression of selected $GABA_A$ receptors subunits specifically in these subpopulations, in order to evaluate then the functional outcome.

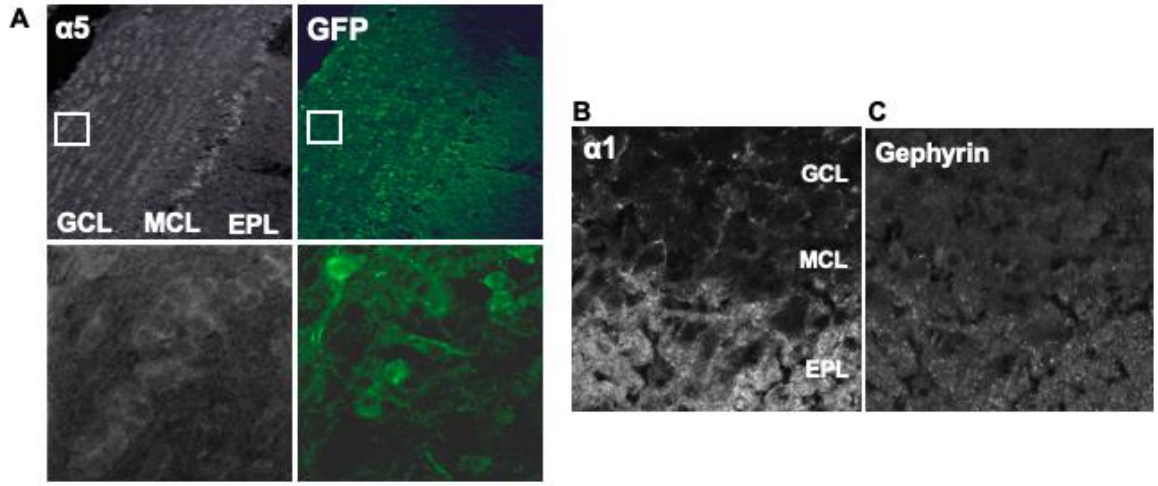

Figure 4.1: Expression of some $GABA_A$ receptors subunits and gephyrin in the OB and by CaMKIIα+ GCs

A. Representative image of an immunohistochemistry against the α5 $GABA_A$ receptor subunit in the OB (white). CaMKIIα-expressing cells are here expressing GFP following injection of a pCaMKIIα-expressing AAV vector. Note that α5 subunit is highly expressed at the level of the MCL but also in the GCL, and that it is expressed by CaMKIIα+ GCs. **B.** Representative image of an immunohistochemistry against the α1 $GABA_A$ receptor subunit in the OB. Here we can see that the GCL seem to be devoid of a strong labelling as opposed to the EPL.

The expression of CaMKIIα and CR were used only as markers to differentiate between subtypes of GCs. This raises the question of whether the functional differences we observed between GCs subpopulations are linked of the presence and functions of CaMKIIα and CR. CaMKIIα is important for the decoding of calcium signaling and plays a major role in the synaptic plasticity (De Koninck and Schulman, 1998; Giese et al., 1998; Lemieux et al., 2012; Lledo et al., 1995). Its expression is usually associated and restricted to excitatory neurons (Benson et al., 1992; Jones et al., 1994), however immunohistochemical analyzes of its expression revealed that in the OB, CaMKIIα is expressed only by the interneuronal population (Neant-Fery

et al., 2012; Zou et al., 2002). Interestingly, a single 30min exposure to odors was shown to increase CaMKIIα-mRNA and protein expression at the synaptic level (Neant-Fery et al., 2012). In addition, blocking CaMKIIα translocation at dendrites impaired mice' ability to perform an odor associative learning task (Neant-Fery et al., 2012). Therefore, considering also the electrophysiological differences we observed between CaMKIIα-expressing adult-born GCs and the general population of adult-born GCs, it is assumable that knocking down CaMKIIα expression in the GCL, via the use of a virus encoding for a CaMKIIα-shRNA could potentially alter OB physiology but also mice abilities to perform tasks in which we showed their involvement.

One of the main observations we made when comparing the role of different subpopulations of GCs was their differential involvement in several olfactory tasks. We showed in the first study that CaMKIIα-expressing cells are highly activated following several olfactory tasks and are required for the completion of a spontaneous olfactory discrimination task, and a go/no-go odor operant condition one, when complex odor mixture are involved. On the opposite, we revealed that tasks such as perceptual learning would require more the activation of CaMKIIα-negative cells. In the second study, we show that CR are also activated following odor discrimination-based tasks (spontaneous and go/no-go), and their inhibition alter mice ability to correctly discriminate between two closely related odorants in a reward-associated discrimination task. In addition of determining the involvement of the two GCs subtypes studies in this thesis, the effect of their inhibition on the completion of other tasks such as long-term associative memory, spontaneous odor discrimination (for CR-expressing cells) and on the odor detection threshold could also be performed using the same chemogenetic approach to further investigate their role in odor behavior. Nevertheless, although we clearly show that animals' discrimination abilities are disrupted with an inhibition of CR+ or CaMKIIα+ activity, we cannot rule out that an inhibition of GCs not expressing these markers would also have an impact on mice performances. To answer this question, experiments involving a Cre-Off strategy to either chemogenetically (DREADDs-Gi) or

optogenetically (expression of a halorhodopsin or NpHR) inactivate CR- or CaMKIIα- cells would be required.

Using dual-color two-photon calcium imaging, we (Malvaut et al., 2017) and previous reports (Kato et al., 2012; Wienisch and Murthy, 2016) revealed that GCs taken as an ensemble, already present a functional heterogeneity. The same heterogeneity was observed when we compared the *in vivo* calcium responses of CaMKIIα+ GCs to the general GCs subpopulation. It is noteworthy that the *in vivo* calcium imaging experiments performed here were done on anesthetized animals. However, wakefulness was shown to have a strong impact on recorded *in vivo* calcium dynamics, especially in our case on OB cells ones (Kato et al., 2012). Therefore, to correlate more with physiological conditions, calcium dynamics of the different subpopulations of interest, both in basal and odor contexts, would benefit from being recorded in awake head restrained animals. This approach is now being used in several reports investigating OB network functioning and allows to perform odorant stimulation while performing *in vivo* imaging of GCs for instance (Kato et al., 2012; Platel et al., 2019; Wallace et al., 2017). It also allows to perform several behavioral tasks in a modified version fitting animals' head fixation. This is for instance the case for go/no-go operant conditioning (Gschwend et al., 2015; Yamada et al., 2017). In our study, we saw that CaMKIIα+ and CR+ GCs are required and activated during go/no-go odor discrimination. However, one still need to determine which parameter of this task activates these cells populations. Performing calcium *in vivo* imaging in animals while performing in the meantime such a task would allow to follow cell populations' activation at every step of learning. Will one observe a progressive recruiting of specific cell populations along learning and trials whereas others would progressively disengage? Would specific cell population be more reactive to the reward-associated odorant (S+ odor) as compared to the S- one being presented without reward? Using the same transgenic mouse line as used in chapter 2 (i.e Calretinin-Cre mice) coupled to a viral injection of a cre-dependant RCaMP virus for instance and a GCaMP vector under the CaMKIIα promoter could for instance allow to compare calcium dynamics of 2 subpopulations of cells in basal or

odor stimulation conditions, but also to compare these dynamics in animals acquiring an operant odor discrimination task.

As discussed above, performing *in vivo* two-photon calcium in awake animals represents a very useful tool that can allow to better understand olfactory processing in the olfactory bulb as well as the role of cellular subpopulations in olfactory behavior. In addition, it does not alter mice ability to learn the task and giving similar results than those obtained in a classical go/no-go odor discrimination task were animals can freely behave in the test chamber (Abraham et al., 2012). However, performing odor discrimination with head restrained animals misses several parameters that can be important in a context of behavioral readout: animals' motivation to perform the task and self-initiation of task trials for tasks like go/no-go. Hence, studying the involvement and recruitment of GCs subpopulations during other behavioral tasks like spontaneous odor discrimination, short-term memory of perceptual learning or long-term associative memory while performing two-photons imaging in head restrained awake animals is impossible since the behavioral readout in these tasks is the time spend by the animal exploring the odors. Another tool was developed in the last years allowing to perform longitudinal calcium imaging in freely behaving animals: miniature endoscopes. In fact, these miniature microscopes allow to image cell activity (using calcium indicators for instance) with a good resolution in regions ranging sometimes up to more than 5mm in depth. It also allows to perform recordings in a context allowing for animals to behave in a way close to their natural behavior, some parameters such as food or water consumption or some sensory modalities being at the same time evaluated (Patel et al., 2019). A dual-color imaging system is also commercially available, opening the way for the recording of different subgroups or subpopulations of cells at the same time in the same region of interest. Such a tool would definitely help investigate the engagement and involvement of GCs subtypes in spontaneous odor behavior. However, although really promising and useful, the current versions of the existing miniature endoscopes cannot be implanted at the level of the OB, its bulkiness preventing it from being installed in very anterior brain regions.

2. Towards a differential wiring of GCs subtypes

As discussed above, the functional differences observed between the GC subtypes could be explained partly by the electrophysiological differences. As presented more extensively in the introduction chapter, it is also assumable that another level of heterogeneity exists among the population of GCs, a heterogeneity introduced by the inputs the OB receives from other brain structures. In fact the GCL is targeted by projections arriving from structures such as the piriform area, the anterior amygdalar area, the dorsal raphe nucleus, but also the basal forebrain (Hintiryan et al., 2012; Niedworok et al., 2012; Padmanabhan et al., 2016) (see also ***Figure 1.13***). Moreover, the functional implication of the vast neuromodulatory inputs that the OB receives was investigated, highlighting for instance that modulating GABAergic or cholinergic projections in the GCL can affect the physiology of M/T cells but also have an impact on animal's performances on olfactory based tasks such as odor discrimination or olfactory fear conditioning (Chaudhury et al., 2009; Escanilla et al., 2012; Gracia-Llanes et al., 2010; Mandairon et al., 2006a; Nunez-Parra et al., 2013). For all the reasons presented, we hypothesized that the different subpopulations of GCs, in addition of being defined by the expression of different neurochemical markers, are also defined by potentially different inputs they may receive from higher brain regions. But it is important to note that these inputs can be different in terms of the brain regions they come from, but also in term of the type of projections they are (i.e inhibitory or excitatory). Current work in the lab is directed toward that end and I will briefly present the methodology we intend to use as well as the preliminary results I have already obtained.

A. Identification of olfactory bulb projecting regions (OPR) of interest

As shown on ***Figure 1.13***, data obtained by the Allen Brain institute confirmed that the OB receives projections from different brain regions. To validate and investigate further the connections that GC subpopulations receive, we took advantage of trans-synaptic spread of serotype 1 Cre-expressing AAV virus (Zingg et al., 2017) and injected it in Cre-dependant GFP reporter animals, in some brain

regions previously shown to project to the OB. This allows the expression of GFP after recombination by OB cells receiving inputs from the targeted OPR where the Cre virus was injected (***Figure 4.2***). We confirmed for instance that the OB receives projection from several regions such as the anterior amygdalar area, the dorsal taenia tecta or the horizontal diagonal band. The labelling clearly also reveals the differential targeting of OB cell populations. There is in our case a strong labelling of OB principal cells when the transsynaptic vector was injected at the level of the anterior amygdalar area, or a sparse GCL labelling when injections were performed either in the horizontal diagonal band or the dorsal taenia tecta.

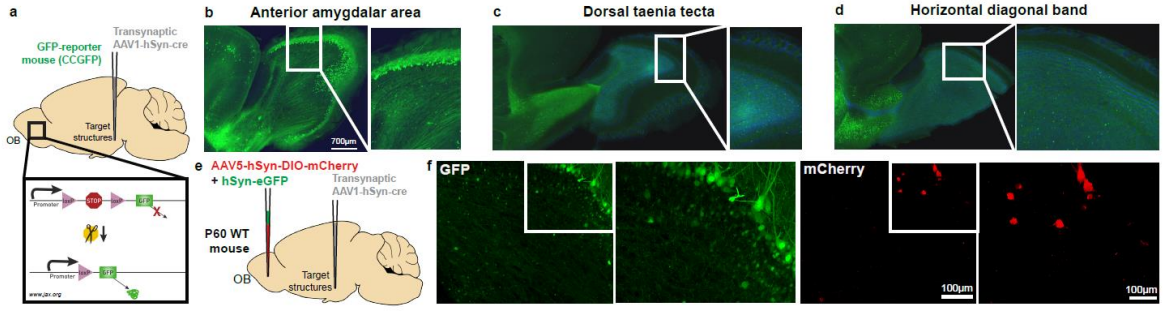

Figure 4.2: Transsynaptic identification of OB projecting regions

A. Schematic representation of the injection in OPRs of a transsynaptic AAV1-hSyn-cre vector in CCGFP animals, 4 wpi. **B-D**. Representative confocal images of OPR targeted cells in the OB. Transsynaptic Cre AAV1 was injected in regions such as the anterior amygdalar area (**B**), dorsal taenia tecta (**C**) or horizontal diagonal band (**D**). **E**. Schematic representation of the injection in the OPRs of a transsynaptic AAV1-hSyn-Cre, and a combination of AAV5-hSyn-DIO-mCherry and hSyn-eGFP in the OB of P60 WT animals. This approach allows for the expression of mCherry by OB cells receiving inputs from the OPR of interest, and of GFP by the general population of bulbar cells. **F**. Representative confocal images of horizontal diagonal band targeted cells in the OB. Left panel shows GFP-expressing resident cells in the OB, whereas right panel shows OB cells specifically contacted by projections coming from the basal forebrain. *Data from Tiziano Siri*.

Using this approach, we are aiming at characterizing more specifically GCs depending on the regions they receive projection from. For instance, using an injection of a combination of a Cre-dependant mCherry virus and a non Cre-dependant GFP one in the OB or the RMS (to label more specifically adult-born cells), we can investigate both morphology and electrophysiological properties of the infected GCs, depending on the OPR were the transsynaptic Cre virus was injected

(***Figure 4.2***). This technique can also allow to phenotype the OPR-contacted cells using neurochemical markers GCs are known to express. It would also be of interest to record calcium activity of GCs specifically contacted by some OPR and compare it to the general GC population, or to see the effect of stimulating OPR-projections on OB physiology and olfactory behavior. Finally, using a retrograde Cre-expressing AAV virus at the level of the GCL and a Cre-dependant reporter virus in OPRs, one can investigate the cell types that are more particularly projecting to GCs from this structure and compare its activity with the other resident cells in the OPR.

B. The role of basal forebrain inputs in olfactory processing

Among the OPR we are investigating, we are currently focusing on one of them more particularly: the basal forebrain (BF). This region is the main cholinergic brain region and represent a hub for many ascending and descending pathways (Blake and Boccia, 2018). It was also shown to be involved in a broad range of brain functions such as arousal, several cognitive functions but also attention and memory. The OB, and more specifically the GCL receives important both GABAergic and cholinergic inputs from this region (Gracia-Llanes et al., 2010; Niedworok et al., 2012; Nunez-Parra et al., 2013). Therefore, we are presently interested to investigate the role that this structure may also play in olfactory function. To do so, we injected GCaMP6s-expressing AAV at the level of the BF and implanted at the same level a miniature endoscope to record *in vivo* Ca^{2+} activity in freely behaving animals. Very interestingly, our preliminary observations revealed that an increase in Ca^{2+} activity in the BF seem to be linked to animal exploration. Since in rodents such as mice, exploration is relying mostly on the sense of smell and so its sniffing behavior, we decided to record animals' respiration and activity in the BF simultaneously (***Figure 4.3***). To this end, animals were also implanted with a thermistor in one of their nostril, a probe that is minimally invasive and reliably records small changes in temperature at the level of the nasal cavity (McAfee et al., 2016). In fact, depending on the frequency of the events recorded by the thermistor, it is possible to discriminate between normal breathing periods and sniffing periods (having a higher event frequency) (***Figure 4.3***). This dual-modality imaging

technique allow us to investigate the activity of BF in response of stimuli with different modality and valences such as a novel odor, natural and neuronal odorants or even another conspecific for socially-relevant odors.

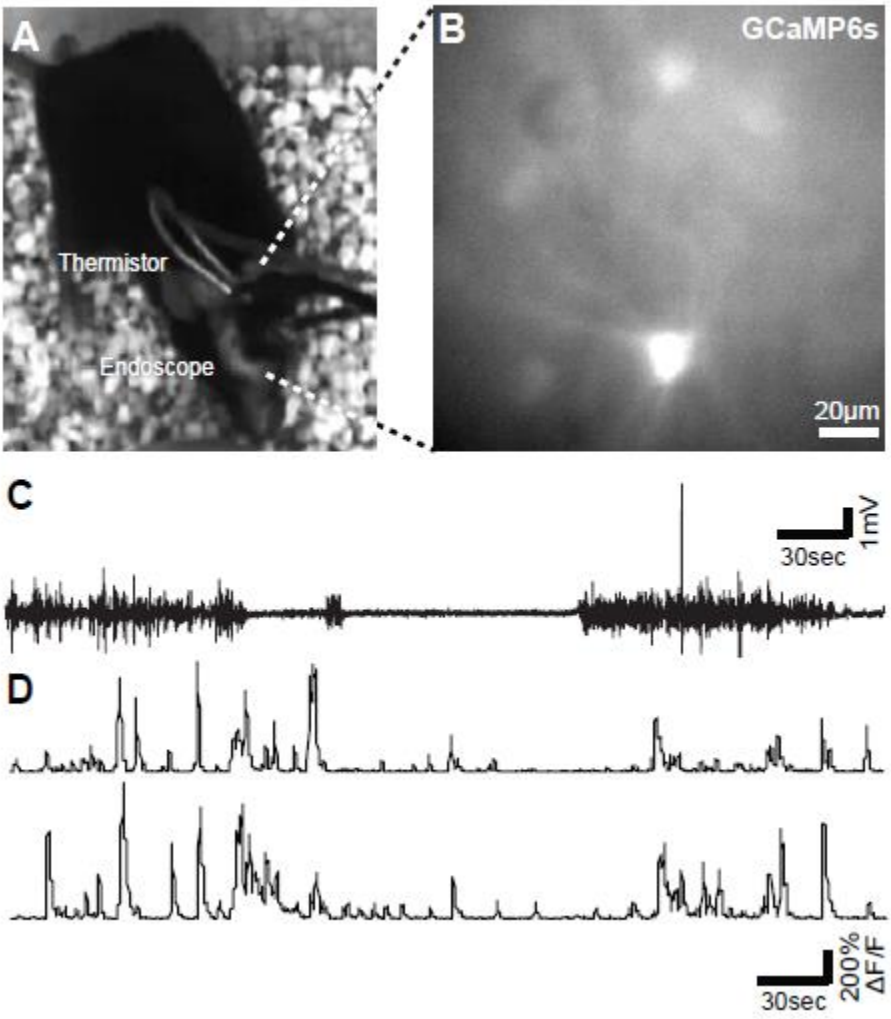

Figure 4.2: Basal forebrain activity is linked to sniffing

A. Photograph of an animal implanted with a miniature endoscope at the level of the BF and a thermistor in a nostril. **B.** Example of GCaMP6s infected cells in the BF. **C.** Example of a respiratory trace recorded with a thermistor. **D.** Examples of Ca^{2+} traces from two BF cells.

GENERAL CONCLUSION

Unravelling and understanding brain structure and function has and will always remain a fascinating topic, notably because of its neuronal heterogeneity and circuitry complexity. In case of the OB, which is important and indispensable for processing of incoming olfactory inputs, several subtypes of the most numerous cell population in this structure (i.e GCs) exists. With our work, we were able to show that each of these subpopulations of cells may contribute in a very unique way to the OB network, thanks to different functional properties, but also to olfactory behaviors. However, the subtypes we studied here only represent a fraction of the cellular pool of the OB. Further investigations focusing on other subtypes, some of them still remaining to be discovered, would be needed to fully understand the heterogeneity in the OB but also its functioning.

In the case of the OB, another remarkable process, adult neurogenesis, occurs on a daily basis and constantly rejuvenate the structure with new neurons that can fully integrate. This process is tightly regulated by different molecules and mechanisms but is also highly sensitive to experience, which can influence the level of incoming newborn neurons in the OB. Moreover, it represents an excellent model of neuronal development and integration of immature cells in a complex neuronal network. Therefore, it could be used as a scaffold to study those processes in a context of healthy or even disease-modeling cells grafting, allowing to better understand pathologies like neurodevelopmental diseases that are known to affect several steps of neuronal development. Finally, in an era where research is oriented towards cell replacement therapies for patients with neurodegenerative diseases for instance, it is necessary to fully understand the neuronal diversity, in order to establish efficient therapies. This in fact involves a control of the integration of specific neuronal subtypes and that the precise role every of these subtypes plays in targeted brain regions that can potentially be affected by cerebral pathologies, is fully understood.

REFERENCES

Abraham, N.M., Egger, V., Shimshek, D.R., Renden, R., Fukunaga, I., Sprengel, R., Seeburg, P.H., Klugmann, M., Margrie, T.W., Schaefer, A.T.*, et al.* (2010). Synaptic inhibition in the olfactory bulb accelerates odor discrimination in mice. Neuron *65*, 399-411.

Abraham, N.M., Guerin, D., Bhaukaurally, K., and Carleton, A. (2012). Similar odor discrimination behavior in head-restrained and freely moving mice. PLoS One *7*, e51789.

Alexander, G.M., Rogan, S.C., Abbas, A.I., Armbruster, B.N., Pei, Y., Allen, J.A., Nonneman, R.J., Hartmann, J., Moy, S.S., Nicolelis, M.A.*, et al.* (2009). Remote control of neuronal activity in transgenic mice expressing evolved G protein-coupled receptors. Neuron *63*, 27-39.

Alonso, M., Lepousez, G., Sebastien, W., Bardy, C., Gabellec, M.M., Torquet, N., and Lledo, P.M. (2012). Activation of adult-born neurons facilitates learning and memory. Nat Neurosci *15*, 897-904.

Alonso, M., Viollet, C., Gabellec, M.M., Meas-Yedid, V., Olivo-Marin, J.C., and Lledo, P.M. (2006). Olfactory discrimination learning increases the survival of adult-born neurons in the olfactory bulb. J Neurosci *26*, 10508-10513.

Altman, J. (1969). Autoradiographic and histological studies of postnatal neurogenesis. IV. Cell proliferation and migration in the anterior forebrain, with special reference to persisting neurogenesis in the olfactory bulb. J Comp Neurol *137*, 433-457.

Alvarez-Buylla, A., and Garcia-Verdugo, J.M. (2002). Neurogenesis in adult subventricular zone. J Neurosci *22*, 629-634.

Arevian, A.C., Kapoor, V., and Urban, N.N. (2008). Activity-dependent gating of lateral inhibition in the mouse olfactory bulb. Nat Neurosci *11*, 80-87.

Armbruster, B.N., Li, X., Pausch, M.H., Herlitze, S., and Roth, B.L. (2007). Evolving the lock to fit the key to create a family of G protein-coupled receptors potently activated by an inert ligand. Proc Natl Acad Sci U S A *104*, 5163-5168.

Arruda-Carvalho, M., Akers, K.G., Guskjolen, A., Sakaguchi, M., Josselyn, S.A., and Frankland, P.W. (2014). Posttraining ablation of adult-generated olfactory granule cells degrades odor-reward memories. J Neurosci *34*, 15793-15803.

Baker, H., Liu, N., Chun, H.S., Saino, S., Berlin, R., Volpe, B., and Son, J.H. (2001). Phenotypic differentiation during migration of dopaminergic progenitor cells to the olfactory bulb. J Neurosci *21*, 8505-8513.

Baker, H., Morel, K., Stone, D.M., and Maruniak, J.A. (1993). Adult naris closure profoundly reduces tyrosine hydroxylase expression in mouse olfactory bulb. Brain Res *614*, 109-116.

Bastien-Dionne, P.O., David, L.S., Parent, A., and Saghatelyan, A. (2010). Role of sensory activity on chemospecific populations of interneurons in the adult olfactory bulb. J Comp Neurol *518*, 1847-1861.

Bath, K.G., Mandairon, N., Jing, D., Rajagopal, R., Kapoor, R., Chen, Z.Y., Khan, T., Proenca, C.C., Kraemer, R., Cleland, T.A.*, et al.* (2008). Variant brain-derived neurotrophic factor (Val66Met) alters adult olfactory bulb neurogenesis and spontaneous olfactory discrimination. J Neurosci *28*, 2383-2393.

Bathellier, B., Buhl, D.L., Accolla, R., and Carleton, A. (2008). Dynamic ensemble odor coding in the mammalian olfactory bulb: sensory information at different timescales. Neuron *57*, 586-598.

Batista-Brito, R., Close, J., Machold, R., and Fishell, G. (2008). The distinct temporal origins of olfactory bulb interneuron subtypes. J Neurosci *28*, 3966-3975.

Beckervordersandforth, R., Tripathi, P., Ninkovic, J., Bayam, E., Lepier, A., Stempfhuber, B., Kirchhoff, F., Hirrlinger, J., Haslinger, A., Lie, D.C.*, et al.* (2010). In vivo fate mapping and expression analysis reveals molecular hallmarks of prospectively isolated adult neural stem cells. Cell Stem Cell *7*, 744-758.

Belluzzi, O., Benedusi, M., Ackman, J., and LoTurco, J.J. (2003). Electrophysiological differentiation of new neurons in the olfactory bulb. J Neurosci *23*, 10411-10418.

Belnoue, L., Grosjean, N., Abrous, D.N., and Koehl, M. (2011). A critical time window for the recruitment of bulbar newborn neurons by olfactory discrimination learning. J Neurosci *31*, 1010-1016.

Belnoue, L., Malvaut, S., Ladevèze, E., Abrous, D.N., and Koehl, M. (2016). Plasticity in the olfactory bulb of the maternal mouse is prevented by gestational stress. Scientific Reports *6*, 37615.

Benson, D.L., Isackson, P.J., Gall, C.M., and Jones, E.G. (1992). Contrasting patterns in the localization of glutamic acid decarboxylase and Ca2+/calmodulin protein kinase gene expression in the rat central nervous system. Neuroscience *46*, 825-849.

Blake, M.G., and Boccia, M.M. (2018). Basal Forebrain Cholinergic System and Memory. Curr Top Behav Neurosci *37*, 253-273.

Bolteus, A.J., and Bordey, A. (2004). GABA release and uptake regulate neuronal precursor migration in the postnatal subventricular zone. J Neurosci *24*, 7623-7631.

Boyd, A.M., Sturgill, J.F., Poo, C., and Isaacson, J.S. (2012). Cortical feedback control of olfactory bulb circuits. Neuron *76*, 1161-1174.

Brandt, M.D., Jessberger, S., Steiner, B., Kronenberg, G., Reuter, K., Bick-Sander, A., von der Behrens, W., and Kempermann, G. (2003). Transient calretinin expression defines early postmitotic step of neuronal differentiation in adult hippocampal neurogenesis of mice. Mol Cell Neurosci *24*, 603-613.

Breton-Provencher, V., Bakhshetyan, K., Hardy, D., Bammann, R.R., Cavarretta, F., Snapyan, M., Cote, D., Migliore, M., and Saghatelyan, A. (2016). Principal cell activity induces spine relocation of adult-born interneurons in the olfactory bulb. Nature Communications *7*, 12659.

Breton-Provencher, V., Lemasson, M., Peralta, M.R., 3rd, and Saghatelyan, A. (2009). Interneurons produced in adulthood are required for the normal functioning of the olfactory bulb network and for the execution of selected olfactory behaviors. J Neurosci *29*, 15245-15257.

Breton-Provencher, V., and Saghatelyan, A. (2012). Newborn neurons in the adult olfactory bulb: unique properties for specific odor behavior. Behavioral Brain Research *227*, 480-489.

Brus, M., Meurisse, M., Keller, M., and Levy, F. (2014). Interactions with the young down-regulate adult olfactory neurogenesis and enhance the maturation of olfactory neuroblasts in sheep mothers. Front Behav Neurosci *8*, 53.

Calof, A.L., Mumm, J.S., Rim, P.C., and Shou, J. (1998). The neuronal stem cell of the olfactory epithelium. J Neurobiol *36*, 190-205.

Camillo, D., Levelt, C.N., and Heimel, J.A. (2014). Lack of functional specialization of neurons in the mouse primary visual cortex that have expressed calretinin. Front Neuroanat *8*, 89.

Carleton, A., Petreanu, L.T., Lansford, R., Alvarez-Buylla, A., and Lledo, P.M. (2003). Becoming a new neuron in the adult olfactory bulb. Nat Neurosci *6*, 507-518.

Cavallin, M.A., Powell, K., Biju, K.C., and Fadool, D.A. (2010). State-dependent sculpting of olfactory sensory neurons is attributed to sensory enrichment, odor deprivation, and aging. Neurosci Lett *483*, 90-95.

Chaker, Z., Aid, S., Berry, H., and Holzenberger, M. (2015). Suppression of IGF-I signals in neural stem cells enhances neurogenesis and olfactory function during aging. Aging Cell *14*, 847-856.

Chaudhury, D., Escanilla, O., and Linster, C. (2009). Bulbar acetylcholine enhances neural and perceptual odor discrimination. J Neurosci *29*, 52-60.

Codega, P., Silva-Vargas, V., Paul, A., Maldonado-Soto, A.R., Deleo, A.M., Pastrana, E., and Doetsch, F. (2014). Prospective identification and purification of quiescent adult neural stem cells from their in vivo niche. Neuron *82*, 545-559.

Corona, R., and Levy, F. (2015). Chemical olfactory signals and parenthood in mammals. Horm Behav *68*, 77-90.

Corona, R., Meurisse, M., Cornilleau, F., Moussu, C., Keller, M., and Levy, F. (2017). Exposure to young preferentially activates adult-born neurons in the main olfactory bulb of sheep mothers. Brain Struct Funct *222*, 1219-1229.

Corotto, F.S., Henegar, J.R., and Maruniak, J.A. (1994). Odor deprivation leads to reduced neurogenesis and reduced neuronal survival in the olfactory bulb of the adult mouse. Neuroscience *61*, 739-744.

Cummings, D.M., Henning, H.E., and Brunjes, P.C. (1997). Olfactory bulb recovery after early sensory deprivation. J Neurosci *17*, 7433-7440.

Cummings, D.M., Snyder, J.S., Brewer, M., Cameron, H.A., and Belluscio, L. (2014). Adult neurogenesis is necessary to refine and maintain circuit specificity. J Neurosci *34*, 13801-13810.

Daroles, L., Gribaudo, S., Doulazmi, M., Scotto-Lomassese, S., Dubacq, C., Mandairon, N., Greer, C.A., Didier, A., Trembleau, A., and Caille, I. (2016). Fragile X Mental Retardation Protein and Dendritic Local Translation of the Alpha Subunit of the Calcium/Calmodulin-Dependent Kinase II Messenger RNA Are Required for the Structural Plasticity Underlying Olfactory Learning. Biol Psychiatry *80*, 149-159.

David, L.S., Schachner, M., and Saghatelyan, A. (2013). The extracellular matrix glycoprotein tenascin-R affects adult but not developmental neurogenesis in the olfactory bulb. J Neurosci *33*, 10324-10339.

Davis, R.L. (2004). Olfactory learning. Neuron *44*, 31-48.

Davison, I.G., and Katz, L.C. (2007). Sparse and selective odor coding by mitral/tufted neurons in the main olfactory bulb. J Neurosci *27*, 2091-2101.

De Koninck, P., and Schulman, H. (1998). Sensitivity of CaM kinase II to the frequency of Ca2+ oscillations. Science *279*, 227-230.

De Marchis, S., Bovetti, S., Carletti, B., Hsieh, Y.C., Garzotto, D., Peretto, P., Fasolo, A., Puche, A.C., and Rossi, F. (2007). Generation of distinct types of periglomerular olfactory bulb interneurons during development and in adult mice: implication for intrinsic properties of the subventricular zone progenitor population. J Neurosci *27*, 657-664.

Deprez, F., Pallotto, M., Vogt, F., Grabiec, M., Virtanen, M.A., Tyagarajan, S.K., Panzanelli, P., and Fritschy, J.M. (2015). Postsynaptic gephyrin clustering controls the development of adult-born granule cells in the olfactory bulb. J Comp Neurol *523*, 1998-2016.

Deshpande, A., Bergami, M., Ghanem, A., Conzelmann, K.K., Lepier, A., Gotz, M., and Berninger, B. (2013). Retrograde monosynaptic tracing reveals the temporal evolution of inputs onto new neurons in the adult dentate gyrus and olfactory bulb. Proc Natl Acad Sci U S A *110*, E1152-1161.

Didier, A., Carleton, A., Bjaalie, J.G., Vincent, J.D., Ottersen, O.P., Storm-Mathisen, J., and Lledo, P.M. (2001). A dendrodendritic reciprocal synapse provides a recurrent excitatory connection in the olfactory bulb. Proc Natl Acad Sci U S A *98*, 6441-6446.

Doetsch, F., Caille, I., Lim, D.A., Garcia-Verdugo, J.M., and Alvarez-Buylla, A. (1999). Subventricular zone astrocytes are neural stem cells in the adult mammalian brain. Cell *97*, 703-716.

Drobizhev, M., Tillo, S., Makarov, N.S., Hughes, T.E., and Rebane, A. (2009). Absolute two-photon absorption spectra and two-photon brightness of orange and red fluorescent proteins. J Phys Chem B *113*, 855-859.

Enwere, E., Shingo, T., Gregg, C., Fujikawa, H., Ohta, S., and Weiss, S. (2004). Aging results in reduced epidermal growth factor receptor signaling, diminished olfactory neurogenesis, and deficits in fine olfactory discrimination. J Neurosci *24*, 8354-8365.

Escanilla, O., Alperin, S., Youssef, M., Ennis, M., and Linster, C. (2012). Noradrenergic but not cholinergic modulation of olfactory bulb during processing of near threshold concentration stimuli. Behav Neurosci *126*, 720-728.

Fantana, A.L., Soucy, E.R., and Meister, M. (2008). Rat olfactory bulb mitral cells receive sparse glomerular inputs. Neuron *59*, 802-814.

Farbman, A.I., Brunjes, P.C., Rentfro, L., Michas, J., and Ritz, S. (1988). The effect of unilateral naris occlusion on cell dynamics in the developing rat olfactory epithelium. J Neurosci *8*, 3290-3295.

Farrant, M., and Nusser, Z. (2005). Variations on an inhibitory theme: phasic and tonic activation of GABA(A) receptors. Nat Rev Neurosci *6*, 215-229.

Feierstein, C.E. (2012). Linking adult olfactory neurogenesis to social behavior. Front Neurosci *6*, 173.

Feierstein, C.E., Lazarini, F., Wagner, S., Gabellec, M.M., de Chaumont, F., Olivo-Marin, J.C., Boussin, F.D., Lledo, P.M., and Gheusi, G. (2010). Disruption of Adult Neurogenesis in the Olfactory Bulb Affects Social Interaction but not Maternal Behavior. Front Behav Neurosci *4*, 176.

Flores, C.E., Nikonenko, I., Mendez, P., Fritschy, J.M., Tyagarajan, S.K., and Muller, D. (2015). Activity-dependent inhibitory synapse remodeling through gephyrin phosphorylation. Proc Natl Acad Sci U S A *112*, E65-72.

Fogli Iseppe, A., Pignatelli, A., and Belluzzi, O. (2016). Calretinin-Periglomerular Interneurons in Mice Olfactory Bulb: Cells of Few Words. Front Cell Neurosci *10*, 231.

Forest, J., Chalencon, L., Midroit, M., Terrier, C., Caille, I., Sacquet, J., Benetollo, C., Martin, K., Richard, M., Didier, A.*, et al.* (2019). Role of Adult-Born Versus Preexisting Neurons Born at P0 in Olfactory Perception in a Complex Olfactory Environment in Mice. Cereb Cortex.

Fritschy, J.M., and Mohler, H. (1995). GABAA-receptor heterogeneity in the adult rat brain: differential regional and cellular distribution of seven major subunits. J Comp Neurol *359*, 154-194.

Fuentealba, L.C., Rompani, S.B., Parraguez, J.I., Obernier, K., Romero, R., Cepko, C.L., and Alvarez-Buylla, A. (2015). Embryonic Origin of Postnatal Neural Stem Cells. Cell *161*, 1644-1655.

Fukunaga, I., Herb, J.T., Kollo, M., Boyden, E.S., and Schaefer, A.T. (2014). Independent control of gamma and theta activity by distinct interneuron networks in the olfactory bulb. Nat Neurosci *17*, 1208-1216.

Furutachi, S., Miya, H., Watanabe, T., Kawai, H., Yamasaki, N., Harada, Y., Imayoshi, I., Nelson, M., Nakayama, K.I., Hirabayashi, Y.*, et al.* (2015). Slowly dividing neural progenitors are an embryonic origin of adult neural stem cells. Nat Neurosci *18*, 657-665.

Gengatharan, A., Bammann, R.R., and Saghatelyan, A. (2016). The Role of Astrocytes in the Generation, Migration, and Integration of New Neurons in the Adult Olfactory Bulb. Front Neuroscience *10*, 149.

Gheusi, G., Cremer, H., McLean, H., Chazal, G., Vincent, J.D., and Lledo, P.M. (2000). Importance of newly generated neurons in the adult olfactory bulb for odor discrimination. Proc Natl Acad Sci U S A *97*, 1823-1828.

Ghosh, S., Larson, S.D., Hefzi, H., Marnoy, Z., Cutforth, T., Dokka, K., and Baldwin, K.K. (2011). Sensory maps in the olfactory cortex defined by long-range viral tracing of single neurons. Nature *472*, 217-220.

Giese, K.P., Fedorov, N.B., Filipkowski, R.K., and Silva, A.J. (1998). Autophosphorylation at Thr286 of the alpha calcium-calmodulin kinase II in LTP and learning. Science *279*, 870-873.

Gracia-Llanes, F.J., Crespo, C., Blasco-Ibanez, J.M., Nacher, J., Varea, E., Rovira-Esteban, L., and Martinez-Guijarro, F.J. (2010). GABAergic basal forebrain afferents innervate selectively GABAergic targets in the main olfactory bulb. Neuroscience *170*, 913-922.

Graziadei, P.P., and Graziadei, G.A. (1979). Neurogenesis and neuron regeneration in the olfactory system of mammals. I. Morphological aspects of differentiation and structural organization of the olfactory sensory neurons. J Neurocytol *8*, 1-18.

Greer, C.A. (1987). Golgi analyses of dendritic organization among denervated olfactory bulb granule cells. J Comp Neurol *257*, 442-452.

Grelat, A., Benoit, L., Wagner, S., Moigneu, C., Lledo, P.M., and Alonso, M. (2018). Adult-born neurons boost odor-reward association. Proc Natl Acad Sci U S A *115*, 2514-2519.

Gribaudo, S., Bovetti, S., Garzotto, D., Fasolo, A., and De Marchis, S. (2009). Expression and localization of the calmodulin-binding protein neurogranin in the adult mouse olfactory bulb. J Comp Neurol *517*, 683-694.

Grosenick, L., Marshel, J.H., and Deisseroth, K. (2015). Closed-loop and activity-guided optogenetic control. Neuron *86*, 106-139.

Gschwend, O., Abraham, N.M., Lagier, S., Begnaud, F., Rodriguez, I., and Carleton, A. (2015). Neuronal pattern separation in the olfactory bulb improves odor discrimination learning. Nat Neurosci *18*, 1474-1482.

Guthrie, K.M., Anderson, A.J., Leon, M., and Gall, C. (1993). Odor-induced increases in c-fos mRNA expression reveal an anatomical "unit" for odor processing in olfactory bulb. Proc Natl Acad Sci U S A *90*, 3329-3333.

Hack, I., Bancila, M., Loulier, K., Carroll, P., and Cremer, H. (2002). Reelin is a detachment signal in tangential chain-migration during postnatal neurogenesis. Nat Neurosci *5*, 939-945.

Hack, M.A., Saghatelyan, A., de Chevigny, A., Pfeifer, A., Ashery-Padan, R., Lledo, P.M., and Gotz, M. (2005). Neuronal fate determinants of adult olfactory bulb neurogenesis. Nat Neurosci *8*, 865-872.

Hintiryan, H., Gou, L., Zingg, B., Yamashita, S., Lyden, H.M., Song, M.Y., Grewal, A.K., Zhang, X., Toga, A.W., and Dong, H.W. (2012). Comprehensive connectivity of the mouse main olfactory bulb: analysis and online digital atlas. Front Neuroanat *6*, 30.

Ihrie, R.A., and Alvarez-Buylla, A. (2011). Lake-front property: a unique germinal niche by the lateral ventricles of the adult brain. Neuron *70*, 674-686.

Imamura, F., Nagao, H., Naritsuka, H., Murata, Y., Taniguchi, H., and Mori, K. (2006). A leucine-rich repeat membrane protein, 5T4, is expressed by a subtype of granule cells with dendritic arbors in specific strata of the mouse olfactory bulb. J Comp Neurol *495*, 754-768.

Imayoshi, I., Sakamoto, M., Ohtsuka, T., Takao, K., Miyakawa, T., Yamaguchi, M., Mori, K., Ikeda, T., Itohara, S., and Kageyama, R. (2008). Roles of continuous neurogenesis in the structural and functional integrity of the adult forebrain. Nat Neurosci *11*, 1153-1161.

In 't Zandt, E.E., Cansler, H.L., Denson, H.B., and Wesson, D.W. (2019). Centrifugal Innervation of the Olfactory Bulb: A Reappraisal. eNeuro *6*.

Inaki, K., Takahashi, Y.K., Nagayama, S., and Mori, K. (2002). Molecular-feature domains with posterodorsal-anteroventral polarity in the symmetrical sensory maps of the mouse olfactory bulb: mapping of odourant-induced Zif268 expression. Eur J Neurosci *15*, 1563-1574.

Isaacson, J.S., and Strowbridge, B.W. (1998). Olfactory reciprocal synapses: dendritic signaling in the CNS. Neuron *20*, 749-761.

Jacobowitz, D.M., and Winsky, L. (1991). Immunocytochemical localization of calretinin in the forebrain of the rat. J Comp Neurol *304*, 198-218.

Jahr, C.E., and Nicoll, R.A. (1982). An intracellular analysis of dendrodendritic inhibition in the turtle in vitro olfactory bulb. J Physiol *326*, 213-234.

Jakobsson, J., Ericson, C., Jansson, M., Bjork, E., and Lundberg, C. (2003). Targeted transgene expression in rat brain using lentiviral vectors. J Neurosci Res *73*, 876-885.

Jiang, M., and Swann, J.W. (1997). Expression of calretinin in diverse neuronal populations during development of rat hippocampus. Neuroscience *81*, 1137-1154.

Jones, E.G., Huntley, G.W., and Benson, D.L. (1994). Alpha calcium/calmodulin-dependent protein kinase II selectively expressed in a subpopulation of excitatory neurons in monkey sensory-motor cortex: comparison with GAD-67 expression. J Neurosci *14*, 611-629.

Jones, S.V., Choi, D.C., Davis, M., and Ressler, K.J. (2008). Learning-dependent structural plasticity in the adult olfactory pathway. J Neurosci *28*, 13106-13111.

Kaneko, N., Marin, O., Koike, M., Hirota, Y., Uchiyama, Y., Wu, J.Y., Lu, Q., Tessier-Lavigne, M., Alvarez-Buylla, A., Okano, H.*, et al.* (2010). New neurons clear the path of astrocytic processes for their rapid migration in the adult brain. Neuron *67*, 213-223.

Kaneko, N., Sawada, M., and Sawamoto, K. (2017). Mechanisms of neuronal migration in the adult brain. J Neurochem *141*, 835-847.

Kato, H.K., Chu, M.W., Isaacson, J.S., and Komiyama, T. (2012). Dynamic sensory representations in the olfactory bulb: modulation by wakefulness and experience. Neuron *76*, 962-975.

Kelsch, W., Lin, C.W., and Lois, C. (2008). Sequential development of synapses in dendritic domains during adult neurogenesis. Proc Natl Acad Sci U S A *105*, 16803-16808.

Kelsch, W., Lin, C.W., Mosley, C.P., and Lois, C. (2009). A critical period for activity-dependent synaptic development during olfactory bulb adult neurogenesis. J Neurosci *29*, 11852-11858.

Kim, W.R., Kim, Y., Eun, B., Park, O.H., Kim, H., Kim, K., Park, C.H., Vinsant, S., Oppenheim, R.W., and Sun, W. (2007). Impaired migration in the rostral migratory stream but spared olfactory function after the elimination of programmed cell death in Bax knock-out mice. J Neurosci *27*, 14392-14403.

Kopel, H., Schechtman, E., Groysman, M., and Mizrahi, A. (2012). Enhanced synaptic integration of adult-born neurons in the olfactory bulb of lactating mothers. J Neurosci *32*, 7519-7527.

Kosaka, K., Aika, Y., Toida, K., Heizmann, C.W., Hunziker, W., Jacobowitz, D.M., Nagatsu, I., Streit, P., Visser, T.J., and Kosaka, T. (1995). Chemically defined neuron groups and their subpopulations in the glomerular layer of the rat main olfactory bulb. Neurosci Res *23*, 73-88.

Kosaka, K., and Kosaka, T. (2007). Chemical properties of type 1 and type 2 periglomerular cells in the mouse olfactory bulb are different from those in the rat olfactory bulb. Brain Res *1167*, 42-55.

Kosaka, K., Toida, K., Aika, Y., and Kosaka, T. (1998). How simple is the organization of the olfactory glomerulus?: the heterogeneity of so-called periglomerular cells. Neurosci Res *30*, 101-110.

Kosaka, T., and Kosaka, K. (2005). Structural organization of the glomerulus in the main olfactory bulb. Chem Senses *30 Suppl 1*, i107-108.

Kovalchuk, Y., Homma, R., Liang, Y., Maslyukov, A., Hermes, M., Thestrup, T., Griesbeck, O., Ninkovic, J., Cohen, L.B., and Garaschuk, O. (2015). In vivo odourant response properties of migrating adult-born neurons in the mouse olfactory bulb. Nat Commun *6*, 6349.

Lagace, D.C., Whitman, M.C., Noonan, M.A., Ables, J.L., DeCarolis, N.A., Arguello, A.A., Donovan, M.H., Fischer, S.J., Farnbauch, L.A., Beech, R.D.*, et al.* (2007). Dynamic contribution of nestin-expressing stem cells to adult neurogenesis. J Neurosci *27*, 12623-12629.

Lagier, S., Carleton, A., and Lledo, P.M. (2004). Interplay between local GABAergic interneurons and relay neurons generates gamma oscillations in the rat olfactory bulb. J Neurosci *24*, 4382-4392.

Lagier, S., Panzanelli, P., Russo, R.E., Nissant, A., Bathellier, B., Sassoe-Pognetto, M., Fritschy, J.M., and Lledo, P.M. (2007). GABAergic inhibition at dendrodendritic synapses tunes gamma oscillations in the olfactory bulb. Proc Natl Acad Sci U S A *104*, 7259-7264.

Larsen, C., and Grattan, D.R. (2010). Prolactin-Induced Mitogenesis in the Subventricular Zone of the Maternal Brain during Early Pregnancy Is Essential for Normal Postpartum Behavioral Responses in the Mother. Endocrinology *151*, 3805-3814.

Laurie, D.J., Wisden, W., and Seeburg, P.H. (1992). The distribution of thirteen GABAA receptor subunit mRNAs in the rat brain. III. Embryonic and postnatal development. J Neurosci *12*, 4151-4172.

Lazarini, F., and Lledo, P.M. (2011). Is adult neurogenesis essential for olfaction? Trends Neurosci *34*, 20-30.

Lazarini, F., Mouthon, M.A., Gheusi, G., de Chaumont, F., Olivo-Marin, J.C., Lamarque, S., Abrous, D.N., Boussin, F.D., and Lledo, P.M. (2009). Cellular and behavioral effects of cranial irradiation of the subventricular zone in adult mice. PLoS One *4*, e7017.

Lemasson, M., Saghatelyan, A., Olivo-Marin, J.C., and Lledo, P.M. (2005). Neonatal and adult neurogenesis provide two distinct populations of newborn neurons to the mouse olfactory bulb. J Neurosci *25*, 6816-6825.

Lemieux, M., Labrecque, S., Tardif, C., Labrie-Dion, E., Lebel, E., and De Koninck, P. (2012). Translocation of CaMKII to dendritic microtubules supports the plasticity of local synapses. J Cell Biol *198*, 1055-1073.

Lepousez, G., and Lledo, P.M. (2013). Odor discrimination requires proper olfactory fast oscillations in awake mice. Neuron *80*, 1010-1024.

Lepousez, G., Nissant, A., Bryant, A.K., Gheusi, G., Greer, C.A., and Lledo, P.M. (2014). Olfactory learning promotes input-specific synaptic plasticity in adult-born neurons. Proc Natl Acad Sci U S A *111*, 13984-13989.

Lepousez, G., Nissant, A., and Lledo, P.M. (2015). Adult neurogenesis and the future of the rejuvenating brain circuits. Neuron *86*, 387-401.

Lin, C.W., Sim, S., Ainsworth, A., Okada, M., Kelsch, W., and Lois, C. (2010). Genetically increased cell-intrinsic excitability enhances neuronal integration into adult brain circuits. Neuron *65*, 32-39.

Lisman, J., Schulman, H., and Cline, H. (2002). The molecular basis of CaMKII function in synaptic and behavioural memory. Nat Rev Neurosci *3*, 175-190.

Livneh, Y., Adam, Y., and Mizrahi, A. (2014). Odor processing by adult-born neurons. Neuron, 1097-1110.

Livneh, Y., Feinstein, N., Klein, M., and Mizrahi, A. (2009). Sensory input enhances synaptogenesis of adult-born neurons. J Neurosci *29*, 86-97.

Livneh, Y., and Mizrahi, A. (2012). Experience-dependent plasticity of mature adult-born neurons. Nat Neurosci *15*, 26-28.

Lledo, P.M., Hjelmstad, G.O., Mukherji, S., Soderling, T.R., Malenka, R.C., and Nicoll, R.A. (1995). Calcium/calmodulin-dependent kinase II and long-term potentiation enhance synaptic transmission by the same mechanism. Proc Natl Acad Sci U S A *92*, 11175-11179.

Lledo, P.M., Merkle, F.T., and Alvarez-Buylla, A. (2008). Origin and function of olfactory bulb interneuron diversity. Trends Neurosci *31*, 392-400.

Lledo, P.M., Saghatelyan, A., and Lemasson, M. (2004). Inhibitory interneurons in the olfactory bulb: from development to function. Neuroscientist *10*, 292-303.

Lois, C., and Alvarez-Buylla, A. (1994). Long-distance neuronal migration in the adult mammalian brain. Science *264*, 1145-1148.

Lois, C., Garcia-Verdugo, J.M., and Alvarez-Buylla, A. (1996). Chain migration of neuronal precursors. Science *271*, 978-981.

Luskin, M.B. (1993). Restricted proliferation and migration of postnatally generated neurons derived from the forebrain subventricular zone. Neuron *11*, 173-189.

Magavi, S.S., Mitchell, B.D., Szentirmai, O., Carter, B.S., and Macklis, J.D. (2005). Adult-born and preexisting olfactory granule neurons undergo distinct experience-dependent modifications of their olfactory responses in vivo. J Neurosci *25*, 10729-10739.

Majewska, A., and Sur, M. (2003). Motility of dendritic spines in visual cortex in vivo: changes during the critical period and effects of visual deprivation. Proc Natl Acad Sci U S A *100*, 16024-16029.

Mak, G.K., Enwere, E.K., Gregg, C., Pakarainen, T., Poutanen, M., Huhtaniemi, I., and Weiss, S. (2007). Male pheromone–stimulated neurogenesis in the adult female brain: possible role in mating behavior. Nature Neuroscience *10*, 1003.

Mak, G.K., and Weiss, S. (2010). Paternal recognition of adult offspring mediated by newly generated CNS neurons. Nature Neuroscience *13*, 753.

Malvaut, S., Gribaudo, S., Hardy, D., David, L.S., Daroles, L., Labrecque, S., Lebel-Cormier, M.A., Chaker, Z., Cote, D., De Koninck, P.*, et al.* (2017). CaMKIIalpha Expression Defines Two Functionally Distinct Populations of Granule Cells Involved in Different Types of Odor Behavior. Curr Biol *27*, 3315-3329 e3316.

Malvaut, S., and Saghatelyan, A. (2016). The Role of Adult-Born Neurons in the Constantly Changing Olfactory Bulb Network. Neural Plast *2016*, 1614329.

Mandairon, N., Didier, A., and Linster, C. (2008). Odor enrichment increases interneurons responsiveness in spatially defined regions of the olfactory bulb correlated with perception. Neurobiol Learn Mem *90*, 178-184.

Mandairon, N., Ferretti, C.J., Stack, C.M., Rubin, D.B., Cleland, T.A., and Linster, C. (2006a). Cholinergic modulation in the olfactory bulb influences spontaneous olfactory discrimination in adult rats. Eur J Neurosci *24*, 3234-3244.

Mandairon, N., Sacquet, J., Garcia, S., Ravel, N., Jourdan, F., and Didier, A. (2006b). Neurogenic correlates of an olfactory discrimination task in the adult olfactory bulb. Eur J Neurosci *24*, 3578-3588.

Mandairon, N., Stack, C., Kiselycznyk, C., and Linster, C. (2006c). Enrichment to odors improves olfactory discrimination in adult rats. Behav Neurosci *120*, 173-179.

Mandairon, N., Stack, C., and Linster, C. (2006d). Olfactory enrichment improves the recognition of individual components in mixtures. Physiol Behav *89*, 379-384.

Mandairon, N., Sultan, S., Nouvian, M., Sacquet, J., and Didier, A. (2011). Involvement of newborn neurons in olfactory associative learning? The operant or non-operant component of the task makes all the difference. J Neurosci *31*, 12455-12460.

Mantamadiotis, T., Lemberger, T., Bleckmann, S.C., Kern, H., Kretz, O., Martin Villalba, A., Tronche, F., Kellendonk, C., Gau, D., Kapfhammer, J.*, et al.* (2002). Disruption of CREB function in brain leads to neurodegeneration. Nat Genet *31*, 47-54.

Markopoulos, F., Rokni, D., Gire, D.H., and Murthy, V.N. (2012). Functional properties of cortical feedback projections to the olfactory bulb. Neuron *76*, 1175-1188.

Marsden, K.C., Shemesh, A., Bayer, K.U., and Carroll, R.C. (2010). Selective translocation of Ca2+/calmodulin protein kinase IIalpha (CaMKIIalpha) to inhibitory synapses. Proc Natl Acad Sci U S A *107*, 20559-20564.

Matsutani, S., and Yamamoto, N. (2008). Centrifugal innervation of the mammalian olfactory bulb. Anat Sci Int *83*, 218-227.

McAfee, S.S., Ogg, M.C., Ross, J.M., Liu, Y., Fletcher, M.L., and Heck, D.H. (2016). Minimally invasive highly precise monitoring of respiratory rhythm in the mouse using an epithelial temperature probe. J Neurosci Methods *263*, 89-94.

Mechawar, N., Saghatelyan, A., Grailhe, R., Scoriels, L., Gheusi, G., Gabellec, M.M., Lledo, P.M., and Changeux, J.P. (2004). Nicotinic receptors regulate the survival of newborn neurons in the adult olfactory bulb. Proc Natl Acad Sci U S A *101*, 9822-9826.

Merkle, F.T., Fuentealba, L.C., Sanders, T.A., Magno, L., Kessaris, N., and Alvarez-Buylla, A. (2014). Adult neural stem cells in distinct microdomains generate previously unknown interneuron types. Nat Neurosci *17*, 207-214.

Merkle, F.T., Mirzadeh, Z., and Alvarez-Buylla, A. (2007). Mosaic organization of neural stem cells in the adult brain. Science *317*, 381-384.

Mirzadeh, Z., Merkle, F.T., Soriano-Navarro, M., Garcia-Verdugo, J.M., and Alvarez-Buylla, A. (2008). Neural stem cells confer unique pinwheel architecture to the ventricular surface in neurogenic regions of the adult brain. Cell Stem Cell *3*, 265-278.

Miyamichi, K., Amat, F., Moussavi, F., Wang, C., Wickersham, I., Wall, N.R., Taniguchi, H., Tasic, B., Huang, Z.J., He, Z.*, et al.* (2011). Cortical representations of olfactory input by trans-synaptic tracing. Nature *472*, 191-196.

Miyamichi, K., Shlomai-Fuchs, Y., Shu, M., Weissbourd, B.C., Luo, L., and Mizrahi, A. (2013). Dissecting local circuits: parvalbumin interneurons underlie broad feedback control of olfactory bulb output. Neuron *80*, 1232-1245.

Mizrahi, A. (2007). Dendritic development and plasticity of adult-born neurons in the mouse olfactory bulb. Nat Neurosci *10*, 444-452.

Mombaerts, P. (2001). How smell develops. Nat Neurosci *4 Suppl*, 1192-1198.

Mombaerts, P., Wang, F., Dulac, C., Chao, S.K., Nemes, A., Mendelsohn, M., Edmondson, J., and Axel, R. (1996). Visualizing an olfactory sensory map. Cell *87*, 675-686.

Moreno, M.M., Bath, K., Kuczewski, N., Sacquet, J., Didier, A., and Mandairon, N. (2012). Action of the noradrenergic system on adult-born cells is required for olfactory learning in mice. J Neurosci *32*, 3748-3758.

Moreno, M.M., Linster, C., Escanilla, O., Sacquet, J., Didier, A., and Mandairon, N. (2009). Olfactory perceptual learning requires adult neurogenesis. Proc Natl Acad Sci U S A *106*, 17980-17985.

Mori, K., Takahashi, Y.K., Igarashi, K.M., and Yamaguchi, M. (2006). Maps of odorant molecular features in the Mammalian olfactory bulb. Physiol Rev *86*, 409-433.

Mouret, A., Gheusi, G., Gabellec, M.M., de Chaumont, F., Olivo-Marin, J.C., and Lledo, P.M. (2008). Learning and survival of newly generated neurons: when time matters. J Neurosci *28*, 11511-11516.

Murata, K., Imai, M., Nakanishi, S., Watanabe, D., Pastan, I., Kobayashi, K., Nihira, T., Mochizuki, H., Yamada, S., Mori, K.*, et al.* (2011). Compensation of depleted neuronal subsets by new neurons in a local area of the adult olfactory bulb. J Neurosci *31*, 10540-10557.

Murray, R.C., and Calof, A.L. (1999). Neuronal regeneration: lessons from the olfactory system. Semin Cell Dev Biol *10*, 421-431.

Muthusamy, N., Zhang, X., Johnson, C.A., Yadav, P.N., and Ghashghaei, H.T. (2017). Developmentally defined forebrain circuits regulate appetitive and aversive olfactory learning. Nat Neurosci *20*, 20-23.

Nagayama, S., Homma, R., and Imamura, F. (2014). Neuronal organization of olfactory bulb circuits. Front Neural Circuits *8*, 98.

Nagayama, S., Takahashi, Y.K., Yoshihara, Y., and Mori, K. (2004). Mitral and tufted cells differ in the decoding manner of odor maps in the rat olfactory bulb. J Neurophysiol *91*, 2532-2540.

Nakamura, T., Colbert, M.C., and Robbins, J. (2006). Neural crest cells retain multipotential characteristics in the developing valves and label the cardiac conduction system. Circ Res *98*, 1547-1554.

Nassi, J.J., Cepko, C.L., Born, R.T., and Beier, K.T. (2015). Neuroanatomy goes viral! Front Neuroanat *9*, 80.

Neant-Fery, M., Peres, E., Nasrallah, C., Kessner, M., Gribaudo, S., Greer, C., Didier, A., Trembleau, A., and Caille, I. (2012). A role for dendritic translation of CaMKIIalpha mRNA in olfactory plasticity. PLoS One *7*, e40133.

Niedworok, C.J., Schwarz, I., Ledderose, J., Giese, G., Conzelmann, K.K., and Schwarz, M.K. (2012). Charting monosynaptic connectivity maps by two-color light-sheet fluorescence microscopy. Cell Rep *2*, 1375-1386.

Ninkovic, J., Mori, T., and Gotz, M. (2007). Distinct modes of neuron addition in adult mouse neurogenesis. J Neurosci *27*, 10906-10911.

Nissant, A., Bardy, C., Katagiri, H., Murray, K., and Lledo, P.M. (2009). Adult neurogenesis promotes synaptic plasticity in the olfactory bulb. Nat Neurosci *12*, 728-730.

Nunes, D., and Kuner, T. (2015). Disinhibition of olfactory bulb granule cells accelerates odour discrimination in mice. Nat Commun *6*, 8950.

Nunez-Parra, A., Maurer, R.K., Krahe, K., Smith, R.S., and Araneda, R.C. (2013). Disruption of centrifugal inhibition to olfactory bulb granule cells impairs olfactory discrimination. Proc Natl Acad Sci U S A *110*, 14777-14782.

Nusser, Z., Kay, L.M., Laurent, G., Homanics, G.E., and Mody, I. (2001). Disruption of GABA(A) receptors on GABAergic interneurons leads to increased oscillatory power in the olfactory bulb network. J Neurophysiol *86*, 2823-2833.

Obernier, K., and Alvarez-Buylla, A. (2019). Neural stem cells: origin, heterogeneity and regulation in the adult mammalian brain. Development *146*.

Obernier, K., Cebrian-Silla, A., Thomson, M., Parraguez, J.I., Anderson, R., Guinto, C., Rodas Rodriguez, J., Garcia-Verdugo, J.M., and Alvarez-Buylla, A. (2018). Adult Neurogenesis Is Sustained by Symmetric Self-Renewal and Differentiation. Cell Stem Cell *22*, 221-234 e228.

Orona, E., Scott, J.W., and Rainer, E.C. (1983). Different granule cell populations innervate superficial and deep regions of the external plexiform layer in rat olfactory bulb. J Comp Neurol *217*, 227-237.

Padmanabhan, K., Osakada, F., Tarabrina, A., Kizer, E., Callaway, E.M., Gage, F.H., and Sejnowski, T.J. (2016). Diverse Representations of Olfactory Information in Centrifugal Feedback Projections. J Neurosci *36*, 7535-7545.

Pallotto, M., Nissant, A., Fritschy, J.M., Rudolph, U., Sassoe-Pognetto, M., Panzanelli, P., and Lledo, P.M. (2012). Early formation of GABAergic synapses governs the development of adult-born neurons in the olfactory bulb. J Neurosci *32*, 9103-9115.

Panzanelli, P., Bardy, C., Nissant, A., Pallotto, M., Sassoe-Pognetto, M., Lledo, P.M., and Fritschy, J.M. (2009). Early synapse formation in developing interneurons of the adult olfactory bulb. J Neurosci *29*, 15039-15052.

Parrish-Aungst, S., Shipley, M.T., Erdelyi, F., Szabo, G., and Puche, A.C. (2007). Quantitative analysis of neuronal diversity in the mouse olfactory bulb. J Comp Neurol *501*, 825-836.

Pastrana, E., Cheng, L.C., and Doetsch, F. (2009). Simultaneous prospective purification of adult subventricular zone neural stem cells and their progeny. Proc Natl Acad Sci U S A *106*, 6387-6392.

Patel, J.M., Swanson, J., Ung, K., Herman, A., Hanson, E., Ortiz-Guzman, J., Selever, J., Tong, Q., and Arenkiel, B.R. (2019). Sensory perception drives food avoidance through excitatory basal forebrain circuits. Elife *8*.

Pavesi, E., Gooch, A., Lee, E., and Fletcher, M.L. (2012). Cholinergic modulation during acquisition of olfactory fear conditioning alters learning and stimulus generalization in mice. Learn Mem *20*, 6-10.

Petreanu, L., and Alvarez-Buylla, A. (2002). Maturation and death of adult-born olfactory bulb granule neurons: role of olfaction. J Neurosci *22*, 6106-6113.

Petrini, E.M., Ravasenga, T., Hausrat, T.J., Iurilli, G., Olcese, U., Racine, V., Sibarita, J.B., Jacob, T.C., Moss, S.J., Benfenati, F.*, et al.* (2014). Synaptic recruitment of gephyrin regulates surface GABAA receptor dynamics for the expression of inhibitory LTP. Nat Commun *5*, 3921.

Platel, J.C., Angelova, A., Bugeon, S., Wallace, J., Ganay, T., Chudotvorova, I., Deloulme, J.C., Beclin, C., Tiveron, M.C., Core, N.*, et al.* (2019). Neuronal integration in the adult mouse olfactory bulb is a non-selective addition process. Elife *8*.

Platel, J.C., Dave, K.A., and Bordey, A. (2008). Control of neuroblast production and migration by converging GABA and glutamate signals in the postnatal forebrain. J Physiol *586*, 3739-3743.

Pressler, R.T., and Strowbridge, B.W. (2006). Blanes cells mediate persistent feedforward inhibition onto granule cells in the olfactory bulb. Neuron *49*, 889-904.

Price, J.L., and Powell, T.P. (1970). The synaptology of the granule cells of the olfactory bulb. J Cell Sci *7*, 125-155.

Qin, J.Y., Zhang, L., Clift, K.L., Hulur, I., Xiang, A.P., Ren, B.Z., and Lahn, B.T. (2010). Systematic comparison of constitutive promoters and the doxycycline-inducible promoter. PLoS One *5*, e10611.

Ravi, N., Sanchez-Guardado, L., Lois, C., and Kelsch, W. (2017). Determination of the connectivity of newborn neurons in mammalian olfactory circuits. Cell Mol Life Sci *74*, 849-867.

Redmond, S.A., Figueres-Onate, M., Obernier, K., Nascimento, M.A., Parraguez, J.I., Lopez-Mascaraque, L., Fuentealba, L.C., and Alvarez-Buylla, A. (2019). Development of Ependymal and Postnatal Neural Stem Cells and Their Origin from a Common Embryonic Progenitor. Cell Rep *27*, 429-441 e423.

Reinert, J.K., Sonntag, I., Sonntag, H., Sprengel, R., Pelzer, P., Lessle, S., Kaiser, M., and Kuner, T. (2019). retroLEAP: rAAV-based retrograde trans-synaptic labeling, expression and perturbation. bioRxiv.

Rochefort, C., Gheusi, G., Vincent, J.D., and Lledo, P.M. (2002). Enriched odor exposure increases the number of newborn neurons in the adult olfactory bulb and improves odor memory. J Neurosci *22*, 2679-2689.

Rochefort, C., and Lledo, P.M. (2005). Short-term survival of newborn neurons in the adult olfactory bulb after exposure to a complex odor environment. Eur J Neurosci *22*, 2863-2870.

Rogan, S.C., and Roth, B.L. (2011). Remote control of neuronal signaling. Pharmacol Rev *63*, 291-315.

Rojas-Libano, D., and Kay, L.M. (2008). Olfactory system gamma oscillations: the physiological dissection of a cognitive neural system. Cogn Neurodyn *2*, 179-194.

Ross, J.M., Bendahmane, M., and Fletcher, M.L. (2019). Olfactory Bulb Muscarinic Acetylcholine Type 1 Receptors Are Required for Acquisition of Olfactory Fear Learning. Front Behav Neurosci *13*, 164.

Roth, B.L. (2016). DREADDs for Neuroscientists. Neuron *89*, 683-694.

Sagar, S.M., Sharp, F.R., and Curran, T. (1988). Expression of c-fos protein in brain: metabolic mapping at the cellular level. Science *240*, 1328-1331.

Saghatelyan, A. (2009). Role of blood vessels in the neuronal migration. Semin Cell Dev Biol *20*, 744-750.

Saghatelyan, A., de Chevigny, A., Schachner, M., and Lledo, P.M. (2004). Tenascin-R mediates activity-dependent recruitment of neuroblasts in the adult mouse forebrain. Nat Neurosci *7*, 347-356.

Saghatelyan, A., Roux, P., Migliore, M., Rochefort, C., Desmaisons, D., Charneau, P., Shepherd, G.M., and Lledo, P.M. (2005). Activity-dependent adjustments of the inhibitory network in the olfactory bulb following early postnatal deprivation. Neuron *46*, 103-116.

Sailor, K.A., Valley, M.T., Wiechert, M.T., Riecke, H., Sun, G.J., Adams, W., Dennis, J.C., Sharafi, S., Ming, G.L., Song, H.*, et al.* (2016). Persistent Structural Plasticity Optimizes Sensory Information Processing in the Olfactory Bulb. Neuron *91*, 384-396.

Sakamoto, M., Imayoshi, I., Ohtsuka, T., Yamaguchi, M., Mori, K., and Kageyama, R. (2011). Continuous neurogenesis in the adult forebrain is required for innate olfactory responses. Proceedings of the National Academy of Sciences.

Saliba, R.S., Kretschmannova, K., and Moss, S.J. (2012). Activity-dependent phosphorylation of GABAA receptors regulates receptor insertion and tonic current. EMBO J *31*, 2937-2951.

Scotto-Lomassese, S., Nissant, A., Mota, T., Neant-Fery, M., Oostra, B.A., Greer, C.A., Lledo, P.M., Trembleau, A., and Caille, I. (2011). Fragile X mental retardation protein regulates new neuron differentiation in the adult olfactory bulb. J Neurosci *31*, 2205-2215.

Serguera, C., Triaca, V., Kelly-Barrett, J., Banchaabouchi, M.A., and Minichiello, L. (2008). Increased dopamine after mating impairs olfaction and prevents odor interference with pregnancy. Nat Neurosci *11*, 949-956.

Shepherd, G.M. (1972). Synaptic organization of the mammalian olfactory bulb. Physiol Rev *52*, 864-917.

Shepherd, G.M., Chen, W.R., and Greer, C.A. (2004). Olfactory Bulb. In The Synaptic Organization of the Brain, G.M. Shepherd, ed., pp. 165–216.

Shepherd, G.M., Chen, W.R., Willhite, D., Migliore, M., and Greer, C.A. (2007). The olfactory granule cell: from classical enigma to central role in olfactory processing. Brain Res Rev *55*, 373-382.

Shingo, T., Gregg, C., Enwere, E., Fujikawa, H., Hassam, R., Geary, C., Cross, J.C., and Weiss, S. (2003). Pregnancy-stimulated neurogenesis in the adult female forebrain mediated by prolactin. Science *299*, 117-120.

Snapyan, M., Lemasson, M., Brill, M.S., Blais, M., Massouh, M., Ninkovic, J., Gravel, C., Berthod, F., Gotz, M., Barker, P.A.*, et al.* (2009). Vasculature guides migrating neuronal precursors in the adult mammalian forebrain via brain-derived neurotrophic factor signaling. J Neurosci *29*, 4172-4188.

Sosulski, D.L., Bloom, M.L., Cutforth, T., Axel, R., and Datta, S.R. (2011). Distinct representations of olfactory information in different cortical centres. Nature *472*, 213-216.

Sultan, S., Mandairon, N., Kermen, F., Garcia, S., Sacquet, J., and Didier, A. (2010). Learning-dependent neurogenesis in the olfactory bulb determines long-term olfactory memory. FASEB J *24*, 2355-2363.

Sultan, S., Rey, N., Sacquet, J., Mandairon, N., and Didier, A. (2011). Newborn neurons in the olfactory bulb selected for long-term survival through olfactory learning are prematurely suppressed when the olfactory memory is erased. J Neurosci *31*, 14893-14898.

Takahashi, H., Ogawa, Y., Yoshihara, S., Asahina, R., Kinoshita, M., Kitano, T., Kitsuki, M., Tatsumi, K., Okuda, M., Tatsumi, K.*, et al.* (2016). A Subtype of Olfactory Bulb Interneurons Is Required for Odor Detection and Discrimination Behaviors. J Neurosci *36*, 8210-8227.

Taniguchi, H., He, M., Wu, P., Kim, S., Paik, R., Sugino, K., Kvitsiani, D., Fu, Y., Lu, J., Lin, Y., *et al.* (2011). A resource of Cre driver lines for genetic targeting of GABAergic neurons in cerebral cortex. Neuron *71*, 995-1013.

Tervo, D.G., Hwang, B.Y., Viswanathan, S., Gaj, T., Lavzin, M., Ritola, K.D., Lindo, S., Michael, S., Kuleshova, E., Ojala, D.*, et al.* (2016). A Designer AAV Variant Permits Efficient Retrograde Access to Projection Neurons. Neuron *92*, 372-382.

Tseng, C.S., Chao, H.W., Huang, H.S., and Huang, Y.S. (2017). Olfactory-Experience- and Developmental-Stage-Dependent Control of CPEB4 Regulates c-Fos mRNA Translation for Granule Cell Survival. Cell Rep *21*, 2264-2276.

Tseng, C.S., Chou, S.J., and Huang, Y.S. (2019). CPEB4-Dependent Neonate-Born Granule Cells Are Required for Olfactory Discrimination. Front Behav Neurosci *13*, 5.

Tsuchiya, R., Yoshiki, F., Kudo, Y., and Morita, M. (2002). Cell type-selective expression of green fluorescent protein and the calcium indicating protein, yellow cameleon, in rat cortical primary cultures. Brain Res *956*, 221-229.

Urban, N.N. (2002). Lateral inhibition in the olfactory bulb and in olfaction. Physiol Behav *77*, 607-612.

Valley, M.T., Henderson, L.G., Inverso, S.A., and Lledo, P.M. (2013). Adult neurogenesis produces neurons with unique GABAergic synapses in the olfactory bulb. J Neurosci *33*, 14660-14665.

Valley, M.T., Mullen, T.R., Schultz, L.C., Sagdullaev, B.T., and Firestein, S. (2009). Ablation of mouse adult neurogenesis alters olfactory bulb structure and olfactory fear conditioning. Front Neurosci *3*, 51.

Veilleux, I., Spencer, J.A., Biss, D.P., Cote, D., and Lin, C.P. (2008). In Vivo Cell Tracking With Video Rate Multimodality Laser Scanning Microscopy. IEEE Journal of selected topics in quantum electronics *14*.

Vinograd, A., Fuchs-Shlomai, Y., Stern, M., Mukherjee, D., Gao, Y., Citri, A., Davison, I., and Mizrahi, A. (2017). Functional Plasticity of Odor Representations during Motherhood. Cell Rep *21*, 351-365.

Waclaw, R.R., Ehrman, L.A., Pierani, A., and Campbell, K. (2010). Developmental origin of the neuronal subtypes that comprise the amygdalar fear circuit in the mouse. J Neurosci *30*, 6944-6953.

Wallace, J.L., Wienisch, M., and Murthy, V.N. (2017). Development and Refinement of Functional Properties of Adult-Born Neurons. Neuron *96*, 883-896 e887.

Wang, W., Pan, Y.W., Wietecha, T., Zou, J., Abel, G.M., Kuo, C.T., and Xia, Z. (2013). Extracellular signal-regulated kinase 5 (ERK5) mediates prolactin-stimulated adult neurogenesis in the subventricular zone and olfactory bulb. J Biol Chem *288*, 2623-2631.

Watt, W.C., Sakano, H., Lee, Z.Y., Reusch, J.E., Trinh, K., and Storm, D.R. (2004). Odorant stimulation enhances survival of olfactory sensory neurons via MAPK and CREB. Neuron *41*, 955-967.

Weinhard, L., di Bartolomei, G., Bolasco, G., Machado, P., Schieber, N.L., Neniskyte, U., Exiga, M., Vadisiute, A., Raggioli, A., Schertel, A.*, et al.* (2018). Microglia remodel synapses by presynaptic trogocytosis and spine head filopodia induction. Nat Commun *9*, 1228.

Wen, P., Rao, X., Xu, L., Zhang, Z., Jia, F., He, X., and Xu, F. (2019). Cortical Organization of Centrifugal Afferents to the Olfactory Bulb: Mono- and Trans-synaptic Tracing with Recombinant Neurotropic Viral Tracers. Neurosci Bull *35*, 709-723.

Whitman, M.C., Fan, W., Rela, L., Rodriguez-Gil, D.J., and Greer, C.A. (2009). Blood vessels form a migratory scaffold in the rostral migratory stream. J Comp Neurol *516*, 94-104.

Whitman, M.C., and Greer, C.A. (2007). Synaptic integration of adult-generated olfactory bulb granule cells: basal axodendritic centrifugal input precedes apical dendrodendritic local circuits. J Neurosci *27*, 9951-9961.

Wienisch, M., and Murthy, V.N. (2016). Population imaging at subcellular resolution supports specific and local inhibition by granule cells in the olfactory bulb. Sci Rep *6*, 29308.

Winner, B., Cooper-Kuhn, C.M., Aigner, R., Winkler, J., and Kuhn, H.G. (2002). Long-term survival and cell death of newly generated neurons in the adult rat olfactory bulb. Eur J Neurosci *16*, 1681-1689.

Woo, C.C., Hingco, E.E., Taylor, G.E., and Leon, M. (2006). Exposure to a broad range of odorants decreases cell mortality in the olfactory bulb. Neuroreport *17*, 817-821.

Yamada, Y., Bhaukaurally, K., Madarasz, T.J., Pouget, A., Rodriguez, I., and Carleton, A. (2017). Context- and Output Layer-Dependent Long-Term Ensemble Plasticity in a Sensory Circuit. Neuron *93*, 1198-1212 e1195.

Yamaguchi, M., and Mori, K. (2005). Critical period for sensory experience-dependent survival of newly generated granule cells in the adult mouse olfactory bulb. Proc Natl Acad Sci U S A *102*, 9697-9702.

Yokoi, M., Mori, K., and Nakanishi, S. (1995). Refinement of odor molecule tuning by dendrodendritic synaptic inhibition in the olfactory bulb. Proc Natl Acad Sci U S A *92*, 3371-3375.

Yoshihara, S., Takahashi, H., Nishimura, N., Naritsuka, H., Shirao, T., Hirai, H., Yoshihara, Y., Mori, K., Stern, P.L., and Tsuboi, A. (2012). 5T4 glycoprotein regulates the sensory input-dependent development of a specific subtype of newborn interneurons in the mouse olfactory bulb. J Neurosci *32*, 2217-2226.

Young, K.M., Fogarty, M., Kessaris, N., and Richardson, W.D. (2007). Subventricular zone stem cells are heterogeneous with respect to their embryonic origins and neurogenic fates in the adult olfactory bulb. J Neurosci *27*, 8286-8296.

Zhang, F., Wang, L.P., Brauner, M., Liewald, J.F., Kay, K., Watzke, N., Wood, P.G., Bamberg, E., Nagel, G., Gottschalk, A.*, et al.* (2007). Multimodal fast optical interrogation of neural circuitry. Nature *446*, 633-639.

Zhou, Z., and Belluscio, L. (2008). Intrabulbar projecting external tufted cells mediate a timing-based mechanism that dynamically gates olfactory bulb output. J Neurosci *28*, 9920-9928.

Zingg, B., Chou, X.L., Zhang, Z.G., Mesik, L., Liang, F., Tao, H.W., and Zhang, L.I. (2017). AAV-Mediated Anterograde Transsynaptic Tagging: Mapping Corticocollicular Input-Defined Neural Pathways for Defense Behaviors. Neuron *93*, 33-47.

Zou, D.J., Greer, C.A., and Firestein, S. (2002). Expression pattern of alpha CaMKII in the mouse main olfactory bulb. J Comp Neurol *443*, 226-236.

ANNEX: THE ROLE OF ADULT-BORN NEURONS IN THE CONSTANTLY CHANGING OLFACTORY BULB NETWORK

Sarah Malvaut[1] and Armen Saghatelyan[1,2]

Affiliations

[1] Cellular Neurobiology Unit, Centre de recherche de l'Institut Universitaire en Santé Mentale de Québec, Québec City, Québec, Canada G1J2G3

[2] Department of Psychiatry and Neuroscience, Université Laval, Québec City, Québec, Canada G1K7P4

Correspondence should be addressed to Armen Saghatelyan; armen.saghatelyan@fmed.ulaval.ca

Neural Plasticity, 2016, 2016:1614329

1. Abstract

The adult mammalian brain is remarkably plastic and constantly undergoes structuro-functional modifications in response to environmental stimuli. In many brain regions these plastic changes are manifested by the modifications in the efficacy of existing synaptic connections or synapse formation and elimination. In a few regions, however, plasticity is brought by new neurons that are constantly produced throughout adulthood and integrate into established neuronal networks. This type of neuronal plasticity is particularly prominent in the olfactory bulb (OB) and dentate gyrus of the mammalian brain. In the OB, some 30000-40000 neuronal progenitors are produced on a daily basis in the subventricular zone (SVZ) bordering the lateral ventricle, and migrate along the rostral migratory stream (RMS) towards the OB. In the OB, these neuronal precursors differentiate into local interneurons, reach maturity and functionally integrate into the bulbar network by establishing output synapses with mitral cells (MCs) or tufted cells, the principal neurons in the OB. Despite continuous progress, it is still not understood how normal functioning of the OB is preserved in the constantly remodelling bulbar network and what role adult-born neurons play in odor behaviour. In this review we will discuss different levels of morpho-functional plasticity effected by adult-born neurons, the functional role of new neurons in the adult OB and also highlight the possibility that different sub-populations of adult-born cells may fulfill distinct functions in the OB neuronal network and odor behaviour.

2. Introduction

The olfactory system is essential for the survival of many animal species, providing vital information about food location and influencing social and sexual behaviours. In mammals, odor information is conveyed by olfactory sensory neurons (OSNs) located in the olfactory epithelium. The axon terminals of OSNs establish synaptic contacts in the glomeruli of the OB with MCs. These principal cells then transduce information directly to the olfactory cortex, with no thalamic relay. In the OB, odor information processing is modulated by interneurons: periglomerular cells (PGCs) located in the glomerular layer (GL) and granule cells (GCs) found in the granule cell layer (GCL). GCs are the most abundant population of neurons in the OB and vastly outnumber the bulbar principal neurons by around 100:1 (Shepherd et al., 2004).These GABAergic interneurons form a unique type of synapse on the dendrites of principal cells: the dendro-dendritic reciprocal synapse in which glutamate, released from the principal cells' dendrites, in turn induces the release of GABA from the spines of interneurons back to the principal cells (Isaacson and Strowbridge, 1998; Jahr and Nicoll, 1982; Price and Powell, 1970; Whitman and Greer, 2007).The two subpopulations of interneurons play an important role in the rhythmic activity of the OB. PGCs coordinate theta activity by regulating baseline and odor-evoked inhibition, whereas GCs are involved in the synchronization of MC activity and generation of gamma rhythm (Arevian et al., 2008; Fukunaga et al., 2014; Urban, 2002; Yokoi et al., 1995).

Interestingly, around 10-15% of GCs and 30% of PGCs are continuously renewed during adulthood (Lagace et al., 2007; Ninkovic et al., 2007). This constant renewal affects the distinct subtypes of PGCs and GCs in different ways (Batista-Brito et al., 2008). In fact, among calretinin, calbindin and tyrosine hydroxylase (TH) expressing PGCs, the production of calbindin- and TH-positive cells tends to decrease after birth (Batista-Brito et al., 2008; Kosaka et al., 1998), while calretinin expressing-PGCs are mostly produced during adulthood (Batista-Brito et al., 2008). With regard to GCs, the generation of different subpopulations has not yet been systemically examined and renewal in the adulthood has been shown only for calretinin-expressing, mGluR2-expressing and small numbers of 5T4-expressing GC subpopulations (Batista-Brito et al., 2008; Merkle et al., 2014; Murata et al., 2011; Parrish-Aungst et al., 2007). In general, less is known about the neurochemical heterogeneity of GCs and until now, studies aimed at understanding the role of adult-born neurons in odor information processing and olfactory behaviour have considered these cells a homogenous population of neurons (Alonso et al., 2012; Arruda-Carvalho et al., 2014; Breton-Provencher et al., 2009; Imayoshi et al., 2008; Sultan et al., 2010). It is conceivable, however, that different subtypes of new neurons may be activated by distinct olfactory tasks and play a specific role in different odor behaviours. There is consequently a need to understand the exact contribution of specific sub-populations of adult-born neurons to animal behaviour.

In this review, after presenting adult OB neurogenesis as a remarkable form of neuronal plasticity, we will discuss recent data concerning the functional role of adult-

born neurons and their implications in olfactory behaviour. Finally, we will also discuss the heterogeneity of adult-born neurons and highlight the possibility that different subtypes of new neurons may play distinct roles in the function of the OB network and odor behaviour.

3. Adult OB neurogenesis, an unusual form of structural and functional plasticity

New neurons for the OB are produced in the subventricular zone (SVZ), bordering the lateral ventricles, where adult neural stem cells proliferate to give rise to rapidly dividing transient amplifying cells, which in turn divide to produce neuroblasts (Alvarez-Buylla and Garcia-Verdugo, 2002; Doetsch et al., 1999; Luskin, 1993). Neuroblasts migrate tangentially in chains, along the blood vessels through the rostral migratory stream (RMS) towards the OB (Lois et al., 1996; Snapyan et al., 2009; Whitman et al., 2009). Once in the OB, they start to migrate radially (David et al., 2013; Hack et al., 2002; Saghatelyan et al., 2004), reach maturity and integrate into pre-existing neuronal networks (Belluzzi et al., 2003; Carleton et al., 2003; Panzanelli et al., 2009; Petreanu and Alvarez-Buylla, 2002; Whitman and Greer, 2007). The vast majority of adult-born neurons, around 97%, differentiate into GCs, while the other 3% become PGCs (Winner et al., 2002).

The constant neuronal turnover occurring in the OB imposes on the olfactory system the never-ending challenge of preserving normal odor information processing despite persistent morpho-functional changes in the large number of interneurons and their synaptic connections with principal cells. The mechanisms enabling the maintenance of this fine equilibrium between normal OB function and the constant rewiring of its neuronal network are not well understood. These mechanisms are driven, however, in an activity-dependent manner and sensory stimulation plays an important role in the maturation, survival and integration of new neurons in the OB (Alonso et al., 2006; Corotto et al., 1994; Mandairon et al., 2006b; Moreno et al., 2009; Petreanu and Alvarez-Buylla, 2002; Rochefort et al., 2002; Saghatelyan et al., 2005; Sultan et al., 2010; Yamaguchi and Mori, 2005). Adult-born neurons may adjust the morpho-functional properties of the bulbar network at several different levels. Firstly, the addition of new neurons may be considered as the topmost level of plasticity along with the continuous formation of new functional synaptic units with principal cells that replace existing connections. Secondly, adult-born neurons may bring to the OB properties that are not present in pre-existing cells, which may make the neuronal network more adaptable to changing environmental conditions. Finally, new neurons may change their own morpho-functional properties in response to external stimuli to uphold the functioning of the bulbar network.

A. Plasticity in the OB network by the addition of new neurons

The adult OB is constantly supplied with new cells to be integrated into the pre-existing neuronal network. *In vivo* calcium imaging has shown that adult-born PGCs begin to express spontaneous and odor-evoked responses soon after their arrival in the OB network, even if they have the molecular phenotype of immature cells (Kovalchuk et al., 2015). In addition, other *in vivo* time-lapse imaging studies have shown that new interneurons remain structurally dynamic not only during their maturation and integration phases (Kovalchuk et al., 2015; Mizrahi, 2007), but also well beyond their synaptic integration (Livneh and Mizrahi, 2012). New spines are constantly forming, retracting and stabilizing on the dendrites of adult-born cells and even six months after their birth and these cells have a higher synaptic density than their pre-existing counterparts (Livneh and Mizrahi, 2012). Moreover, young adult-born neurons become more selective to particular odors as they mature (Livneh et al., 2014). These data suggest that adult-born neurons are continuously rewiring the bulbar network, and represent a population of cells enabling the OB to adapt to an ever-changing odor environment.

In accordance with this, it has recently been demonstrated that the lack of neurogenesis in the adult OB alters the anatomical organization of the bulbar network by modifying the precision and size of intrabulbar projections of principal cells (Cummings et al., 2014). Suppression of adult neurogenesis has also been shown to affect synchronized activity of MCs *in vitro* (Breton-Provencher et al., 2009). Adult-born neurons provide an important inhibitory input to the bulbar principal cells (Breton-Provencher et al., 2009) and *in vivo* experiments have shown that a disruption to the excitation/inhibition balance received by MCs deregulates the ability of animals to discriminate between odors (Lepousez and Lledo, 2013). Thus, the constant supply of new neurons to the OB is a form of morpho-functional plasticity, allowing permanent reorganization of the bulbar network to suit changing environmental conditions.

B. Adult-born neurons, a population of cells remarkably different from their pre-existing counterparts

During maturation, adult-born GCs receive synaptic inputs on the soma and the proximal part of their apical dendrites before forming their output dendro-dendritic synapses (Kelsch et al., 2008; Whitman and Greer, 2007). This maturational profile of adult-born GCs distinguishes them from their pre-existing counterparts that form input and output synapses simultaneously (Kelsch et al., 2008). The sequential acquisition of input synapses before forming the output ones allows these cells to “silently” integrate into the operational bulbar network (Kelsch et al., 2008). However, when adult-born neurons are fully mature they display greater excitability than early-born ones (Belluzzi et al., 2003; Carleton et al., 2003). This increased excitability of adult-born cells enhances their overall inhibitory drive on the principal cells. This is supported by data which shows that ablation of neurogenesis for 28 days results in a decrease of around 45% in the inhibitory input received by MCs (Breton-

Provencher et al., 2009). In addition, synapses of adult-born interneurons impinging on the dendrites of principal cells differ from those made by pre-existing interneurons in terms of sensitivity to GABA(B) receptors-induced suppression of GABA release (Valley et al., 2013). This is due to the different localization of GABA(B) receptors which confers adult-born GCs with synapses different from their pre-existing counterparts (Valley et al., 2013). These data suggest that adult-born neurons provide stronger inhibitory modulation of the principal cells and have unique features that distinguish them from early-born neurons.

At two to three weeks after birth, adult-born neurons have also been shown to be more responsive to incoming new odors than their older counterparts (Belnoue et al., 2011; Magavi et al., 2005). This increased responsiveness of adult-born neurons during their development may be due to the critical period during which adult-born cells (at least the PGCs) are less selective to odorant stimuli (Livneh et al., 2014). Odor selectivity of these cells can be increased by housing animals in an olfactory enriched environment, which suggests that activity-dependent mechanisms play a part in the functional maturation of these cells (Livneh et al., 2014). During this critical period adult-born cells also display long-term potentiation (LTP) at the glutamatergic input impinging on the proximal dendrites of GCs (Nissant et al., 2009).

Altogether, the results presented above demonstrate that the adult OB receives a population of interneurons distinguishable from the neurons produced during early development and that these cells play a unique role in olfactory information processing.

C. Plasticity through changing morpho-functional properties of new neurons

OB neurogenesis is a process sensitive to the level of sensory experience. Several studies have shown that exposing animals to an olfactory enriched environment (Moreno et al., 2009; Rochefort et al., 2002; Rochefort and Lledo, 2005) or learning of an associative olfactory task (Alonso et al., 2006; Sultan et al., 2010) increases survival of adult-born neurons in the OB. Conversely, depriving animals of olfactory input by closing one of their nostrils reduces survival of new neurons (Corotto et al., 1994; Petreanu and Alvarez-Buylla, 2002; Saghatelyan et al., 2005; Yamaguchi and Mori, 2005). Sensory activity is essential for the development and expression of dopaminergic phenotypes, but not GABAergic, calretinin- or calbindin-positive ones, suggesting that the acquisition and maintenance of chemospecific phenotypes by different PGCs can be affected differently by odor-induced activity (Baker et al., 1993; Bastien-Dionne et al., 2010). It has recently been proposed that mechanisms exist to allow the replacement of pre-existing neurons of a particular phenotype, by newborn cells of the same phenotype, thereby maintaining in the OB a constant level of GCs of the same neurochemical subset (Murata et al., 2011). In fact, at least for the population of mGluR2-expressing cells, ablation of pre-existing GCs of this particular phenotype resulted in a recovery of the density of cells

belonging to this subtype (Murata et al., 2011). Moreover, adult-born mGluR2-expressing adult-born GCs presented enlarged spines, a characteristic that may aid in compensating for the loss of cells of the same subpopulation (Murata et al., 2011).

Sensory stimulation is required not only for the survival of new neurons, but also for their maturation, since sensory enrichment enhances synaptogenesis of PGCs , whereas sensory deprivation affects the density of spines on the distal dendrites of adult-born GCs (Kelsch et al., 2009; Saghatelyan et al., 2005).Interestingly, this decreased spine density on the distal dendrites of GCs is accompanied by increased spine density on the apical dendrites (Kelsch et al., 2009). These data suggest a form of structural plasticity among distinct compartments of adult-born GCs that may allow cells to receive stronger input to compensate for a decreased number of output synapses. Further evidence for activity-dependent modifications in the morpho-functional properties of adult-born neurons are observations showing that sensory deprivation triggers an increase in the excitability of new neurons (Saghatelyan et al., 2005). These sensory-deprivation-induced alterations in the morphology and function of GCs are specific to the adult-born population, since sensory deprivation does not affect the maturation and excitability of pre-existing neurons (Saghatelyan et al., 2005). To understand whether odor stimulation provides a specific pattern of activity or overall membrane depolarization to adult-born neurons which may be required for the survival and maturation of these cells, Lin and colleagues modulated the intrinsic activity of new neurons via overexpression of Kir2.1 potassium and bacterial sodium channels and assessed the survival and integration of new cells in the OB network (Lin et al., 2010). These experiments revealed that the intrinsic activity of adult-born neurons plays an important role in their survival, but not their synaptogenesis (Lin et al., 2010). Therefore, the plasticity in the morpho-functional properties of adult-born cells themselves may be used to uphold the function of these cells in the OB and allow adjustment of the bulbar network to environmental stimuli. The above data reveal that neurogenesis in the adult OB is tightly linked to sensory experience and represents an important process by which the functioning of the OB network is adjusted to the constantly changing olfactory environment. This is accomplished by different levels of morpho-functional plasticity that are brought by adult-born neurons to the bulbar network.

4. Implication of adult-born neurons in olfactory behaviour

The fact that a substantial number of adult-born neurons are integrated into the OB neuronal network on a daily basis suggests that these cells may contribute significantly to olfactory behaviour. In this review we will discuss the role of adult-born neurons in spontaneous odor exploration, odor discrimination and associative memory tasks. The involvement of adult neurogenesis in odor-based social interactions has been discussed elsewhere (Breton-Provencher and Saghatelyan, 2012; Corona and Levy, 2015; Feierstein, 2012) and will not be covered here.

A number of studies have been aimed at determining the potential role of adult-born neurons in various spontaneous odor behaviour tasks. First, odor enrichment (Moreno et al., 2009; Rochefort et al., 2002; Rochefort and Lledo, 2005) that increased the survival of adult-born neurons in the OB, also resulted in an improvement of short-term odor memory (Rochefort et al., 2002; Rochefort and Lledo, 2005). Irradiation which decreased the number of adult-born neurons produced, however, no change in short-term odor memory (Lazarini et al., 2009). This is likely due to a compensatory increase in the survival of the pre-existing population of GCs (Lazarini et al., 2009). Indeed, complete suppression of adult OB neurogenesis using anti-mitotic drug cytosine β-D-arabinofuranoside (AraC), which had no effect on GCs born before AraC infusion, led to impaired short-term olfactory memory (Breton-Provencher et al., 2009). It has also been demonstrated that blocking adult neurogenesis with an anti-mitotic drug during odor enrichment prevents the enhancement in discrimination abilities of animals (Moreno et al., 2009), supporting the involvement of neurogenesis in the ability to discriminate between similar odors. It appears that adult-born cells are involved specifically in the discrimination of similar odors, since inhibition of neurogenesis with an anti-mitotic drug had no effect on the ability of mice to discriminate between dissimilar odorants (Breton-Provencher et al., 2009). This was recently confirmed in another study which took advantage of the optogenetic approach to reveal that the specific activation of adult-born neurons facilitates animals' learning to discriminate between two odors, but only when the task is difficult, involving perceptually similar odorants (Alonso et al., 2012). What are the cellular mechanisms underlying these behavioural modulations? One possibility, as highlighted by electrophysiological recordings at the cellular and network levels following ablation of adult-born cells, is a reduced number of inhibitory synapses made by adult-born GCs on principal cell dendrites which altered inhibitory input and affected synchronized oscillatory activity of principal neurons (Breton-Provencher et al., 2009). Moreover, an optogenetic study has shown that the activation of adult-born neurons improves animal performances in an operant discrimination task of two perceptually similar odorants (Alonso et al., 2012). It is likely that activation of GCs increases the contrast between MCs since light stimulation triggers an inhibition of MCs with a low firing rate (Alonso et al., 2012). While these studies highlight some mechanisms of affected odor performances following manipulation in the number or activity of adult-born neurons, there is still a need to better understand the cellular and network mechanisms underlying the role of adult-born interneurons in the processing of olfactory information.

Associative olfactory learning, which evaluates the capacity of an animal to associate an odor with reward or noxious stimuli, is another test widely used to evaluate the implications of adult-born neurons in odor behaviour. Paradigms such as associative olfactory learning, especially those employing perceptually dissimilar odorants, increase the survival of adult-born cells in the OB (Alonso et al., 2006; Belnoue et al., 2011; Mouret et al., 2008; Sultan et al., 2010). However, modulation of the levels of neurogenesis had mixed consequences for animals' ability to learn an associative memory task, in some cases having no effect (Breton-Provencher et

al., 2009; Imayoshi et al., 2008), while in others performances were clearly altered (Lazarini et al., 2009; Sultan et al., 2010). A possible explanation for such differences could stem from the type of odor associative tasks used in these studies (Breton-Provencher and Saghatelyan, 2012; Lazarini and Lledo, 2011). In associative learning procedures, it is possible to differentiate in operant conditioning tasks from non-operant conditioning ones. With operant conditioning tasks, the active behaviour adopted by animals during the learning phase determines whether or not they receive a reward. On the other hand, in non-operant conditioning tasks, during the learning phase animals make a passive association between the odorant stimuli and the reward. Indeed, Mandairon and colleagues have shown that adult-born neurons play an important role only in operant conditioning tasks, since only these types of task seem to have an impact on the level of neurogenesis (Mandairon et al., 2011).

Another question to take into consideration, which may also explain discrepancies in the literature, is whether adult-born neurons are involved in the acquisition, retrieval and storage of odor-associated memories. Several studies have shown that pharmacological or genetic suppression of adult neurogenesis prior to the task of acquisition does not affect animals' performances (Arruda-Carvalho et al., 2014; Breton-Provencher et al., 2009; Imayoshi et al., 2008; Sultan et al., 2010), suggesting that adult-born neurons are not involved in the acquisition of odor-associated memories. Recent observations using a transgenic mouse line based on the "tag-and-ablate" strategy showed, however, that adult-born neurons are involved in the expression of odor-reward memories (Arruda-Carvalho et al., 2014). In this model, a tamoxifen treatment makes it possible to target or "tag" a large population of adult-born neurons with diphtheria toxin receptor in nestin-positive cells and their progeny. This is followed by a second treatment with diphtheria toxin that ablates the entire tagged cell population. The advantage of this model compared to general adult neurogenesis suppression studies is that adult-born neurons can be specifically ablated during particular phases of memory acquisition, retrieval or storage. Using this model, the authors demonstrated that in an associative learning task, the ablation of mature newborn neurons just after the training phase resulted in altered olfactory memory. Although this study shows that bulbar adult-born neurons play a key role in the expression of odor-reward memories, this effect appears to be transient. Ablation of adult-born GCs 28 days after training did not produce a memory deficit, suggesting that with time, recall of odor-reward memory becomes independent from adult-neurogenesis in the OB (Arruda-Carvalho et al., 2014). Thus these data indicate that in order to more fully understand the role of adult-born neurons in odor memory tasks, there is a need for more detailed analyses that take into account the different steps of memory formation, execution and storage.

One approach to address this issue would be to directly modulate the activity of adult-born neurons that are already integrated into the bulbar network. To achieve this, it is possible to take advantage of optogenetic activation or silencing of neurons, a method that has been used extensively over the last decade in many different fields of research (Grosenick et al., 2015; Zhang et al., 2007). This technique enables the selective activation or inhibition of the activity of particular cell

populations via expression at their membrane opsin receptors which are sensitive to light stimulation at a particular wavelength. Alonso and colleagues used this technique to investigate the involvement of adult-born interneurons in olfactory behaviour in the context of associative learning (Alonso et al., 2012). They showed that specifically activating adult-born neurons during learning of an operant olfactory discrimination task not only decreased the time necessary for the animals to learn the task, but also improved their memory of it. Animals in which adult-born neurons were activated were able to remember the task longer, as compared to control mice (Alonso et al., 2012). Other tools available to modulate the activity of different cellular populations are Designed Receptors Exclusively Activated by Designer Drugs (DREADDs), G protein-coupled muscarinic receptors genetically modified to respond exclusively to a pharmacologically inert molecule, clozapine-N-Oxide (CNO) (Alexander et al., 2009; Armbruster et al., 2007). When coupled to Gi family proteins, CNO treatment has an inhibitory effect on DREADD-expressing cells, whereas those coupled to Gq proteins are activated by CNO.

The tools presented above will enable investigation of the involvement of adult-born interneurons in olfactory behaviour during particular phases of odor task performance and there is urgent need for the implementation of these approaches to dissect the function of new cells in the OB.

5. Adult-born neurons: distinct functions for different sub-populations of cells?

Adult-born interneurons are produced in a region-specific manner and may be sub-divided into different subsets based on the expression of neurochemical markers. Hack and colleagues showed that different subpopulations of adult-born neurons are produced in the region-specific manner in the SVZ and RMS (Hack et al., 2005). Using retroviral labelling in these regions, the authors revealed that TH+ PGCs are generated in large numbers in the RMS (Hack et al., 2005). Merkle and colleagues, by targeting stem cells, have further shown that both neonatally- and adult-born cells in the OB are produced in a region-specific manner along SVZ-RMS pathway (Merkle et al., 2007). These data suggest that diverse subpopulations of interneurons are derived from a heterogeneous pool of stem cells.

The different subpopulations of adult-born neurons are produced not only in specific sub-regions, but also with a distinct temporal pattern throughout an animal lifetime. As briefly presented in the introduction, the GL contains at least three subpopulations of PGCs based on the expression of TH, calretinin and calbindin (Kosaka et al., 1995; Kosaka and Kosaka, 2005; Parrish-Aungst et al., 2007). Using dye labelling and homochronic/heterochronic transplantation, it has been shown that calbindin-positive PGCs are largely generated during neonatal life, whereas calretinin- and TH-expressing neurons are mainly produced during adulthood (De Marchis et al., 2007). By contrast, using inducible genetic fate mapping of Dlx1/2 precursors, it has been shown that the production of TH-expressing PGCs is

maximal during early embryogenesis (Batista-Brito et al., 2008). More consensus exists for the temporal pattern of calretinin and calbindin-expressing PGCs production, as genetic fate mapping has revealed that the production of calbindin interneurons is maximal during late embryogenesis and declines postnatally, whereas calretinin cell production is low during embryogenesis and increases postnatally (Batista-Brito et al., 2008). The different subpopulations of adult-born PGCs are responsive to odor stimulation as shown by *in vivo* two-photon Ca^{2+} imaging and targeted patch-clamp recordings (Kovalchuk et al., 2015; Livneh et al., 2014). Moreover, their responses to olfactory stimulation are shaped in an experience-dependent manner (Livneh et al., 2014). However, the role of different subpopulations of adult-born PGCs in OB network function and odor behaviour remains unknown. Some morpho-functional differences are observed between different subtypes of PGCs indicating that they may play distinct roles in the OB. For example, it has been shown that TH-expressing PGCs are the only population of interneurons that receive input from the olfactory nerve (Kosaka and Kosaka, 2007). By contrast, other populations of PGCs send their dendrites to intraglomerular zones that are not in contact with the sensory neuron's terminals (Kosaka and Kosaka, 2007). Therefore, TH-expressing PGCs may be more sensitive to the level of sensory input. This is supported by observations showing that social odor perception after mating is associated with an increased level of TH expression in PGCs and dopaminergic transmission in the OB (Serguera et al., 2008). This increase in dopaminergic transmission upholds presynaptic inhibition of sensory neurons and hampers neuronal activation in the OB thus leading to the modulation of social odor perception detrimental to pregnancy (Serguera et al., 2008). The relative contributions of adult-born and pre-existing TH-expressing cells to this effect have yet to be studied, as have the roles of calbindin- and calretinin-positive PGCs in odor behaviour.

The OB also contains parvalbumin-expressing interneurons located in the external plexiform layer (EPL) (Batista-Brito et al., 2008; Miyamichi et al., 2013). These interneurons are produced only during the perinatal period (Batista-Brito et al., 2008) and play an important role in feedback control of the OB output (Miyamichi et al., 2013).

GCs are the largest population of neurons in the OB. Despite this, very little is known about neurochemical heterogeneity of these cells and how different subtypes of GCs shape odor information processing in the OB and olfactory behaviour. Indeed, until now essentially all of the studies investigating the role of adult-born neurons in olfactory behaviour have considered these cells a homogenous population of neurons (Alonso et al., 2012; Arruda-Carvalho et al., 2014; Breton-Provencher et al., 2009; Imayoshi et al., 2008; Sultan et al., 2010). It is conceivable, however, that each subtype of adult-born GCs plays a specific role in odor information processing. Among the different subtypes that have been described so far are calretinin-expressing GCs found in the superficial GCL; glycoprotein 5T4-expressing cells located in the mitral cell layer (MCL); and mGluR2-, CaMKIV- and CaMKII-expressing ones found throughout the GCL (Imamura et al., 2006;

Jacobowitz and Winsky, 1991; Murata et al., 2011; Zou et al., 2002). Of these, calretinin- and mGluR2-expressing neurons, and at lower level 5T4-expressing cells, have been shown to be renewed in adulthood (Batista-Brito et al., 2008; Merkle et al., 2014; Murata et al., 2011), while the renewal of other subtypes have not been yet reported. Moreover, GCs with different morphology to their early-born counterparts have recently been described as type 1 deep branching GCs, type 2 shrub GCs, type 3 perimitral GCs and type 4 satellite cells (Merkle et al., 2014). What is the role of these neurons as well as other, as yet undiscovered, subtypes of GCs in odor information processing and odor behaviour? Interestingly, as with PGCs, some morpho-functional differences have been observed in GCs. While these data are still rudimentary, they imply that each subtype of GCs may play a distinct role in the OB. For example, it is well known that calretinin-expressing cells are located at the superficial GCL and may thus specifically contact tufted cells (Batista-Brito et al., 2008; Parrish-Aungst et al., 2007). Since tufted cells are involved in the synchronization of isofunctional odor columns in the OB (Zhou and Belluscio, 2008) and GCs play a crucial role in the synchronization of principal cell activity (Arevian et al., 2008; Fukunaga et al., 2014; Urban, 2002; Yokoi et al., 1995), it is conceivable that calretinin-expressing GCs may be specifically involved in odor discrimination paradigms, especially those involving complex tasks based on the discrimination of similar odors. With regard to newly described subpopulations of adult-born GCs (Merkle et al., 2014), some morphological differences were also documented. It has been shown that the dendrites of type 1 GCs do not reach the MCL or EPL but branch primarily in deeper regions of the OB. Type 2 shrub GCs extend a single primary dendrite into the deep layer of the EPL where they branch extensively, giving rise to many small dendrites decorated with numerous spine-like protrusions. The cell bodies of type 3 perimitral GCs are confined to the MCL, from which they extend thin spineless processes that branch above and below the MCL. Type 4 cells are located in the EPL and have branched dendrites with varicosities and few spines (Merkle et al., 2014). While the functional role of these new subtypes of GCs is not yet known, based on their morphology and location in the OB it has been hypothesized that type 1 and 2 GCs may inhibit the cell bodies and proximal dendrites of principal neurons and thus mediate columnar inhibition and localized lateral inhibition; whereas type 3 and 4 cells may inhibit the output of principal neurons and their dendrites (Merkle et al., 2014). The above data demonstrate growing evidence for the heterogeneity of adult-born interneurons in the OB. While several subpopulations of PGCs and GCs have already been described, it is conceivable that other subpopulations will emerge in the near future. Some of this data implies that various subpopulations may differ functionally, something that must be studied further to increase our understanding of how olfactory information is processed in the OB. Hence, further investigation is needed to determine whether and how each adult-born (and pre-existing) cell subpopulation makes a unique contribution to bulbar circuitry, and if so, whether there are preferential conditions under which their involvement is required. Moreover, if such differences can be revealed, it will be crucial to understand the impact of each subpopulation of interneurons on different olfactory behaviours.

6. Conclusion

Adult neurogenesis is an extraordinary process which constantly supplies the OB with new interneurons, a cell population that plays an important role in regulating information sent by principal cells to higher brain regions. This mode of maintaining the plasticity of the OB allows fine adaptation of the bulbar circuitry to the constantly changing environment. The question of the functional role played by these cells has to be better understood. In fact, studies aimed at determining the involvement of adult neurogenesis in different olfactory behaviours have produced dissenting data. There is therefore a need for a different approach to resolve this problem and the advent of new techniques over recent years will certainly aid in advancing our knowledge in this field of research. Moreover, the fact that different subpopulations of adult-born cells in the OB have been clearly identified implies that we can no longer consider neurogenesis as the birth of a homogeneous population of interneurons, but of different subsets that each makes a unique contribution to olfactory processing and network activity.

7. References

Alexander, G.M., Rogan, S.C., Abbas, A.I., Armbruster, B.N., Pei, Y., Allen, J.A., Nonneman, R.J., Hartmann, J., Moy, S.S., Nicolelis, M.A.*, et al.* (2009). Remote control of neuronal activity in transgenic mice expressing evolved G protein-coupled receptors. Neuron *63*, 27-39.

Alonso, M., Lepousez, G., Sebastien, W., Bardy, C., Gabellec, M.M., Torquet, N., and Lledo, P.M. (2012). Activation of adult-born neurons facilitates learning and memory. Nat Neurosci *15*, 897-904.

Alonso, M., Viollet, C., Gabellec, M.M., Meas-Yedid, V., Olivo-Marin, J.C., and Lledo, P.M. (2006). Olfactory discrimination learning increases the survival of adult-born neurons in the olfactory bulb. J Neurosci *26*, 10508-10513.

Alvarez-Buylla, A., and Garcia-Verdugo, J.M. (2002). Neurogenesis in adult subventricular zone. J Neurosci *22*, 629-634.

Arevian, A.C., Kapoor, V., and Urban, N.N. (2008). Activity-dependent gating of lateral inhibition in the mouse olfactory bulb. Nat Neurosci *11*, 80-87.

Armbruster, B.N., Li, X., Pausch, M.H., Herlitze, S., and Roth, B.L. (2007). Evolving the lock to fit the key to create a family of G protein-coupled receptors potently activated by an inert ligand. Proc Natl Acad Sci U S A *104*, 5163-5168.

Arruda-Carvalho, M., Akers, K.G., Guskjolen, A., Sakaguchi, M., Josselyn, S.A., and Frankland, P.W. (2014). Posttraining ablation of adult-generated olfactory granule cells degrades odor-reward memories. J Neurosci *34*, 15793-15803.

Baker, H., Morel, K., Stone, D.M., and Maruniak, J.A. (1993). Adult naris closure profoundly reduces tyrosine hydroxylase expression in mouse olfactory bulb. Brain Res *614*, 109-116.

Bastien-Dionne, P.O., David, L.S., Parent, A., and Saghatelyan, A. (2010). Role of sensory activity on chemospecific populations of interneurons in the adult olfactory bulb. J Comp Neurol *518*, 1847-1861.

Batista-Brito, R., Close, J., Machold, R., and Fishell, G. (2008). The distinct temporal origins of olfactory bulb interneuron subtypes. J Neurosci *28*, 3966-3975.

Belluzzi, O., Benedusi, M., Ackman, J., and LoTurco, J.J. (2003). Electrophysiological differentiation of new neurons in the olfactory bulb. J Neurosci *23*, 10411-10418.

Belnoue, L., Grosjean, N., Abrous, D.N., and Koehl, M. (2011). A critical time window for the recruitment of bulbar newborn neurons by olfactory discrimination learning. J Neurosci *31*, 1010-1016.

Breton-Provencher, V., Lemasson, M., Peralta, M.R., 3rd, and Saghatelyan, A. (2009). Interneurons produced in adulthood are required for the normal functioning of the olfactory bulb network and for the execution of selected olfactory behaviors. J Neurosci *29*, 15245-15257.

Breton-Provencher, V., and Saghatelyan, A. (2012). Newborn neurons in the adult olfactory bulb: unique properties for specific odor behavior. Behavioral Brain Research *227*, 480-489.

Carleton, A., Petreanu, L.T., Lansford, R., Alvarez-Buylla, A., and Lledo, P.M. (2003). Becoming a new neuron in the adult olfactory bulb. Nat Neurosci *6*, 507-518.

Corona, R., and Levy, F. (2015). Chemical olfactory signals and parenthood in mammals. Horm Behav *68*, 77-90.

Corotto, F.S., Henegar, J.R., and Maruniak, J.A. (1994). Odor deprivation leads to reduced neurogenesis and reduced neuronal survival in the olfactory bulb of the adult mouse. Neuroscience *61*, 739-744.

Cummings, D.M., Snyder, J.S., Brewer, M., Cameron, H.A., and Belluscio, L. (2014). Adult neurogenesis is necessary to refine and maintain circuit specificity. J Neurosci *34*, 13801-13810.

David, L.S., Schachner, M., and Saghatelyan, A. (2013). The extracellular matrix glycoprotein tenascin-R affects adult but not developmental neurogenesis in the olfactory bulb. J Neurosci *33*, 10324-10339.

De Marchis, S., Bovetti, S., Carletti, B., Hsieh, Y.C., Garzotto, D., Peretto, P., Fasolo, A., Puche, A.C., and Rossi, F. (2007). Generation of distinct types of periglomerular olfactory bulb interneurons during development and in adult mice: implication for intrinsic properties of the subventricular zone progenitor population. J Neurosci *27*, 657-664.

Doetsch, F., Caille, I., Lim, D.A., Garcia-Verdugo, J.M., and Alvarez-Buylla, A. (1999). Subventricular zone astrocytes are neural stem cells in the adult mammalian brain. Cell *97*, 703-716.

Feierstein, C.E. (2012). Linking adult olfactory neurogenesis to social behavior. Front Neurosci *6*, 173.

Fukunaga, I., Herb, J.T., Kollo, M., Boyden, E.S., and Schaefer, A.T. (2014). Independent control of gamma and theta activity by distinct interneuron networks in the olfactory bulb. Nat Neurosci *17*, 1208-1216.

Grosenick, L., Marshel, J.H., and Deisseroth, K. (2015). Closed-loop and activity-guided optogenetic control. Neuron *86*, 106-139.

Hack, I., Bancila, M., Loulier, K., Carroll, P., and Cremer, H. (2002). Reelin is a detachment signal in tangential chain-migration during postnatal neurogenesis. Nat Neurosci *5*, 939-945.

Hack, M.A., Saghatelyan, A., de Chevigny, A., Pfeifer, A., Ashery-Padan, R., Lledo, P.M., and Gotz, M. (2005). Neuronal fate determinants of adult olfactory bulb neurogenesis. Nat Neurosci *8*, 865-872.

Imamura, F., Nagao, H., Naritsuka, H., Murata, Y., Taniguchi, H., and Mori, K. (2006). A leucine-rich repeat membrane protein, 5T4, is expressed by a subtype of granule cells with dendritic arbors in specific strata of the mouse olfactory bulb. J Comp Neurol *495*, 754-768.

Imayoshi, I., Sakamoto, M., Ohtsuka, T., Takao, K., Miyakawa, T., Yamaguchi, M., Mori, K., Ikeda, T., Itohara, S., and Kageyama, R. (2008). Roles of continuous neurogenesis in the structural and functional integrity of the adult forebrain. Nat Neurosci *11*, 1153-1161.

Isaacson, J.S., and Strowbridge, B.W. (1998). Olfactory reciprocal synapses: dendritic signaling in the CNS. Neuron *20*, 749-761.

Jacobowitz, D.M., and Winsky, L. (1991). Immunocytochemical localization of calretinin in the forebrain of the rat. J Comp Neurol *304*, 198-218.

Jahr, C.E., and Nicoll, R.A. (1982). An intracellular analysis of dendrodendritic inhibition in the turtle in vitro olfactory bulb. J Physiol *326*, 213-234.

Kelsch, W., Lin, C.W., and Lois, C. (2008). Sequential development of synapses in dendritic domains during adult neurogenesis. Proc Natl Acad Sci U S A *105*, 16803-16808.

Kelsch, W., Lin, C.W., Mosley, C.P., and Lois, C. (2009). A critical period for activity-dependent synaptic development during olfactory bulb adult neurogenesis. J Neurosci *29*, 11852-11858.

Kosaka, K., Aika, Y., Toida, K., Heizmann, C.W., Hunziker, W., Jacobowitz, D.M., Nagatsu, I., Streit, P., Visser, T.J., and Kosaka, T. (1995). Chemically defined neuron groups and their subpopulations in the glomerular layer of the rat main olfactory bulb. Neurosci Res *23*, 73-88.

Kosaka, K., and Kosaka, T. (2007). Chemical properties of type 1 and type 2 periglomerular cells in the mouse olfactory bulb are different from those in the rat olfactory bulb. Brain Res *1167*, 42-55.

Kosaka, K., Toida, K., Aika, Y., and Kosaka, T. (1998). How simple is the organization of the olfactory glomerulus?: the heterogeneity of so-called periglomerular cells. Neurosci Res *30*, 101-110.

Kosaka, T., and Kosaka, K. (2005). Structural organization of the glomerulus in the main olfactory bulb. Chem Senses *30 Suppl 1*, i107-108.

Kovalchuk, Y., Homma, R., Liang, Y., Maslyukov, A., Hermes, M., Thestrup, T., Griesbeck, O., Ninkovic, J., Cohen, L.B., and Garaschuk, O. (2015). In vivo odourant response properties of migrating adult-born neurons in the mouse olfactory bulb. Nat Commun *6*, 6349.

Lagace, D.C., Whitman, M.C., Noonan, M.A., Ables, J.L., DeCarolis, N.A., Arguello, A.A., Donovan, M.H., Fischer, S.J., Farnbauch, L.A., Beech, R.D.*, et al.* (2007). Dynamic contribution of nestin-expressing stem cells to adult neurogenesis. J Neurosci *27*, 12623-12629.

Lazarini, F., and Lledo, P.M. (2011). Is adult neurogenesis essential for olfaction? Trends Neurosci *34*, 20-30.

Lazarini, F., Mouthon, M.A., Gheusi, G., de Chaumont, F., Olivo-Marin, J.C., Lamarque, S., Abrous, D.N., Boussin, F.D., and Lledo, P.M. (2009). Cellular and behavioral effects of cranial irradiation of the subventricular zone in adult mice. PLoS One *4*, e7017.

Lepousez, G., and Lledo, P.M. (2013). Odor discrimination requires proper olfactory fast oscillations in awake mice. Neuron *80*, 1010-1024.

Lin, C.W., Sim, S., Ainsworth, A., Okada, M., Kelsch, W., and Lois, C. (2010). Genetically increased cell-intrinsic excitability enhances neuronal integration into adult brain circuits. Neuron *65*, 32-39.

Livneh, Y., Adam, Y., and Mizrahi, A. (2014). Odor processing by adult-born neurons. Neuron, 1097-1110.

Livneh, Y., and Mizrahi, A. (2012). Experience-dependent plasticity of mature adult-born neurons. Nat Neurosci *15*, 26-28.

Lois, C., Garcia-Verdugo, J.M., and Alvarez-Buylla, A. (1996). Chain migration of neuronal precursors. Science *271*, 978-981.

Luskin, M.B. (1993). Restricted proliferation and migration of postnatally generated neurons derived from the forebrain subventricular zone. Neuron *11*, 173-189.

Magavi, S.S., Mitchell, B.D., Szentirmai, O., Carter, B.S., and Macklis, J.D. (2005). Adult-born and preexisting olfactory granule neurons undergo distinct experience-dependent modifications of their olfactory responses in vivo. J Neurosci *25*, 10729-10739.

Mandairon, N., Sacquet, J., Garcia, S., Ravel, N., Jourdan, F., and Didier, A. (2006b). Neurogenic correlates of an olfactory discrimination task in the adult olfactory bulb. Eur J Neurosci *24*, 3578-3588.

Mandairon, N., Sultan, S., Nouvian, M., Sacquet, J., and Didier, A. (2011). Involvement of newborn neurons in olfactory associative learning? The operant or non-operant component of the task makes all the difference. J Neurosci *31*, 12455-12460.

Merkle, F.T., Fuentealba, L.C., Sanders, T.A., Magno, L., Kessaris, N., and Alvarez-Buylla, A. (2014). Adult neural stem cells in distinct microdomains generate previously unknown interneuron types. Nat Neurosci *17*, 207-214.

Merkle, F.T., Mirzadeh, Z., and Alvarez-Buylla, A. (2007). Mosaic organization of neural stem cells in the adult brain. Science *317*, 381-384.

Miyamichi, K., Shlomai-Fuchs, Y., Shu, M., Weissbourd, B.C., Luo, L., and Mizrahi, A. (2013). Dissecting local circuits: parvalbumin interneurons underlie broad feedback control of olfactory bulb output. Neuron *80*, 1232-1245.

Mizrahi, A. (2007). Dendritic development and plasticity of adult-born neurons in the mouse olfactory bulb. Nat Neurosci *10*, 444-452.

Moreno, M.M., Linster, C., Escanilla, O., Sacquet, J., Didier, A., and Mandairon, N. (2009). Olfactory perceptual learning requires adult neurogenesis. Proc Natl Acad Sci U S A *106*, 17980-17985.

Mouret, A., Gheusi, G., Gabellec, M.M., de Chaumont, F., Olivo-Marin, J.C., and Lledo, P.M. (2008). Learning and survival of newly generated neurons: when time matters. J Neurosci *28*, 11511-11516.

Murata, K., Imai, M., Nakanishi, S., Watanabe, D., Pastan, I., Kobayashi, K., Nihira, T., Mochizuki, H., Yamada, S., Mori, K.*, et al.* (2011). Compensation of depleted neuronal subsets by new neurons in a local area of the adult olfactory bulb. J Neurosci *31*, 10540-10557.

Ninkovic, J., Mori, T., and Gotz, M. (2007). Distinct modes of neuron addition in adult mouse neurogenesis. J Neurosci *27*, 10906-10911.

Nissant, A., Bardy, C., Katagiri, H., Murray, K., and Lledo, P.M. (2009). Adult neurogenesis promotes synaptic plasticity in the olfactory bulb. Nat Neurosci *12*, 728-730.

Panzanelli, P., Bardy, C., Nissant, A., Pallotto, M., Sassoe-Pognetto, M., Lledo, P.M., and Fritschy, J.M. (2009). Early synapse formation in developing interneurons of the adult olfactory bulb. J Neurosci *29*, 15039-15052.

Parrish-Aungst, S., Shipley, M.T., Erdelyi, F., Szabo, G., and Puche, A.C. (2007). Quantitative analysis of neuronal diversity in the mouse olfactory bulb. J Comp Neurol *501*, 825-836.

Petreanu, L., and Alvarez-Buylla, A. (2002). Maturation and death of adult-born olfactory bulb granule neurons: role of olfaction. J Neurosci *22*, 6106-6113.

Price, J.L., and Powell, T.P. (1970). The synaptology of the granule cells of the olfactory bulb. J Cell Sci *7*, 125-155.

Rochefort, C., Gheusi, G., Vincent, J.D., and Lledo, P.M. (2002). Enriched odor exposure increases the number of newborn neurons in the adult olfactory bulb and improves odor memory. J Neurosci *22*, 2679-2689.

Rochefort, C., and Lledo, P.M. (2005). Short-term survival of newborn neurons in the adult olfactory bulb after exposure to a complex odor environment. Eur J Neurosci *22*, 2863-2870.

Saghatelyan, A., de Chevigny, A., Schachner, M., and Lledo, P.M. (2004). Tenascin-R mediates activity-dependent recruitment of neuroblasts in the adult mouse forebrain. Nat Neurosci *7*, 347-356.

Saghatelyan, A., Roux, P., Migliore, M., Rochefort, C., Desmaisons, D., Charneau, P., Shepherd, G.M., and Lledo, P.M. (2005). Activity-dependent adjustments of the inhibitory network in the olfactory bulb following early postnatal deprivation. Neuron *46*, 103-116.

Serguera, C., Triaca, V., Kelly-Barrett, J., Banchaabouchi, M.A., and Minichiello, L. (2008). Increased dopamine after mating impairs olfaction and prevents odor interference with pregnancy. Nat Neurosci *11*, 949-956.

Shepherd, G.M., Chen, W.R., and Greer, C.A. (2004). Olfactory Bulb. In The Synaptic Organization of the Brain, G.M. Shepherd, ed., pp. 165–216.

Snapyan, M., Lemasson, M., Brill, M.S., Blais, M., Massouh, M., Ninkovic, J., Gravel, C., Berthod, F., Gotz, M., Barker, P.A.*, et al.* (2009). Vasculature guides migrating neuronal precursors in the adult mammalian forebrain via brain-derived neurotrophic factor signaling. J Neurosci *29*, 4172-4188.

Sultan, S., Mandairon, N., Kermen, F., Garcia, S., Sacquet, J., and Didier, A. (2010). Learning-dependent neurogenesis in the olfactory bulb determines long-term olfactory memory. FASEB J *24*, 2355-2363.

Urban, N.N. (2002). Lateral inhibition in the olfactory bulb and in olfaction. Physiol Behav *77*, 607-612.

Valley, M.T., Henderson, L.G., Inverso, S.A., and Lledo, P.M. (2013). Adult neurogenesis produces neurons with unique GABAergic synapses in the olfactory bulb. J Neurosci *33*, 14660-14665.

Whitman, M.C., Fan, W., Rela, L., Rodriguez-Gil, D.J., and Greer, C.A. (2009). Blood vessels form a migratory scaffold in the rostral migratory stream. J Comp Neurol *516*, 94-104.

Whitman, M.C., and Greer, C.A. (2007). Synaptic integration of adult-generated olfactory bulb granule cells: basal axodendritic centrifugal input precedes apical dendrodendritic local circuits. J Neurosci *27*, 9951-9961.

Winner, B., Cooper-Kuhn, C.M., Aigner, R., Winkler, J., and Kuhn, H.G. (2002). Long-term survival and cell death of newly generated neurons in the adult rat olfactory bulb. Eur J Neurosci *16*, 1681-1689.

Yamaguchi, M., and Mori, K. (2005). Critical period for sensory experience-dependent survival of newly generated granule cells in the adult mouse olfactory bulb. Proc Natl Acad Sci U S A *102*, 9697-9702.

Yokoi, M., Mori, K., and Nakanishi, S. (1995). Refinement of odor molecule tuning by dendrodendritic synaptic inhibition in the olfactory bulb. Proc Natl Acad Sci U S A *92*, 3371-3375.

Zhang, F., Wang, L.P., Brauner, M., Liewald, J.F., Kay, K., Watzke, N., Wood, P.G., Bamberg, E., Nagel, G., Gottschalk, A.*, et al.* (2007). Multimodal fast optical interrogation of neural circuitry. Nature *446*, 633-639.

Zhou, Z., and Belluscio, L. (2008). Intrabulbar projecting external tufted cells mediate a timing-based mechanism that dynamically gates olfactory bulb output. J Neurosci *28*, 9920-9928.

Zou, D.J., Greer, C.A., and Firestein, S. (2002). Expression pattern of alpha CaMKII in the mouse main olfactory bulb. J Comp Neurol *443*, 226-236.